The Dissertation Committee for Ling Huang Certifies that this is the approved version of the following dissertation:

The Effects of Drought on Predicted Air Quality in Texas

Committee:

David T. Allen, Co-Supervisor

Elena McDonald-Buller, Co-Supervisor

Lea Hildebrandt Ruiz

Rong Fu

Gary T. Rochelle

The Effects of Drought on Predicted Air Quality in Texas

by

Ling Huang, B.E.; M.S.E.

Dissertation

Presented to the Faculty of the Graduate School of

The University of Texas at Austin

in Partial Fulfillment

of the Requirements

for the Degree of

Doctor of Philosophy

The University of Texas at Austin

August 2015

Dedication

To my family.

Acknowledgements

First of all, I would like to express my deepest gratitude to my advisors – Dr. Elena McDonald-Buller and Dr. David Allen – for their continuous guidance and support through my Ph.D. studies at the University of Texas at Austin. I also want to thank Gary McGaughey and Yosuke Kimura for their tremendous help and encouragement that walked me through numerous difficulties. Finally, I want to thank my parents and my husband for their unconditional love and support that makes me who I am right now.

The Effects of Drought on Predicted Air Quality in Texas

Ling Huang, Ph.D.

The University of Texas at Austin, 2015

Co-Supervisor: David T. Allen

Co-Supervisor: Elena McDonald-Buller

Drought is a natural disaster that has profound and complex social, economic, and environmental impacts. As drought is predicted to occur more frequently within Texas with changes in future climate, it is critical to understand its impacts on regional air quality as the State endeavors to achieve and maintain attainment with National Ambient Air Quality Standards for ozone and fine particulate matter. Drought-induced changes in various natural systems, including emissions of biogenic hydrocarbons from vegetation and the physical removal of pollutants by vegetation via dry deposition, have the potential to effect air quality. This work characterizes land cover for eastern Texas climate regions during years with severe to exceptional drought conditions as well as years with average to above average precipitation patterns. Variability in meteorological conditions, biogenic emissions, and dry deposition rates is explored with widely applied global and regional models that have been configured specifically for multi-year analysis of eastern Texas conditions. The Comprehensive Air Quality Model with Extensions (CAMx), which has been used for air quality planning and management efforts in Texas, is used to quantify the relative contributions of various physical and chemical processes to ground-level ozone formation and changes in ground-level ozone concentrations

during representative drought and wet periods. The analyses indicate that drought influences air quality in complex ways. This work suggests that the two largest drought driven changes to the physical and chemical processes that influence air quality are increased biogenic emissions due to elevated temperatures and decreased air pollutant removal through dry deposition due to changes in leaf-level processes. Both of these changes degrade air quality and their combined effect can be as large as an increase of approximately 5 ppb in ground level, 8-hour averaged ozone concentrations in parts of eastern Texas. The effects of soil moisture on biogenic emissions estimates can be as significant as temperature, but current land surface model configurations and the adequacy of the Model of Emissions of Gases and Aerosols Nature (MEGAN) algorithm to fully represent short and long-term responses to soil moisture remain highly uncertain. The characterization of soil moisture through ground and satellite-based measurement programs and validation of global and regional-scale land cover distributions should continue to be high priorities to support air quality planning in Texas.

Table of Contents

List of Tables

List of Figures

Chapter 1: Introduction

1.1 Research Motivation

Drought is broadly recognized as abnormally dry conditions relative to the local normal (Dai, 2011) due to a precipitation deficit over an extended period of time. Ranked as the first natural hazard with respect to the number of people affected (Obasi, 1994; Hewitt, 1997; Wilhite, 2000), drought has unique characteristics relative to other natural hazards (Wilhite, 2000; Mishra and Singh, 2010). For example, the onset and end of a drought can be difficult to determine, and the impacts may linger over a considerable period of time. Unlike floods, hurricanes, and earthquakes, droughts seldom cause apparent structural damages, but the effects can spread over large geographical areas leading to difficulties in their quantification. In addition to natural causes, human activities, such as deforestation, agricultural operations, and the over-exploitation of water resources, also contribute, resulting in a complex "interplay between a natural event (i.e., precipitation deficiencies) and the demand placed on water and other natural resources by human-use systems" (Wilhite and Vanyarkho, 2000).

Droughts can occur over most parts of the world, even in wet and humid regions, and vary substantially in intensity, severity, duration, and spatial extent (Zargar et al., 2011). Large-scale intensive droughts have been observed throughout the world during the past century (Sheffield and Wood, 2012a). The famed Dust Bowl of the 1930s, compounded with the Great Depression, was one of the worst natural disasters in United States history (Sheffield and Wood, 2012a). Others historical events have included unprecedented severe droughts in West Africa since the late 1960s (Mishra and Singh, 2010), the 1996 drought in the United States (Wilhite and Vanyarkho, 2000), frequent severe droughts in 1997 and 1999 through 2002 in northern China (Zhang, 2003), the 2003 drought across large parts of Europe (Marsh, 2004), the droughts of 1999 through

2004-2005 in the Canadian Prairies (Fang and Pomeroy, 2008), the 2005 drought that plagued much of the southern and western parts of the Amazon River basin (Sheffield and Wood, 2012a), the 'millennium' drought that lasted for almost a decade in Australia (Bond et al., 2008), and the recent 2010-2012 drought in the southern United States.

The American Meteorological Society (AMS, 1997) has classified drought into four categories: meteorological, agricultural, hydrological, and socio-economic, described in Table 1-1. Mishra and Singh (2010) suggested groundwater drought as a fifth type. Figure 1-1 indicates that the five drought types generally occur in a particular sequence. Globally, the use of indices has become a popular approach for characterizing drought (Tsakiris et al., 2002). Drought indices attempt to assimilate meteorological, hydrological and/or other data into a single numerical value (Tsakiris et al., 2002; Zargar et al., 2011) to provide simple, quantitative assessments of the intensity, duration, and spatial extent of drought (Hayes et al. 2000). More than 150 indices have been developed with different intents and purposes (Byun and Wilhite, 1999; Heim, 2002; Ntale and Gan, 2003; Niemeyer, 2008; Bayarjargal et al., 2006, Mishra and Singh, 2010; Sivakumar et al., 2010; Dai, 2011; Zargar et al., 2011). Table 1-1 summarizes five drought indices (i.e. PDSI, SPI, KBDI, ESI, USDM) as representative examples.

Table 1-1: Classification of droughts. Summarized from Wilhite (2000); Mishra and Singh (2010); NDMC website (http://drought.unl.edu/DroughtBasics/TypesofDrought.aspx).

Types of Droughts	Definition	Causes	Main Indicator	Characteristics
Meteorological	Below-normal precipitation over a region for a period of months to years	Low precipitation	Precipitation	Definitions of meteorological droughts are region specific. It precedes other drought types.
Agricultural	Period when soil moisture is declining as a result of below-average precipitation with consequent reduced crop production and plant growth	Low precipitation and high evaporation; anthropogenic causes such as poor water management, overfarming, deforestation, etc.	Soil moisture	In addition to the loss of precipitation, agricultural droughts can also be triggered by other factors, such as more intense but less frequent precipitation, poor water management, and erosion.
Hydrological	Period when surface and subsurface water storages drop below long-term statistical average	Same as agricultural droughts.	Streamflow	Hydrological droughts develop more slowly because they involve stored water that is used but not refilled. Like agricultural droughts, hydrological droughts can also be triggered by more than a lack of precipitation.
Socio-economic	Imbalance between the demand and supply for an economic good as a result of a weather-related shortage in water supply	Reduction of supply caused by the above droughts.	Water demand and supply	Unlike the other types of droughts, the identification of socio-economic droughts depends on the temporal and spatial distribution of supply and demand.
Groundwater	Decrease of groundwater recharge followed by drop of groundwater levels and discharge	Low precipitation possibly with high evapotranspiration; overexploitation.	Groundwater level	Groundwater droughts are caused by low precipitation possibly with high evapotranspiration. In addition, overexploitation can also create a groundwater drought.

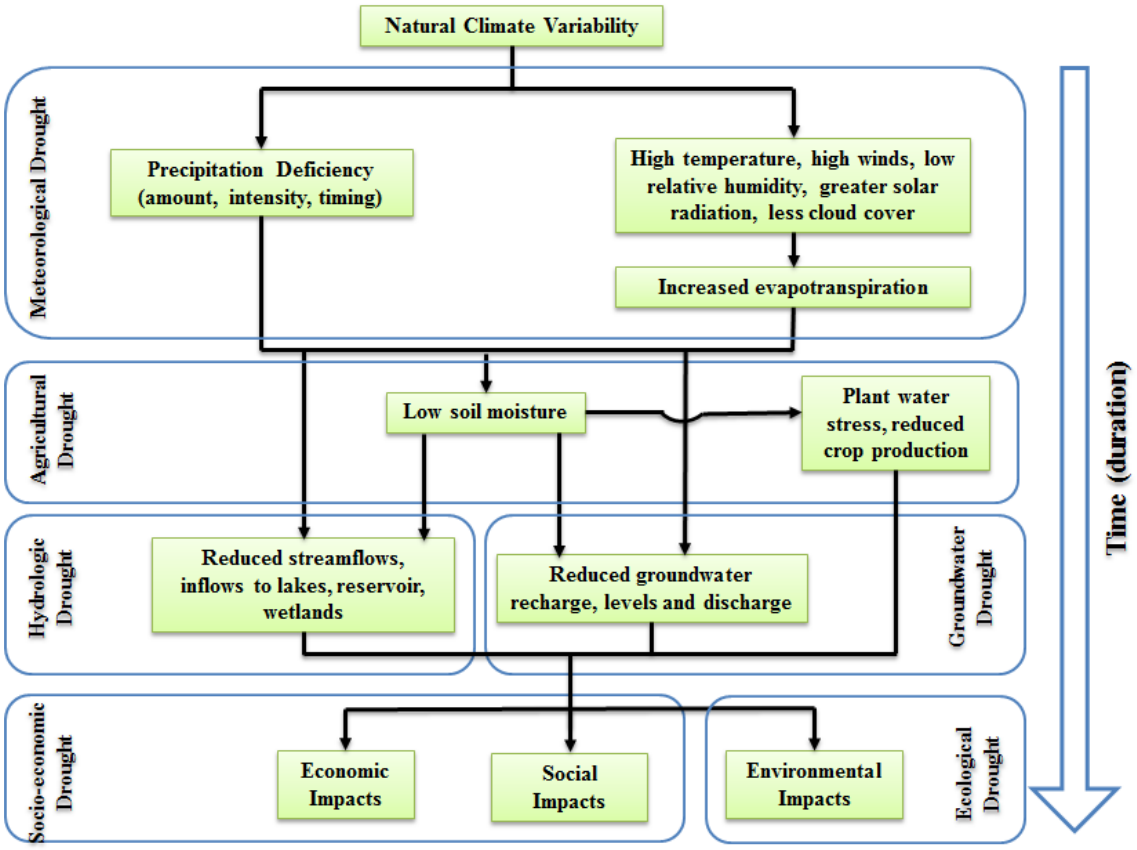

Figure 1-1: Sequence of drought types. Source: Adopted from the US National Drought Mitigation Center (NDMC) and Sheffield and Wood (2012b)

Table 1-2: Summaries of five representative drought indices. M: Meteorological, A: Agricultural, RS: Remote-Sensing, Agre: Aggregate, P: Precipitation, T: Temperature, ET: Evapotranspiration, SM: Soil Moisture, SF: Streamflow, LST: Land Surface Temperature, TIR: Thermal-Infrared.

Index Name	Type	Inputs	Notes	Reference
Palmer Drought Severity Index (PDSI)	M/A	P,T,ET,SM,SF	Measures the departure from normal conditions and is based on a two layer soil model which considers moisture input, output and storage components; most widely used drought index.	Palmer (1965)
Standardized Precipitation Index (SPI)	M/A	P	Standardized precipitation anomaly for various time scales after long-term precipitation record is fitted and transformed to a normal distribution.	McKee et al. (1993)
Keetch-Byram Drought Index (KBDI)	M	P,T	A daily water budgeting procedure is used to analyze P and SM; widely used in wildfire monitoring and prediction (Heim, 2002).	Keetch and Byram (1968)
Evaporative Stress Index (ESI)	RS	LST, TIR	Based on the ratio of actual ET to potential ET, derived using satellite data and the Atmosphere-Land Exchange Inverse (ALEXI) model.	Anderson and Kustas (2008)
US Drought Monitor (USDM)	Agre	SPI, PDSI, vegetation and hydrologic conditions	First created in 1999; integrates multiple drought indices (e.g. SPI, PDSI) and indicators for vegetation and hydrologic conditions into a weekly map of drought.	Svoboda et al (2002)

Drought imposes complex and profound social, economic, and environmental effects. These include threats to food security due to losses in crop yields and livestock production (Liverman, 1990; Webb and Reardon, 1992), increases in the cost of water transport (Logar and Bergh, 2011), changes in water quality (Van Vliet and Zwolsman, 2008), air quality (Prosperop and Nees, 1986), and forest biodiversity (Frédéric and Volkmar, 2006), and threats to public health and quality of life (Webb and Reardon, 1992; Wilhite and Vanyarkho, 2000). For example, the impacts of drought on food security in East Africa (also referred as the Horn of Africa) have been particularly severe, necessitating international humanitarian relief efforts and prompting greater recognition of the need for early drought warning systems. An ecological impact of drought is regional-scale forest die-off, which has been observed in the United States (Breshears et al., 2005; Shaw et al., 2005; Voelker et al., 2008; Allen et al., 2010; Texas A&M Forest Service, 2012) as well as other regions of the world (Logan et al., 2003; Van Nieuwstadt and Sheil, 2004; Allen and Breshears, 2007; Fensham et al., 2008). Drought impacts can be described as direct or indirect (Wilhite and Vanyarkho 2000). Direct (also referred to as primary) impacts are usually of a biophysical nature, such as reduced crop yields and water levels and increased fire hazard and wildlife mortality rates; the consequences of these direct impacts represent indirect or secondary impacts (Logar and Bergh 2011; Wilhite et al. 2007). Indirect losses associated with drought often exceed direct losses and are likely to be underestimated since they may occur months or years after the event has started (Logar and Bergh 2011; Wilhite et al. 2007). Overall, the effects of drought are highly dependent on the preparedness and coping capabilities of a population through drought monitoring, planning, and policies (Wilhite and Knutson, 2008).

Drought has been a recurring phenomenon in the southeastern United States. Figure 1-2 shows time series of three drought indices (i.e. 3-month SPI, 12-month SPI,

monthly PDSI) for eastern Texas climate regions during 2006 through 2011. Figure 1-3 shows the U.S. Drought Monitor maps released in the month of September during 2006-2011 and on June 16, 2015. As shown by both figures, the severity of drought varies spatially and temporally. The drought effects in Texas during 2011 were among the worst of the 2010-2012 drought in the southern United States; Texas was still faced with continuing challenges to its water resources in the aftermath. In October 2011, 88% of Texas was under exceptional drought conditions, with only 3% of the state not classified as experiencing extreme or exceptional drought conditions. According to the Texas AgriLife Extension Service, the 2011 Texas drought caused a record $7.62 billion in agricultural losses (Fannin, 2012), exceeding the previous record of $4.1 billion during 2006. The drought and associated heat were also associated with 31,453 wildfires with more than 4 million acres burned and 2,947 Texas homes destroyed, making 2011 the worst year for wildfires in Texas history (Texas A&M Forest Service, 2013). According to the Texas A&M Forest Service (2012), the devastating 2011 drought also led to the die-off of 301 million trees across the state with the die-off of 5.6 million within urban forests. As Figure 1-4 indicates, the Southern Great Plains are projected to experience drier conditions with higher numbers of hot days and consecutive dry days (Melillo et al., 2014).

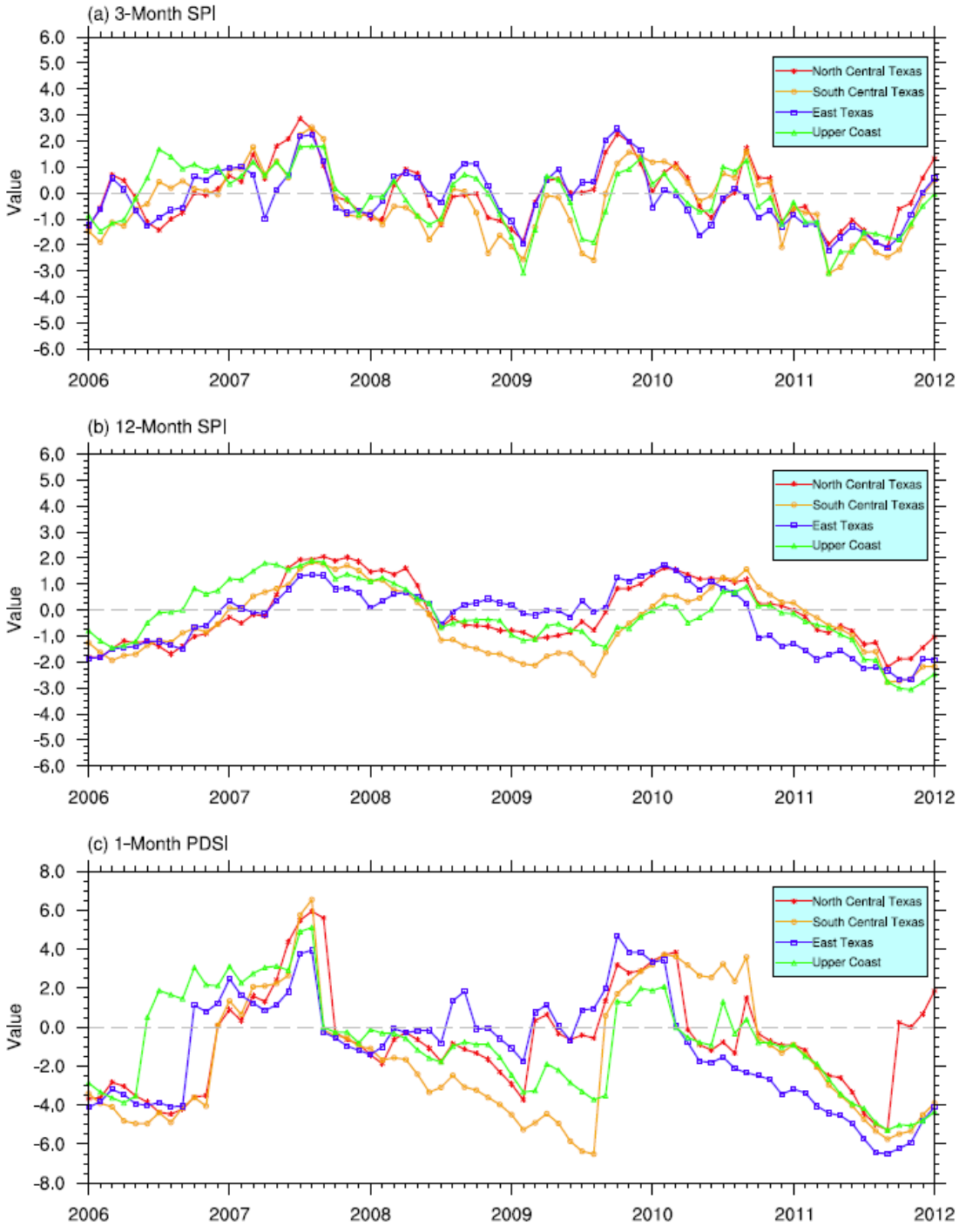

Figure 1-2: Time series of (a) 3-month SPI, (b) 12-month SPI and (c) monthly PDSI for four eastern Texas climate regions during 2006-2011. Source: National Climatic Data Center.

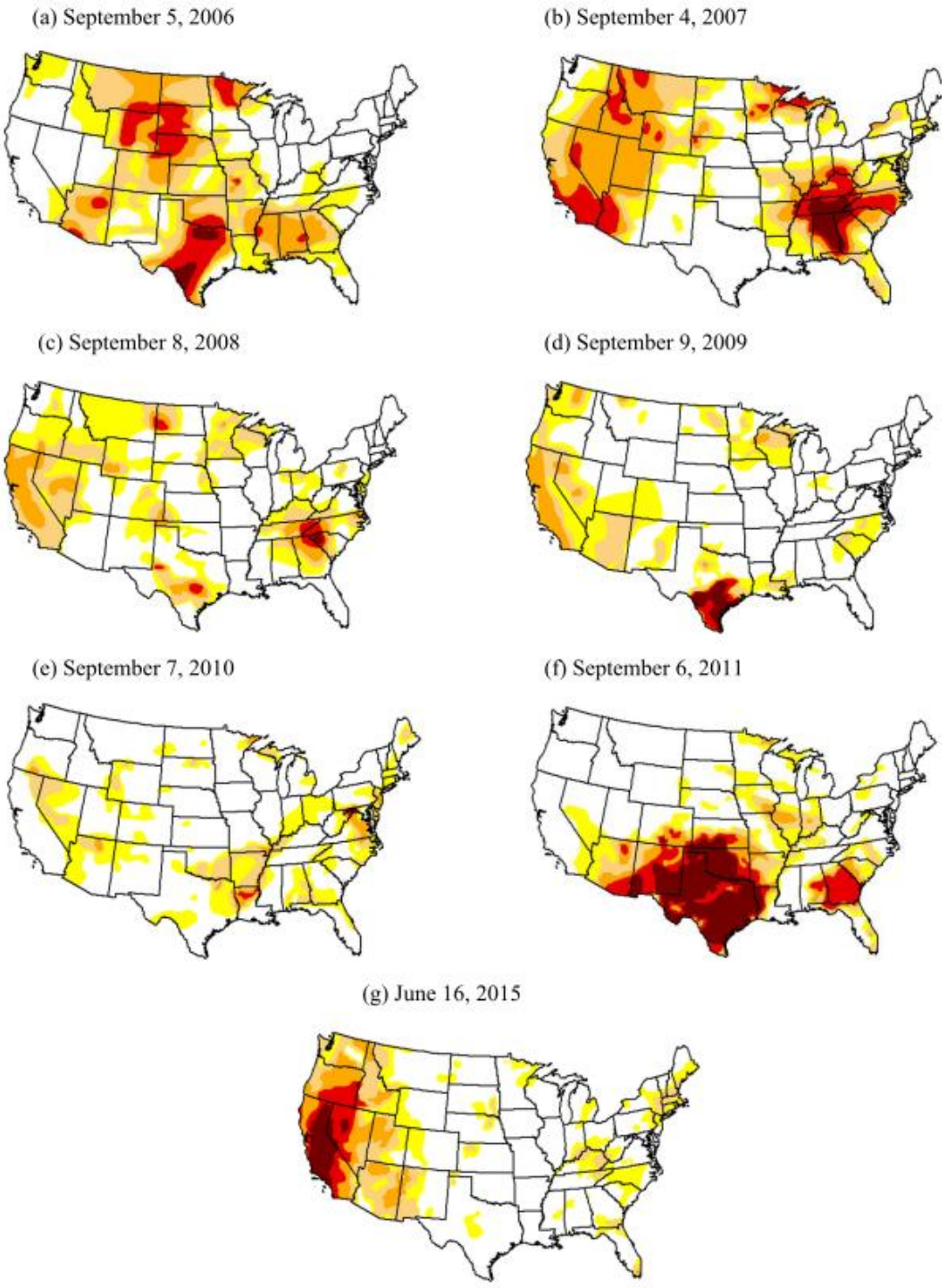

Figure 1-3: U.S. Drought Monitor, released on (a) September 5, 2006, (b) September 4, 2007, (c) September 8, 2008, (d) September 9, 2009, (e) September 7, 2010, (f) September 6, 2011 and (g) June 16, 2015. Source: http://droughtmonitor.unl.edu/.

(a) (b)

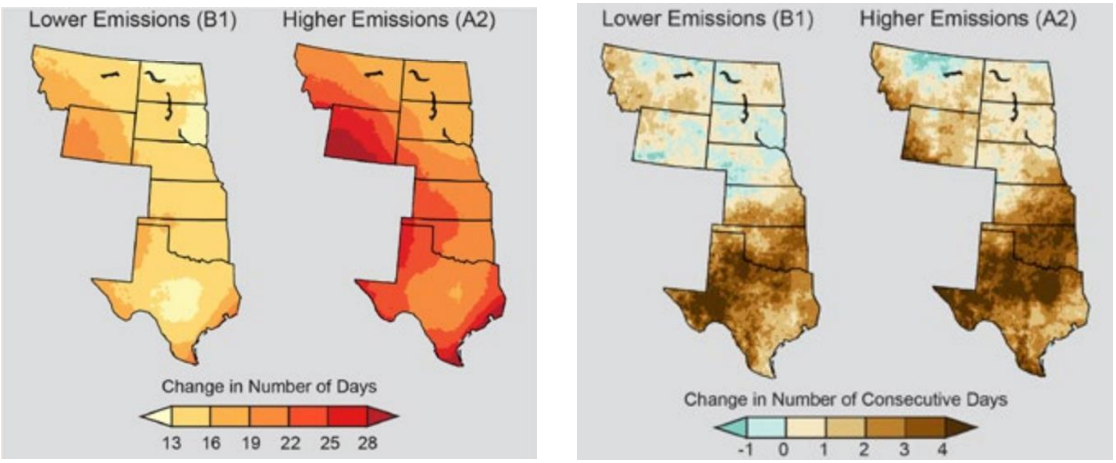

Figure 1-4: Projected changes in (a) number of days with the hottest temperatures and (b) number of consecutive dry days in Great Plains by mid-century (2041-2070). Figure source: NOAA NCDC / CICS-NC.

Drought-induced changes in natural, managed, and cultivated land cover systems, including emissions of biogenic hydrocarbons from vegetation and the removal of atmospheric pollutants by vegetation via dry deposition, have the potential to affect air quality. Vegetation is a primary source of hydrocarbons, with levels that can exceed those emitted from anthropogenic activities (Purves et al., 2004). Biogenic hydrocarbons, primarily isoprene and monoterpenes, are important precursors for tropospheric ozone and secondary organic aerosols (Atkinson, 2000; Claeys et al., 2004), both of which have well-documented adverse impacts on human health (Dockery et al., 1993; Lippmann, 1989). Dry deposition refers to the process by which trace gases and particulates in the atmosphere are transferred to the Earth's surface, including soil, vegetation, and water. Substantial removal of air pollutants by dry deposition to vegetation via leaf stomata can influence urban air quality (Nowak et al., 2006); in Texas, dry deposition is the most important physical removal mechanism for ozone during the summer season (McDonald-Buller et al., 2001).

Texas has highly diverse climatic conditions and land use/land cover profiles over its 10 climate regions (Figure 1-5a). Both temperature and precipitation gradually decrease inland from the Gulf of Mexico and across the state: average annual temperature decreases from approximately 68 ºF in the Lower Rio Grande Valley to 52 ºF in the northern Panhandle (Figure 1-5b); average annual precipitation decreases from over 55 inches in Upper Coast to less than 10 inches in west Trans-Pecos (Figure 1-5c). This work focuses on four climate regions in eastern Texas—North Central Texas, South Central Texas, East Texas, and Upper Coast—which include most large metropolitan areas in the state and most of the regions that exceed National Ambient Air Quality Standards (NAAQS). Major land cover types change from grasses/crops in central regions to dense forest in East Texas. As Texas's population has increased by 20% (to 26 million) over the past decade (Source: U.S. Census Bureau), especially in major urban centers, areas of agricultural and forest land adjacent to cities have been consumed by suburbanization. Future changes in land use/land cover due to urbanization are predicted to influence air quality in urban centers and surrounding regions (Jiang et al., 2008). As drought is predicted to occur more frequently within Texas, which concurrently faces requirements to achieve and maintain attainment with the National Ambient Air Quality Standards for ozone and fine particulate matter, it is important to understand the effects of drought on regional air quality.

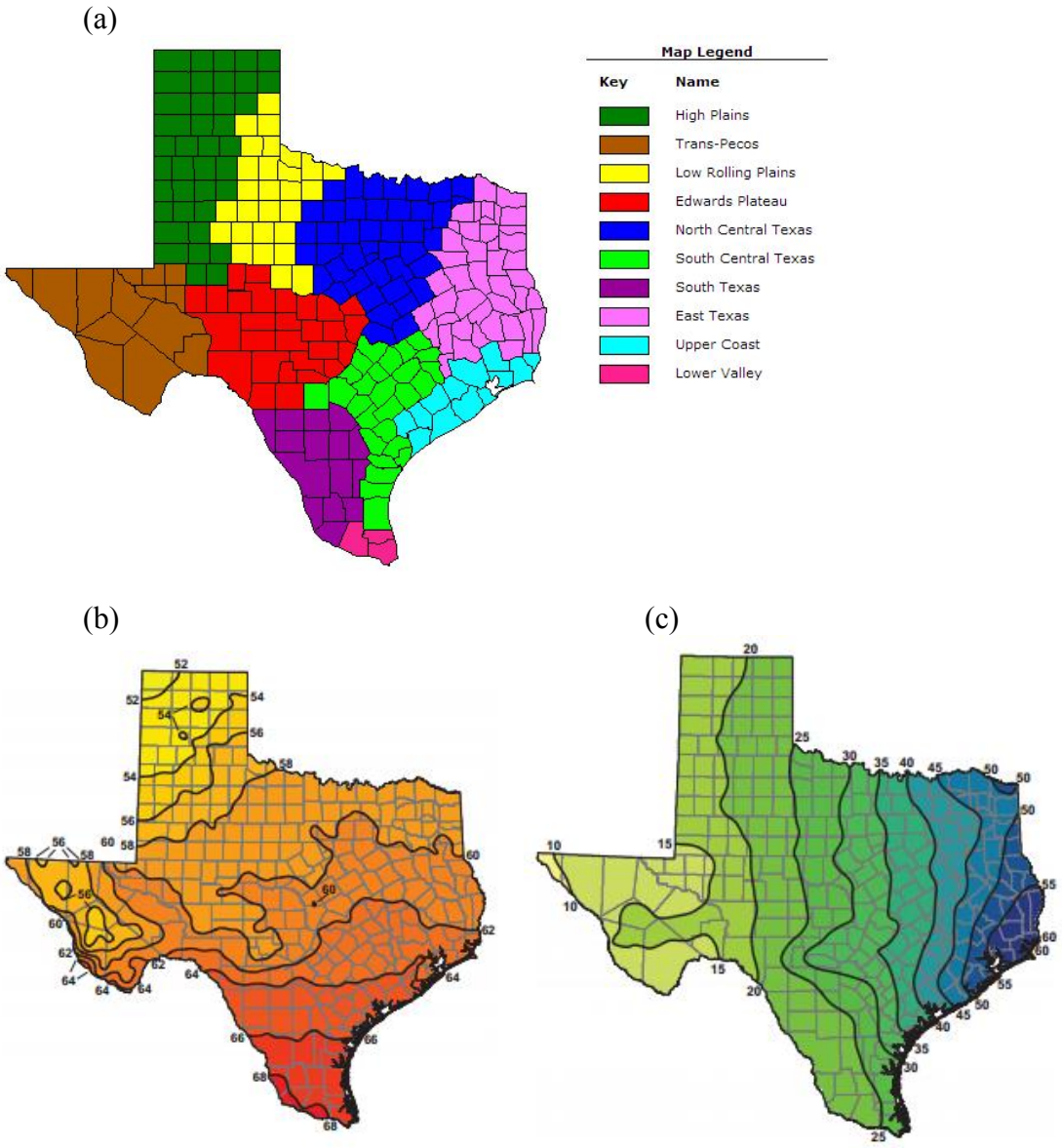

Figure 1-5: (a) Texas climate divisions (Source: United States Department of Agricultural-National Agricultural Statistics Service); (b) Average annual temperature for 1981 to 2010 in F and (c) Average annual precipitation for 1981 to 2010 in inches (Source: Texas Water Development Board).

1.2 RESEARCH OBJECTIVES

This work characterizes land cover for eastern Texas climate regions during 2006-2011, including years with severe to exceptional drought conditions as well as years with average to above average precipitation patterns. Variability in meteorological conditions, biogenic emissions, and dry deposition rates is explored with widely applied global and regional models that have been configured specifically for multi-year analyses of conditions in eastern Texas climate regions. The Comprehensive Air Quality Model with Extensions (CAMx), which has been used to support air quality planning and management efforts in Texas, is used to evaluate ground-level ozone concentrations during drought and wet periods. This work has five specific objectives:

1. To quantify and contrast annual and seasonal variations in leaf area index (LAI) derived from satellite observations and the influence of LAI on estimates of emissions of biogenic hydrocarbons using the Model of Emissions of Gases and Aerosols from Nature (MEGAN) (**Chapter 3**).
2. To evaluate the relative effects of other meteorological and environmental factors, including temperature, soil moisture, and photosynthetically active radiation (PAR), on biogenic emissions estimates using MEGAN (**Chapter 4**).
3. To characterize the influence of a high-resolution (30 m) regional land cover product and a widely used global land cover product on biogenic emissions estimates and ozone predictions in eastern Texas (**Chapter 5**).
4. To simulate drought effects on meteorological fields using the Weather Research and Forecasting (WRF) model and examine seasonal and interannual changes in estimated ozone dry deposition velocities and component resistances over eastern Texas using an offline version of CAMx dry deposition algorithm (**Chapter 6**).

5. To quantify the relative contributions of different physical and chemical processes on predicted ground-level ozone concentrations using the process analysis diagnostic tool in CAMx during representative drought and wet periods (**Chapter 7**).

1.3 OVERVIEW OF CHAPTERS

Chapter 2 provides a general literature review that describes biogenic emissions, dry deposition, and drought effects on both processes. Chapter 3 presents the investigation of interannual variability of LAI and isoprene and monoterpene emissions estimates over eastern Texas during 2006-2011. Chapter 4 quantifies seasonal and interannual contributions of individual environmental factors on isoprene and monoterpene emissions estimates. Chapter 5 examines the effects of two different land cover products on estimated biogenic emissions by MEGAN and ground-level ozone concentrations predicted by CAMx. Chapter 6 investigates the impacts of drought on ozone dry deposition velocities and component resistances/conductances during representative drought and wet periods. Chapter 7 explores the relative contributions of individual chemical and physical processes on predicted ground-level ozone concentrations under drought and wet conditions. Chapter 8 summarizes the major findings of the research and proposes recommendations for future studies.

1.4 REFERENCES

Allen, C. D., & Breshears, D. D. (2007). Climate-induced forest dieback as an emergent global phenomenon. *Eos, Transactions American Geophysical Union, 88*(47), 504.

Allen, C. D., Macalady, A. K., Chenchouni, H., Bachelet, D., McDowell, N., Vennetier, M., … Cobb, N. (2010). A global overview of drought and heat-induced tree mortality reveals emerging climate change risks for forests. *Forest Ecology and Management, 259*(4), 660–684. doi:10.1016/j.foreco.2009.09.001

American Meteorological Society (AMS). (1997). Meteorological drought—policy statement. *Bullutin of the American Meteorological Society, 78*, 847–849. Retrieved from http://www.ametsoc.org/policy/drought2.html

Anderson, M. C., & Kustas, W. P. (2008). Mapping evapotranspiration and drought at local to continental scales with a thermal-based surface energy balance model. In *Meeting Abstract*.

Atkinson, R. (2000). Atmospheric chemistry of VOCs and NO_x. *Atmospheric Environment, 34*(12), 2063-2101.

Bayarjargal, Y., Karnieli, A, Bayasgalan, M., Khudulmur, S., Gandush, C., & Tucker, C. (2006). A comparative study of NOAA–AVHRR derived drought indices using change vector analysis. *Remote Sensing of Environment, 105*(1), 9–22. doi:10.1016/j.rse.2006.06.003

Bond, N. R., Lake, P. S., & Arthington, A. H. (2008). The impacts of drought on freshwater ecosystems: an Australian perspective. *Hydrobiologia, 600*(1), 3–16. doi:10.1007/s10750-008-9326-z

Breshears, D. D., Cobb, N. S., Rich, P. M., Price, K. P., Allen, C. D., Balice, R. G., … Meyer, C. W. (2005). Regional vegetation die-off in response to global-change-type drought. *Proceedings of the National Academy of Sciences of the United States of America*, 102, 15144–15148. doi:10.1073/pnas.0505734102

Byun, H. R., & Wilhite, D. A. (1999). Objective quantification of drought severity and duration. *Journal of Climate, 12*(9), 2747-2756.

Claeys, M., Graham, B., Vas, G., Wang, W., Vermeylen, R., Pashynska, V., … Maenhaut, W. (2004). Formation of secondary organic aerosols through photooxidation of isoprene. *Science, 303*(5661), 1173-1176.

Dai, A. (2011). Drought under global warming: a review. *Wiley Interdisciplinary Reviews: Climate Change*, *2*(1), 45–65. doi:10.1002/wcc.81

Dockery, D. W., Pope, C. A., Xu, X., Spengler, J. D., Ware, J. H., Fay, M. E., … Speizer, F. E. (1993). An association between air pollution and mortality in six US cities. *New England Journal of Medicine*, *329*(24), 1753-1759.

Fang, X., & Pomeroy, J. W. (2008). Drought impacts on Canadian prairie wetland snow hydrology. *Hydrological Processes*, *22*(15), 2858–2873.

Fannin, B. (2012). Updated 2011 Texas agricultural drought losses total $7.62 billion. Retrieved July 5, 2015, from http://today.agrilife.org/2012/03/21/updated-2011-texas-agricultural-drought-losses-total-7-62-billion/

Fensham, R. J., Fairfax, R. J., & Ward, D. P. (2008). Drought-induced tree death in savanna. *Global Change Biology*, *15*(2), 380–387.

Frédéric, A., & Volkmar, W. (2006). Impact of summer drought on forest biodiversity : what do we know ? *Annals of Forest Science*, *63*(6), 645–652.

Hayes, M., Svoboda, M., & Wilhite, D. A. (2000). Monitoring Drought Using the Standardized Precipitation Index. *Drought: A Global Assessment* (pp. 168–180). London/New York: Taylor and Francis Group.

Heim Jr, R. R. (2002). A review of twentieth-century drought indices used in the United States. *Bulletin of the American Meteorological Society*, *83*(8), 1149-1165.

Hewitt, K. (1997). *Regions of risk: A geographical introduction to disasters* (pp. 189-213). Harlow: Longman.

Jiang, X., Wiedinmyer, C., Chen, F., Yang, Z. L., & Lo, J. C. F. (2008). Predicted impacts of climate and land use change on surface ozone in the Houston, Texas, area. *Journal of Geophysical Research: Atmospheres (1984–2012)*, *113*(D20).

Keetch, J. J. & Byram, G. M. (1968). A drought index for forest fire control. US Department of Agriculture, Forest Service, Southeastern Forest Experiment Station.

Lippmann, M. (1989). Health effects of ozone a critical review. *Japca*, *39*(5), 672-695.

Liverman, D. M. (1990). Drought impacts in Mexico: climate, agriculture, technology, and land tenure in Sonora and Puebla. *Annals of the Association of American Geographers*, *80*(1), 49-72.

Logan, J. A., Regniere, J., & Powell, J. A. (2003). Assessing the impacts of global warming on forest pest dynamics. *Frontiers in Ecology and the Environment*, *1*(3), 130–137.

Logar, I., & van den Bergh, J. C. J. M. (2011). *Methods for assessment of the costs of droughts* (pp. 1–58). CONHAZ Report. Retrieved from http://conhaz.org/CONHAZ%20REPORT%20WP05_1_FINAL.pdf

Marsh, T. J. (2004). The UK drought of 2003: a hydrological review. *Weather*, *59*(8), 224–230. doi:10.1256/wea.79.04

McDonald-Buller, E., Wiedinmyer, C., Kimura, Y., & Allen, D. (2001). Effects of land use data on dry deposition in a regional photochemical model for eastern Texas. *Journal of the Air & Waste Management Association*, *51*(8), 1211–1218. doi:10.1080/10473289.2001.10464340

McKee, T. B., Doesken, N. J., & Kleist, J. (1993). The relationship of drought frequency and duration to time scale. *Proceedings of 8th Conference on Applied Climatology, American Meteorological Society* (pp. 179–184). Boston.

Melillo, J.M., Richmond, T.C., & Yohe, G.W. (2014). Climate Change Impacts in the United States. *Third National Climate Assessment*. US Global Change Research Program.

Mishra, A. K., & Singh, V. P. (2010). A review of drought concepts. *Journal of Hydrology*, *391*(1-2), 202–216. doi:10.1016/j.jhydrol.2010.07.012

Niemeyer, S. (2008). New drought indices. In *Proceedings of the 1st international conference "Drought management: Scientific and technological innovations", Zaragoza, Spain* (pp. 12-14).

Nowak, D. J., Crane, D. E., & Stevens, J. C. (2006). Air pollution removal by urban trees and shrubs in the United States. *Urban Forestry & Urban Greening*,*4*(3), 115-123.

Ntale, H. K., & Gan, T. Y. (2003). Drought indices and their application to East Africa. *International Journal of Climatology*, *23*(11), 1335–1357. doi:10.1002/joc.931

Obasi, G. O. P. (1994). WMO's role in the international decade for natural disaster reduction. *Bulletin of the American Meteorological Society*, 75(9), 1655-1661.

Palmer, W. C. (1965). *Meteorological Drought*. Washington, DC: US Department of Commerce, Weather Bureau.

Prosperop, J. M., & Nees, R. T. (1986). Impact of the North African drought and El Nino on mineral dust in the Barbados trade winds. *Nature, 320,* 735 – 738.

Purves, D. W., Caspersen, J. P., Moorcroft, P. R., Hurtt, G. C., & Pacala, S. W. (2004). Human-induced changes in US biogenic volatile organic compound emissions: evidence from long-term forest inventory data. *Global Change Biology*, *10*(10), 1737-1755.

Shaw, J. D., Steed, B. E., & Deblander, L. T. (2005). Forest Inventory and Analysis (FIA) annual inventory answers the question: What is happening to pinyon-juniper woodlands? *Journal of Forestry*, *103*(6), 280–285.

Sheffield, J., & Wood, E. F. (2012a). Major drought events of the 20th century. *Drought: Past Problems and Future Scenarios* (pp. 123–164). Routledge.

Sheffield, J., & Wood, E. F. (2012b). What is drought? *Drought: Past Problems and Future Scenarios* (p. 12). Routledge.

Sivakumar, M. V. K., Stone, R., Sentelhas, P. C., Svoboda, M., Omondi, P., Sarkar, J., & Wardlow, B. (2010). Agricultural drought indices: summary and recommendations. *Agricultural Drought Indices Proceedings of an Expert Meeting* (pp. 172–197). Murcia, Spain.

Svoboda, M., LeComte, D., Hayes, M., Heim, R., Gleason, K., Angel, J., & Stephens, S. (2002). The drought monitor. *Bulletin of the American Meteorological Society*, *83*, 1181–1190.

Texas A&M Forest Service (2012). Texas A&M Forest Service Survey Shows 301 Million Trees Killed by Drought, Retrieved February 19, 2014 from http://texasforestservice.tamu.edu/main/popup.aspx?id=16509

Texas A&M Forest Service (2013). 2011 Texas Wildfires Common Denominators of Home Destruction, Retrieved July 5, 2015, from http://texasforestservice.tamu.edu/uploadedFiles/TFSMain/Preparing_for_Wildfires/Prepare_Your_Home_for_Wildfires/Contact_Us/2011%20Texas%20Wildfires.pdf

Tsakiris, G., Loukas, A., Pangalou, D., Vangelis, H., Tigkas, D., Rossi, G., & Cancelliere, A. (2002). Drought characterization. *Options Méditerranéennes, Ser. B*(58), 85–102.

Van Nieuwstadt, M. G. L., & Sheil, D. (2004). Drought, fire and tree survival in a Borneo rain forest, East Kalimantan, Indonesia. *Journal of Ecology*, *93*(1), 191–201. doi:10.1111/j.1365-2745.2005.00954.x

Van Vliet, M. T. H., & Zwolsman, J. J. G. (2008). Impact of summer droughts on the water quality of the Meuse river. *Journal of Hydrology*, *353*(1), 1–17. doi:10.1016/j.jhydrol.2008.01.001

Voelker, S. L., Muzika, R., & Guyette, R. P. (2008). Individual tree and stand level influences on the growth, vigor, and decline of Red Oaks in the Ozarks. *Forest Science*, *54*(1), 8–20.

Webb, P., & Reardon, T. (1992). Drought impact and household response in East and West Africa. *Quarterly Journal of International Agriculture*, *31*, 230–246.

Wilhite, D.A. (2000). Drought as a Natural Harzard: Concepts and Definitions. In D.A. Wilhite (Ed.), *Drought: A Global Assessment* (pp. 3–18). London/New York: Routledge.

Wilhite, D. A., & Knutson, C. L. (2008). Drought management planning: conditions for success. *Options Mediterraneennes Series A*, *80*, 141-148.

Wilhite, D.A., Svoboda, M. D., & Hayes, M. J. (2007). Understanding the complex impacts of drought: A key to enhancing drought mitigation and preparedness. *Water Resources Management*, *21*(5), 763–774. doi:10.1007/s11269-006-9076-5

Wilhite, D.A., & Vanyarkho, O. (2000). Drought: Pervasive impacts of a creeping phenomenon. *Drought: A Global Assessment* (ed., pp. 245–255). London/New York.

Zargar, A., Sadiq, R., Naser, B., & Khan, F. I. (2011). A review of drought indices. *Environmental Reviews*, *19*, 333–349. doi:10.1139/A11-013

Zhang, Q. (2003). Drought and its impacts. *China Climate Impact Assessment (2002)*, edited by H. Chen, pp. 12–18. China Meteorol Press. Beijing

Chapter 2: Drought Effects on Vegetation – Biogenic Emissions and Dry Deposition

2.1 BIOGENIC EMISSIONS

Although uncertainties exist, it has been estimated that approximately 1,150 Tg C yr^{-1} of volatile organic compounds (VOCs) are emitted into the atmosphere by vegetation (Guenther et al., 1995), contributing around 90% of global non-methane hydrocarbons emissions each year (Ashworth et al., 2013). Among hundreds of biogenic volatile organic compounds (BVOCs) that have been identified, isoprene (2-mehtyl-1,3-butadiene, C_5H_8) represents more than half of the total emissions, and is quantitatively the most important (Guenther et al., 2006). Other significant biogenic emissions include monoterpenes (a class of terpenes made of two isoprene units, Guenther et al., 1995), methanol (Jacob et al., 2005) and acetone (Jacob et al., 2002). Previous studies have focused on quantification of global and regional isoprene and monoterpene emissions, either by observations (e.g. Pressley et al., 2004; Kuhn et al., 2007; etc.) or model predictions (e.g. Palmer et al., 2003, 2006; Guenther et al., 2006, 2012; Sakulyanontvittaya et al., 2008; etc.); however, large uncertainties remain in estimates of these compounds for many regions and for most other BVOCs (Guenther et al., 2012). Figure 2-1 and Figure 2-2 show predicted isoprene and monoterpene emissions in eastern Texas from March to October averaged over 2006-2011. Emissions of isoprene and monoterpenes show a strong seasonal pattern with the highest emissions during the summer. Spatially, emissions correspond well to the distributions of live oak (isoprene-emitter) in the Edwards Plateau and pine forests (monoterpene-emitter) in East Texas (Texas A&M Forest Service, 2014). Biogenic emissions contribute approximately 30% of all VOCs emitted in urban areas in the eastern half of Texas; for example, biogenic emissions during 2008 accounted for 29% and 40% of all VOCs emitted in the

Dallas/Fort Worth and Houston/Galveston/Brazoria ozone nonattainment areas, respectively (fractions based on 2008 National Emission Inventory, EPA, 2013).

2.1.1 Roles of biogenic emissions in atmospheric chemistry and climate

Biogenic VOCs play a crucial role in atmospheric chemistry and climate at regional and global scales (Fehsenfeld et al., 1992; Chameides et al., 1988; Tsigaridis and Kanakidou, 2003; Sanderson et al., 2003; Pacifico et al., 2009). The impacts of BVOC emissions on ozone formation have been investigated using various atmospheric modeling systems (e.g. Situ et al., 2013; Curci et al., 2009; Thunis and Cuvelier, 2000; Scholes and Andreae, 2000, Wu et al., 2008) and through field measurement campaigns (e.g. Li et al., 2007; Lee et al., 2006). Ground-level ozone (O_3) is formed in the presence of sunlight by photochemical reactions involving oxides of nitrogen (NO_x =NO+NO_2) and VOCs (Atkinson, 2000). Owing to their high reactivity, isoprene and monoterpenes and their oxidation products are important ozone precursors when NO_x is abundant (Atkinson and Arey, 2003). In addition, the oxidation of BVOCs generates carbon monoxide (Fehsenfeld et al., 1992; Bergamaschi et al., 2000), which has a long atmospheric lifetime and plays a major role in the control of hydroxyl radical concentrations in the atmosphere (Fehsenfeld et al., 1992; Lerdau et al., 1997). Organic nitrates such as peroxyacetylnitrates (PANs) and peroxymetharcrylic nitric anhydrides (MPANs) are formed from reactions between BVOC oxidation products and NO_x (Fehsenfeld et al., 1992). The relatively longer atmospheric lifetimes of PANs and MPANs compared to NO_x enable them to act as reactive nitrogen carriers that can be transported over large distances and once thermally decomposed in warmer air, contribute to ozone formation in remote areas (Poisson et al., 2000).

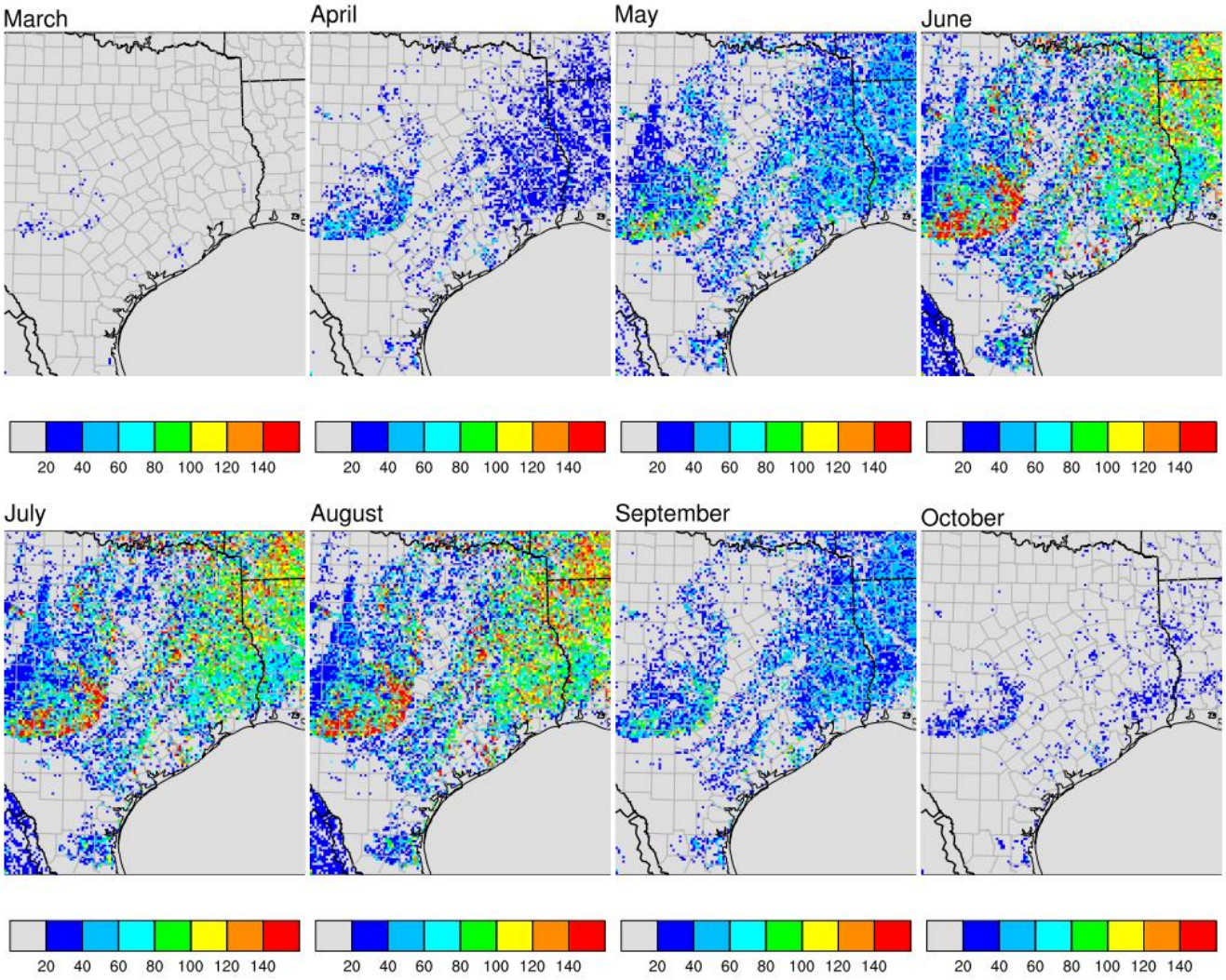

Figure 2-1: Isoprene emissions (kg/day/km^2) from March through October in eastern Texas averaged over 2006-2011.

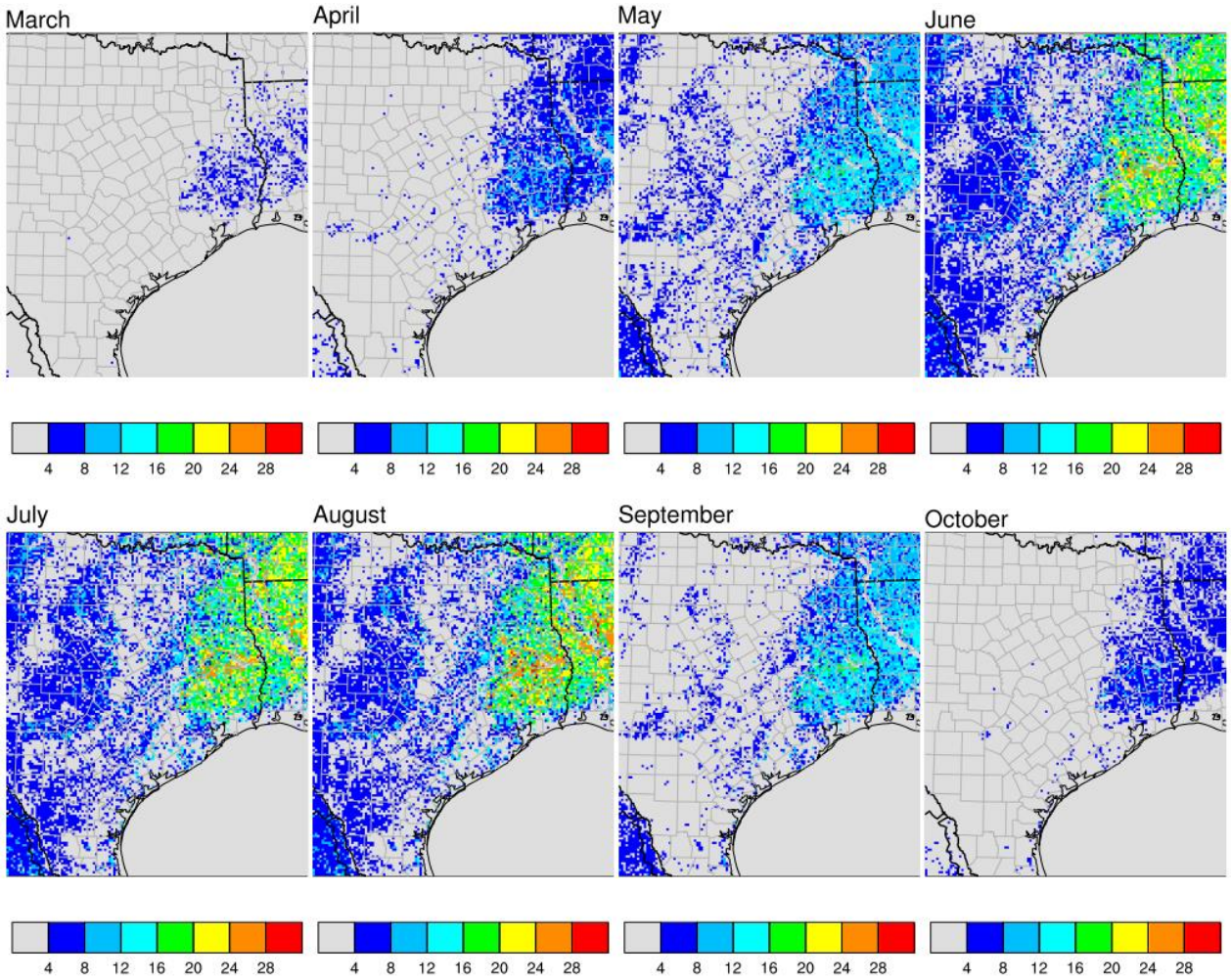

Figure 2-2: Monoterpene emissions (kg/day/km^2) from March through October in eastern Texas averaged over 2006-2011.

Formation of secondary organic aerosols (SOA) is a second relevant process for atmospheric chemistry and climate in which BVOCs play a key role. Aerosols are linked to adverse health effects, impaired visibility (Turpin and Huntzicker, 1995), and climate change. Aerosols can directly influence climate by scattering and absorbing solar radiation (Andreae and Crutzen, 1997) or indirectly by serving as cloud condensation nuclei, changing cloud albedo and leading to net cooling (Novako and Penner, 1993). Monoterpenes, and more recently isoprene, have been shown to be important SOA precursors (Hoffmann et al., 1997; Carlton et al., 2009; Claeys et al., 2004). Although the SOA yield from isoprene is relatively low compared with monoterpenes, the overall contribution could be significant owing to the large source strength.

Methane is the third most important greenhouse gas after water vapor and CO_2; it requires attack by hydroxyl radical (OH) as the first oxidation step. Since isoprene and monoterpenes more readily react with OH, BVOC emissions can serve to reduce OH availability and increase the atmospheric lifetime of methane, thus indirectly influencing the Earth's radiation balance (Wuebbles et al., 1989). Both the greenhouse warming caused by increased methane concentrations and the potential cooling effects by SOA may in turn modulate the temperature-dependent BVOC emissions from plants thereby exhibiting positive/negative feedbacks between BVOC emissions, atmospheric chemistry, and climate (Pacifico et al., 2009).

2.1.2 Drought effects on biogenic emissions

Numerous studies have been conducted to characterize the effects of drought on biogenic emissions, particularly isoprene and monoterpene emissions, both at leaf- (Fang et al., 1996; Pegoraro et al., 2004b, 2007; Funk et al., 2005; Tani et al., 2011; Lavoir et al., 2009, etc.) and ecosystem- levels (Pegoraro et al., 2005, 2006, 2007; Potosnak et al., 2014; Pressley et al., 2006; Seco et al., 2015; Nogués et al., 2015). Leaf-level

experiments have mostly been performed on a single leaf/branch of potted seedlings or saplings under simulated drought conditions, either by manipulation of water vapor deficit (e.g. Pegoraro et al., 2004a), withholding watering (e.g. Brilli et al., 2007), or intercepting precipitation (e.g. Lavoir et al., 2009). Previous studies have suggested that leaf-level isoprene emissions rates are less sensitive to drought initially and recover more rapidly than photosynthetic rates and stomatal conductance (e.g. Rodríguez-Calcerrada et al., 2013; Centritto et al., 2011; Brilli et al., 2007; Funk et al., 2005). However, the responses of leaf-level isoprene and monoterpene emissions rates to mild water stress have been inconsistent (e.g. Pegoraro et al., 2007; Brilli et al., 2007; Staudt et al., 2008). For example, Tingey et al. (1981) found that isoprene emissions from live oak trees (*Quercus virginiana* Mill.) were not inhibited during short-term drought (four days) while slightly reduced isoprene emission rates from kudzu (*Pueraria lobata* (Willd) Ohwi.) were observed by Sharkey and Loreto (1993). On the other hand, stimulation of isoprene emissions by drought was observed in a study of a resurrection plant (*Xerphyta humilis*) before a relative water content of 80% was reached (Beckett et al., 2012). Based upon a conceptual model of leaf-level isoprene response to drought stress (Niinemets, 2010), Potosnak et al. (2014) proposed that emissions are initially stimulated by increased leaf temperatures due to reduction in stomatal conductance; continued drought stress suppresses emissions by reductions in substrate availability and/or isoprene synthase activity. Ryan et al. (2014) noted a lack of consensus regarding the effects of drought on reported isoprene emissions and the potential protection afforded to plants under drought stress by isoprene, indicating a need for further study. Leaf-level monoterpene emissions were also found to increase (e.g. Staudt et al., 2008) or remain unchanged (e.g. Ormeno et al., 2007; Nogués et al., 2015) in response to moderate water stress, depending on the species and protocol applied.

The sustained or even stimulated isoprene/monoterpene emissions during mild drought despite large reductions in photosynthesis may be associated with (1) higher leaf temperature due to lower latent heat dissipation caused by stomatal closure (Pegoraro et al., 2004b); (2) lower intercellular CO_2 concentrations (C_i), again a consequence of drought-induced stomatal closure (Pegoraro et al., 2004a, 2005); or (3) utilization of alternative carbon sources (e.g. starch and soluble sugars) for isoprene synthesis (Brilli et al., 2007; Rodríguez-Calcerrada et al., 2013). Severe droughts are generally found to cause a significant decrease in isoprene and monoterpene emissions (e.g. Brilli et al. 2007; Lavoir et al., 2009; Pegoraro et al., 2007), attributed to inhibition of specific enzymes in the biosynthesis pathway (Fortunati et al., 2008) or depletion of alternative carbon pools (Brüggemann and Schnitzler, 2002).

Compared to leaf-level experiments, studies of the impact of drought on ecosystem-level isoprene and monoterpene emissions are relatively rare. Enhancement of ecosystem-scale isoprene emissions caused by simulated or natural drought has been observed (e.g. Pressley et al., 2006; Pegoraro et al., 2005, 2006, 2007; Potosnak et al., 2014; Seco et al., 2015). For example, Pegoraro et al. (2007) examined both leaf and ecosystem isoprene emissions from cottonwood trees (*Populus deltoides*) under simulated drought conditions; increases in ecosystem-level isoprene emission rates were measured while leaf-level rates decreased slightly or remained constant. To explain this uncoupled leaf- and ecosystem-level response, the author proposed several hypotheses, including increases in canopy surface temperature during drought, increased light penetration into the canopy due to changes in leaf angle, reduced isoprene sink strength of the soil and decreases in mean intercellular CO_2 concentration of leaves (Pegoraro et al., 2007). Seco et al. (2015) measured the isoprene and monoterpenes fluxes from a temperate forest ecosystem in the Ozark region of the central U.S. spanning over the start

and end of an extreme 2012 drought event. They observed increase in isoprenoid emissions during early drought stage and later decrease when the drought intensified. Potosnak et al. (2014) proposed a two-phase ecosystem-level isoprene response to drought, consisting of an initial (short-term) emissions enhancement due to increases in leaf temperature caused by drought-induced stomatal closure followed by a decline (long-term) in isoprene emissions due to reductions in substrate availability and/or isoprene synthase transcription during the more severe phase of drought.

Because the intensity and severity of droughts may increase under a changing future climate (Dai, 2013; Melillo et al., 2014), it will be crucial to understand the mechanisms underlying drought-induced tree mortality in order to model water and carbon fluxes and to predict the impacts on ecosystems and climate (Adams et al., 2010; Allen et al., 2010; Anderegg et al., 2012). Despite recent studies (McDowell et al., 2008; Breshears et al., 2009; Sala et al., 2010; McDowell, 2011; Anderegg et al., 2012), the mechanisms through which drought drives tree mortality and forest die-off are still subject to extensive debate (Sala et al., 2010; Zeppel et al., 2013). Previous studies have suggested that tree mortality may be associated with complex interactions involving carbon starvation, hydraulic failure, and biotic attack (Allen et al., 2010; McDowell, 2011; Mitchell et al., 2013; Sevanto et al., 2014). In addition, increases in the frequency and severity of wildfires under drought conditions threaten forest survival (McDowell et al., 2008).

2.1.3 The Model of Emissions of Gases and Aerosols from Nature (MEGAN)

Regional air quality models, such as CAMx and the Community Multi-scale Air Quality (CMAQ) modeling system, require spatially and temporally resolved estimates of biogenic emissions. Commonly used models have included the Biogenic Emission Inventory System (BEIS, third generation; Schwede et al., 2005), Global Biosphere

Emissions and Interactions System (GloBEIS, third generation, Yarwood et al., 2002), and the Model of Emissions of Gases and Aerosols from Nature (MEGAN version 2.1; Guenther et al., 2012). Although regulatory air quality model applications in Texas during the past decade have relied on estimates of biogenic emissions from GloBEIS, MEGAN is currently being used for modeling and regulatory purposes by the Texas Commission on Environmental Quality (TCEQ). Therefore, MEGAN was selected for this work.

MEGAN is a modeling framework for estimating the net fluxes of gases and aerosols between terrestrial ecosystems and the atmosphere (Guenther et al., 2006), which was developed by the Biosphere-Atmosphere Interaction (BAI) group of the Atmospheric Chemistry Division (ACD) at the National Center for Atmospheric Research (NCAR) and is currently supported by the Laboratory for Atmospheric Research at Washington State University (http://lar.wsu.edu/megan/guides.html). As a global model, MEGAN can be run alone, offline, or as an on-line component with land surface and atmospheric chemistry models (Guenther et al., 2012; Lawrence et al., 2011). The offline version of MEGAN2.1 can be obtained from http://lar.wsu.edu/megan/guides.html and was used throughout this work.

MEGAN2.1 estimates emissions rates (F_i) of chemical species i from terrestrial landscapes in unit of flux (μg m^{-2} ground area h^{-1}) as:

$$F_i = \gamma_i \sum \varepsilon_{i,j} \chi_j \qquad \text{Eq. 2-1}$$

where $\varepsilon_{i,j}$ (μg m^{-2} ground area h^{-1}) is the basal emission factor representing the net primary emission rate for vegetation type j with fractional coverage χ_j; it represents the emission rate under standard environmental conditions defined in Guenther et al. (2006; 2012); γ_i is the overall emission activity factor that accounts for variations in environmental conditions including temperature, light, soil moisture, LAI and etc.

Descriptions of individual activity factors are presented in Table A-1. MEGAN2.1 adopted the 16 Plant Functional Types (PFTs) scheme from the Community Land Model (CLM4, Lawrence et al. 2011; Table A-2). Basal emission factors are specified for each compound class based on each PFT (ref. Table 2 in Guenther et al., 2012). In order to account for the emission variability within each PFT, the base MEGAN2.1 land cover includes more than 2000 ecoregions, allowing the PFT-based emission factors to differ by region (Guenther et al., 2012). To drive MEGAN simulations, input data including emission factor maps, PFT distributions, observational or modeled meteorological parameters (e.g. solar radiation, air temperature, wind speed, and soil moisture) and LAI distributions are needed. Table A-3 describes each of the driving parameters and examples of datasets used in this work.

MEGAN simulates the drought response of isoprene emissions through a soil moisture activity factor (γ_{SM}) based on the observations of Pegoraro et al. (2004b). The soil moisture activity factor scales between 0 and 1 depending on the soil moisture and wilting point (the soil moisture content below which plants cannot extract water from soil), representing a negative influence on isoprene emissions under drought conditions (Figure 2-3). Potosnak et al. (2014) compared observed and MEGAN-simulated canopy-level isoprene emissions from an oak-dominated temperate forest during periods of natural drought and concluded that MEGAN was not able to capture the response of canopy-level isoprene emissions to drought stress. In addition, predicted isoprene emissions are sensitive to the specific soil moisture and wilting point datasets (Müller et al., 2008; Tawfik et al., 2012), which themselves are associated with large uncertainties.

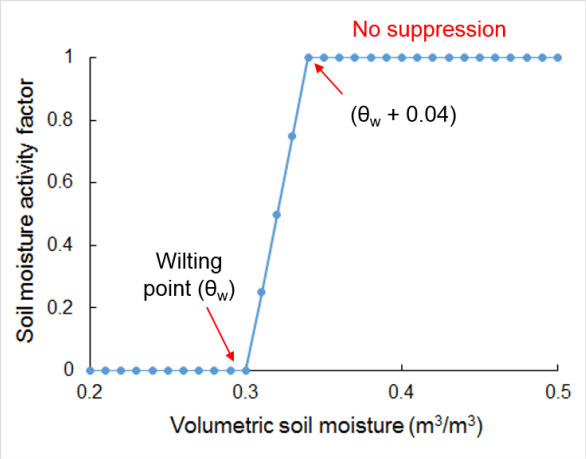

Figure 2-3: Illustration of soil moisture acitivty factor (γ_{SM}) as a function of soil moisture in MEGAN. A wilting point of 0.3 m^3/m^3 is used as an example.

2.2 DRY DEPOSITION

Dry deposition is broadly defined as the transport of gaseous and particulate species from the atmosphere by turbulent transfer to surfaces in the absence of precipitation (Seinfeld and Pandis, 2012). There exist strong connections between tropospheric ozone concentrations and ozone dry deposition (Emberson et al., 2013). Chemical destruction and dry deposition to Earth's surface represent two primary pathways of ozone removal from the troposphere, of which 20-25% is estimated to be attributable to the latter process globally (Lelieveld and Dentener, 2000; Wild, 2007). In Texas, dry deposition represents the most important physical removal mechanism for ozone during the warm spring through early fall seasons (McDonald-Buller et al., 2001). The majority of ozone deposition occurs to vegetation, which is through the stomatal pores of plants and non-stomatal sinks, e.g. deposition to soils, stems, leaf cuticles or any other external surfaces (e.g. Wesely et al., 1989). Stomatal ozone uptake is regarded as a major mechanism for ozone damage to plants (UNECE, 2004). When exposed to ozone, reactive oxygen species (ROS), such as hydrogen peroxide (H_2O_2), are formed via

chemical reactions (Kangasjärvi, et al., 2005) and are responsible for reduced productivity of crops (Morgan et al., 2006; Emberson et al., 2009) and forest (Wittig et al., 2009; Ashmore et al., 2005). Thus accurate estimates of ozone dry deposition are critical for both human health and ecosystem risk assessments (Pleijel et al., 2007; Mills et al., 2011; Emberson et al., 2013). Nevertheless, ozone dry deposition remains one of the major uncertainties in modeling ozone in the troposphere (Wild, 2007) and current model results are subject to substantial errors compared to observations (Pleim and Ran, 2011). Hardacre et al. (2015) compared ozone dry deposition across 15 global chemistry transport models and noted differences of up to a factor of two compared to measurements in Europe and North America.

The magnitude of ozone deposition is reflected in the combined removal through stomatal and non-stomatal pathways; their relative contributions depend on both the canopy type and the surface meteorological conditions (Lamaud et al., 2009; Rannik et al., 2012; Fares et al., 2012; Neirynck et al., 2012), which is responsible for the uncertainties in esimating dry deposition processes (Hardacre et al., 2015). Numerous studies have reported a wide range of stomatal vs. non-stomatal relative contributions for various surface types (e.g. Fares et al., 2010; Cieslik 2004; Gerosa et al., 2005; Hogg et al., 2007). Rannik et al. (2012) reported 26-44% of daytime ozone deposition through non-stomatal removal during the growing season over a boreal forest in Southern Finland. Measurements at a mixed hardwood forest in northern Michigan showed the non-stomatal sink representing 63% of total ozone removal (Hogg et al., 2007). Gerosa et al. (2005) reported only 31.5% of total ozone flux was attributable to stomatal pathways over a Mediterranean evergreen forest in central Italy. Stomata control the exchange of water and CO_2; stomatal aperture is influenced by various local environmental variables including light, temperature, air humidity, soil water status and atmospheric CO_2

concentrations (e.g. Jarvis 1976; Monteith, 1995; Ainsworth and Rogers, 2007). On the other hand, the detailed mechanism of the non-stomatal pathway is not known (Cape et al., 2009) and is influenced by surface wetness (Altimir et al., 2006). Many studies have emphasized the importance of gas-phase chemical reactions between ozone and nitric oxide (NO) or BVOCs in the canopy space on ozone deposition (e.g. Goldstein et al., 2004; Hogg et al., 2007; Neirynck et al., 2012).

2.2.1 Comparison of Wesely's and Zhang's dry deposition algorithm

Although various techniques have been developed to measure dry deposition fluxes (e.g. eddy covariance, gradient method, see summaries in Seinfeld and Pandis, 2012), model parameterization is required to provide dry deposition estimations for desired regions and time periods. In general, dry deposition is treated as a first-order removal mechanism and the dry deposition mass flux density is calculated as:

$$F_{c,i} = V_{d,i} \cdot C_{z,i} \qquad \text{Eq. 2-2}$$

where $F_{c,i}$ is the dry deposition flux of gas (ppb_v m/s), i, of interest, V_d is the dry deposition velocity (m/s), and $C_{z,i}$ is the concentration or mixing ratio of i at height z (ppb_v). In CAMx, two dry deposition algorithms are available to calculate V_d: the widely used Wesely's algorithm (Wesely 1989; Slinn and Slinn, 1980) and a more recently developed Zhang's algorithm (Zhang et al. 2001, 2003). For both algorithms, the dry deposition velocity is modeled using an approach analogous to Ohm's law in electrical circuits as shown in Eq. 2-3:

$$V_d = (R_a + R_b + R_c)^{-1} \qquad \text{Eq. 2-3}$$

where R_a, R_b, R_c represent the aerodynamic resistance, the quasi-laminar sublayer resistance and the canopy resistance. The Wesely scheme uses 11 land use categories while the Zhang scheme uses 26 land use categories. The two algorithms differ in the

calculation of the canopy resistance (R_c). Table A-4 contrasts the calculations of R_c between Wesely's and Zhang's algorithm (see Table A-5 for nomenclature).

Two major differences exist between the Wesely's and Zhang's algorithms. First, in Wesley's algorithm, stomatal resistance (R_{st}) responds only to changes in temperature and solar radiation while in Zhang's algorithm, two additional parameters (i.e. water vapor pressure deficit and leaf water potential) are incorporated. The inclusion of the response to water stress is especially relevant to this work as drought could affect dry deposition of ozone through changes in stomatal uptake. A second difference is that Wesely's algorithm specifies the various surface resistances by five seasons (spring, summer, fall, winter, winter with snow cover) while leaf area index (LAI) is used by Zhang's algorithm to scale pollutant uptake by vegetation. LAI is an important parameter in Zhang's algorithm as it appears explicitly in the calculation of in-canopy resistance (R_{ac}), cuticle resistance (R_{cut}), and implicitly in the aerodynamic (R_a) and quasi-laminar (R_b) resistances through roughness length z_0. The inclusion of LAI represents another potential impact of drought on ozone dry deposition through drought-induced LAI reductions, especially in central Texas as will be demonstrated in Chapter 3. Zhang's algorithm was shown to result lower ozone deposition fluxes compared to Wesely' algorithm, thus leading to higher predicted ozone concentrations (ENVIRON, 2014). Considering the advantage of utilizing LAI in its parameterization, Zhang's algorithm is used in this work.

2.2.2 Drought effects on ozone dry deposition

The impact of drought on ozone dry deposition is mainly associated with the reductions in the stomatal conductance as plants tend to reduce evaporation for water conservation. For example, stomatal conductance of adult beech trees (*Fagus sylvatica*) was lowered by drought during the summer of 2003 in Central Europe (Löw et al., 2006).

Panek and Goldstein (2001) observed ~40% less ozone deposition (ozone concentration times stomatal conductance) to ponderosa pine (*Pinus ponderosa* Dougl. *ex* Laws.) under typical Mediterranean-climate summer drought conditions. Drought and ozone episodes can often occur together as both are favored under similar meteorological conditions. Drought-induced stomatal closure has been proposed as a protective mechanism against ozone exposure. However, there are conflicting findings regarding the concurrent effects between drought and ozone (e.g. Biswas and Jiang, 2011; Bohler et al., 2013; Iyer et al., 2013; Alonso et al., 2014). For instance, *Medicago truncatula* cultivar Jemalong showed improved tolerance when subjected to combined ozone and drought stress (Iyer et al., 2012). Alonso et al. (2014), on the contrary, observed no drought related protection for *Q. ilex* from ozone effects. Bohler et al. (2015) listed many factors that have been shown to affect the interactive effects between ozone and drought stress, including species, order of occurrence, and season. While reductions in stomatal ozone uptake under drought conditions may be considered as a protective mechanism for vegetation from ozone damage, reduced dry deposition could lead to substantial increase in ground-level ozone concentrations (Pio et al., 2000; Solberg et al., 2008; Vieno et al., 2010), which has implications for human health (Emberson et al., 2013).

2.3 REFERENCES

Adams, H. D., Macalady, A. K., Breshears, D. D., Allen, C. D., Stephenson, N. L., Saleska, S. R., & Huxman, T. E. (2010). Climate-Induced Tree Mortality: Earth System Consequences. *Eos, Transactions American Geophysical Union*, *91*(17), 153-154.

Ainsworth, E. A., & Rogers, A. (2007). The response of photosynthesis and stomatal conductance to rising [CO_2]: mechanisms and environmental interactions. *Plant, Cell & Environment*, *30*(3), 258-270.

Allen, C. D., Macalady, A. K., Chenchouni, H., Bachelet, D., McDowell, N., Vennetier, M., . . . Cobb, N. (2010). A global overview of drought and heat-induced tree mortality reveals emerging climate change risks for forests. *Forest Ecology and Management*, *259*(4), 660–684. doi:10.1016/j.foreco.2009.09.001

Alonso, R., Elvira, S., González-Fernández, I., Calvete, H., García-Gómez, H., & Bermejo, V. (2014). Drought stress does not protect Quercus ilex L. from ozone effects: results from a comparative study of two subspecies differing in ozone sensitivity. *Plant Biology*, *16*(2), 375-384.

Altimir, N., Kolari, P., Tuovinen, J. P., Vesala, T., Bäck, J., Suni, T., & Hari, P. (2006). Foliage surface ozone deposition: a role for surface moisture? *Biogeosciences Discussions*, *2*(6), 1739-1793.

Anderegg, W. R., Berry, J. A., Smith, D. D., Sperry, J. S., Anderegg, L. D., & Field, C. B. (2012). The roles of hydraulic and carbon stress in a widespread climate-induced forest die-off. *Proceedings of the National Academy of Sciences*, *109*(1), 233-237.

Andreae, M. O., & Crutzen, P. J. (1997). Atmospheric aerosols: Biogeochemical sources and role in atmospheric chemistry. *Science*, *276*(5315), 1052-1058.

Ashmore, M. R. (2005). Assessing the future global impacts of ozone on vegetation. *Plant, Cell & Environment*, *28*(8), 949-964.

Ashworth, K., Boissard, C., Folberth, G., Lathière, J., & Schurgers, G. (2013). Global modelling of volatile organic compound emissions. In *Biology, controls and models of tree volatile organic compound emissions* (pp. 451-487). Springer Netherlands.

Atkinson, R. (2000). Atmospheric chemistry of VOCs and NO_x. *Atmospheric Environment*, *34*(12), 2063-2101.

Atkinson, R., & Arey, J. (2003). Gas-phase tropospheric chemistry of biogenic volatile organic compounds: a review. *Atmospheric Environment*, *37*, 197-219.

Beckett, M., Loreto, F., Velikova, V., Brunetti, C., Di Ferdinando, M., Tattini, M., ... & Farrant, J. M. (2012). Photosynthetic limitations and volatile and non-volatile isoprenoids in the poikilochlorophyllous resurrection plant Xerophyta humilis during dehydration and rehydration. *Plant, cell & environment*, *35*(12), 2061-2074.

Bergamaschi, P., Hein, R., Heimann, M., & Crutzen, P. J. (2000). Inverse modeling of the global CO cycle: 1. Inversion of CO mixing ratios. *Journal of Geophysical Research: Atmospheres (1984–2012)*, *105*(D2), 1909-1927.

Biswas, D. K., & Jiang, G. M. (2011). Differential drought-induced modulation of ozone tolerance in winter wheat species. *Journal of Experimental Botany*, doi: 10.1093/jxb/err104

Bohler, S., Cuypers, A., & Vangronsveld, J. (2015). *Combined Stresses in Plants.* (pp. 147–157). Springer International Publishing.

Bohler, S., Sergeant, K., Jolivet, Y., Hoffmann, L., Hausman, J. F., Dizengremel, P., & Renaut, J. (2013). A physiological and proteomic study of poplar leaves during ozone exposure combined with mild drought. *Proteomics*,*13*(10-11), 1737-1754.

Breshears, D. D., Myers, O. B., Meyer, C. W., Barnes, F. J., Zou, C. B., Allen, C. D., ... & Pockman, W. T. (2008). Tree die-off in response to global change-type drought: mortality insights from a decade of plant water potential measurements. *Frontiers in Ecology and the Environment*, *7*(4), 185-189.

Brilli, F., Barta, C., Fortunati, A., Lerdau, M., Loreto, F., & Centritto, M. (2007). Response of isoprene emission and carbon metabolism to drought in white poplar (*Populus alba*) saplings. *New Phytologist*, *175*(2), 244-254.

Brüggemann, N., & Schnitzler, J. P. (2002). Comparison of isoprene emission, intercellular isoprene concentration and photosynthetic performance in water-limited oak (*Quercus pubescens* Willd. and *Quercus robur* L.) saplings. *Plant Biology*, *4*(4), 456-463.

Cape, J. N., Hamilton, R., & Heal, M. R. (2009). Reactive uptake of ozone at simulated leaf surfaces: implications for 'non-stomatal'ozone flux. *Atmospheric Environment*, *43*(5), 1116-1123.

Carlton, A. G., Wiedinmyer, C., & Kroll, J. H. (2009). A review of Secondary Organic Aerosol (SOA) formation from isoprene. *Atmospheric Chemistry and Physics*, *9*(14), 4987-5005.

Centritto, M., Brilli, F., Fodale, R., & Loreto, F. (2011). Different sensitivity of isoprene emission, respiration and photosynthesis to high growth temperature coupled with drought stress in black poplar (*Populus nigra*) saplings. *Tree Physiology*, tpq112.

Chameides, W. L., Lindsay, R. W., Richardson, J., & Kiang, C. S. (1988). The role of biogenic hydrocarbons in urban photochemical smog: Atlanta as a case study. *Science*, *241*(4872), 1473-1475.

Cieslik, S. A. (2004). Ozone uptake by various surface types: a comparison between dose and exposure. *Atmospheric Environment*, *38*(15), 2409-2420.

Claeys, M., Graham, B., Vas, G., Wang, W., Vermeylen, R., Pashynska, V., ... & Maenhaut, W. (2004). Formation of secondary organic aerosols through photooxidation of isoprene. *Science*, *303*(5661), 1173-1176.

Curci, G., Beekmann, M., Vautard, R., Smiatek, G., Steinbrecher, R., Theloke, J., & Friedrich, R. (2009). Modelling study of the impact of isoprene and terpene biogenic emissions on European ozone levels. *Atmospheric Environment*, *43*(7), 1444-1455.

Dai, A. (2013). Increasing drought under global warming in observations and models. *Nature Climate Change*, *3*(1), 52-58.

Emberson, L. D., Büker, P., Ashmore, M. R., Mills, G., Jackson, L. S., Agrawal, M., ... & Wahid, A. (2009). A comparison of North American and Asian exposure–response data for ozone effects on crop yields. *Atmospheric Environment*, *43*(12), 1945-1953.

Emberson, L. D., Kitwiroon, N., Beevers, S., Büker, P., & Cinderby, S. (2013). Scorched Earth: how will changes in the strength of the vegetation sink to ozone deposition affect human health and ecosystems? *Atmospheric Chemistry and Physics*, *13*(14), 6741-6755.

ENVIRON. (2014). User's guide Comprehensive Air Quality Model with Extension (CAMx), version 6.10. Retrieved April 17, 2015, from http://www.camx.com/files/camxusersguide_v6-10.txt

EPA. (2013). 2008 National Emission Inventory, version 3 Technical Support Document Draft, Retrived July 8, 2015, from http://www.epa.gov/ttn/chief/net/2008neiv3/2008_neiv3_tsd_draft.pdf

Fang, C., Monson, R. K., & Cowling, E. B. (1996). Isoprene emission, photosynthesis, and growth in sweetgum (*Liquidambar styraciflua*) seedlings exposed to short-and long-term drying cycles. *Tree Physiology*, *16*(4), 441-446.

Fares, S., McKay, M., Holzinger, R., & Goldstein, A. H. (2010). Ozone fluxes in a Pinus ponderosa ecosystem are dominated by non-stomatal processes: evidence from long-term continuous measurements. *Agricultural and Forest Meteorology*, *150*(3), 420-431.

Fares, S., Weber, R., Park, J.-H., Gentner, D., Karlik, J., & Goldstein, A. H. (2012). Ozone deposition to an orange orchard: Partitioning between stomatal and non-stomatal sinks. *Environmental Pollution*, *169*, 258–266. doi:10.1016/j.envpol.2012.01.030

Fehsenfeld, F., Calvert, J., Fall, R., Goldan, P., Guenther, A. B., Hewitt, C. N., ... & Zimmerman, P. (1992). Emissions of volatile organic compounds from vegetation and the implications for atmospheric chemistry. *Global Biogeochemical Cycles*, *6*(4), 389-430.

Fortunati, A., Barta, C., Brilli, F., Centritto, M., Zimmer, I., Schnitzler, J. P., & Loreto, F. (2008). Isoprene emission is not temperature-dependent during and after severe drought-stress: a physiological and biochemical analysis. *The Plant Journal*, 55(4), 687-697.

Funk, J. L., Jones, C. G., Gray, D. W., Throop, H. L., Hyatt, L. A., & Lerdau, M. T. (2005). Variation in isoprene emission from *Quercus rubra*: sources, causes, and consequences for estimating fluxes. *Journal of Geophysical Research: Atmospheres (1984–2012)*, *110*(D4).

Gerosa, G., Vitale, M., Finco, A., Manes, F., Denti, A. B., & Cieslik, S. (2005). Ozone uptake by an evergreen Mediterranean forest (Quercus ilex) in Italy. Part I: Micrometeorological flux measurements and flux partitioning. *Atmospheric Environment*, *39*(18), 3255-3266.

Goldstein, A. H., McKay, M., Kurpius, M. R., Schade, G. W., Lee, A., Holzinger, R., & Rasmussen, R. A. (2004). Forest thinning experiment confirms ozone deposition to forest canopy is dominated by reaction with biogenic VOCs. *Geophysical research letters*, *31*(22).

Guenther, A., Hewitt, C. N., Erickson, D., Fall, R., Geron, C., Graedel, T., ... & Zimmerman, P. (1995). A global model of natural volatile organic compound emissions. *Journal of Geophysical Research: Atmospheres (1984–2012),100*(D5), 8873-8892.

Guenther, A. B., Jiang, X., Heald, C. L., Sakulyanontvittaya, T., Duhl, T., Emmons, L. K., & Wang, X. (2012). The Model of Emissions of Gases and Aerosols from Nature version 2.1 (MEGAN2. 1): an extended and updated framework for modeling biogenic emissions, *Geoscientific Model Development Discussions*, 5, 1503-1560.

Guenther, A., Karl, T., Harley, P., Wiedinmyer, C., Palmer, P. I., & Geron, C. (2006). Estimates of global terrestrial isoprene emissions using MEGAN (Model of Emissions of Gases and Aerosols from Nature). *Atmospheric Chemistry and Physics*, *6*(11), 3181-3210.

Hardacre, C., Wild, O., & Emberson, L. (2015). An evaluation of ozone dry deposition in global scale chemistry climate models. *Atmospheric Chemistry and Physics*, *15*(11), 6419-6436.

Hoffmann, T., Odum, J. R., Bowman, F., Collins, D., Klockow, D., Flagan, R. C., & Seinfeld, J. H. (1997). Formation of organic aerosols from the oxidation of biogenic hydrocarbons. *Journal of Atmospheric Chemistry*,*26*(2), 189-222.

Hogg, A., Uddling, J., Ellsworth, D., Carroll, M. A., Pressley, S., Lamb, B., & Vogel, C. (2007). Stomatal and non-stomatal fluxes of ozone to a northern mixed hardwood forest. *Tellus B*, *59*(3), 514–525.

Iyer, N. J., Tang, Y., & Mahalingam, R. (2013). Physiological, biochemical and molecular responses to a combination of drought and ozone in Medicago truncatula. *Plant, Cell & Environment*, *36*(3), 706-720.

Jacob, D. J., Field, B. D., Jin, E. M., Bey, I., Li, Q., Logan, J. A., ... & Singh, H. B. (2002). Atmospheric budget of acetone. *Journal of Geophysical Research: Atmospheres (1984–2012)*, *107*(D10), ACH-5.

Jacob, D. J., Field, B. D., Li, Q., Blake, D. R., De Gouw, J., Warneke, C., ... & Guenther, A. (2005). Global budget of methanol: Constraints from atmospheric observations. *Journal of Geophysical Research: Atmospheres (1984–2012)*,*110*(D8).

Jarvis, P. G. (1976). The interpretation of the variations in leaf water potential and stomatal conductance found in canopies in the field. *Philosophical Transactions of the Royal Society of London B: Biological Sciences*, *273*(927), 593-610.

Kangasjärvi, J., Jaspers, P., & Kollist, H. (2005). Signalling and cell death in ozone-exposed plants. *Plant, Cell & Environment*, *28*(8), 1021-1036.

Kuhn, U., Andreae, M. O., Ammann, C., Araújo, A. C., Brancaleoni, E., Ciccioli, P., ... & Kesselmeier, J. (2007). Isoprene and monoterpene fluxes from Central Amazonian rainforest inferred from tower-based and airborne measurements, and implications on the atmospheric chemistry and the local carbon budget. *Atmospheric Chemistry and Physics*, *7*(11), 2855-2879.

Lamaud, E., Loubet, B., Irvine, M., Stella, P., Personne, E., & Cellier, P. (2009). Partitioning of ozone deposition over a developed maize crop between stomatal and

non-stomatal uptakes, using eddy-covariance flux measurements and modelling. *Agricultural and Forest Meteorology*, *149*(9), 1385–1396. doi:10.1016/j.agrformet.2009.03.017

Lavoir, A. V., Staudt, M., Schnitzler, J. P., Landais, D., Massol, F., Rocheteau, A., ... & Rambal, S. (2009). Drought reduced monoterpene emissions from the evergreen Mediterranean oak Quercus ilex: results from a throughfall displacement experiment. *Biogeosciences*, *6*, p-1167.

Lawrence, D. M., Oleson, K. W., Flanner, M. G., Thornton, P. E., Swenson, S. C., Lawrence, P. J., ... & Slater, A. G. (2011). Parameterization improvements and functional and structural advances in version 4 of the Community Land Model. *Journal of Advances in Modeling Earth Systems*, *3*(1).

Lee, J. D., Lewis, A. C., Monks, P. S., Jacob, M., Hamilton, J. F., Hopkins, J. R., ... & Jenkin, M. E. (2006). Ozone photochemistry and elevated isoprene during the UK heatwave of August 2003. *Atmospheric Environment*, *40*(39), 7598-7613.

Lehning, A., Zimmer, I., Steinbrecher, R., Brüggemann, N., & Schnitzler, J. P. (1999). Isoprene synthase activity and its relation to isoprene emission in *Quercus robur* L. leaves. *Plant, Cell & Environment*, 22(5), 495-504.

Lelieveld, J., & Dentener, F. J. (2000). What controls tropospheric ozone ? *Journal of Geophysical Research: Atmospheres (1984–2012)*, *105*(1999), 3531–3551.

Lerdau, M., Guenther, A., & Monson, R. (1997). Plant production and emission of volatile organic compounds. *Bioscience*, 373-383.

Li, G., Zhang, R., Fan, J., & Tie, X. (2007). Impacts of biogenic emissions on photochemical ozone production in Houston, Texas. *Journal of Geophysical Research: Atmospheres (1984–2012)*, *112*(D10).

Löw, M., Herbinger, K., Nunn, A. J., Häberle, K. H., Leuchner, M., Heerdt, C., ... & Matyssek, R. (2006). Extraordinary drought of 2003 overrules ozone impact on adult beech trees (Fagus sylvatica). *Trees*, *20*(5), 539-548.

McDonald-Buller, E., Wiedinmyer, C., Kimura, Y., & Allen, D. (2001). Effects of land use data on dry deposition in a regional photochemical model for eastern Texas. *Journal of the Air & Waste Management Association*, *51*(8), 1211–1218. doi:10.1080/10473289.2001.10464340

McDowell, N. G. (2011). Mechanisms linking drought, hydraulics, carbon metabolism, and vegetation mortality. *Plant Physiology*, *155*(3), 1051–9. doi:10.1104/pp.110.170704

McDowell, N., Pockman, W. T., Allen, C. D., Breshears, D. D., Cobb, N., Kolb, T., ... & Yepez, E. A. (2008). Mechanisms of plant survival and mortality during drought: why do some plants survive while others succumb to drought? *New phytologist*, *178*(4), 719-739.

Melillo, J.M., Richmond, T.C., & Yohe, G.W. (2014). Climate Change Impacts in the United States. *Third National Climate Assessment*. US Global Change Research Program.

Mills, G., Hayes, F., Simpson, D., Emberson, L., Norris, D., Harmens, H., & Büker, P. (2011). Evidence of widespread effects of ozone on crops and (semi-) natural vegetation in Europe (1990–2006) in relation to AOT40-and flux-based risk maps. *Global Change Biology*, *17*(1), 592–613.

Mitchell, P. J., O'Grady, A. P., Tissue, D. T., White, D. A., Ottenschlaeger, M. L., & Pinkard, E. A. (2013). Drought response strategies define the relative contributions of hydraulic dysfunction and carbohydrate depletion during tree mortality. *New Phytologist*, *197*(3), 862-872.

Monteith, J. L. (1995). A reinterpretation of stomatal responses to humidity. *Plant, Cell & Environment*, *18*(4), 357-364.

Morgan, P. B., Mies, T. A., Bollero, G. A., Nelson, R. L., & Long, S. P. (2006). Season-long elevation of ozone concentration to projected 2050 levels under fully open-air conditions substantially decreases the growth and production of soybean. *New Phytologist*, *170*(2), 333-343.

Müller, J. F., Stavrakou, T., Wallens, S., Smedt, I. D., Roozendael, M. V., Potosnak, M. J., et al. (2008). Global isoprene emissions estimated using MEGAN, ECMWF analyses and a detailed canopy environment model. *Atmospheric Chemistry and Physics*, *8*(5), 1329-1341.

Neirynck, J., Gielen, B., Janssens, I. A, & Ceulemans, R. (2012). Insights into ozone deposition patterns from decade-long ozone flux measurements over a mixed temperate forest. *Journal of Environmental Monitoring*, *14*(6), 1684–1695. doi:10.1039/c2em10937a

Niinemets, U. (2010). Mild versus severe stress and BVOCs: thresholds, priming and consequences. *Trends in Plant Science*, *15*(3), 145–53. doi:10.1016/j.tplants.2009.11.008

Nogués, I., Medori, M., & Calfapietra, C. (2015). Limitations of monoterpene emissions and their antioxidant role in Cistus sp. under mild and severe treatments of drought and warming. *Environmental and Experimental Botany*.

Novakov, T., & Penner, J. E. (1993). Large contribution of organic aerosols to cloud-condensation-nuclei concentrations. *Nature*, *365*(6449), 823-826.

Ormeno, E., Mevy, J. P., Vila, B., Bousquet-Melou, A., Greff, S., Bonin, G., & Fernandez, C. (2007). Water deficit stress induces different monoterpene and sesquiterpene emission changes in Mediterranean species. Relationship between terpene emissions and plant water potential. *Chemosphere*, 67(2), 276-284.

Pacifico, F., Harrison, S. P., Jones, C. D., & Sitch, S. (2009). Isoprene emissions and climate. *Atmospheric Environment*, *43*(39), 6121-6135.

Palmer, P. I., Abbot, D. S., Fu, T. M., Jacob, D. J., Chance, K., Kurosu, T. P., ... & Sumner, A. L. (2006). Quantifying the seasonal and interannual variability of North American isoprene emissions using satellite observations of the formaldehyde column. *Journal of Geophysical Research: Atmospheres (1984–2012)*, *111*(D12).

Palmer, P. I., Jacob, D. J., Fiore, A. M., Martin, R. V., Chance, K., & Kurosu, T. P. (2003). Mapping isoprene emissions over North America using formaldehyde column observations from space. *Journal of Geophysical Research: Atmospheres (1984–2012)*, *108*(D6).

Panek, J. A., & Goldstein, A. H. (2001). Response of stomatal conductance to drought in ponderosa pine: implications for carbon and ozone uptake. *Tree physiology*, *21*(5), 337-344.

Pegoraro, E., Potosnak, M. J., Monson, R. K., Rey, A., Barron-Gafford, G., & Osmond, C. B. (2007). The effect of elevated CO_2, soil and atmospheric water deficit and seasonal phenology on leaf and ecosystem isoprene emission. *Functional Plant Biology*, 34(9), 774-784.

Pegoraro, E., Rey, A. N. A., Abrell, L., Haren, J., & Lin, G. (2006). Drought effect on isoprene production and consumption in Biosphere 2 tropical rainforest. *Global Change Biology*, 12(3), 456-469.

Pegoraro, E., Rey, A., Barron-Gafford, G., Monson, R., Malhi, Y., & Murthy, R. (2005). The interacting effects of elevated atmospheric CO_2 concentration, drought and leaf-to-air vapour pressure deficit on ecosystem isoprene fluxes. *Oecologia*, 146(1), 120-129.

Pegoraro, E., Rey, A., Bobich, E. G., Barron-Gafford, G., Grieve, K. A., Malhi, Y., & Murthy, R. (2004a). Effect of elevated CO_2 concentration and vapour pressure deficit on isoprene emission from leaves of Populus deltoides during drought. *Functional Plant Biology*, *31*(12), 1137-1147.

Pegoraro, E., Rey, A., Greenberg, J., Harley, P., Grace, J., Malhi, Y., & Guenther, A. (2004b). Effect of drought on isoprene emission rates from leaves of *Quercus virginiana* Mill. *Atmospheric Environment*, *38*(36), 6149-6156.

Pio, C. A., Feliciano, M. S., Vermeulen, A. T., & Sousa, E. C. (2000). Seasonal variability of ozone dry deposition under southern European climate conditions, in Portugal. *Atmospheric Environment*, *34*, 195–205.

Pleijel, H., Danielsson, H., Emberson, L., Ashmore, M. R., & Mills, G. (2007). Ozone risk assessment for agricultural crops in Europe: Further development of stomatal flux and flux–response relationships for European wheat and potato. *Atmospheric Environment*, *41*(14), 3022–3040. doi:10.1016/j.atmosenv.2006.12.002

Pleim, J., & Ran, L. (2011). Surface flux modeling for air quality applications. *Atmosphere*, *2*(4), 271–302. doi:10.3390/atmos2030271

Poisson, N., Kanakidou, M., & Crutzen, P. J. (2000). Impact of non-methane hydrocarbons on tropospheric chemistry and the oxidizing power of the global troposphere: 3-dimensional modelling results. *Journal of Atmospheric Chemistry*, *36*(2), 157-230.

Potosnak, M. J., LeStourgeon, L., Pallardy, S. G., Hosman, K. P., Gu, L., Karl, T., ... & Guenther, A. B. (2014). Observed and modeled ecosystem isoprene fluxes from an oak-dominated temperate forest and the influence of drought stress. *Atmospheric Environment*, *84*, 314-322.

Pressley, S., Lamb, B., Westberg, H., & Vogel, C. (2006). Relationships among canopy scale energy fluxes and isoprene flux derived from long-term, seasonal eddy covariance measurements over a hardwood forest. *Agricultural and Forest Meteorology*, 136(3), 188-202.

Pressley, S., Lamb, B., Westberg, H., Guenther, A., Chen, J., & Allwine, E. (2004). Monoterpene emissions from a Pacific Northwest Old-Growth Forest and impact on regional biogenic VOC emission estimates. *Atmospheric Environment*, *38*(19), 3089-3098.

Rannik, Ü., Altimir, N., Mammarella, I., Bäck, J., Rinne, J., Ruuskanen, T. M., ... & Kulmala, M. (2012). Ozone deposition into a boreal forest over a decade of observations: evaluating deposition partitioning and driving variables.*Atmospheric Chemistry and Physics*, *12*(24), 12165-12182.

Ryan, A. C., Hewitt, C. N., Possell, M., Vickers, C. E., Purnell, A., Mullineaux, P. M., ... & Dodd, I. C. (2014). Isoprene emission protects photosynthesis but reduces plant

productivity during drought in transgenic tobacco (Nicotiana tabacum) plants. *New Phytologist*, *201*(1), 205-216.

Rodríguez-Calcerrada, J., Buatois, B., Chiche, E., Shahin, O., & Staudt, M. (2013). Leaf isoprene emission declines in *Quercus pubescens* seedlings experiencing drought–Any implication of soluble sugars and mitochondrial respiration? *Environmental and Experimental Botany*, 85, 36-42.

Sakulyanontvittaya, T., Duhl, T., Wiedinmyer, C., Helmig, D., Matsunaga, S., Potosnak, M., ... & Guenther, A. (2008). Monoterpene and sesquiterpene emission estimates for the United States. *Environmental science & technology*,*42*(5), 1623-1629.

Sala, A., Piper, F., and Hoch, G. (2010). Physiological mechanisms of drought-induced tree mortality are far from being resolved. *New Phytologist*, *186*, 274–281.

Scholes, M., & Andreae, M. O. (2000). Biogenic and pyrogenic emissions from Africa and their impact on the global atmosphere. *AMBIO: A Journal of the Human Environment*, *29*(1), 23-29.

Schwede, D., Pouliot, G., & Pierce, T. (2005). Changes to the biogenic emissions inventory system version 3 (BEIS3). In *4th Annual CMAS Models-3 Users' Conference, September* (Vol. 26, p. 28).

Seco, R., Karl, T., Guenther, A., Hosman, K. P., Pallardy, S. G., Gu, L., ... & Kim, S. (2015). Ecosystem-scale VOC fluxes during an extreme drought in a broad-leaf temperate forest of the Missouri Ozarks (central USA). *Global change biology*.

Seinfeld, J. H., & Pandis, S. N. (2012). *Atmospheric chemistry and physics: from air pollution to climate change*. John Wiley & Sons.

Sevanto, S., McDowell, N. G., Dickman, L. T., Pangle, R., & Pockman, W. T. (2014). How do trees die? A test of the hydraulic failure and carbon starvation hypotheses.*Plant, Cell & Environment*, *37*(1), 153-161.

Sharkey, T. D. (2005). Effects of moderate heat stress on photosynthesis: importance of thylakoid reactions, rubisco deactivation, reactive oxygen species, and thermotolerance provided by isoprene. *Plant, Cell & Environment*,28(3), 269-277.

Sharkey, T. D., & Loreto, F. (1993). Water stress, temperature, and light effects on the capacity for isoprene emission and photosynthesis of kudzu leaves. *Oecologia*, 95(3), 328-333.

Situ, S., Guenther, A., Wang, X., Jiang, X., Turnipseed, A., Wu, Z., & Bai, J. (2013). Impacts of seasonal and regional variability in biogenic VOC emissions on surface

ozone in the Pearl River delta region, China. *Atmospheric Chemistry and Physics*, *13*(23), 11803-11817.

Slinn, S. A., & Slinn, W. G. N. (1980). Predictions for particle deposition on natural waters. *Atmospheric Environment (1967)*, *14*(9), 1013-1016.

Solberg, S., Hov, Ø., Søvde, A., Isaksen, I. S. A., Coddeville, P., De Backer, H., ... & Uhse, K. (2008). European surface ozone in the extreme summer 2003. *Journal of Geophysical Research: Atmospheres (1984–2012)*, *113*(D7).

Staudt, M., Ennajah, A., Mouillot, F., & Joffre, R. (2008). Do volatile organic compound emissions of Tunisian cork oak populations originating from contrasting climatic conditions differ in their responses to summer drought? *Canadian Journal of Forest Research*, 38(12), 2965-2975.

Tani, A., Tozaki, D., Okumura, M., Nozoe, S., & Hirano, T. (2011). Effect of drought stress on isoprene emission from two major *Quercus* species native to East Asia. *Atmospheric Environment*, 45(34), 6261-6266.

Tawfik, A. B., Stöckli, R., Goldstein, A., Pressley, S., & Steiner, A. L. (2012). Quantifying the contribution of environmental factors to isoprene flux interannual variability. *Atmospheric Environment*, 54, 216-224.

Texas A&M Forest Service. (2014). Texas ecoregions. Retrieved July 5, 2015, from http://texastreeid.tamu.edu/content/texasecoregions/

Thunis, P., & Cuvelier, C. (2000). Impact of biogenic emissions on ozone formation in the Mediterranean area–a BEMA modelling study. *Atmospheric Environment*, *34*(3), 467-481.

Tingey, D. T., Evans, R., & Gumpertz, M. (1981). Effects of environmental conditions on isoprene emission from live oak. *Planta*, 152(6), 565-570.

Tsigaridis, K., & Kanakidou, M. (2003). Global modelling of secondary organic aerosol in the troposphere: a sensitivity analysis. *Atmospheric Chemistry and Physics*, *3*(5), 1849-1869.

Turpin, B. J., & Huntzicker, J. J. (1995). Identification of secondary organic aerosol episodes and quantitation of primary and secondary organic aerosol concentrations during SCAQS. *Atmospheric Environment*, *29*(23), 3527-3544.

UNECE. (2004). Revised Manual on Methodologies and Criteria for Mapping Critical Levels/loads and Geographical Areas where they are Exceeded. www.icpmapping.org.

Vieno, M., Dore, A. J., Stevenson, D. S., Doherty, R., Heal, M. R., Reis, S., ... & Sutton, M. A. (2010). Modelling surface ozone during the 2003 heat-wave in the UK. *Atmospheric Chemistry and Physics*, *10*(16), 7963-7978.

Wesely, M. L. (1989). Parameterization of surface resistances to gaseous dry deposition in regional-scale numerical models. *Atmospheric Environment*, *23*(6), 1293–1304.

Wild, O. (2007). Modelling the global tropospheric ozone budget : exploring the variability in current models. *Atmospheric Chemistry and Physics*, *7*(10), 2643–2660.

Wittig, V. E., Ainsworth, E. A., Naidu, S. L., Karnosky, D. F., & Long, S. P. (2009). Quantifying the impact of current and future tropospheric ozone on tree biomass, growth, physiology and biochemistry: a quantitative meta-analysis.*Global Change Biology*, *15*(2), 396-424.

Wu, S., Mickley, L. J., Leibensperger, E. M., Jacob, D. J., Rind, D., & Streets, D. G. (2008). Effects of 2000–2050 global change on ozone air quality in the United States. *Journal of Geophysical Research: Atmospheres (1984–2012)*, *113*(D6).

Wuebbles, D. J., Grant, K. E., Connell, P. S., & Penner, J. E. (1989). The role of atmospheric chemistry in climate change. *JAPCA*, *39*(1), 22-28.

Yarwood, G., Wilson, G., Shepard, S., & Guenther, A. (2002). User's guide to the global biosphere emissions and interactions system (GloBEIS) version 3. *ENVIRON International Corporation*, *773*.

Zeppel, M. J. B., Anderegg, W. R. L., & Adams, H. D. (2013). Meetings Forest mortality due to drought : latest insights , evidence and unresolved questions on physiological pathways and consequences of tree death. *New Phytologist*, *197*, 372–374.

Zhang, L., Brook, J. R., & Vet, R. (2003). A revised parameterization for gaseous dry deposition in air-quality models. *Atmospheric Chemistry and Physics*, *3*(6), 2067-2082.

Zhang, L., Gong, S., Padro, J., & Barrie, L. (2001). A size-segregated particle dry deposition scheme for an atmospheric aerosol module. *Atmospheric Environment*, *35*(3), 549-560.

Chapter 3: Annual Variability in Leaf Area Index and Isoprene and Monoterpene emissions during Drought Years in Texas

The material presented in this Chapter has been published in *Atmospheric Environment*
Huang, L.; McDonald-Buller, E. C.; McGaughey, G.; Kimura, Y.; Allen, D. T.
Atmospheric Environment. **2014**, *92*, doi:10.1016/j.atmosenv.2014.04.016
Dr. Elena McDonald-Buller and Dr. David Allen are the co-supervisors of this work, providing comments and final reviews of this work. Mr. Gary McGaughey and Dr. Yosuke Kimura are research scientists, contributing to suggestions and part of data analysis and modeling work.

3.1 INTRODUCTION

Isoprene and monoterpenes are quantitatively among the most important biogenic volatile organic compounds (BVOCs) emitted globally from vegetation (Fehsenfeld et al., 1992; Guenther et al., 1995; Guenther et al., 2006). Annual biogenic emissions in Texas ranked first within the continental United States in the 2008 National Emission Inventory (EPA, 2013), with 30% of the contribution from the dense hardwood and coniferous forests of east Texas. Recognition of the roles of BVOCs in tropospheric ozone and organic aerosol formation has been critical for air quality planning efforts in the state. In 2008, for example, biogenic emissions accounted for 29% and 40% of the total VOC inventories in the Dallas/Fort Worth and Houston/Galveston/Brazoria ozone nonattainment areas, respectively.

Droughts have been a recurring phenomenon throughout the southwestern United States. Most climate models suggest that droughts will persist in the future as climate changes in response to increased concentrations of greenhouse gases and other radiative forcing species in the atmosphere (U.S. Global Change Research Program, 2009). In recent years, effects in Texas have been among the most severe; during 2011, more than 80% of Texas was under exceptional drought, which was associated with record agricultural losses and the worst year for wildfires in the state's history (Fannin, 2011).

Understanding the effects of drought on vegetation and biogenic emissions is important as the state concurrently faces requirements to achieve and maintain attainment with the National Ambient Air Quality Standard (NAAQS) for ozone in several large metropolitan areas.

Previous studies have suggested that the impacts of drought on isoprene and monoterpene emissions depend on its severity, with relatively small effects during mild drought but more significant reductions during prolonged and extreme conditions (Brilli et al., 2007; Fang et al., 1996; Fortunati et al., 2008; Funk et al., 2005; Lavoir et al., 2009; Niinemets, 2010; Pegoraro et al., 2004). For example, Lavoir et al. (2009) found a factor of two decrease in monoterpene emissions from *Quercus ilex* in Southern France during pronounced summer drought. Leaf isoprene emissions rates have been shown to be less sensitive to water stress and recover more rapidly than photosynthetic rates and stomatal conductance (Brilli et al., 2007; Funk et al., 2005; Pegoraro et al., 2004). Based upon a conceptual model of leaf-level isoprene response to drought stress (Niinemets, 2010), Potosnak et al. (2014) proposed that emissions are initially stimulated by increased leaf temperatures due to reduction in stomatal conductance; continued drought stress suppresses emissions by reductions in substrate availability and/or isoprene synthase activity. Ryan et al. (2014) noted a lack of consensus regarding the effects of drought on reported isoprene emissions and the potential protection afforded to plants under drought stress by isoprene, indicating a need for further study.

Gulden et al. (2007) estimated interannual variability in fluxes of isoprene and monoterpenes to be 25% and 19%, respectively, in Texas. These estimates were within the range of 5% to 35% reported for interannual variations in isoprene fluxes elsewhere (Abbot et al., 2003; Pressley et al., 2005; Lathiere et al., 2006; Palmer et al., 2006; Duncan et al., 2009; Arneth et al., 2011; Tawfik et al., 2012). One pathway through

which drought may affect BVOC emissions is through reductions in leaf area (Vilagrosa et al., 2003; Limousin et al., 2009; Hummel et al., 2010). Leaf area index (LAI), representing the ratio of total upper leaf surface of vegetation to land surface area, is a key input parameter, along with local meteorological fields, land use/land cover classification, and soil moisture, in biogenic emissions models. Interannual variability in LAI was found to result in weak (~4%) variations in annual isoprene emissions estimates globally, but variations exceeded 30% for specific regions and months (Guenther et al., 2006). Gulden et al. (2007) identified LAI as a significant contributor to interannual variations of biogenic emissions estimates in Texas.

This chapter quantifies and contrasts annual and seasonal variability in the 4-day LAI product derived from the Moderate Resolution Imaging Spectroradiometer (MODIS) instrument and the relative influence of LAI on predictions of biogenic emissions using MEGAN across four climate regions in eastern Texas. The analysis focuses on 2006 – 2011, which included years with extreme to exceptional droughts as well as years with average and above average precipitation patterns (see Appendix B.1 for descriptions of climatology for 2006-2011).

3.2 METHODOLOGY

3.2.1 Climatology and land cover of eastern Texas

The National Oceanic and Atmospheric Administration, National Climatic Data Center (NOAA - NCDC) divides Texas into 10 climate regions, shown in Figure 3-1. Most large metropolitan areas in the state are located within one of four climate regions: North Central Texas (sub-tropical steppe or semi-arid savanna), South Central Texas (sub-tropical sub-humid mixed prairie, savanna and woodlands), East Texas (sub-tropical humid mixed evergreen-deciduous forestland) and Upper Coast (sub-tropical humid

marine prairies and marshes) (Texas Water Development Board, 2012); rural areas lie between population centers. Both temperature and precipitation gradually decrease inland from the Gulf of Mexico and across the state (Texas Water Development Board, 2012). Figure 3-2 shows the 12-month Standardized Precipitation Index (SPI) (McKee et al., 1993) and monthly Palmer Drought Severity Index (PDSI) (Palmer, 1965; Alley, 1984) during 2006-2011 as well as annual precipitation distributions as the departure from normal. In 2007 Texas had a relatively wetter and cooler weather pattern throughout the state, and 2011 had record heat, low rainfall, and more than 85% of the state in exceptional drought by late September. Figure 3-2 indicates not only interannual variability in the onset and persistence of drought in eastern Texas, but also its spatial variability between the four climate regions. For example, spring 2006 had drought conditions over most of Texas with the southern third of the state classified as extreme to exceptional. July rainfall ended the drought in coastal areas while a continuation of the hotter and drier than normal weather pattern during the fall caused the persistence of extreme drought in central and northern Texas.

Figure 3-1 also shows 36 land use/land cover types across the eastern half of the state from a recent effort (Popescu et al., 2011) sponsored by the Texas Commission on Environmental Quality (TCEQ). The MODIS 4-day LAI product used in this work relied on the Collection 5 MODIS land cover product (MOD12Q1), a global land cover dataset (Friedl et al., 2010; Myneni et al., 2002). However, this work used land cover data from the TCEQ for the spatial and temporal analysis of LAI because of its regional specificity. Discrepancies existed between land cover classifications in the global and regional products, which highlighted the need for validation of global satellite products and consideration of the effects of land cover on the LAI retrieval scheme (Fang et al., 2013b).

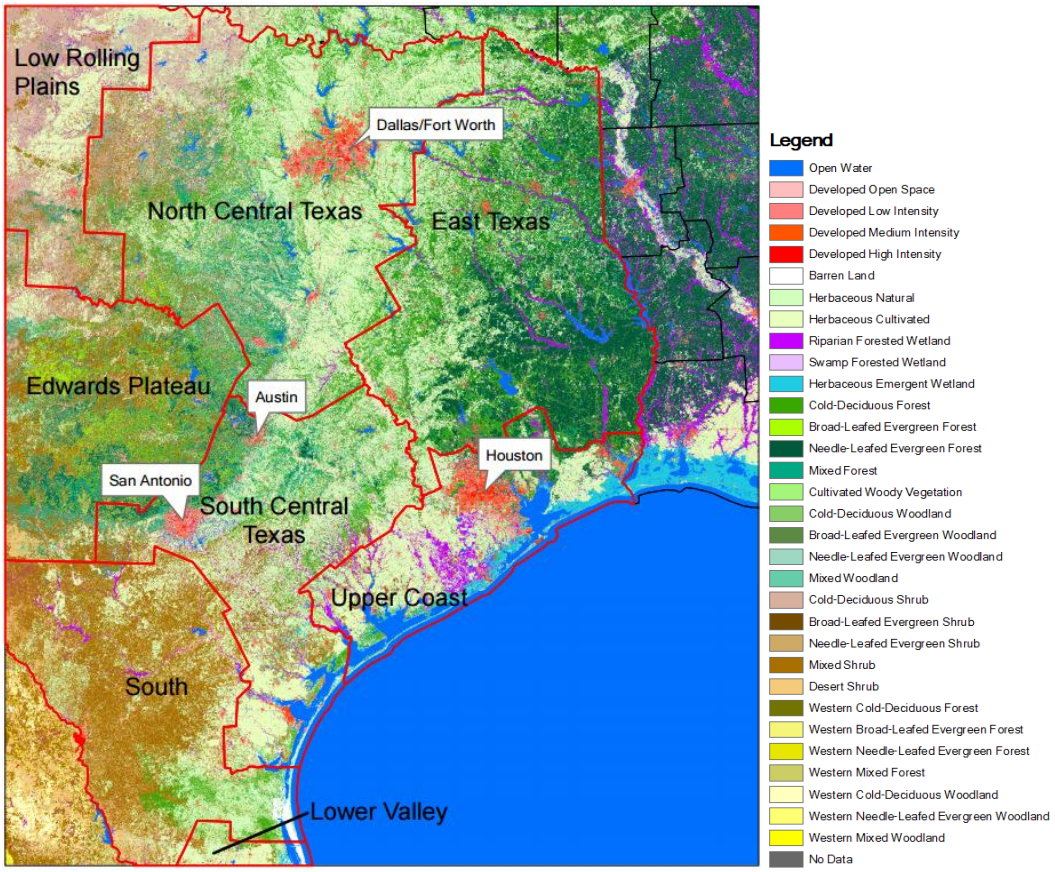

Figure 3-1: Thirty-six land cover/land use types in eastern Texas (Source: Popescu et al., 2011) with boundaries of Texas climate divisions (Source: National Oceanic and Atmospheric Administration). Developed metropolitan areas are shown in red. Dallas and Fort Worth are located in North Central Texas, Austin and San Antonio in South Central Texas, and Houston in the Upper Coast.

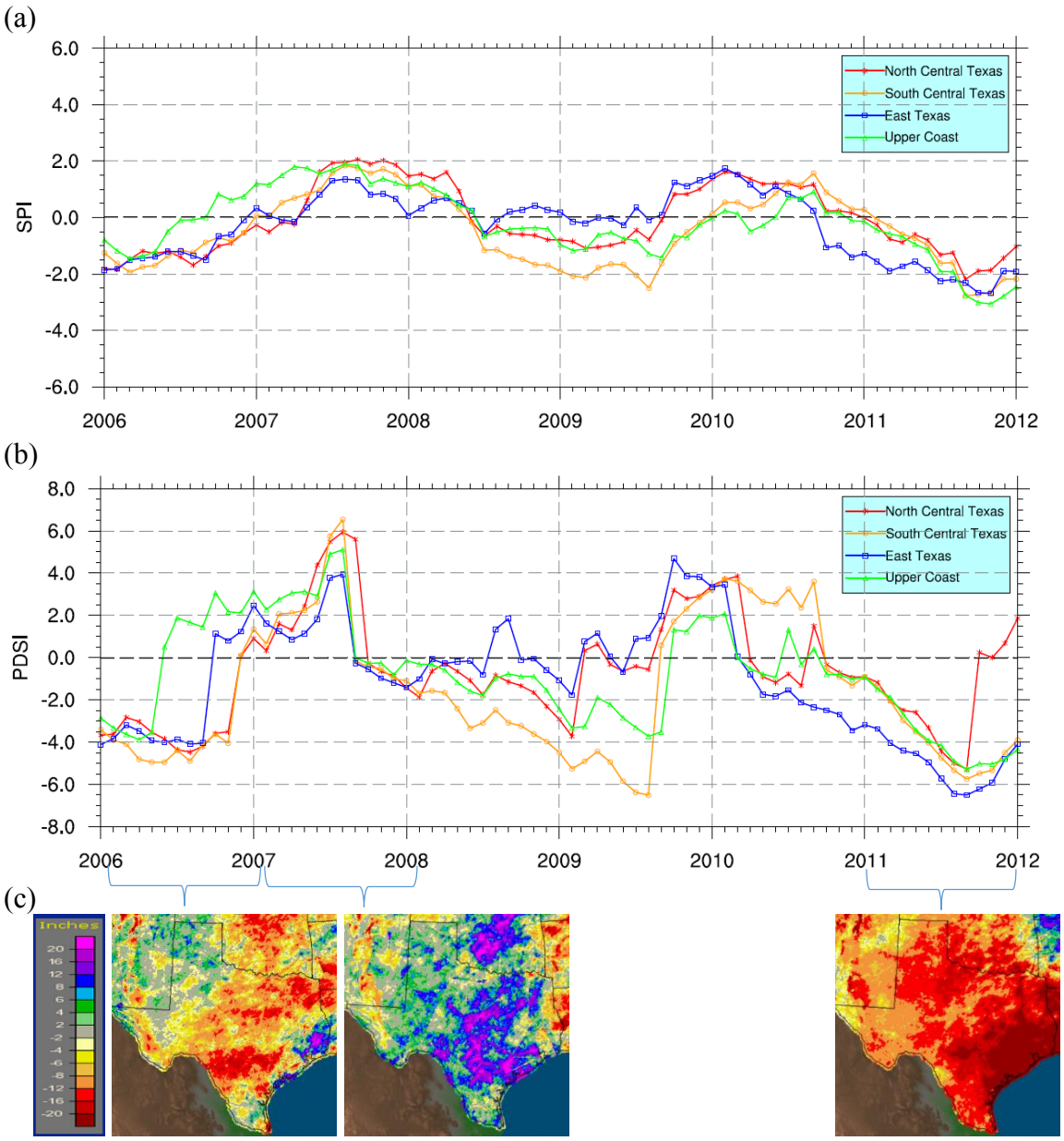

Figure 3-2: (a) 12-month SPI and (b) monthly PDSI for 2006 through 2011 for the North Central Texas, South Central Texas, East Texas, and Upper Coast climate regions. Positive SPI and PDSI values suggest wet conditions while negative suggest drought. Note differences in scales between plots. Source: National Climatic Data Center. (c) Annual precipitation distribution (as departure from normal in inches) for Texas during 2006, 2007, and 2011. Source: National Weather Service – Advanced Hydrologic Prediction Service.

3.2.2 MODIS LAI product

The Land Processes Distributed Active Archive Center (LP DAAC) currently provides two versions of Level-4 combined Terra and Aqua MODIS LAI products: an 8-day LAI composite (MCD15A2) and a 4-day LAI composite (MCD15A3). The 4-day LAI product is a recent release that is available only with MODIS Collection 5 (De Kauwe et al., 2011; Shabanov et al., 2007). Both the 8-day and 4-day LAI products are based on the same retrieval algorithms and are synchronously composited with a standard scheme every 8 days and 4 days, respectively (Knyazikhin et al., 1999). The 8-day LAI product has been used as a critical model parameter in the estimation of biogenic emissions (Guenther and Sakulyanontvittaya, 2011; Stavrakou et al., 2011) and has undergone more extensive validation (Cohen, et al., 2006; Fang, et al., 2013a; Xue et al., 2011; Yang et al., 2006) than the more recent 4-day LAI product (Heiskanen et al., 2012). However, with its increased temporal frequency, the 4-day LAI product has the potential to capture rapid changes in vegetation that may be important in the estimation of biogenic emissions. A comparison between the 4-day LAI and the 8-day LAI products is described in Appendix B.2. Overall, the two datasets were directionally consistent and exhibited reasonable agreement, with the 4-day LAI values showing greater fluctuations between composite periods. Differences between the products were associated with the presence of clouds and aerosols that affected the input surface reflectance, as well as with the compositing logic.

3.2.3 MEGAN biogenic emissions model

MEGAN2.1 (Guenther et al., 2012) estimates emissions rate (F_i) of chemical species i from terrestrial landscapes in unit of flux (μg m^{-2} ground area h^{-1}) as

$$F_i = \gamma_i \sum \varepsilon_{i,j} \chi_j \qquad \text{Eq. 3-1}$$

where $\varepsilon_{i,j}$ (μg m^{-2} ground area h^{-1}) is the standard emission factor representing the net primary emission rate for vegetation type j with fractional coverage χ_j, γ_i is the overall activity factor that accounts for variations in light (γ_P), temperature (γ_T), LAI (γ_{LAI}), leaf age (γ_A), soil moisture (γ_{SM}), and CO_2 inhibition (γ_C =1). For light, temperature, and leaf area index activity factors, MEGAN2.1 separates emissions of each compound class into a light-dependent fraction (LDF) and a light-independent fraction (LIF) which are then added to give the overall activity factor:

$$\gamma = \gamma_A \gamma_{SM} \gamma_C (LDF \cdot \gamma_{LAI\_LDF} \cdot \gamma_{P\_LDF} \cdot \gamma_{T\_LDF} + (1 - LDF) \cdot \gamma_{LAI\_LIF} \cdot \gamma_{T\_LIF}) \quad \text{Eq. 3-2}$$

Basal emission factors for isoprene and monoterpene over eastern Texas are shown in Figure 3-3; the highest isoprene emission factors are found in regions dominated by live oak (Edwards Plateau) and pine (East Texas) while monoterpene emissions are largest in the East Texas pine forests. MEGAN requires meteorological fields for air temperature, solar radiation, relative humidity, wind speed and soil moisture, and vegetation parameters including Plant Functional Type (PFT) fractions, LAI, and base emission rates (Guenther et al., 2012). MEGAN2.1 was modified to accept the 4-day LAI product as an alternative to the 8-day LAI product. LAI values for urban areas were not reported in the MODIS product but were estimated for this work as an average LAI from surrounding 5-km buffer regions. Assigning suburban LAI values to urban areas may cause an overestimation in LAI values and subsequent estimations of biogenic emissions in urban regions. Meteorological variables, except Photosynthetically Active Radiation (PAR), were obtained from the National Centers for Environmental Prediction (NCEP) North American Regional Reanalysis (NARR) products. NARR data with a 3-hour temporal and 32-km (nominal) spatial resolution were interpolated to a 1-km grid and a 1-hour resolution. Hourly surface insolation from the Geostationary Operational Environmental Satellite (GOES, generated by University of Alabama in Huntsville) with

a spatial resolution of 4-km were re-gridded into a 1-km grid and converted to PAR based on a conversion factor of 0.45 (McNider, 2013; ENVIRON, 2011). The TCEQ land cover data had a spatial resolution of 30 m with 36 Texas Land Classification System classes that were mapped to MEGAN's 16 PFTs. For each MEGAN 1-km grid cell, the fractional coverage of each PFT was determined by summing the number of 30-m resolution cells whose centroid fell within a given grid cell. MEGAN2.1 sets the default soil moisture activity factor to a value of one; source codes were modified to include the direct impact of soil moisture on isoprene emissions (Guenther et al. 2006, 2012). In this work, predictions of soil moisture were provided by the newly-developed Noah land surface model with multiparameterization options (Noah-MP, Cai et al., 2014).

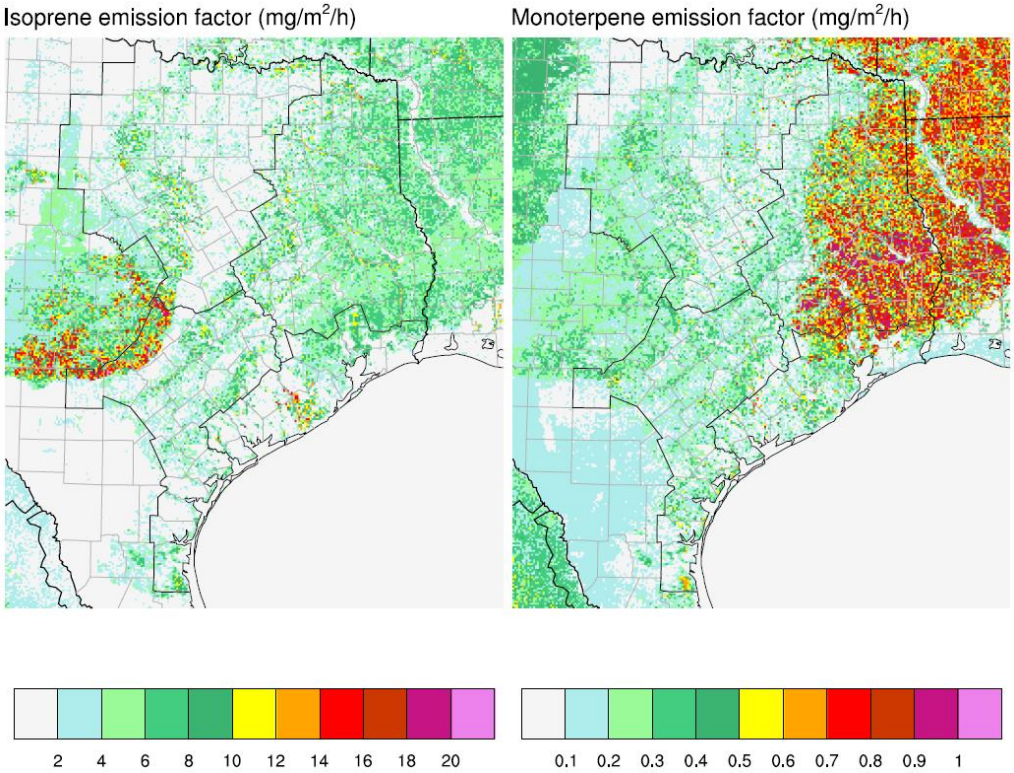

Figure 3-3: Emission factors (mg/m^2/h) for isoprene (left) and monoterpenes (right) over eastern Texas. Boundaries of the four climate divisions are outlined in black. Note differences in scales between plots.

Four types of simulations were conducted with MEGAN2.1 for the months of March to October during 2006-2011. The first (SM1) considered both annual LAI and meteorological fields for each year from 2006 – 2011, in order to characterize the interannual variability in emissions of isoprene and monoterpenes; the second (SM2) utilized meteorological fields and PAR for 2010, but varied LAI for each of the six years; the third (SM3) utilized a single LAI representation for 2010, but varied meteorological fields for each year; the fourth simulation (SM4) was identical to SM1 but the modified version of MEGAN was used to investigate the impact of soil moisture on isoprene emissions.

3.3 LAI IN EASTERN TEXAS CLIMATE REGIONS

3.3.1 Spatial and interannual variability

The spatial and temporal variability of MODIS 4-day LAI was examined for major (i.e., coverage area > 10%) land cover types during 2006 – 2011 in the four eastern Texas climate regions. Area-averaged LAI for all climate regions and land cover types had a strong seasonal pattern with the lowest values in winter and highest during April through September (Figure B-6), results that were consistent with earlier studies (Fang et al., 2013a; Tian et al., 2004). Interannual variations of LAI (Table B-1), as well as temperature and precipitation (Table B-2), were examined by calculating the standard deviations of monthly averaged values; in the case of LAI this was done to reduce fluctuations between composite periods potentially associated with cloud interference. Interannual variations in LAI were generally greater in North and South Central Texas than East Texas and Upper Coast. Maximum normalized monthly interannual variations were above 20% for all land cover types in North and South Central Texas, but less than 20% in East Texas and Upper Coast. Interannual LAI variations had a seasonal pattern

that was congruent to the seasonal trend in LAI; monthly interannual LAI variations peaked in summer, but were negligible in winter.

Two land cover types, grasses and broadleaf forest, were common to all four climate regions. However, LAI for these classes varied between climate regions, with higher values in East Texas, followed by the Upper Coast, and North/South Central Texas (Figure B-7); a result that was consistent with temperature and precipitation distributions. Some exceptions existed that could be associated with precipitation events or the lack thereof. Within a climate region, East Texas and Upper Coast showed substantial LAI variations across different land cover types, while LAI values in North and South Central Texas were more consistent (Figure B-8). In East Texas, area-averaged LAI by land cover type ranged from 1.9 m^2/m^2 for grasses, 2.8 m^2/m^2 for broadleaf forest, to 3.5 m^2/m^2 for needleleaf forest during April through September. In-situ LAI values in East Texas during May-July 2004 from Zhao and Popescu (2009) ranged within 1.0-3.5 m^2/m^2 for pine and hardwood forests, similar to values observed in this work. In North Central Texas (as well as South Central Texas), LAI values for broadleaf forest were only slightly higher, by 0.5 m^2/m^2, than other low-growing vegetation. These could represent actual conditions or could be associated with biome misclassification by the MODIS land cover product (Fang et al., 2013b). With the exception of data for East Texas from Zhao and Popescu (2009), in-situ LAI measurements are not currently available for comparison with MODIS products in other areas of the state. In-situ LAI values in other parts of U.S. have been reported by previous studies (e.g. Buermann et al., 2002; Viña et al., 2011; Brantley et al., 2011).

3.3.2 Response to the onset and persistence of drought

The response of LAI to the onset and persistence of drought contrasted 2007, a year with greater than average precipitation, with 2006 and 2011, years that had extreme

to exceptional drought within some or most of the four eastern Texas climate regions (Figure 3-4). Temperature and precipitation patterns during these three years are shown in Figure B-9. In North Central Texas, LAI values for the first three months were quite similar between 2007 and 2011 with slightly higher values (< 0.2 m^2/m^2) in 2007. By the end of March, LAI reductions associated with the 2011 drought exceeded 0.5 m^2/m^2 and persisted until the end of October. A similar response in LAI was evident during 2006; by the end of May, reductions in LAI were substantial (> 0.5 m^2/m^2) for all land cover types and prevailed until October. Shrubs showed the most significant decrease (over 1 m^2/m^2) in LAI during summer and fall in 2011. South Central Texas had similar land cover composition and temperature and precipitation patterns as North Central Texas during the three years. Average absolute LAI reductions in South Central Texas were substantial during April to October during drought years, exceeding 0.5 m^2/m^2 for all land cover types. July 2006 was an exception as South Central Texas received greater than average rainfall that resulted in increases in LAI, especially for low-growing vegetation.

In East Texas, LAI values for broadleaf and needleleaf forests, which comprised 60% of the land cover, were relatively consistent among the three years with smaller interannual variability than that observed for land cover types in North and South Central Texas. Vicente-Serrano (2007) indicated that factors that influence the spatial heterogeneity of the response of vegetation to drought are diverse and include land cover type, topoclimatic conditions, vegetation characteristics, and drought time-scale. Dry farming, shrubs, and pasture-lands generally exhibit greater vulnerability than irrigated lands and deciduous forest; coniferous forests can also be affected (Vicente-Serrano, 2007). Differences in the predominance of low-growing vegetation versus forests together with temperature and precipitation patterns may explain the smaller interannual variability in LAI for East Texas than Central Texas. Field surveys of tree mortality by

the Texas A&M Forest Service (2012) suggested widespread, but disproportionate impacts of the 2011 drought. In particular, far eastern Texas experienced relatively lower mortality than other regions of the state, while portions of Central Texas experienced the highest. The analysis in this work considered the association between precipitation and temperature on the LAI response to drought; however, other factors, such as soil composition and conditions, irrigation, wildfires, and pests, may also influence LAI.

3.3.3 Interannual variability of BVOC emissions and the influence of LAI

With contemporaneous annual meteorological fields and LAI (i.e., MEGAN SM1 simulation), isoprene exceeded monoterpene emissions by approximately a factor of six in eastern Texas; emissions of both BVOCs peaked during the summer months (JJA) of all years (Figure 2-1, Figure 2-2, Figure B-10). East Texas had the highest isoprene/monoterpene emissions among the four climate regions due to its dense forest coverage. Reductions of PAR and emissions could be associated with the timing of precipitation events, for example in South Central Texas and the Upper Coast in July 2007 and 2010. Average interannual variability, according to the approach of Tawfik et al. (2012), between March and October ranged from 18.3% in Upper Coast to 23.5% in East Texas, but decreased during the summer months. Interannual variability of isoprene emissions peaked in April for all regions, ranging from 27.3% in Upper Coast to 34.8% in North Central Texas (Table 3-1). Seasonal patterns of monoterpene emissions (Table 3-2) were similar to that of isoprene, but with weaker yearly variations. This result may be attributable to differences in the LDFs assigned by MEGAN2.1 (Guenther et al. 2012); estimates of isoprene, which is assigned an LDF of one, respond to changes in LAI, temperature and PAR; in contrast, estimates of monoterpenes, which are assigned LDFs of less than one, are fractionally dependent on LAI, temperature, and PAR or only LAI and temperature.

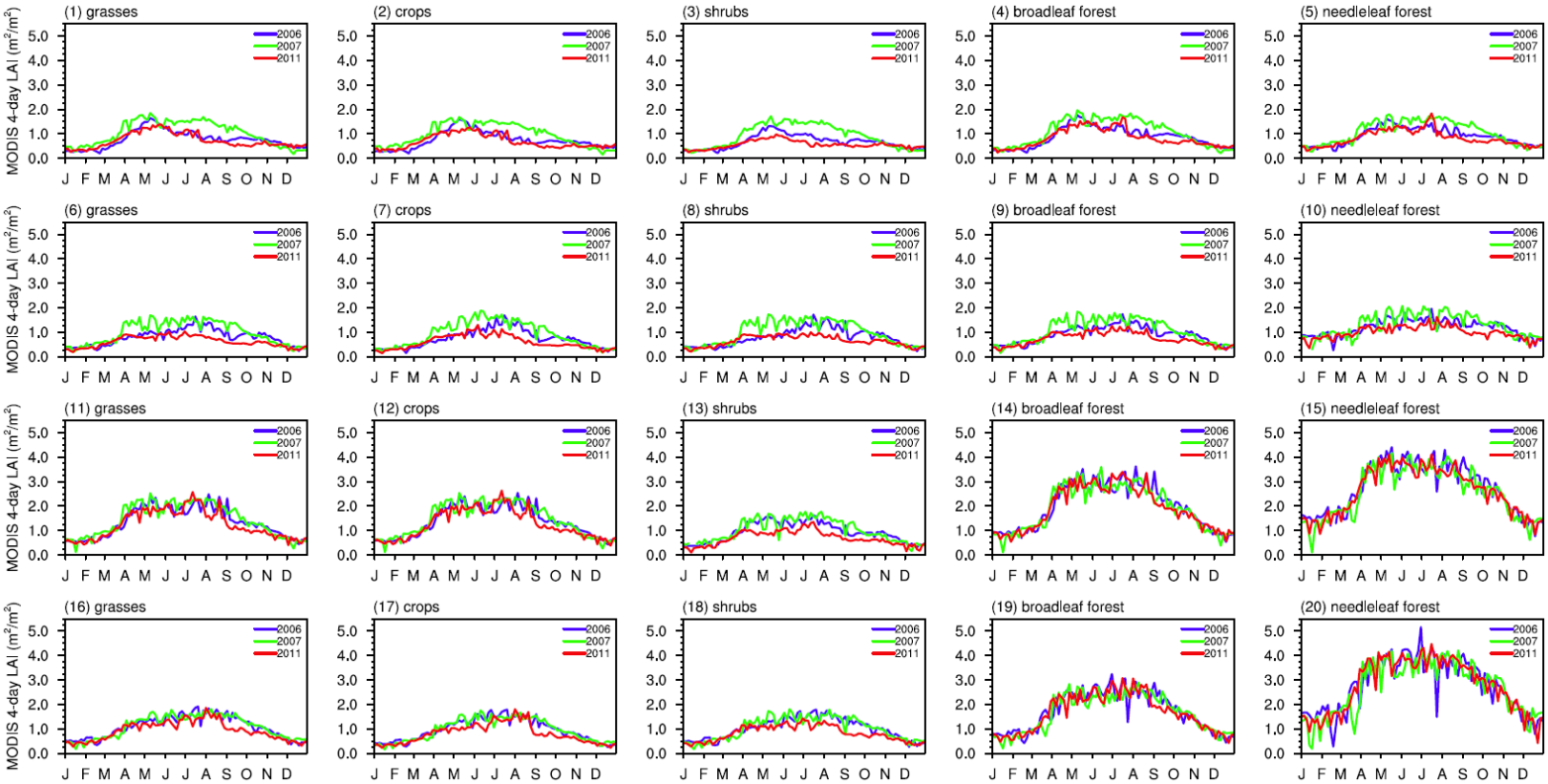

Figure 3-4: Time series of MODIS 4-day LAI during 2006, 2007, and 2011 for major land cover types in North Central Texas (1st row), South Central Texas (2nd row), East Texas (3rd row), and Upper Coast (4th row). Note differences in scales for LAI between plots.

Table 3-1: Interannual variability* of isoprene emissions by climate region and month during 2006-2011. SM1 had consistent annual LAI and meteorological fields; SM2 utilized meteorological fields for 2010, but varied annual LAI; SM3 used a 2010 LAI representation, but varied annual meteorological fields; SM4 was identical to SM1 except the impact of soil moisture on isoprene emissions was included. Maximum values are bolded.

Isoprene								
North Central Texas	Mar	Apr	May	June	Jul	Aug	Sep	Oct
SM1	19.2%	**34.8%**	22.9%	20.9%	17.0%	20.5%	17.4%	32.0%
SM2	10.8%	6.8%	8.5%	5.1%	5.0%	13.0%	**14.1%**	14.0%
SM3	14.6%	**27.3%**	18.1%	19.4%	21.2%	23.8%	17.8%	20.6%
SM4	16.9%	**31.7%**	21.8%	19.3%	14.6%	19.1%	17.9%	30.6%
South Central Texas	Mar	Apr	May	June	Jul	Aug	Sep	Oct
SM1	20.1%	**34.3%**	15.7%	15.0%	16.7%	20.5%	19.7%	20.5%
SM2	**18.6%**	11.4%	6.5%	3.6%	2.8%	10.5%	11.9%	7.5%
SM3	17.6%	**28.6%**	11.4%	15.5%	17.1%	18.9%	14.4%	11.2%
SM4	19.1%	**31.0%**	14.6%	12.2%	14.0%	18.1%	18.5%	19.7%
East Texas	Mar	Apr	May	June	Jul	Aug	Sep	Oct
SM1	15.9%	**31.5%**	25.9%	23.9%	18.2%	26.5%	24.6%	21.8%
SM2	8.9%	2.7%	**10.7%**	7.4%	5.0%	4.5%	10.3%	8.7%
SM3	17.3%	**26.7%**	16.3%	20.3%	15.1%	24.1%	19.5%	16.3%
SM4	15.9%	**30.8%**	25.7%	21.9%	17.1%	24.4%	23.3%	21.5%
Upper Coast	Mar	Apr	May	June	Jul	Aug	Sep	Oct
SM1	15.3%	**27.3%**	14.8%	15.6%	20.9%	20.9%	17.4%	13.9%
SM2	11.2%	2.8%	6.7%	3.9%	7.8%	6.4%	**12.7%**	5.3%
SM3	13.9%	**22.4%**	9.8%	13.7%	14.4%	17.7%	11.3%	8.0%
SM4	15.3%	**26.6%**	14.4%	14.3%	20.4%	19.8%	16.8%	13.7%

*Interannual variability (IAV) was determined as the average absolute percent departure from the 2006 through 2011 mean according to the approach of Tawfik et al. (2012):

$$IAV = \frac{1}{n}\sum_{y=1}^{n}\left|\frac{x_{y,m} - \overline{x_m}}{\overline{x_m}}\right| \times 100$$

where $x_{y,m}$ is the isoprene/monoterpene emission for year, y, and month, m, $\overline{x_m}$ is the average monthly emission across all years (2006 – 2011), n is the number of years simulated (n=6; for October 2008, n=5 due to missing PAR data).

Table 3-2: Interannual variability* of monoterpene emissions by climate region and month during 2006-2011. SM1 had consistent annual LAI and meteorological fields; SM2 utilized meteorological fields for 2010, but varied annual LAI; SM3 used a 2010 LAI representation, but varied annual meteorological fields. Maximum values are bolded.

Monoterpenes								
North Central Texas	Mar	Apr	May	June	Jul	Aug	Sep	Oct
SM1	17.3%	20.0%	9.7%	12.9%	9.1%	11.8%	15.1%	**20.1%**
SM2	8.2%	8.9%	3.9%	5.4%	11.6%	12.5%	**13.7%**	6.5%
SM3	12.6%	**22.0%**	12.5%	15.0%	15.8%	19.0%	12.9%	12.1%
South Central Texas	Mar	Apr	May	June	Jul	Aug	Sep	Oct
SM1	12.5%	**19.3%**	8.5%	6.3%	8.7%	12.3%	13.7%	11.3%
SM2	9.6%	13.0%	8.4%	9.8%	13.3%	13.5%	**14.7%**	8.2%
SM3	12.2%	**23.1%**	8.0%	10.1%	12.3%	12.9%	9.3%	7.2%
East Texas	Mar	Apr	May	June	Jul	Aug	Sep	Oct
SM1	15.2%	**20.9%**	9.5%	11.7%	10.2%	14.2%	12.2%	12.0%
SM2	1.7%	3.2%	3.1%	1.8%	3.4%	4.5%	**5.6%**	2.6%
SM3	13.3%	**20.8%**	11.7%	14.5%	10.5%	17.9%	13.3%	8.9%
Upper Coast	Mar	Apr	May	June	Jul	Aug	Sep	Oct
SM1	12.2%	**18.2%**	6.6%	6.1%	6.2%	9.9%	9.2%	7.8%
SM2	4.8%	4.4%	3.7%	3.8%	6.5%	4.8%	**7.1%**	3.3%
SM3	11.7%	**17.2%**	7.4%	9.1%	9.0%	11.7%	8.9%	5.0%

*Interannual variability (IAV) was determined as the average absolute percent departure from the 2006 through 2011 mean according to the approach of Tawfik et al. (2012):

$$IAV = \frac{1}{n}\sum_{y=1}^{n}\left|\frac{x_{y,m}-\overline{x_m}}{\overline{x_m}}\right|\times 100$$

where $x_{y,m}$ is the isoprene/monoterpene emission for year, y, and month, m, $\overline{x_m}$ is the average monthly emission across all years (2006 – 2011), n is the number of years simulated (n=6; for October 2008, n=5 due to missing PAR data).

Meteorological fields for 2010 were also used with year-specific LAI as the single variant (MEGAN SM2 simulation). Interannual variability in isoprene (monoterpene) emissions over North Central Texas ranged from 5.0% (3.9%) in July (May) to 14.1% (13.7%) in September (Table 3-1 and Table 3-2), which was less than when meteorological fields and LAI were both varied annually. Interannual variability in isoprene and monoterpene emissions in South Central Texas was similar to that of North Central Texas, but weaker in East Texas and the Upper Coast due to smaller interannual variations in LAI in more heavily forested areas. Deviations of isoprene and monoterpene emissions from the six-year (2006 – 2011) mean were well correlated with the corresponding deviations of LAI (R^2 of 0.59 – 0.98). Figure 3-5 contrasts deviations in monthly isoprene and monoterpene emissions and LAI from their six-year means during 2006, 2007 and 2011. In the two central regions, isoprene and monoterpene emissions were lower (for example, by as much as -24% in September 2011 for monoterpenes in North Central Texas) than their six-year means during the summers of 2006 and 2011, due to significant reductions in LAI during these time periods. The annual variability may be influenced by consideration of a longer time period or different reference metric; the years of 2007 and 2011 represented the wettest and driest on record during 2001-2011 (http://climatexas.tamu.edu/images/files/fnep_climdiv.txt).

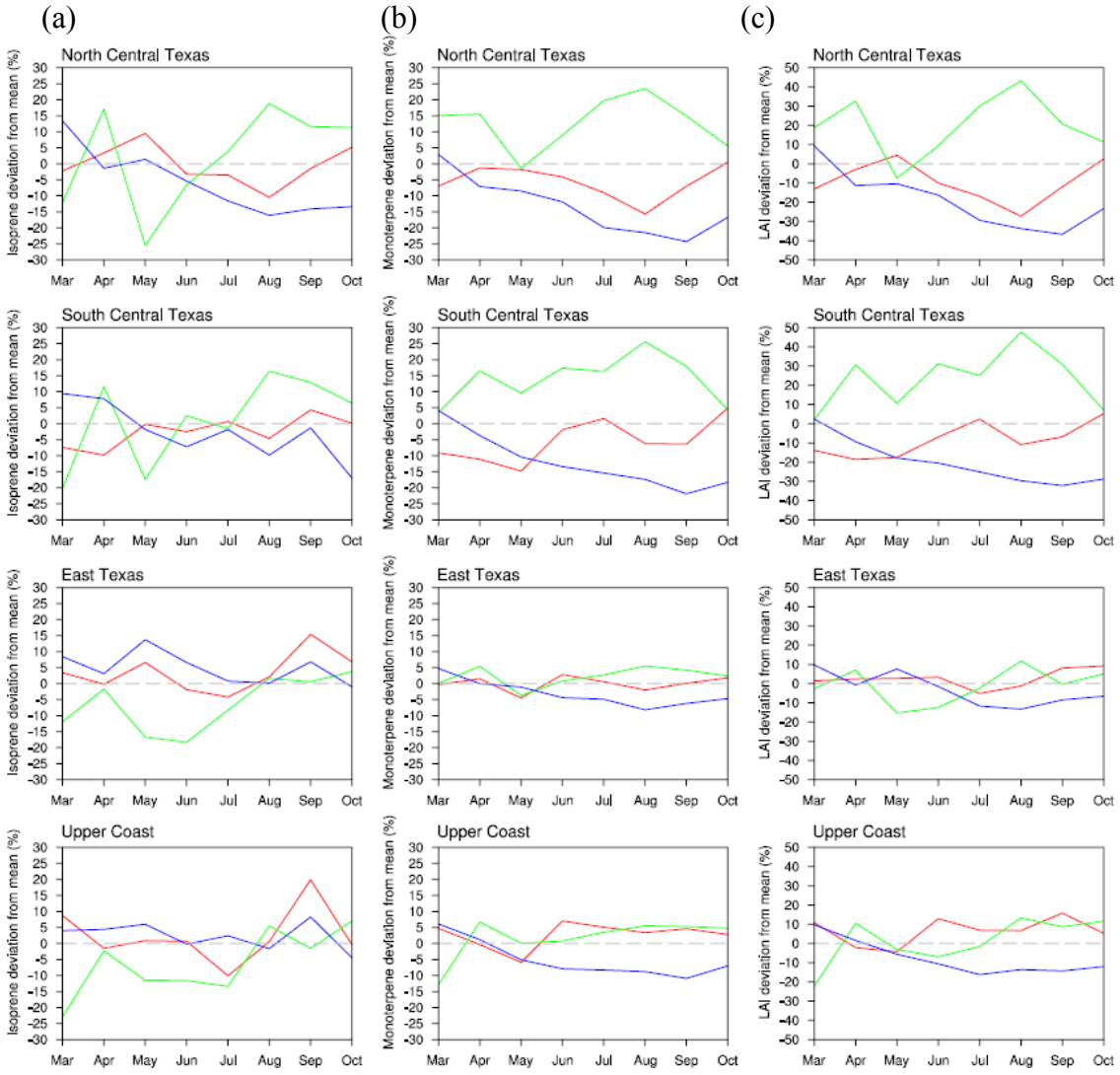

Figure 3-5: Deviations in monthly isoprene and monoterpene emissions and LAI from the six-year (2006-2011) mean during 2006 (red), 2007 (green), and 2011 (blue) by Texas climate region for the MEGAN SM2 simulation (consistent meteorological fields for 2010 with year-specific LAI).

The findings suggested that isoprene and monoterpene emissions may be affected by drought through changes in LAI and were similar to that of Gulden et al. (2007). Tawfik et al. (2012) indicated that the influence of LAI to interannual variability in isoprene fluxes in the U.S. during the summer were negligible relative to temperature and

soil moisture. Differences in the spatial resolution of the LAI data used by Tawfik et al. (2012) (half a degree) and this work (1 km) and the inclusion of the direct impact of soil moisture in Tawfik et al. (2012) may contribute to discrepancies. In addition, regional specificity in land use/land cover across the eastern Texas climate regions was considered in the analyses presented here, but may not be reflected in national- or global-scale data. Chavez-Figueroa et al. (2012) analyzed two 8-day LAI products originating from the MODIS instrument for a ten-year period (2001-2010) over the continental U.S. Interannual LAI variations across different land cover types were evident in Texas and elsewhere. Although the two years presented by Chavez-Figueroa et al. (2012), 2005 and 2007, had average to above average precipitation within eastern Texas, consideration of PDSI maps illustrated drought-correspondent LAI depression during August in other areas of the country. Similar to this work, positive LAI anomalies were evident in eastern Texas due to above average precipitation in 2007. Chavez-Figueroa et al. (2012) noted small LAI increases in certain regions of the U.S. even in areas experiencing severe drought in August; a hypothesis for future investigation is that use of a 4-day LAI product, with its higher temporal frequency, may capture sudden LAI increases after precipitation events during drought periods. Chavez-Figueroa et al. (2012) used constant meteorological fields to drive MEGAN and isolate the influence of LAI on isoprene emissions. Interannual variations in isoprene emissions were substantially reduced (< 15%) compared to those of LAI within eastern Texas.

In order to investigate the relative influence of LAI and meteorological fields, a third MEGAN simulation (SM3) varied meteorological fields annually with a 2010 representation of LAI. Similarities between the results of the MEGAN SM1 and SM3 simulations (Table 3-1) suggested that meteorological fields had a greater collective influence on the interannual variability in isoprene and monoterpene emissions than LAI

alone. However, LAI and meteorological variables may have competing effects on these emissions. Reductions in LAI were associated with declines in isoprene and monoterpene emissions during drought years, but less cloudiness and greater surface insolation could enhance isoprene emissions. As an example, when only the months of June, July and August were considered during the six-year period, interannual variability in monoterpene emissions from SM3, in which the LAI influence was removed, consistently equaled or exceeded that from SM1, in which annual LAI and meteorological influences were included. This was most notable in North and South Central Texas and indirectly suggested potential competing impacts of LAI and meteorological fields, such as temperature and PAR, on monoterpene emissions. In addition to temperature and PAR, soil moisture is also reported to be an important contributor to interannual variations of isoprene emissions (e.g., Tawfik et al., 2012; Potosnak et al., 2014). A fourth MEGAN simulation (SM4), which was the same as SM1 but incorporated the soil moisture algorithm, was performed as a preliminary evaluation of the effects of soil moisture on isoprene emissions. The impact of soil moisture variations led to maximum decreases in monthly isoprene emissions of 14% (August 2006) and 13% (August 2011) for North and South Central Texas, respectively. Impacts were smaller for East Texas and Upper Coast with a maximum decrease of 9% (August 2011) in East Texas. Table 3-1 shows that the SM4 monthly interannual isoprene variations were slightly less than those for SM1 (with largest differences of a few % for North and South Central Texas) suggesting that the exclusion of soil moisture did not impact the overall trends for our study. Additional investigation of the impact of soil moisture on isoprene emissions is on-going.

3.4 CONCLUSIONS

Biogenic emissions represent a significant fraction of the VOC inventories in eastern Texas ozone nonattainment areas, and consequently, have a critical role in air

quality planning efforts. This work investigated interannual variability in the MODIS 4-day LAI product and isoprene and monoterpene emissions estimates from MEGAN during time periods with extreme to exceptional drought in eastern Texas climate regions that had diverse climatology and land cover. Interannual variability of LAI in climate regions with low-growing vegetation was greater than in more heavily forested areas and exceeded 20%, with reductions of LAI exceeding 0.5 m^2/m^2 in drought years. Estimates of isoprene and monoterpene emissions were influenced by potentially competing effects of LAI and meteorological fields, such as temperature and solar insolation, during drought years. Maximum interannual variability in estimated monthly isoprene emissions exceeded 30%. These findings suggest the need for in situ validation of LAI derived from satellite observations and biogenic emissions during changing climatic conditions. As efforts to examine the effects of drought on vegetation health and mortality in Texas and other information are incorporated into a better understanding of land cover change in the future, it will be important to consider the effects on biogenic emissions.

3.5 REFERENCES

Abbot, D. S., Palmer, P. I., Martin, R. V., Chance, K. V., & Jacob, D. J. (2003). Seasonal and interannual variability of North American isoprene emissions as determined by formaldehyde column measurements from space. *Geophysical Research Letters*, *30*(17). doi:10.1029/2003GL017336

Alley, W. M. (1984). The Palmer drought severity index: limitations and assumptions. *J. Climate Appl. Meteorol.,* 23(7), pp. 1100-1109

Arneth, A., Schurgers, G., Lathiere, J., Duhl, T., Beerling, D. J., Hewitt, C. N., ... & Guenther, A. (2011). Global terrestrial isoprene emission models: sensitivity to variability in climate and vegetation. *Atmospheric Chemistry and Physics*, *11*(15), 8037-8052.

Brantley, S. T., Zinnert, J. C., & Young, D. R. (2011). Application of hyperspectral vegetation indices to detect variations in high leaf area index temperate shrub thicket canopies. *Remote Sensing of Environment*, *115*(2), 514–523. doi:10.1016/j.rse.2010.09.020

Brilli, F., Barta, C., Fortunati, A., Lerdau, M., Loreto, F., & Centritto, M. (2007). Response of isoprene emission and carbon metabolism to drought in white poplar (*Populus alba*) saplings. *The New Phytologist*, *175*(2), 244–54. doi:10.1111/j.1469-8137.2007.02094.x

Buermann, W., Wang, Y., Dong, J., Zhou, L., Zeng, X., Dickinson, R. E., ... & Myneni, R. B. (2002). Analysis of a multiyear global vegetation leaf area index data set. *Journal of Geophysical Research: Atmospheres (1984–2012)*,*107*(D22), ACL-14.

Cai, X., Yang, Z. L., David, C. H., Niu, G. Y., & Rodell, M. (2014). Hydrological evaluation of the Noah-MP land surface model for the Mississippi River Basin. *Journal of Geophysical Research: Atmospheres*.119, doi:10.1002/2013JD020792

Chavez-Figueroa, E. M., Cohan, D. S., Aghedo, A. M., Lash, B., Bi, J., & Myneni, R. (October, 2012). Impact of vegetation variability on biogenic emissions. Unpublished paper presented at the 11th Annual CMAS Conference, Chapel Hill, NC.

Cohen, W. B., Maiersperger, T. K., Turner, D. P., Ritts, W. D., Pflugmacher, D., Kennedy, R. E., ... & Gower, S. T. (2006). MODIS land cover and LAI collection 4 product quality across nine sites in the western hemisphere.*Geoscience and Remote Sensing, IEEE Transactions on*, *44*(7), 1843-1857.

De Kauwe, M. G., Disney, M. I., Quaife, T., Lewis, P., & Williams, M. (2011). An assessment of the MODIS collection 5 leaf area index product for a region of mixed coniferous forest. *Remote Sensing of Environment*, *115*(2), 767–780. doi:10.1016/j.rse.2010.11.004

Duncan, B. N., Yoshida, Y., Damon, M. R., Douglass, A. R., & Witte, J. C. (2009). Temperature dependence of factors controlling isoprene emissions. *Geophysical Research Letters*, *36*(5), L05813.

ENVIRON International Corporation (2011). Project status updates and isoprene comparisons from using different sources of PAR [PowerPoint Slides]. Retrieved February 19, 2014, from http://www.wrapair2.org/pdf/MGN210_sat_vs_wrf_DecCall14.Final2.ppt

EPA. (2013). 2008 National Emissions Inventory, version 3 Technical Support Document. Retrived Februray 4, 2014, from http://www.epa.gov/ttn/chief/net/2008neiv3/2008_neiv3_tsd_draft.pdf

Fang, C., Monson, R. K., & Cowling, E. B. (1996). Isoprene emission, photosynthesis, and growth in sweetgum (*Liquidambar styraciflua*) seedlings exposed to short- and long-term drying cycles. *Tree Physiology*, *16*(4), 441–446.

Fang, H., Jiang, C., Li, W., Wei, S., Baret, F., & Chen, J. M. (2013a). Characterization and intercomparison of global moderate resolution leaf area index (LAI) products: Analysis of climatologies and theoretical uncertainties. *Journal of Geophysical Research: Biogeosciences*, *118*, 1–20.

Fang, H., Li, W., & Myneni, R. (2013b). The impact of potential land cover misclassification on MODIS leaf area index (LAI) estimation: A statistical perspective. *Remote Sensing*, *5*(2), 830–844. doi:10.3390/rs5020830

Fannin, B. (2011). Texas agricultural drought losses reach record $5.2 billion. *AgriLife Today*. Retrieved May 28, 2013, from http://today.agrilife.org/2011/08/17/texas-agricultural-drought-losses-reach-record-5-2-billion/

Fehsenfeld, F., Calvert, J., Fall, R., Goldan, P., Guenther, A. B., Hewitt, C. N., ... & Zimmerman, P. (1992). Emissions of volatile organic compounds from vegetation and the implications for atmospheric chemistry. *Global Biogeochemical Cycles*, *6*(4), 389-430.

Fortunati, A., Barta, C., Brilli, F., Centritto, M., Zimmer, I., Schnit- zler, J., & Loreto, F. (2008). Isoprene emission is not temperature-dependent during and after severe drought stress: a physiological and biochemical analysis. *Plant J.*, *55*(4), 687–697.

Friedl, M. A., Sulla-Menashe, D., Tan, B., Schneider, A., Ramankutty, N., Sibley, A., & Huang, X. (2010). MODIS Collection 5 global land cover: Algorithm refinements and characterization of new datasets. *Remote Sensing of Environment*, *114*(1), 168–182. doi:10.1016/j.rse.2009.08.016

Funk, J. L., Jones, C. G., Gray, D. W., Throop, H. L., Hyatt, L. A., & Lerdau, M. T. (2005). Variation in isoprene emission from *Quercus rubra* : sources, causes, and consequences for estimating fluxes. *Journal of Geophysical Research: Atmosphere*, *110*(D4), D04301. doi:10.1029/2004JD005229

Guenther, A., & Sakulyanontvittaya, T. (2011). Improved biogenic emission inventories across the West. Retrieved Februray 19, 2014, from http://www.wrapair2.org/pdf/WGA_Task1_TechnicalAnalysisReport_ImprovedBiogenicEmissionInventories.pdf

Guenther, A., Hewitt, C. N., Erickson, D., Fall, R., Geron, C., Graedel, T., ... & Zimmerman, P. (1995). A global model of natural volatile organic compound emissions. *Journal of Geophysical Research: Atmospheres (1984–2012)*,*100*(D5), 8873-8892.

Guenther, A., Karl, T., Harley, P., Wiedinmyer, C., Palmer, P. I., & Geron, C. (2006). Estimates of global terrestrial isoprene emissions using MEGAN (Model of Emissions of Gases and Aerosols from Nature). *Atmospheric Chemistry and Physics*, *6*(1), 107–173. doi:10.5194/acpd-6-107-2006

Guenther, A. B., Jiang, X., Heald, C. L., Sakulyanontvittaya, T., Duhl, T., Emmons, L. K., & Wang, X. (2012). The Model of Emissions of Gases and Aerosols from Nature version 2.1 (MEGAN2.1): an extended and updated framework for modeling biogenic emissions. *Geoscientific Model Development*, *5*(6), 1471–1492. doi:10.5194/gmd-5-1471-2012

Gulden, L. E., Yang, Z. L., & Niu, G. Y. (2007). Interannual variation in biogenic emissions on a regional scale. *Journal of Geophysical Research*, *112*, D14103. doi:10.1029/2006JD008231

Heiskanen, J., Rautiainen, M., Stenberg, P., Mõttus, M., Vesanto, V.-H., Korhonen, L., & Majasalmi, T. (2012). Seasonal variation in MODIS LAI for a boreal forest area in Finland. *Remote Sensing of Environment*, *126*, 104–115. doi:10.1016/j.rse.2012.08.001

Hummel, I., Pantin, F., Sulpice, R., Piques, M., Rolland, G., Dauzat, M., ... & Muller, B. (2010). Arabidopsis plants acclimate to water deficit at low cost through changes of carbon usage: an integrated perspective using growth, metabolite, enzyme, and gene expression analysis. *Plant Physiology*, *154*(1), 357-372.

Knyazikhin, Y., Glassy, J., Privette, J. L., Tian, Y., Lotsch, A., Zhang, Y., … Running, W. (1999). MODIS Leaf Area Index (LAI) and Fraction of Photosynthetically Active Radiation Absorbed by Vegetation (FPAR) Product (MOD15) Algorithm Theoretical Basis Document. Retrieved Feburary 19, 2014, from http://modis.gsfc.nasa.gov/data/atbd/atbd_mod15.pdf

Lathiere, J., Hauglustaine, D. A., Friend, A. D., Noblet-Ducoudré, N. D., Viovy, N., & Folberth, G. A. (2006). Impact of climate variability and land use changes on global biogenic volatile organic compound emissions. *Atmospheric Chemistry and Physics*, *6*(8), 2129–2146.

Lavoir, A. V., Staudt, M., Schnitzler, J. P., Landais, D., Massol, F., Rocheteau, A., ... & Rambal, S. (2009). Drought reduced monoterpene emissions from the evergreen Mediterranean oak Quercus ilex: results from a throughfall displacement experiment. *Biogeosciences*, *6*, p-1167.

Limousin, J. M., Rambal, S., Ourcival, J. M., Rocheteau, A., Joffre, R., & Rodriguez-Cortina, R. (2009). Long-term transpiration change with rainfall decline in a Mediterranean *Quercus ilex* forest. *Global Change Biology*, *15*(9), 2163–2175. doi:10.1111/j.1365-2486.2009.01852.x

LP DAAC (2012). *MODIS LAI_FPAR User's Guide.* Retrieved September 17, 2013, from https://lpdaac.usgs.gov/sites/default/files/public/modis/docs/MODIS-LAI-FPAR-User-Guide.pdf

McKee, T. B., Doesken, N. J., & Kleist, J. (1993). The relationship of drought frequency and duration to time scale. *Proceedings of 8th Conference on Applied Climatology, American Meteorological Society* (pp. 179–184). Boston.

McNider, R., personal communication, July 31, 2013

Myneni, R. B., Hoffman, S., Knyazikhin, Y., Privette, J. L., & Glassy, J. (2002). Global products of vegetation leaf area and fraction absorbed PAR from year one of MODIS data. *Remote Sensing of Environment*, *83*(1-2), 214–231.

National Climate Data Center, Retrieved September 17, 2013, from http://www1.ncdc.noaa.gov/pub/data/cirs/

National Oceanic and Atmospheric Administration, Retrieved September 17, 2013, from http://www.esrl.noaa.gov/psd/data/usclimdivs/boundaries.html

National Weather Service, Advanced Hydrologic Prediction Service, Retrieved September 17, 2013, from http://water.weather.gov/precip/

Niinemets, U. (2010). Mild versus severe stress and BVOCs: thresholds, priming and consequences. *Trends in Plant Science*, *15*(3), 145–53. doi:10.1016/j.tplants.2009.11.008

Palmer, W. C. (1965). *Meteorological drought* (p. 58). Washington, DC, USA: US Department of Commerce, Weather Bureau.

Palmer, P. I., Abbot, D. S., Fu, T. M., Jacob, D. J., Chance, K., Kurosu, T. P., ... & Sumner, A. L. (2006). Quantifying the seasonal and interannual variability of North American isoprene emissions using satellite observations of the formaldehyde column. *Journal of Geophysical Research: Atmospheres (1984–2012)*, *111*(D12).

Pegoraro, E., Rey, A., Greenberg, J., Harley, P., Grace, J., Malhi, Y., & Guenther, A. (2004). Effect of drought on isoprene emission rates from leaves of *Quercus virginiana* Mill. *Atmospheric Environment*, *38*(36), 6149–6156. doi:10.1016/j.atmosenv.2004.07.028

Popescu, S. C., Stukey, J., Mutlu, M., Zhao, K., Sheridan, R., Ku, N.W., & Harper, C. (2011). Expansion of Texas land use/land cover through class crosswalking and Lidar parameterization of arboreal vegetation secondary investigators: Retrieved September 17, 2013, from http://m.tceq.texas.gov/assets/public/implementation/air/am/contracts/reports/oth/5820564593FY0925-20110419-tamu-expension_tx_lulc_arboreal_vegetation.pdf

Potosnak, M. J., LeStourgeon, L., Pallardy, S. G., Hosman, K. P., Gu, L., Karl, T., ... & Guenther, A. B. (2014). Observed and modeled ecosystem isoprene fluxes from an oak-dominated temperate forest and the influence of drought stress. *Atmospheric Environment*, *84*, 314-322.

Pressley, S., Lamb, B., Westberg, H., Flaherty, J., & Chen, J. (2005). Long-term isoprene flux measurements above a northern hardwood forest. *Journal of Geophysical Research*, *110*(D7), D07301. doi:10.1029/2004JD005523

Ryan, A. C., Hewitt, C. N., Possell, M., Vickers, C. E., Purnell, A., Mullineaux, P. M., ... & Dodd, I. C. (2014). Isoprene emission protects photosynthesis but reduces plant productivity during drought in transgenic tobacco (Nicotiana tabacum) plants. *New Phytologist*, *201*(1), 205-216.

Shabanov, N., Samanta, A., Myneni, R. B., Knyazikhin, Y., Votava, P., & Nemani, R. (2007). Collection 5 MODIS LAI and FPAR Products, University of Maryland. Retrieved Februray 19, 2014 from http://modis.gsfc.nasa.gov/sci_team/meetings/c5meeting/pres/day1/shabanov.pdf

Stavrakou, T., Guenther, A., Razavi, A., Clarisse, L., Clerbaux, C., Coheur, P. F., ... & Müller, J. F. (2011). First space-based derivation of the global atmospheric methanol emission fluxes. *Atmospheric chemistry and physics*,*11*(10), 4873-4898.

Tawfik, A. B., Stöckli, R., Goldstein, A., Pressley, S., & Steiner, A. L. (2012). Quantifying the contribution of environmental factors to isoprene flux interannual variability. *Atmospheric Environment*, *54*, 216–224. doi:10.1016/j.atmosenv.2012.02.018

Texas A&M Forest Service. (2012). Texas A&M Forest Service survery shows 301 million trees killed by drought, Retrieved Februray 19, 2014 from http://texasforestservice.tamu.edu/main/popup.aspx?id=16509

Texas Water Development Board. (2012). 2012 State Water Plan. Retrieved September 17, 2013 from http://www.twdb.state.tx.us/publications/state_water_plan/2012/04.pdf

Tian, Y. (2004). Comparison of seasonal and spatial variations of leaf area index and fraction of absorbed photosynthetically active radiation from Moderate Resolution Imaging Spectroradiometer (MODIS) and Common Land Model. *Journal of Geophysical Research*, *109*(D1), D01103. doi:10.1029/2003JD003777

US Global Change Research Program. (2009). Global Climate Change Impacts in the United States. Cambridge University Press. Retrieved Feb 19, 2014, from http://downloads.globalchange.gov/usimpacts/pdfs/climate-impacts-report.pdf

Vicente-Serrano, S. M. (2007). Evaluating the impact of drought using remote sensing in a Mediterranean, semi-arid region. *Natural Hazards*, *40*(1), 173-208.

Vilagrosa, A., Bellot, J., Vallejo, V. R., & Gil-Pelegrin, E. (2003). Cavitation, stomatal conductance, and leaf dieback in seedlings of two co-occurring Mediterranean shrubs during an intense drought. *Journal of Experimental Botany*, *54*(390), 2015–24. doi:10.1093/jxb/erg221

Viña, A., Gitelson, A. A., Nguy-Robertson, A. L., & Peng, Y. (2011). Comparison of different vegetation indices for the remote assessment of green leaf area index of crops. *Remote Sensing of Environment*, *115*(12), 3468–3478. doi:10.1016/j.rse.2011.08.010

Xue, H., Wang, J., & Ping, C. (2011). Validation of collection 5 MODIS LAI product by scaling-up method using field measurements. *Remote Sensing. International Society for Optics and Photonics*, 81742H–81742H.

Yang, W., Tan, B., Huang, D., Rautiainen, M., Shabanov, N. V., Wang, Y., ... & Myneni, R. B. (2006). MODIS leaf area index products: From validation to algorithm improvement. *Geoscience and Remote Sensing, IEEE Transactions on*, *44*(7), 1885-1898.

Zhao, K., & Popescu, S. (2009). Lidar-based mapping of leaf area index and its use for validating GLOBCARBON satellite LAI product in a temperate forest of the southern USA. *Remote Sensing of Environment*, *113*(8), 1628–1645. doi:10.1016/j.rse.2009.03.006

Chapter 4: Quantifying Regional, Seasonal and Interannual Contributions of Environmental Factors on Isoprene and Monoterpene Emissions Estimates over Eastern Texas

The material presented in this Chapter has been published in *Atmospheric Environment*
Huang, L.; McGaughey, G.; McDonald-Buller, E. C.; Kimura, Y.; Allen, D. T.
Atmospheric Environment. **2015**, *106*, doi:10.1016/j.atmosenv.2015.01.072
Dr. Elena McDonald-Buller and Dr. David Allen are the co-supervisors of this work, providing comments and final reviews of this work. Mr. Gary McGaughey and Dr. Yosuke Kimura are research scientists, contributing to suggestions and part of data analysis and modeling work.

4.1 INTRODUCTION

Isoprene (2-methyl-1, 3-butadiene, C_5H_8) and monoterpenes (a class of terpenes composed of two isoprene units) have been widely recognized for their key roles in atmospheric chemistry and climate, including contributions as precursors for tropospheric ozone (Atkinson, 2000) and secondary organic aerosol (SOA) formation (Tsigaridis and Kanakidou, 2003; Claeys et al., 2004). Globally, isoprene and monoterpenes are estimated to comprise 70% and 11%, respectively, of total annual biogenic volatile organic compounds (BVOCs) emitted from vegetation (Sindelarova et al., 2014). Average Texas statewide VOC emissions reported in the EPA 2011 National Emission Inventory (Version 1) were ranked first within the continental United States at approximately 11,650 and 4600 tons per day for biogenic and anthropogenic emissions, respectively.

The Model of Emissions of Gases and Aerosols from Nature (MEGAN) has been utilized extensively for the estimation of BVOC emissions on global and regional scales (Müller et al., 2008; Arneth et al., 2011; Sindelarova et al., 2014; Guenther et al., 2006, 2012; Ferreira et al., 2010; Potosnak et al., 2014; Han et al., 2013) as well as to investigate the impacts of biogenic emissions on atmospheric chemistry (Heald et al., 2008; Fu and Liao, 2012; Geng et al., 2011). Isoprene and monoterpene emissions are

controlled by various environmental factors, including temperature and light (Petron et al., 2001; Tingey et al., 1980; Sharkey et al., 1996), soil moisture (Pegoraro et al., 2004; Ormeno et al., 2007), atmospheric CO_2 concentration (Rosenstiel et al., 2003; Wilkinson et al., 2009), and phenology (Kuhn et al., 2004; Fischbach et al., 2002).

Previous studies have investigated the sensitivities of biogenic emissions (primarily isoprene) estimated by MEGAN to the driving meteorology, basal emission rate, vegetation distribution, and leaf area index (LAI) (Guenther et al., 2006, Wiedinmyer et al., 2006; Müller et al., 2008; Smiatek and Bogacki, 2005). Temperature has an important influence on estimates of emissions of isoprene and monoterpenes and their interannual variations (Stavrakou et al., 2014; Tawfik et al., 2012; Guenther et al., 2006). Solar radiation is an essential driving variable for light-dependent isoprene emissions; recent studies have suggested that solar radiation contributes negligibly to summer variations in sub-regions of the U.S. (Tawfik et al., 2012) but is a primary influence on interannual variations in East Asia (Stavrakou et al., 2014). The emission of de novo biosynthesized monoterpenes is controlled by light on a daily basis and is modeled in a similar way as for isoprene (Guenther et al., 2012).

A limited number of observational studies have suggested that soil water deficits are associated with an overall decline in leaf-level isoprene and monoterpene emissions (Lusebrink et al., 2011; Rodriguez-Calcerrada et al., 2013). The impact of modeled variations of soil moisture on biogenic emissions has been inconsistent and is likely sensitive to the specific soil moisture and wilting point data being employed (Müller et al., 2008; Tawfik et al., 2012; Sindelarova et al., 2014; Potosnak et al., 2014). Modeled impacts of LAI variability on isoprene emissions have shown a wide range (Huang et al., 2014; Gulden et al., 2007; Tawfik et al., 2012; Müller et al., 2008). With respect to uncertainty, recent MEGAN studies that have compared the impact of variability in

environmental inputs on predicted emissions have shown greater sensitivity (suggesting potentially larger uncertainty) for temperature, PAR, and soil moisture compared to other environmental inputs such as LAI (e.g., Holm et al., 2014; Situ et al., 2014; Stravrakou et al., 2014).

Many of the aforementioned studies have utilized MEGAN in support of sensitivity analyses of emissions estimates via perturbations of environmental inputs or climate/vegetation scenarios (e.g., Lathiere et al., 2010; Sindelarova et al., 2014; Chen et al., 2009; Arneth et al., 2011; Guenther et al., 2006, 2012). In MEGANv2.1, activity factors are used to multiplicatively adjust emissions from a standardized set of environmental conditions (Guenther et al., 2012). In order to track the relative changes in these activity factors internal to the MEGAN estimations, the model source codes were modified to enable the examination of individual activity factors for temperature, light, LAI, and soil moisture. The objective of this study is to quantify and interpret the differences in these environmental activity factors between years that had above average rainfall and average temperatures (2007) to years with substantially warmer and drier conditions (2006 and 2011) to assess the influence on isoprene and monoterpene emissions estimates in MEGAN.

4.2 METHODS

4.2.1 Description of MEGANv2.1

The latest version of MEGAN (MEGANv2.1) is described in detail by Guenther et al. (2012). The emissions rate (F_i) of isoprene/monoterpenes from terrestrial landscapes in units of flux (μg m^{-2} ground area h^{-1}) is calculated as:

$$F_i = \gamma_i \sum \varepsilon_{i,j} \chi_j \qquad \text{Eq. 4-1}$$

where ε is the basal emission factor for vegetation type *j* with fractional coverage χ_j ; it represents the emission rate under standard environmental conditions defined in Guenther et al. (2006, 2012) including an air temperature of 303 K, solar angle of 60 degrees, photosynthetic photon flux density (PPFD) transmission of 0.6, LAI of 5 m^2/m^2 consisting of 80% mature, 10% growing and 10% old foliage, and volumetric soil moisture of 0.3 m^3/m^3. γ is the overall emissions activity factor that accounts for variations in environmental conditions, and is constructed differently for isoprene and monoterpenes. For isoprene, emissions are light-dependent with a light dependent fraction (LDF) assigned as unity; the overall activity factor is calculated as:

$$\gamma = \gamma_{age} \cdot \gamma_{SM} \cdot \gamma_{CE} \qquad \text{Eq. 4-2}$$

with each of the individual gammas calculated as below (detailed descriptions of all activity factor variables are provided in Table A-1):

leaf age: $\gamma_{age} = A_{new}F_{new} + A_{gro}F_{gro} + A_{mat}F_{mat} + A_{old}F_{old}$ Eq. 4-3

soil moisture: $\gamma_{SM} = \sum_{i=1}^{4} f_{root}^{i} \max(0, \min(1, (\theta^i - \theta_{wilt})/0.04))$ Eq. 4-4

canopy environment:

$$\gamma_{CE} = 0.56 \cdot \sum_{i=1}^{5} [(\gamma_T^i)_{sun}(\gamma_P^i)_{sun} f_{sun}^i + (\gamma_T^i)_{shade}(\gamma_P^i)_{shade} f_{shade}^i] \cdot LAI^i \qquad \text{Eq. 4-5}$$

The default MEGAN configuration sets the relative emissions rates based on mature leaves. γ_{age} accounts for differences in basal emission rates among four leaf stages – new, growing, mature and old foliage. Emission rates for each leaf stage are assigned based on experimental observations (Guenther, et al., 2006) and the distribution of leaf ages is determined by changes in LAI between the current and previous time steps; a positive difference increases the amount of new and growing leaves and vice versa.

For monoterpenes, the soil moisture effect is not considered (γ_{SM} =1); a LDF of either 0.4 (for β-pinene, limonene, 3-carene, *t*-β-ocimene) or 0.6 (for α-pinene, myrcene, sabinene) is assigned. The overall activity factor is calculated as:

$$\gamma = \gamma_{age} \cdot [(1 - LDF) \cdot \gamma_{T\_LIF} \cdot \gamma_{LAI} + LDF \cdot \gamma_{CE}] \quad \text{Eq. 4-6}$$

with light independent fraction (LIF) related factors calculated as:

$$\text{temperature: } \gamma_{T\_LIF} = \sum_{i=1}^{5} [(\gamma^i_{T\_LIF})_{sun} f^i_{sun} + (\gamma^i_{T\_LIF})_{shade} f^i_{shade}] \quad \text{Eq. 4-7}$$

$$\text{leaf area index: } \gamma_{LAI} = 0.49LAI/(1 + 0.2LAI^2)^{0.5} \quad \text{Eq. 4-8}$$

The canopy environment model within MEGANv2.1 consists of five canopy layers. For each layer, temperature (γ_T , γ_{T_LIF}) and light (γ_P) activity factors are calculated for both sun and shaded leaves based on layer-specific temperature and PPFD, and then summed based on the sun/shaded fractions (f) for each layer. LAI is distributed between the layers using a Gaussian distribution. The sum of the product of γ_T , γ_P and LAI over the five layers provides the canopy environment activity factor (γ_{CE}). The parameters are further described in Table A-1 and Guenther et al. (2012).

4.2.2 MEGAN configuration

MEGAN was run at a 1-km horizontal spatial resolution and configured according to the approach of Huang et al. (2014). Utilized datasets included a regional land cover database with high spatial resolution (~30m, generated by Texas Commission on Environmental Quality) consisting of 36 Land Classification System classes that were mapped to MEGAN's 16 default Plant Functional Types (PFTs), MODIS (Moderate Resolution Imaging Spectroradiometer) 4-day LAI product (MCD15A3, 1-km), National Centers for Environmental Predictions - North American Regional Reanalysis (NCEP – NARR, 32-km) meteorological data, and Photosynthetic Active Radiation (PAR, 4-km)

produced by University of Alabama Huntsville from the Geostationary Operational Environmental Satellites (GOES).

The soil moisture datasets employed in our study were driven by North American Land Data Assimilation System Phase 2 (NLDAS-2) meteorological forcings, which provide hourly temporal and $1/8^{th}$ degree spatial resolution; the NLDAS-2 nonprecipitation fields are provided by NCEP – NARR while the precipitation data are derived from gauged daily rainfall from NCEP/Climate Prediction Center (Cai et al, 2014a). The original NLDAS testbed, which was designed to provide land surface states to coupled weather/climate models (Mitchell et al., 2004), consists of four land surface models (LSMs): the community Noah LSM (Noah) (Ek et al., 2003), the Mosaic LSM (Mosaic) (Koster and Suarez, 1996), the Sacramento Soil Moisture Accounting model (SAC-SMA) (Burnash et al., 1973), and the Variable Infiltration Capacity (VIC) model (Liang et al., 1994). These original NLDAS LSMs do not yet include recent developments in the land model community such as improved physics and new functionalities (e.g., prognostic leaf models, dynamic groundwater, multilayer snow) that have been incorporated into the Community Land Model version 4 (CLM4) (Lawrence et al., 2011) and the multi-parameterization options version of the Noah model (Noah-MP) (Niu et al., 2011). Because Noah-MP has been shown to have good performance for soil moisture in Texas (Cai et al., 2014b), Noah-MP was the primary soil moisture dataset used for our study. Additionally, soil moisture predictions from the Mosaic LSM were used for sensitivity simulations to investigate the impact of soil moisture uncertainty on estimates of isoprene emissions. As stressed by Muller et al. (2008) and Guenther et al. (2012), wilting point values for a given MEGAN simulation were those provided by the specific land surface model employed.

In addition to the default overall activity factor (γ), MEGAN source codes were modified to output each of the individual activity factors (e.g. γ_{age}, γ_{SM}, γ_{CE}, γ_{LAI}, etc.). MEGAN simulations were conducted over eastern Texas (ref. Figure 4-1) for March-October during 2006, 2007 and 2011. As shown by the drought indices as well as annual precipitation distributions anomalies (Figure C-1), 2007 was a relatively wet year with greater than average annual precipitation; in contrast, 2006 and 2011 were characterized by extreme to exceptional drought. Hourly individual activity factors for each 1-km grid cell were averaged by season (spring: March-April-May or MAM; summer: June-July-August or JJA; fall: September-October or SO), eastern Texas climate region (North Central Texas, South Central Texas, East Texas and Upper Coast) and year to generate area- and season- averaged values. Grid cells designated as water by the land cover database were ignored. For isoprene, only hours with non-zero PAR values (i.e. daytime) were considered.

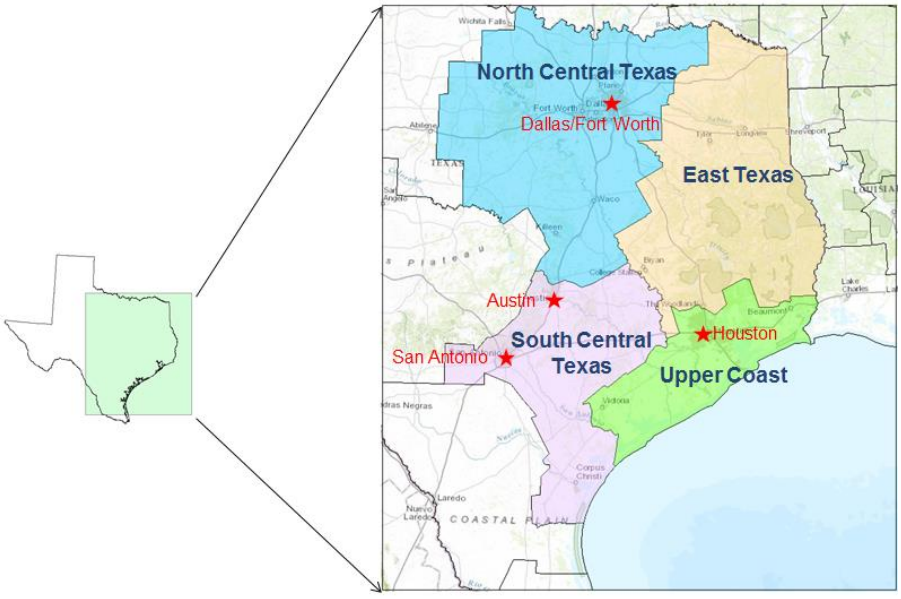

Figure 4-1: The MEGAN domain over eastern Texas including the four eastern Texas climate regions – North Central Texas, South Central Texas, East Texas and Upper Coast (Source: National Oceanic and Atmospheric Administration). The centers of major metropolitan areas are shown by red stars.

4.3 RESULTS

4.3.1 Isoprene and monoterpene emission estimates

Consistent with other studies for the South Central U.S. (Lamb et al., 1993; Kleindienst et al., 2007), Huang et al. (2014) demonstrated that biogenic emissions peak during summer. Table 4-1 shows the 2006-2011 season-averaged isoprene and monoterpene emissions and their variability for the four eastern Texas climate regions from Huang et al. (2014). East Texas exhibits the highest emissions among the four climate regions, primarily due to its densely forested areas; by region, summer emissions can be more than three times greater compared to spring/fall. Isoprene interannual variations ranged from 13.9% during summer in South Central Texas to 24.6% during spring in North Central Texas; monoterpenes exhibited weaker interannual variations by season.

Table 4-1: Averaged isoprene and monoterpene emissions (kg/km^2/day) and interannual variability* (in brackets) during 2006-2011 by season and eastern Texas climate region from Huang et al. (2014).

Climate region	***Isoprene (kg/km^2/day)***			***Monoterpenes (kg/km^2/day)***		
	MAM	**JJA**	**SO**	**MAM**	**JJA**	**SO**
North Central Texas	8.1 (24.6%)	33.4 (15.7%)	8.0 (18.5%)	1.5 (10.6%)	4.2 (9.8%)	1.6 (16.8%)
South Central Texas	13.7 (20.4%)	40.6 (13.9%)	13.7 (17.4%)	1.9 (8.3%)	4.1 (8.4%)	2.1 (12.6%)
East Texas	18.7 (23.6%)	69.3 (19.9%)	22.1 (21.1%)	4.5 (10.1%)	11.8 (12.0%)	5.4 (9.8%)
Upper Coast	9.8 (14.5%)	28.7 (14.6%)	11.6 (16.8%)	2.0 (7.6%)	4.5 (7.2%)	2.4 (8.7%)

*Interannual variability (IAV) was determined as the average absolute percent departure from the 2006-2011 mean according to the approach of Tawfik et al. (2012):

$$IAV = \frac{1}{n}\sum_{y=1}^{n}\left|\frac{x_{y,seas} - \overline{x_{seas}}}{\overline{x_{seas}}}\right| \times 100\%$$

where $x_{y,seas}$ is the isoprene/monoterpene emissions for year, y, and season, seas; $\overline{x_{seas}}$ is the average seasonal emissions across all years (2006–2011); n is the number of years simulated.

4.3.2 canopy-level comparisons

Isoprene

Figure 4-2 shows the canopy-level activity factors for isoprene during 2006, 2007 and 2011 averaged by season for the North Central (predominantly grassland) and East (predominantly forested) regions; analogous results for South Central and Upper Coast are provided in Figure C-2. As expected, the overall activity factors (γ_{tot}) exhibit strong seasonal patterns with highest values during summer regardless of region and year. Because the basal emission factor (ε) and vegetation distributions (χ_j) are assumed constant, the seasonal pattern of the absolute emissions is solely controlled by changes in the overall activity factor.

Across all regions and seasons the leaf age activity factors (γ_{age}) typically range from 0.85-0.94 (with a low of 0.8 during spring 2007 for South Central Texas) and exhibit negligible interannual or seasonal variations. Mature and older leaves have higher isoprene emissions than new and growing leaves; therefore, the leaf age factor is always below unity. As shown in Figure 4-2, the leaf age activity factor during the generally wet year (2007) is always slightly lower than the drought years (i.e. 2006 and 2011) related to the more rapid changes and variations in LAI during 2007.

The soil moisture activity factors also demonstrate low seasonal and interannual variations (<5%). As shown in Figure 4-2, the soil moisture activity factor for 2007 is essentially constant near unity; during the drought years (2006 and 2011), the soil moisture activity factor primarily ranges between 0.94-0.99. During 2011, a year that had

conditions of the all-time record drought throughout most of Texas, the minimum soil moisture activity factor is 0.90 during the North Central Texas summer. The impact of drought on isoprene emissions as currently characterized by MEGANv2.1 may have substantial uncertainty; for example, a recent study by Potosnak et al. (2014) observed a time-dependent response of field isoprene emissions to drought where an initial increase of emissions (about a week) was followed by a subsequent decrease and concluded that the MEGAN time-independent soil moisture algorithm was not able to capture the relevant response of isoprene emissions to drought. Nonetheless, soil moisture represents a primary mechanism by which drought effects are manifested in MEGAN isoprene estimates.

Figure 4-2 illustrates that the majority of changes in the overall activity factor is captured by differences in the canopy environmental factor (γ_{CE}). Seasonal variations are greater than inter-annual variations; year-to-year differences in γ_{CE} diminished in the fall, particularly in East Texas (and Upper Coast shown in Figure C-2). As an example, the seasonal values of γ_{CE} for East Texas during 2011 ranged from 0.53 during the fall to 1.85 during the summer, differing by a factor of 3.5. In contrast, summer γ_{CE} values for 2006 and 2007 are 1.27 and 0.94, respectively.

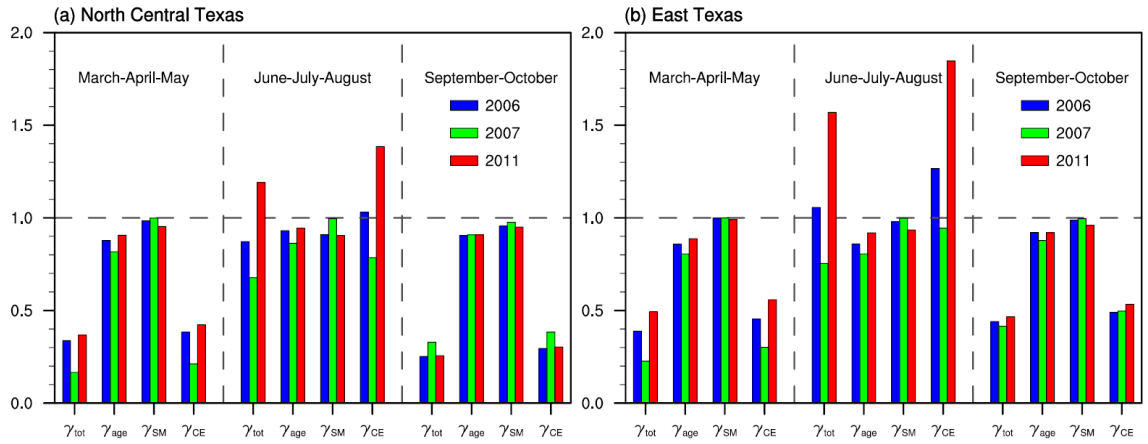

Figure 4-2: Area- and season- averaged MEGAN activity factors for isoprene during 2006, 2007, and 2011 in (a) North Central Texas and (b) East Texas. Results for South Central Texas and Upper Coast are shown in Figure C-2.

Monoterpenes

Figure 4-3 (North Central and East) and Figure C-3 (South Central and Upper Coast) show the canopy-level activity factors for monoterpenes during 2006, 2007 and 2011 averaged by season and climate region. In contrast to the methodology used for isoprene, the hourly-generated activity factors are averaged over the entire period instead of daylight hours because monoterpenes have both light-dependent and light-independent fractions; thus there are two additional activity factors (γ_{T_LIF}, γ_{LAI}) related to light-independent emissions. The use of different light-dependent fractions causes negligible differences in the overall activity factor; thus the seven classes of monoterpenes are considered as one monoterpene class for the purposes of this study.

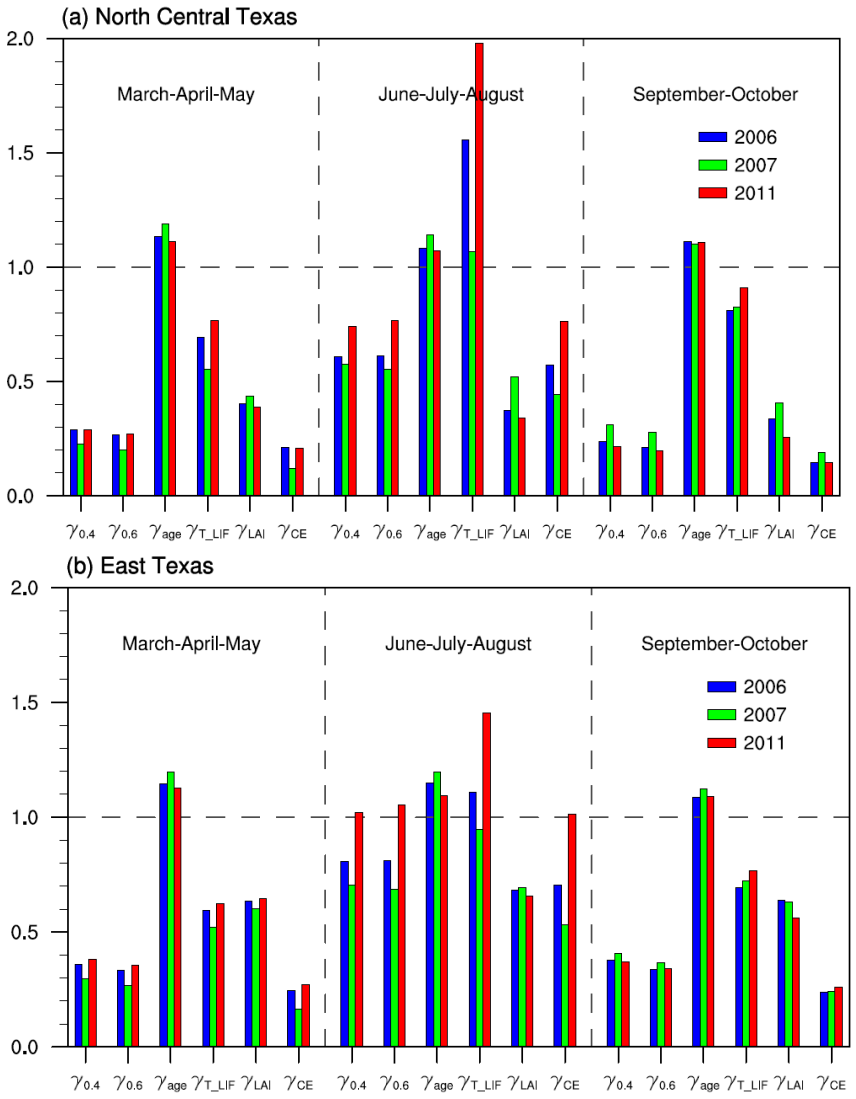

Figure 4-3: Area- and season- averaged MEGAN activity factors for monoterpenes during 2006, 2007, and 2011 in (a) North Central Texas and (b) East Texas. $\gamma_{0.4}$ and $\gamma_{0.6}$ represent the overall activity factor for monoterpene classes with a light dependent fraction of 0.4 and 0.6, respectively. Results for South Central Texas and Upper Coast are shown in Figure C-3.

As shown in Figure 4-3, the light-independent temperature (γ_{T_LIF}) and canopy environment activity (γ_{CE}) factors have substantial seasonal variations. The seasonal variations of the light-independent LAI activity factor (γ_{LAI}) are generally low and reach a maximum value of 14.8% in North Central Texas during 2011; interannual variations

are strong in the two central regions during summer and fall (>15%) but less (<10%) in East Texas; this is consistent with the substantial LAI reductions associated with drought in the central regions as demonstrated by Huang et al. (2014).

In contrast to isoprene, new and growing leaves emit more monoterpenes than mature and old leaves. Thus, the leaf age activity factor for monoterpenes is always above unity and had slightly greater values during the wetter than normal year (2007) compared to the drought years, with a maximum value of 1.2 in spring 2007. Similar to isoprene, leaf age is not a significant contributor to seasonal or interannual monoterpene variations. The soil moisture algorithm is not applied to monoterpenes in MEGAN.

4.3.3 Within-canopy comparisons

Isoprene

The detailed results for γ_{CE}, which describes the variations due to temperature, light and LAI within each of the five canopy layers, have been provided as Figure C-4. MEGAN uses a Gaussian distribution to distribute LAI between the layers such that the middle layer has the largest LAI values. Temperature variability, as demonstrated by the temperature activity factor (γ_T), is relatively low and varies as much as 7% between the top and bottom layers. There is often a substantial change in the light activity factor (γ_P) with top to bottom differences of 10-30%; larger LAI values produce greater attenuation as light passes through the canopy. For example, in North Central Texas during 2011, summer γ_P values decrease from 0.97 at the canopy top to 0.64 at the bottom (a factor of 1.5 attenuation); during the wetter-than-normal year (2007) with relatively larger LAI, γ_P is reduced from 0.85 to 0.45 (a factor of 1.9 attenuation). As shown in Figure C-4, East Texas has the greatest values of LAI as well as the largest layer-to-layer differences in γ_P compared to the other regions.

In order to investigate the seasonal and interannual variations in canopy activity factors, layer-averaged values for LAI, temperature and light activity are shown in Figure 4-4 and Figure C-5. The temperature activity factor has much greater seasonal variation compared to LAI and light for all regions, indicating that temperature is the primary driver of the seasonal variations of the canopy environment activity factor and, thus, isoprene emissions. Seasonal variations of the temperature activity factor were 20-55% with the greatest variation during 2011 in North Central Texas. Interannually, the variability of the LAI activity factor is sometimes comparable to that for temperature. Within seasons, the temperature activity factor varies substantially between years during spring and summer but shows minimal changes (<6%) during fall. LAI has substantial interannual differences during summer and fall in the central regions comparable to (or even greater than) the variations in the temperature activity factor but relatively small year-to-year changes for the East Texas and Upper Coast regions. As noted by Huang et al. (2014), the different regional response in LAI interannual variability is likely related to the dominant land cover types by region; East Texas and the Upper Coast are dominated by broadleaf and needleleaf forest versus low-growing vegetation (e.g., grasses) in the central regions. Sunlight controls isoprene emissions on a daily basis; however, it is not a significant contributor to seasonal or interannual variations in isoprene emissions.

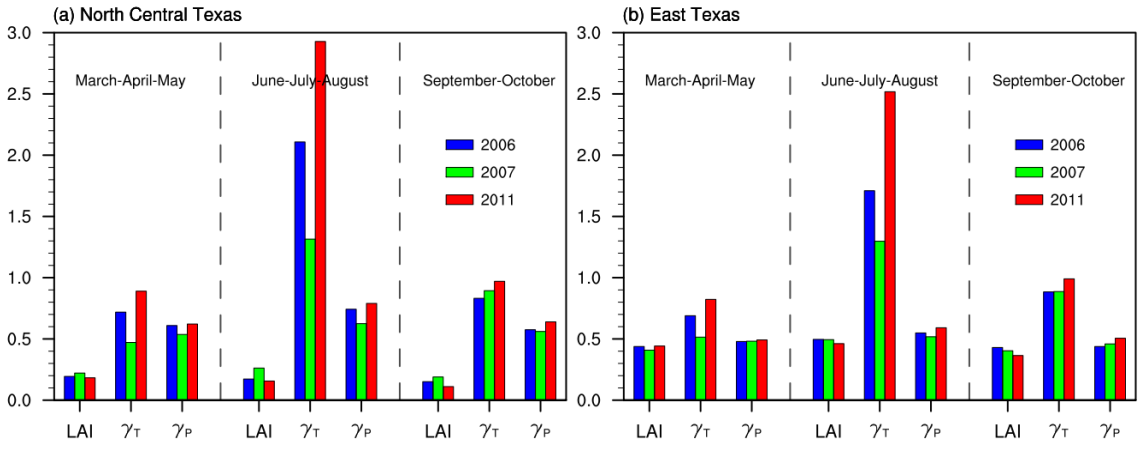

Figure 4-4: Layer-averaged LAI, temperature and light activity factors for isoprene during 2006, 2007, and 2011 by season and region – (a) North Central Texas and (b) East Texas. Results for South Central Texas and Upper Coast are shown in Figure C-5.

Monoterpenes

The by-layer activity factors for monoterpenes (Figure C-6) demonstrate that the relative directional variations in light/temperature activity factors are similar to those for isoprene. Figure 4-5 and Figure C-7 demonstrates that the layer-averaged temperature activity (γ_T) has the greatest seasonal variations and reaches a maximum value of 60% during 2011 in North Central Texas. LAI and light activity factors also show some seasonal variations with values ranging between 10-20% for LAI and 10-15% for light.

Overall, the relative importance of factors that contribute to interannual monoterpene variations are similar to those for isoprene: in central regions, the LAI and temperature activity factors dominate interannual variations while in East Texas and Upper Coast, LAI exhibits relatively smaller interannual changes (<10%). As for isoprene, the contribution of the light activity factor to interannual variations of monoterpene emissions is minimal.

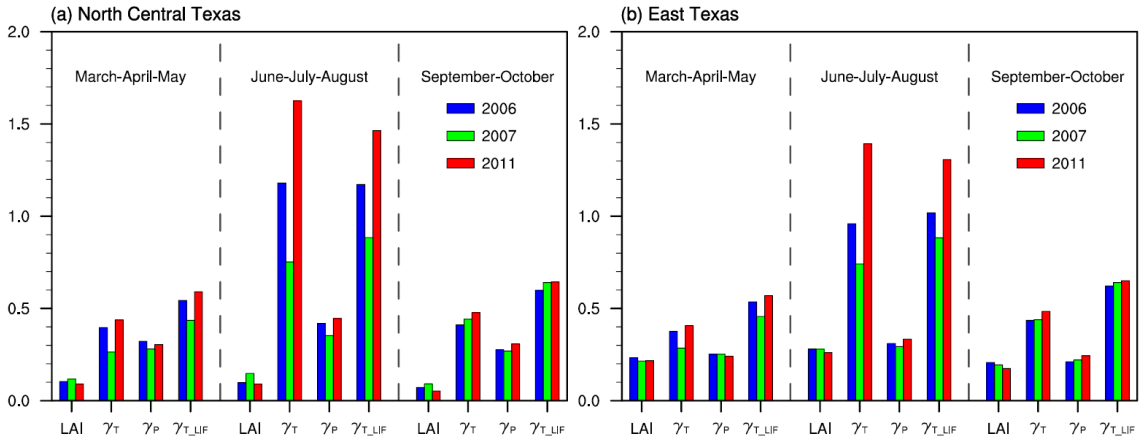

Figure 4-5: Layer-averaged LAI, temperature and light activity factors for monoterpenes during 2006, 2007 and 2011 by season and region – (a) North Central Texas and (b) East Texas. Results for South Central Texas and Upper Coast are shown in Figure C-7.

4.3.4 Uncertainty of isoprene emissions to soil moisture

In order to test the sensitivity of isoprene predictions during drought to the specific soil moisture database employed, MEGAN simulations were conducted for North Central and East Texas using the Mosaic soil moisture database in place of the Noah MP database. As demonstrated in Table 4-2, the Mosaic simulations for the all-time record drought year 2011 predicted dramatically lower isoprene emissions compared to those for the basecase (i.e., impact of soil moisture not considered) and Noah MP runs. Maximum reductions were -69% for the North Central summer compared to -12% for Noah MP. An investigation of upper-level soil moisture values revealed that Mosaic tends to predict lower moisture availability compared to Noah MP; crucially, the Mosaic wilting point values are almost a factor of two greater than those for Noah MP. The difference in the wilting points between the NLDAS-2 databases is significant because θ_{wilt} is a threshold value below which γ_{SM} is set to zero (ref. Eq. 4-4).

Table 4-2: Season-averaged isoprene emissions for the North Central and East Texas climate regions during 2011 for three MEGAN simulations: (1) basecase (impact of soil moisture not considered), (2) basecase utilizing the Noah MP soil moisture database (Noah MP), and (3) basecase utilizing the Mosaic soil moisture database (Mosaic).

Climate Region	**Months during 2011**	**Area-Averaged Daily Total Isoprene Emissions (kg/km^2/day)**			**Percentage Change Relative to Basecase**	
		Basecase	Noah MP	Mosaic	Noah MP	Mosaic
North Central Texas	Apr/May	15.1	14.0	6.7	-7%	-56%
	Jun/Jul/Aug	43.9	38.8	13.5	-12%	-69%
	Sep/Oct	8.5	7.7	2.7	-10%	-68%
East Texas	Apr/May	35.4	35.0	25.0	-1%	-29%
	Jun/Jul/Aug	104.1	96.5	59.6	-7%	-43%
	Sep/Oct	26.9	25.4	16.2	-6%	-40%

During 2011, in-situ measurements of volumetric soil moisture within the root zone were available at three locations in eastern Texas; a comparison between these limited observations and the NLDAS-2 datasets showed that Mosaic and especially Noah MP tended to be too wet in the near-surface layer and too dry at deeper depths compared to observations. The evaluation and validation of simulated soil moisture datasets is important; however, the current spatial coverage of in-situ root-zone measurements is sparse for most of the U.S. (e.g., Ochsner, et al., 2013). In addition to uncertainties in the accurate simulation of soil moisture within land surface models, substantial errors can also be introduced when sharing data between applications because outputs are often highly model-dependent (e.g., Koster et al., 2009). Previous MEGAN studies have typically employed a single soil moisture database; predicted impacts on isoprene emissions have ranged from minimal (e.g., Guenther, et al, 2006; Potosnak et al., 2014) to substantial (e.g., global isoprene reductions of 20-50% for Müller et al., 2008; Tawfik et al., 2012; Sindelarova et al., 2014) suggesting that γ_{SM} is characterized by substantial uncertainty. The high sensitivity of predicted isoprene emissions to soil moisture inputs

suggests a continued need for investigations to evaluate and improve the drought stress parameterizations and/or representations in models such as MEGAN (e.g., Potosnak, et al., 2014).

4.4 DISCUSSIONS

Drought evolves through a complex interaction of land/atmosphere processes; typical components of drought include reductions in volumetric soil moisture and increases in land/atmospheric temperatures. Table 4-3 presents the percentage change in summer activity factors between 2007, which had average-to-wet conditions, and 2011, a year characterized by all-time record drought and heat throughout Texas. The relative change in summer emissions between 2007 and 2011 is also shown. For isoprene, the γ_{SM} and emissions ratio results are provided based on both the Noah MP and Mosaic soil moisture databases.

For all climate regions, higher temperatures between 2007 and 2011 drive a nonlinear increase in the temperature activity factors (γ_T ,γ_{T_LIF}) producing a nonlinear increase in the overall activity factors; for example, the 2011 γ_T in North Central Texas is more than a factor of two greater compared to that for 2007. The light activity factors are also greater during 2011 compared to 2007, while the LAI activity factors (LAI, γ_{LAI}) show decreases. In the two central regions, drought-induced summer LAI reductions are greater than 40%, suggesting a strong negative effect of drought on summer isoprene and monoterpene emissions.

Table 4-3: Percentage change* in MEGAN activity factors and emissions of isoprene and monoterpenes by climate division between the summers of 2007 and 2011. Two soil moisture datasets were considered for isoprene emission estimates.

Isoprene	γ_{age}	LAI	γ_T	γ_P	**Noah MP**		**Mosaic**	
					γ_{SM}	Emissions	γ_{SM}	Emissions
North Central Texas	9%	-40%	123%	26%	-9%	83%	-70%	-30%
South Central Texas	10%	-44%	66%	30%	-8%	51%	-66%	-45%
East Texas	14%	-7%	94%	14%	-6%	117%	-44%	34%
Upper Coast	11%	-15%	46%	18%	-3%	74%	-71%	-46%

Monoterpenes	γ_{age}	LAI	γ_T	γ_P	γ_{T_LIF}	γ_{LAI}	γ_{SM}	Emissions
North Central Texas	-6%	-40%	112%	27%	85%	-34%	na	34%
South Central Texas	-6%	-44%	52%	30%	51%	-37%	na	7%
East Texas	-9%	-6%	78%	14%	54%	-5%	na	54%
Upper Coast	-7%	-15%	33%	18%	28%	-13%	na	23%

*Calculated as $\frac{\gamma_{2011}-\gamma_{2007}}{\gamma_{2007}}\times 100\%$. Note that "na" means not applicable

For the isoprene simulation with Noah MP, the combined negative impacts of LAI and soil moisture are dominated by emissions increases associated with leaf age, PAR and, especially, temperature. In East Texas, LAI shows a small decrease between 2007 and 2011; consequently, summer isoprene emissions increase by a factor of 2.2 compared to factors of 1.8 and 1.5 for North and South Central Texas, respectively. Significantly, if the soil moisture results from the Mosaic simulation better represent actual conditions compared to those that used Noah MP, the substantially larger decreases in isoprene emissions associated with reduced soil moisture availability would overwhelm the increases in emissions caused by warmer temperatures across most regions. The negative impacts of soil moisture and LAI reduce summer emissions by 50% in South Central and Upper Coast for the Mosaic simulation; in East Texas,

relatively lower magnitude reductions associated with LAI and soil moisture results in an emissions increase of 30% for 2011 relative to 2007.

For monoterpenes, the percentage increases in summer emissions between 2007 and 2011 are less than those for isoprene. This attenuated response can be attributed to the differential methodology used by MEGAN to estimate emissions for the two compounds. First, isoprene has a steeper temperature response than monoterpenes (Guenther et al., 2012); thus, a given temperature increase produces a greater percentage change in isoprene compared to monoterpenes. Second, the impact of leaf age on monoterpene emissions is slightly negative compared to slightly positive for isoprene. During the fall, the relative contribution of temperature on both isoprene and monoterpene emissions diminishes substantially; thus, fall isoprene emissions would range from only slightly greater during 2011 compared to 2007 for the Noah MP simulation to substantially lower during 2011 for Mosaic, while monoterpene emissions have slightly greater emissions during 2007 compared to 2011.

4.5 CONCLUSIONS

During recent years, the importance of biogenic emissions to air quality and climate has brought renewed attention to the effects of drought on isoprene and monoterpene emissions rates. Drought is a recurring phenomenon in Texas; similar to most of the central and western U.S., the frequency and intensity of Texas droughts are expected to increase over the coming decades (Melillo et al., 2014). This work quantified the variability of environmental inputs on isoprene and monoterpene emissions in eastern Texas by tracking seasonal and interannual changes in activity factors intrinsic to MEGAN; this methodology maintains an environmentally consistent (i.e., "real-world") set of model inputs. Comparisons of results between drought and non-drought years reinforced the importance of temperature on predicted emissions. Decreases in emissions

associated with reduced LAI during periods of drought were dominated by emission increases caused by much warmer temperatures. MEGAN sensitivity simulations using two different soil moisture datasets demonstrated that the soil moisture activity factor is subject to large uncertainty; dependent on the soil moisture database employed, predicted reductions in isoprene emissions ranged from nearly negligible to almost -70% during the summer of 2011, a time period characterized by all-time record drought in Texas.

4.6 REFERENCES

Arneth, A., Schurgers, G., Lathiere, J., Duhl, T., Beerling, D. J., Hewitt, C. N., ... & Guenther, A. (2011). Global terrestrial isoprene emission models: sensitivity to variability in climate and vegetation. *Atmospheric Chemistry and Physics*, *11*(15), 8037-8052.

Atkinson, R. (2000). Atmospheric chemistry of VOCs and NO_x. *Atmospheric Environment*, *34*(12), 2063-2101.

Burnash, R. J. C., Ferral, R. L., & McGuire, R. A. (1973), A generalized streamflow simulation system: Conceptual models for digital computer. Technical report, joint Federal-State River Forecast Center, Sacramento, Calif.

Cai, X., Yang, Z. L., David, C. H., Niu, G. Y., & Rodell, M. (2014a). Hydrological evaluation of the Noah-MP land surface model for the Mississippi River Basin. *Journal of Geophysical Research: Atmospheres*, *119*(1), 23-38.

Cai, X., Yang, Z.-L., Xia, Y., Huang, M., Wei, H., Leung, L. R. & Ek, M. B. (2014b). Assessment of simulated water balance from Noah, Noah-MP, CLM, and VIC over CONUS using the NLDAS test bed. *Journal of Geophysical Research: Atmospheres*, *119*.

Chen, J., Avise, J., Guenther, A., Wiedinmyer, C., Salathe, E., Jackson, R. B., & Lamb, B. (2009). Future land use and land cover influences on regional biogenic emissions and air quality in the United States. *Atmospheric Environment*, *43*(36), 5771-5780.

Claeys, M., Graham, B., Vas, G., Wang, W., Vermeylen, R., Pashynska, V., ... & Maenhaut, W. (2004). Formation of secondary organic aerosols through photooxidation of isoprene. *Science*, *303*(5661), 1173-1176.

Ek, M. B., Mitchell, K. E., Lin, Y., Rogers, E., Grunmann, P., Koren, V., ... & Tarpley, J. D. (2003). Implementation of Noah land surface model advances in the National Centers for Environmental Prediction operational mesoscale Eta model. *Journal of Geophysical Research: Atmospheres (1984–2012)*, *108*(D22).

Ferreira, J., Reeves, C. E., Murphy, J. G., Garcia-Carreras, L., Parker, D. J., & Oram, D. E. (2010). Isoprene emissions modelling for West Africa: MEGAN model evaluation and sensitivity analysis. *Atmospheric Chemistry and Physics*,*10*(17), 8453-8467.

Fischbach, R. J., Staudt, M., Zimmer, I., Rambal, S., & Schnitzler, J. P. (2002). Seasonal pattern of monoterpene synthase activities in leaves of the evergreen tree Quercus ilex. *Physiologia Plantarum*, *114*(3), 354-360.

Fu, Y., & Liao, H. (2012). Simulation of the interannual variations of biogenic emissions of volatile organic compounds in China: Impacts on tropospheric ozone and secondary organic aerosol. *Atmospheric Environment*, *59*, 170-185.

Geng, F., Tie, X., Guenther, A., Li, G., Cao, J., & Harley, P. (2011). Effect of isoprene emissions from major forests on ozone formation in the city of Shanghai, China. *Atmospheric Chemistry and Physics*, *11*(20), 10449-10459.

Guenther, A. B., Jiang, X., Heald, C. L., Sakulyanontvittaya, T., Duhl, T., Emmons, L. K., & Wang, X. (2012). The Model of Emissions of Gases and Aerosols from Nature version 2.1 (MEGAN2. 1): an extended and updated framework for modeling biogenic emissions, Geoscientific Model Development Discussions, 5, 1503-1560.

Guenther, A., Karl, T., Harley, P., Wiedinmyer, C., Palmer, P. I., & Geron, C. (2006). Estimates of global terrestrial isoprene emissions using MEGAN (Model of Emissions of Gases and Aerosols from Nature). *Atmospheric Chemistry and Physics*, *6*(11), 3181-3210.

Gulden, L. E., Yang, Z. L., & Niu, G. Y. (2007). Interannual variation in biogenic emissions on a regional scale. *Journal of Geophysical Research: Atmospheres (1984–2012)*, *112*(D14).

Han, K. M., Park, R. S., Kim, H. K., Woo, J. H., Kim, J., & Song, C. H. (2013). Uncertainty in biogenic isoprene emissions and its impacts on tropospheric chemistry in East Asia. *Science of The Total Environment*, *463*, 754-771.

Heald, C. L., Henze, D. K., Horowitz, L. W., Feddema, J., Lamarque, J. F., Guenther, A., ... & Fung, I. (2008). Predicted change in global secondary organic aerosol concentrations in response to future climate, emissions, and land use change. *Journal of Geophysical Research: Atmospheres (1984–2012)*,*113*(D5).

Holm, J. A., Jardine, K., Guenther, A. B., Chambers, J. Q., & Tribuzy, E. (2014). Evaluation of MEGAN-CLM parameter sensitivity to predictions of isoprene emissions from an Amazonian rainforest. *Atmospheric Chemistry and Physics Discussions*, *14*, 23995-24041.

Huang, L., McDonald-Buller, E. C., McGaughey, G., Kimura, Y., & Allen, D. T. (2014). Annual variability in leaf area index and isoprene and monoterpene emissions during drought years in Texas. *Atmospheric Environment*, *92*, 240-249.

Kleindienst, T. E., Jaoui, M., Lewandowski, M., Offenberg, J. H., Lewis, C. W., Bhave, P. V., & Edney, E. O. (2007). Estimates of the contributions of biogenic and anthropogenic hydrocarbons to secondary organic aerosol at a southeastern US location. *Atmospheric Environment*, *41*(37), 8288-8300.

Koster, R. D., Guo, Z., Yang, R., Dirmeyer, P. A., Mitchell, K. & Puma, M. J. (2009). On the nature of soil moisture in land surface models. *Journal of Climate, 22,* 4322–4335.

Koster, R., & Suarez, M. (1996). Energy and water balance calculations in the Mosaic LSM. NASA Technical Memorandum, NASA TM-104606, Volume 9, 60 pp.

Kuhn, U., Rottenberger, S., Biesenthal, T., Wolf, A., Schebeske, G., Ciccioli, P., & Kesselmeier, J. (2004). Strong correlation between isoprene emission and gross photosynthetic capacity during leaf phenology of the tropical tree species Hymenaea courbaril with fundamental changes in volatile organic compounds emission composition during early leaf development. *Plant, Cell & Environment*,*27*(12), 1469-1485.

Lamb, B., Gay, D., Westberg, H., & Pierce, T. (1993). A biogenic hydrocarbon emission inventory for the USA using a simple forest canopy model. *Atmospheric Environment. Part A. General Topics*, *27*(11), 1673-1690.

Lathiere, J., Hewitt, C. N., & Beerling, D. J. (2010). Sensitivity of isoprene emissions from the terrestrial biosphere to 20th century changes in atmospheric CO2 concentration, climate, and land use. *Global Biogeochemical Cycles*,*24*(1).

Lawrence, D. M., Oleson, K. W., Flanner, M. G., Thornton, P. E., Swenson, S. C., Lawrence, P. J., ... & Slater, A. G. (2011). Parameterization improvements and functional and structural advances in version 4 of the Community Land Model. *Journal of Advances in Modeling Earth Systems*, *3*(1).

Liang, X., Lettenmaier, D. P., Wood, E. F., & Burges, S. J. (1994). A simple hydrologically based model of land surface water and energy fluxes for general circulation models. *Journal of Geophysical Research, 99*(D7), 14415-14428.

Lusebrink, I., Evenden, M. L., Blanchet, F. G., Cooke, J. E., & Erbilgin, N. (2011). Effect of water stress and fungal inoculation on monoterpene emission from an historical and a new pine host of the mountain pine beetle. *Journal of chemical ecology*, *37*(9), 1013-1026.

Melillo, J.M., Richmond, T.C., & Yohe, G.W. (2014). Climate Change Impacts in the United States. *Third National Climate Assessment*. US Global Change Research Program.

Mitchell, K. E., Lohmann, D., Houser, P. R., Wood, E. F., Schaake, J. C., Robock, A., ... & Bailey, A. A. (2004). The multi-institution North American Land Data Assimilation System (NLDAS): Utilizing multiple GCIP products and partners in a continental distributed hydrological modeling system. *Journal of Geophysical Research: Atmospheres (1984–2012)*, *109*(D7).

Niu, G.-Y., et al. (2011). The community Noah land surface model with multiparameterization options (Noah-MP): 1. Model description and evaluation with local-scale measurements. *Journal of Geophysical Research*, *116*.

Ochsner, T. E., Cosh, M. H., Cuenca, R. H., Dorigo, W. A., Draper, C. S., Hagimoto, Y., ... & Zreda, M. (2013). State of the art in large-scale soil moisture monitoring. *Soil Science Society of America Journal*, *77*(6), 1888-1919.

Ormeno, E., Mevy, J. P., Vila, B., Bousquet-Melou, A., Greff, S., Bonin, G., & Fernandez, C. (2007). Water deficit stress induces different monoterpene and sesquiterpene emission changes in Mediterranean species. Relationship between terpene emissions and plant water potential. *Chemosphere*, *67*(2), 276-284.

Pegoraro, E., Rey, A., Greenberg, J., Harley, P., Grace, J., Malhi, Y., & Guenther, A. (2004). Effect of drought on isoprene emission rates from leaves of *Quercus virginiana* Mill. *Atmospheric Environment*, *38*(36), 6149-6156.

Petron, G., Harley, P., Greenberg, J., & Guenther, A. (2001). Seasonal temperature variations influence isoprene emission. *Geophysical Research Letters*, *28*(9), 1707-1710.

Potosnak, M. J., LeStourgeon, L., Pallardy, S. G., Hosman, K. P., Gu, L., Karl, T., ... & Guenther, A. B. (2014). Observed and modeled ecosystem isoprene fluxes from an oak-dominated temperate forest and the influence of drought stress. *Atmospheric Environment*, *84*, 314-322.

Rodríguez-Calcerrada, J., Buatois, B., Chiche, E., Shahin, O., & Staudt, M. (2013). Leaf isoprene emission declines in *Quercus pubescens* seedlings experiencing drought–Any implication of soluble sugars and mitochondrial respiration?. *Environmental and Experimental Botany*, *85*, 36-42.

Rosenstiel, T. N., Potosnak, M. J., Griffin, K. L., Fall, R., & Monson, R. K. (2003). Increased CO_2 uncouples growth from isoprene emission in an agriforest ecosystem. *Nature*, *421*(6920), 256-259.

Sharkey, T. D., Singsaas, E. L., Vanderveer, P. J., & Geron, C. (1996). Field measurements of isoprene emission from trees in response to temperature and light. *Tree Physiology*, *16*(7), 649-654.

Sindelarova, K., Granier, C., Bouarar, I., Guenther, A., Tilmes, S., Stavrakou, T., ... & Knorr, W. (2014). Global data set of biogenic VOC emissions calculated by the MEGAN model over the last 30 years. *Atmospheric Chemistry and Physics*, *14*(17), 9317-9341.

Situ, S., Wang, X., Guenther, A., Zhang, Y., Wang, X., Huang, M., ... & Xiong, Z. (2014). Uncertainties of isoprene emissions in the MEGAN model estimated for a coniferous and broad-leaved mixed forest in Southern China. *Atmospheric Environment*, *98*, 105-110.

Smiatek, G., & Bogacki, M. (2005). Uncertainty assessment of potential biogenic volatile organic compound emissions from forests with the Monte Carlo method: Case study for an episode from 1 to 10 July 2000 in Poland. *Journal of Geophysical Research: Atmospheres (1984–2012)*, *110*(D23).

Stavrakou, T., Müller, J. F., Bauwens, M., De Smedt, I., Van Roozendael, M., Guenther, A., ... & Xia, X. (2014). Isoprene emissions over Asia 1979–2012: impact of climate and land-use changes. *Atmospheric Chemistry and Physics*,*14*(9), 4587-4605.

Tawfik, A. B., Stöckli, R., Goldstein, A., Pressley, S., & Steiner, A. L. (2012). Quantifying the contribution of environmental factors to isoprene flux interannual variability. *Atmospheric Environment*, 54, 216-224.

Tingey, D. T., Manning, M., Grothaus, L. C., & Burns, W. F. (1980). Influence of light and temperature on monoterpene emission rates from slash pine. *Plant Physiology*, *65*(5), 797-801.

Tsigaridis, K., & Kanakidou, M. (2003). Global modelling of secondary organic aerosol in the troposphere: a sensitivity analysis. *Atmospheric Chemistry and Physics*, *3*(5), 1849-1869.

Wiedinmyer, C., Guenther, A., Estes, M., Strange, I. W., Yarwood, G., & Allen, D. T. (2001). A land use database and examples of biogenic isoprene emission estimates for the state of Texas, USA. *Atmospheric Environment*, *35*(36), 6465-6477.

Wiedinmyer, C., Tie, X., Guenther, A., Neilson, R., & Granier, C. (2006). Future changes in biogenic isoprene emissions: how might they affect regional and global atmospheric chemistry? *Earth Interactions*, *10*(3), 1-19.

Wilkinson, M. J., Monson, R. K., Trahan, N., Lee, S., Brown, E., Jackson, R. B., ... & Fall, R. A. Y. (2009). Leaf isoprene emission rate as a function of atmospheric CO2 concentration. *Global Change Biology*, *15*(5), 1189-1200.

Chapter 5: Comparison of Regional and Global Land Cover Products and the Implications for Biogenic Emissions Modeling

The material presented in this Chapter has been published in *JAWMA*
Huang, L.; McDonald-Buller, E.; McGaughey, G.; Kimura, Y.; Allen, D. T. *Journal of the Air & Waste Management Association*. **2015**, doi:10.1080/10962247.2015.1057302
Dr. Elena McDonald-Buller and Dr. David Allen are the co-supervisors of this work, providing comments and final reviews of this work. Mr. Gary McGaughey and Dr. Yosuke Kimura are research scientists, contributing to suggestions and part of data analysis and modeling work.

5.1 INTRODUCTION

Vegetation is a major source of biogenic volatile organic compound (BVOC) emissions, which have important roles in atmospheric chemistry (Fehsenfeld et al., 1992; Chameides et al., 1988; Kavouras et al., 1998; Tsigaridis and Kanakidou, 2003) and climate (Sanderson et al., 2003; Pacifico et al., 2009). Among the hundreds of BVOCs identified, isoprene and monoterpenes are among the most significant because of their relative abundance (Sindelarova et al., 2014), high chemical reactivity (Atkinson, 2000), and contributions to the formation of ozone (Chameides et al., 1988) and secondary organic aerosols (Hoffmann et al. 1997; Claeys et al., 2004; Carlton et al., 2009). Globally, isoprene and monoterpenes account for 70% and 11% of the total BVOCs emitted annually (Sindelarova et al., 2014). Average Texas statewide daily BVOC emissions were approximately 11,650 tons per day and ranked first within the continental United States in the 2011 National Emission Inventory (NEI) version 1 (EPA, 2014). Estimated emissions in Texas are not homogeneously distributed across the state. As noted by Song et al. (2008), biogenic emissions overwhelm anthropogenic emissions in the heavily forested eastern half of Texas, the latter dominates in highly developed urban areas, and yet a number of transition areas exist where both are important to the overall VOC inventories. Accurate emission inventories from both anthropogenic and biogenic sources are required for air quality models that support the development of air quality

management plans and attainment demonstrations in Texas and elsewhere in the United States where BVOCs comprise substantial fractions of the total VOC emission inventories.

For most biogenic emission models, land cover characterization, i.e. the distribution of plant functional types (PFTs), is an essential driving variable as it determines the phenological emission potential of a region (Kim et al., 2014). For instance, grasses and cropland are generally expected to have lower monoterpene emission potentials (Guenther et al., 2000) than needleleaf evergreen forest (Guenther et al., 1994). Previous studies have reported the influences of different land cover representations on modeled biogenic emissions and subsequent ozone predictions at regional and global scale (e.g. Byun et al., 2005; Guenther et al., 2006; Gulden et al., 2008; Steinbrecher et al., 2009; Kim et al., 2014; Drewniak et al., 2014). For example, Gulden et al. (2008) found that differences in vegetation profiles could lead to variations of a factor of three in mean Texas statewide biogenic emission estimates. Texas has highly diverse land use/land cover profiles over its ten climate regions. Major land cover types change from grasses and crops in the central regions to heavily forested areas towards the east. The objective of this study was to investigate the influences of different land cover representations on the estimation of isoprene and monoterpene emissions by the Model of Emissions of Gases and Aerosols from Nature (MEGAN) over eastern Texas using the Moderate Resolution Imaging Spectroradiometer (MODIS) global land cover product and a regional product with high spatial resolution and detailed land cover categories developed for the Texas Commission on Environmental Quality (TCEQ). In addition, emission estimates generated using MEGAN's default input data, including the default PFT distribution and gridded emission factor maps, were compared with results generated using the MODIS and TCEQ land cover data for eastern Texas. MEGAN

simulations were conducted to examine the influences of different land cover datasets on the standard emission potential and emission activity factors, both separately and simultaneously. Biogenic emissions generated from different land cover scenarios were used to drive air quality simulations using the Comprehensive Air Quality Model with Extensions (CAMx, version 6.10; ENVIRON, 2014) to examine the effects on predicted ground-level ozone concentrations.

5.2 METHODOLOGY

5.2.1 MEGAN default PFT data and emission factor (EF) maps

MEGAN version 2.1 adopts the Community Land Model (CLM4) PFT scheme with a total of 16 plant functional types (Guenther et al., 2012). A default PFT dataset with a spatial resolution of 30 arc-seconds for North America is available from http://lar.wsu.edu/megan/guides.html. Only a subset of these PFTs exists in Texas, including needleleaf evergreen temperate tree (PFT1), needleleaf deciduous boreal tree (PFT2), broadleaf evergreen temperate tree (PFT5), broadleaf deciduous temperate tree (PFT7), broadleaf deciduous temperate shrub (PFT10), cool C3 grass (PFT13), warm C4 grass (PFT14), other crops (PFT15) and corn (PFT16). MEGAN2.1 also provides gridded emission factor (EF) maps based on species composition. The default MEGAN configuration uses the default PFT distribution and gridded EF maps.

5.2.2 MODIS land cover product (MCD12Q1)

The MODIS land cover product is a crucial input for several MODIS products, including the MODIS Leaf Area Index and Fraction of Absorbed Photosynthetically Active Radiation (LAI/fPAR; Knyazikhin et al., 1999) and Gross/Net Primary Productivity (Running et al., 1999). The latest version of the MODIS land cover product - version 051 (MCD12Q1; Friedl et al., 2010) provides five types of land cover

classification schemes at annual time steps and 500 m spatial resolution available since 2001. Type 5 data (shown in Figure 5-1a), with eight plant functional types and four non-vegetated classes (Bonan et al. 2002), was mapped to valid PFTs in Texas (see Table D-1). For example, MODIS grass was mapped to MEGAN cool C3 grass (PFT13) and warm C4 grass (PFT14). The distribution of the two grass types was determined by the area-averaged ratio of C3 to C4 grass of MEGAN's default PFT data. A similar treatment was applied to map MODIS cereal crops and broadleaf crops into crops (PFT15) and corn (PFT16). The fractional coverage of each MEGAN PFT was calculated as the total area of the 500-m grid cells mapped as the corresponding PFT over the area of the 1-km grid cell.

5.2.3 TCEQ land cover product

A regional land cover product for air quality modeling in Texas was developed by Popescu et al. (2011) for the TCEQ by combining three existing databases: LANDFIRE (previously known as the Landscape Fire and Resources Management Planning Tools Project from 2004 to 2009), the 2001 National Land Cover Dataset (NLCD) and the Texas Parks and Wildlife Department (TPWD) Texas Ecological System Classification Project. The LANDFIRE and 2001 NLCD products were derived from Landsat imagery (Rollins et al., 2009; Homer et al., 2007); the TPWD Texas Ecological System Classification Project relied on field data collection and aerial photography to provide a land classification map at 10 m for Texas (http://tpwd.texas.gov/landwater/land/maps/gis/tescp/index.phtml). As shown in Figure 5-1b, this regional land cover product consisted of 36 land cover categories with 30-m spatial resolution. The TCEQ land cover classes were mapped to valid MEGAN's PFTs (see Table D-2). For each 1-km MEGAN grid cell, the fractional coverage of each PFT

was determined by summing the number of 30-m resolution cells whose centroid fell within a given grid cell.

(a)

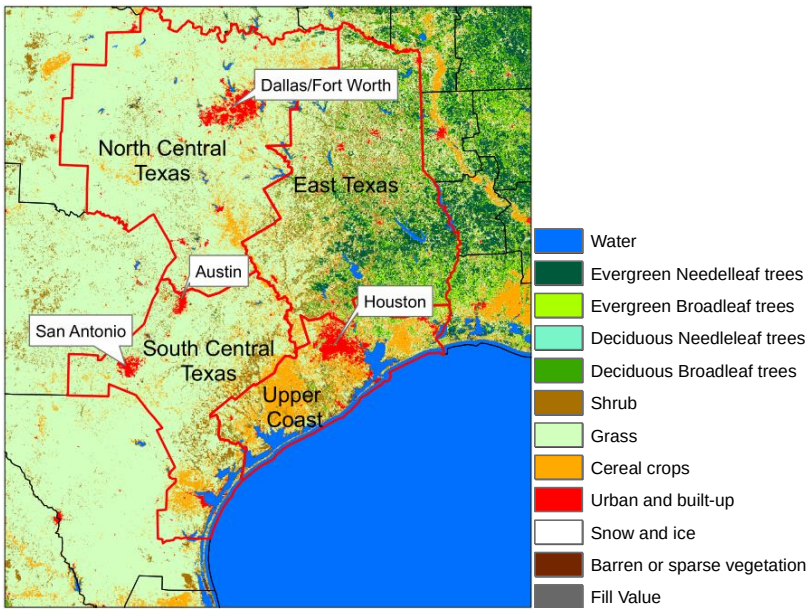

(b)

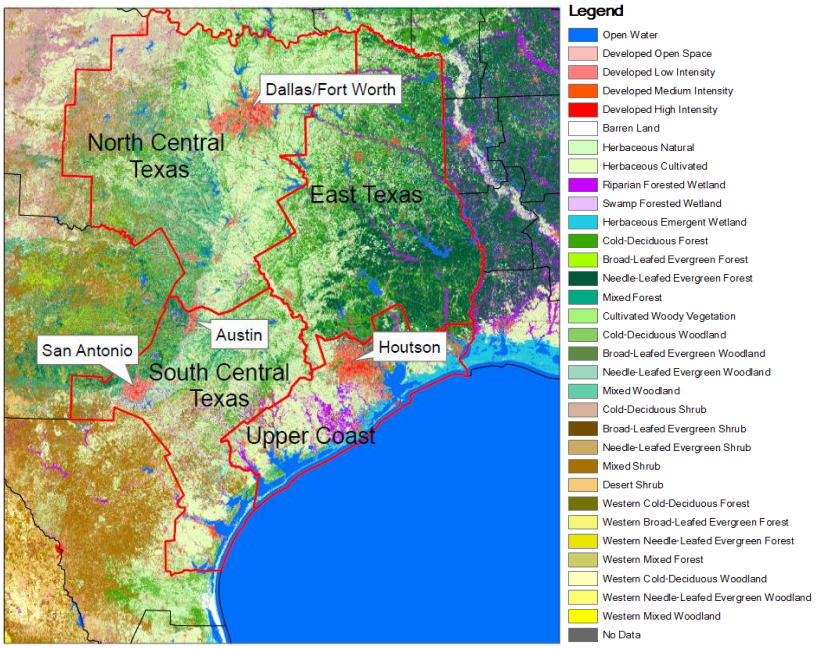

Figure 5-1: (a) MODIS Land Cover Type 5 Product (MCD12Q1) over eastern Texas for 2011. (b) Thirty-six land cover/land use types in eastern Texas developed for the TCEQ by Popescu et al. (2011). Developed metropolitan areas are shown in red.

5.2.4 MEGAN configuration

The emission rate (F) of isoprene/monoterpenes in units of flux (μg m^{-2} ground area h^{-1}) in MEGAN version 2.1 (http://lar.wsu.edu/megan/guides.html) is calculated as:

$$F = \gamma \cdot \sum \varepsilon_j \chi_j \qquad \text{Eq. 5-1}$$

where ε is the basal emission factor for vegetation type j with fractional coverage χ_j within a model grid; it represents the emission rate under standard environmental conditions with an air temperature of 303 K, solar angle of 60°, photosynthetic photon flux density (PPFD) transmission of 0.6, LAI of 5 m^2/m^2 consisting of 80% mature, 10% growing and 10% old foliage (Guenther et al., 2006, 2012). The standard emission potential (SEP) is identified as the summation term ($\sum \varepsilon_j \chi_j$). The SEP can be directly determined by the PFT distribution and PFT-specific emission factors or can be specified from prescribed gridded emission factor maps (Guenther et al., 2012). γ is the overall emission activity factor that is calculated based on the multiplication of several individual activity factors which account for variations in environmental conditions (e.g. temperature, light, leaf area index). Parameters are described in detail by Guenther et al. (2012). In MEGAN's canopy environment model, the distributions of light and temperature within the canopy are influenced by PFT-specific characteristics including canopy height/depth and leaf width/length; thus PFT distribution is also implicitly incorporated within the calculation of the overall activity factor. The soil moisture algorithm was not applied in the MEGAN configuration for this study but has been examined elsewhere (e.g. Tawfik et al., 2012; Potosnak et al., 2014; Huang et al., 2014; 2015).

The MEGAN configuration follows the approach of Huang et al. (2014), which utilized the National Centers for Environmental Predictions – North American Regional Reanalysis (NCEP-NARR) meteorological data (temporal/spatial resolution: 3 h/32 km),

MODIS 4-day LAI product (MCD15A3; spatial resolution: 1 km), Photosynthetically Active Radiation (PAR) produced using the surface insolation data (with a conversion factor of 0.45) from the Geostationary Operational Environmental Satellites (GOES; temporal/spatial resolution: 1 h/4 km) that were obtained from the University of Alabama in Huntsville, and the remapped MODIS or TCEQ land cover products. The horizontal resolution of the MEGAN configuration was 1 km x 1 km.

In order to investigate the influence of differences in land cover characterization on estimates of isoprene and monoterpene emissions, three sets of MEGAN simulations were conducted over eastern Texas. For each set of simulations, parallel MEGAN simulations were conducted using either the year-specific MODIS or the TCEQ land cover product while leaving other inputs (e.g. meteorological inputs, LAI) unchanged. The first set of MEGAN simulations (SM1) characterized the influence of different land cover data on the standard emission potential (SEP) by artificially assigning the activity factor (γ) to be unity. For the second set of simulations (SM2), year-specific meteorological fields and LAI data were used to drive MEGAN simulations for March-October within a six-year-period (2006-2011), during which Texas experienced relatively wet conditions (e.g. 2007) as well as extreme to exceptional drought (e.g. 2006 and 2011; Huang et al., 2014). Emission activity factors (γ) were first compared to investigate the differences associated with different land cover products. Then resulting emissions were contrasted to examine the influences on the SEP and emission activity factor simultaneously. For the third simulation (SM3), MEGAN's default emission factor maps were utilized in both land cover scenarios to demonstrate the use of a prescribed emission factor map. Monthly isoprene and monoterpene emissions (or emission activity factors for SM2) were assessed for four climate regions in eastern Texas – North Central Texas, South Central Texas, East Texas and Upper Coast – which included most large

metropolitan areas in the state (Figure 5-1). Results were also generated using MEGAN's default PFT data and/or default emission factor maps.

5.2.5 CAMx configuration

CAMx simulations were conducted over eastern Texas in order to examine the effects of land cover characterization on predicted ground-level ozone concentrations. An existing CAMx episode was used that spanned May 31 - July 2, 2006. The episode was developed by the TCEQ to support air quality planning efforts across areas in eastern Texas. CAMx version 6.10 was used with Carbon Bond 6 revision 2 (CB6r2) (Yarwood et al., 2012; Ruiz and Yarwood, 2013) as the gas-phase chemistry mechanism and the Zhang algorithm for dry deposition (Zhang et al., 2003). Meteorological fields were developed using the Weather Research and Forecasting (WRF) model. Boundary and initial conditions were generated by the Goddard Earth Observing System chemical transport model (GEOS-Chem). Horizontal grid domains for the episode are shown in Figure D-1; additional information regarding the CAMx configuration and model performance evaluation can be found at https://www.tceq.texas.gov/airquality/airmod/data/tx2006. The 4-km CAMx domain matched the MEGAN modeling domain; biogenic emission estimates from MEGAN that had a horizontal resolution of 1 km were aggregated to a 4-km spatial resolution. Biogenic emission estimates generated from the TCEQ and MODIS land cover data (identified as MEGAN SM2) were used to drive parallel CAMx simulations. The simulations differed only in the substitution of biogenic emissions generated from the different land cover scenarios while the configuration and all other inputs remained identical.

5.3 RESULTS AND DISCUSSION

5.3.1 Intercomparison of land cover products

Figure 5-2 shows the spatial distributions of PFTs from the mappings of the MODIS (averaged during 2006-2011) and TCEQ land cover products over eastern Texas. MEGAN's default PFT data are also shown for comparison. In general for the domain, the MODIS land cover data exhibited the highest coverage of C3 and C4 grasses; TCEQ data indicated the highest tree and shrub coverage while cropland was most abundant in MEGAN's default PFT data. The spatial distributions of the TCEQ and MEGAN's default PFT data were similar although their magnitudes differed. Figure 5-3 shows the area-averaged percent coverage of each PFT by climate region (corresponding values are shown in Table D-3). North and South Central Texas (referred to as Central Texas) were dominated by C3 and C4 grasses in the MODIS land cover product with combined area percentages of 84% and 68%, respectively; tree coverage was negligible (<2%). In contrast, the TCEQ land cover indicated significantly higher tree coverage (~28%; including all tree PFTs) in Central Texas with grass coverage of approximately 35%. MEGAN's default PFT data suggested a similar PFT profile with the TCEQ data in Central Texas, except the former classified large portions of grassland as crops (>30%) in South Central Texas. Less tree (~36%) and more grass (~40%) coverage in the MODIS data was also evident in East Texas relative to the other two products; the TCEQ data suggested more than two-thirds of the area in East Texas was tree coverage while MEGAN's default PFT data indicated comparable coverage of needleleaf evergreen temperate/broadleaf deciduous temperate trees and crops in East Texas. Both the MODIS land cover and MEGAN's default data suggested more substantial crop coverage (~30%) than the TCEQ data within the Upper Coast climate region.

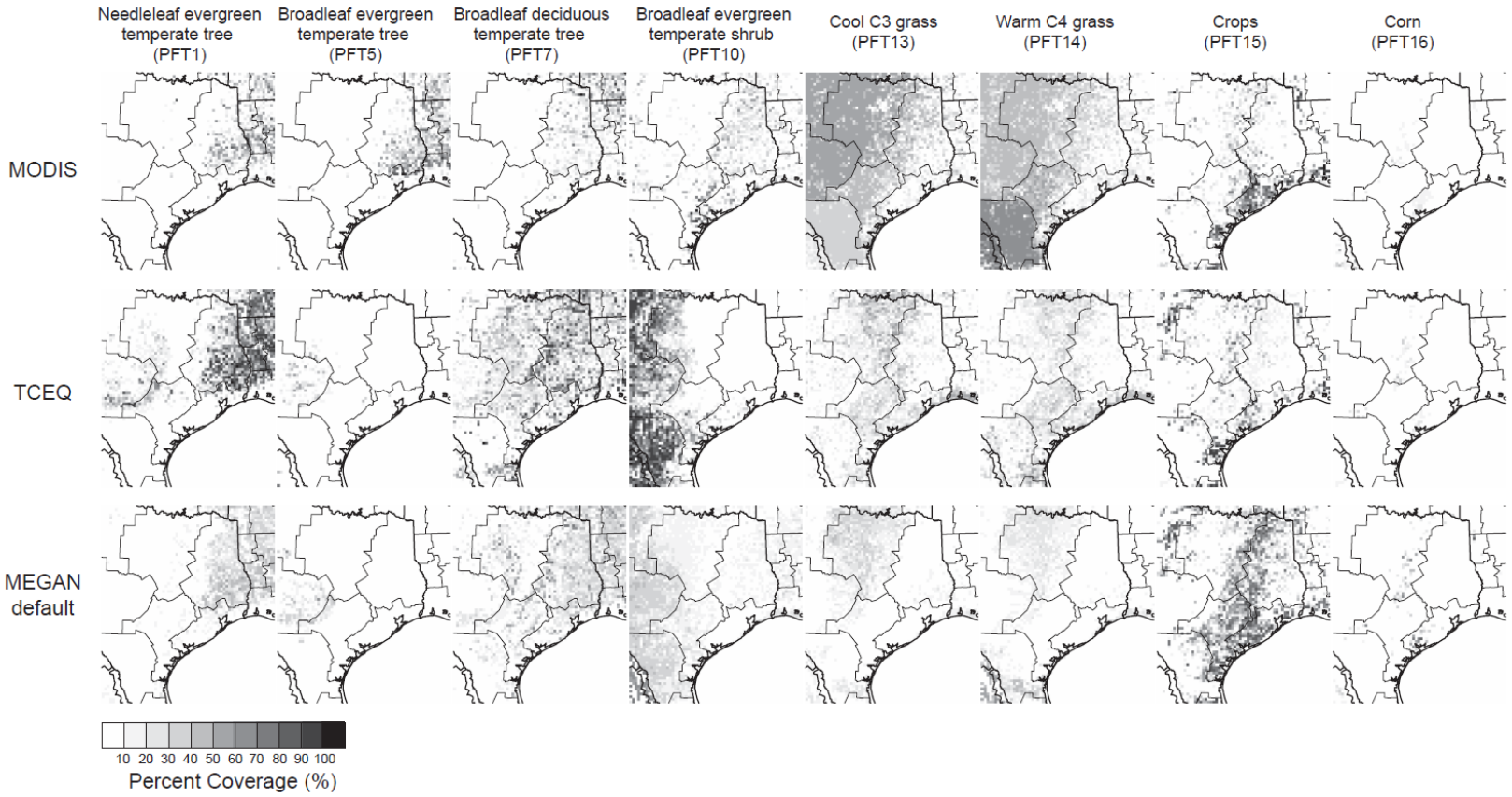

Figure 5-2: Percent coverage of PFTs for the MODIS (averaged during 2006-2011) and TCEQ land cover products and MEGAN's default PFT distribution. Note that needleleaf deciduous boreal tree (PFT2) was not shown due to negligible coverage.

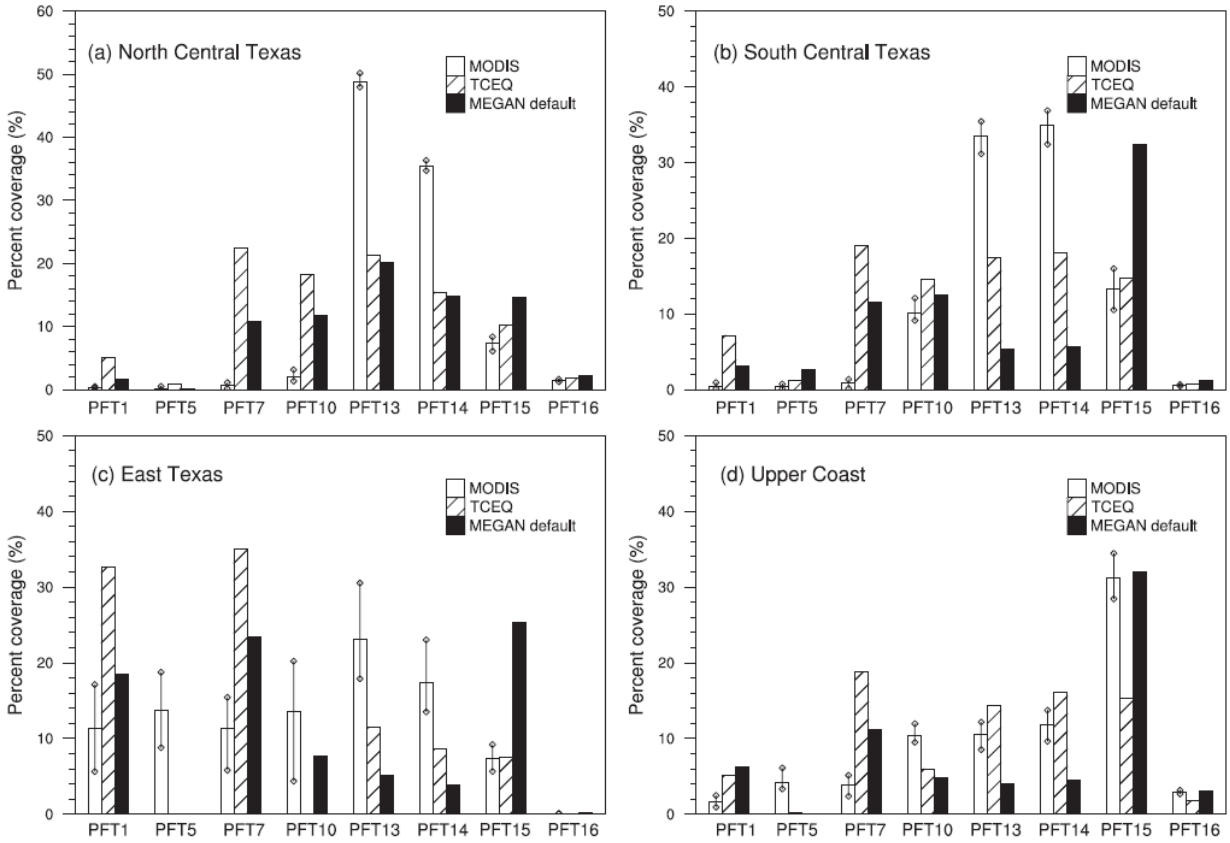

Figure 5-3: Area-averaged percent PFT coverage in (a) North Central Texas, (b) South Central Texas, (c) East Texas and (d) the Upper Coast for the MODIS and TCEQ land cover products and MEGAN's default PFT distribution (see Figure 5-2 for PFT descriptions). Note that needleleaf deciduous boreal tree (PFT2) was not shown due to low coverage. Black lines confine the maximum and minimum range during 2006-2011.

Potential causes for the disagreements between the land cover datasets include differences in the classification methodology, the type of satellite sensors used, uncertainty associated with the reprojection, and differences in the data spatial resolution (McCallum et al., 2006; Pouliot et al., 2014; Quaife et al., 2008). MEGAN's default PFT data were generated for North America for the 2008 time period by combining the 2001 NLCD and the Landsat based Cropland Data Layer (Guenther et al., 2012). The MODIS land cover product was developed using a top-down supervised approach based on 1860

training sites around the globe with an overall accuracy of approximately 75% (Friedl et al., 2002, 2010); yet eastern Texas was not well represented in the training sites. In contrast, the TCEQ land cover was specifically generated for air quality modeling in Texas and was developed by aggregating the much more detailed LANDFIRE classes into the Texas Land Classification System (Popescu et al., 2011). The accuracy of the LANDFIRE product in Texas and neighboring states to the northeast ranges between 60-84% and is expected to be higher when aggregated (Popescu et al., 2011). Reprojection of the MODIS dataset from the original sinusoidal projection to Lambert Conformal conic projection could result in some loss of data as suggested by Pouliot et al. (2014). The coarser spatial resolution of the MODIS land cover product (500 m) could also result in loss of information regarding classifications when mixed land cover types exist within a single pixel (Quaife et al., 2008). However, as shown by Figure 5-3, the year-specific MODIS land cover product exhibits substantial interannual variations, particularly for East Texas. For instance, broadleaf deciduous temperate trees (with high isoprene emission potential; Table D-1) covered approximately 15% of the area of East Texas during 2007, a relatively wetter year, but dropped to 6% during 2011, a historical drought year. Part of this change could be associated with drought-induced tree mortality during 2011 (Texas A&M Forest Service, 2012). The TCEQ land cover data, although it has much higher spatial resolution, may not fully capture recent year-to-year changes in vegetation distributions, particularly during and after 2011, a year with exceptional drought. Nevertheless, discrepancies between the land cover datasets suggest that differences in land cover characterization have the potential to influence model predictions of isoprene and monoterpene emissions through PFT-dependent basal emission factors and emission activity factors.

5.3.2 Sensitivity of isoprene and monoterpene emissions to land cover characterization

Standard emission potential (SEP). With the emission activity factor (γ) assigned as unity (i.e. MEGAN simulation SM1), the resulting isoprene or monoterpene emission rate from eq 1 represents the standard emission potential. Figure D-2 contrasts the spatial distribution of isoprene and monoterpene SEPs over eastern Texas generated using the MODIS (averaged over 2006-2011) and the TCEQ land cover products and PFT-specific basal emission factors, respectively. The spatial distributions of isoprene and monoterpene SEPs were consistent with the distribution of PFTs with strong basal emission rates (i.e. the first four PFTs in Figure 5-2). For example, the significant SEPs in East Texas with the MODIS land cover product were consistent with tree and shrub coverage; even with substantial coverage, grass contributed negligibly to the isoprene and monoterpene SEPs. The SEPs generated using MEGAN's default emission factor maps are also shown in Figure D-2. It should be noted that MEGAN's default emission factor maps were not directly generated from MEGAN's default PFT data and PFT-specific basal emission factors; rather the PFT-specific basal emission factors listed in Table D-1 represent area-weighted global averages of different ecoregions (Guenther et al., 2012).

Figure 5-4 shows area-averaged isoprene and monoterpene SEPs by climate region. East Texas had the highest isoprene and monoterpene SEPs among the four climate regions, attributed to the dense forest coverage. Overall, isoprene SEPs obtained from the TCEQ product were more similar than the MODIS product to MEGAN's default emission factor map; the opposite trend was evident for monoterpene SEPs. In North Central Texas, the MODIS land cover characterization resulted in significantly lower values of isoprene (by 80%) and monoterpene (by 87%) SEPs relative to the TCEQ land cover (Figure 5-4). Findings were similar in South Central Texas. The substantially lower SEPs with the MODIS data were associated with lower tree coverage, because the

basal emission factors for isoprene and monoterpenes (sum of myrcene, sabinene, limonene, 3-carene, α-pinene, β-pinene, and *t*-β-ocimene) assigned for trees were considerably higher than those for grasses and crops (see Table D-1).

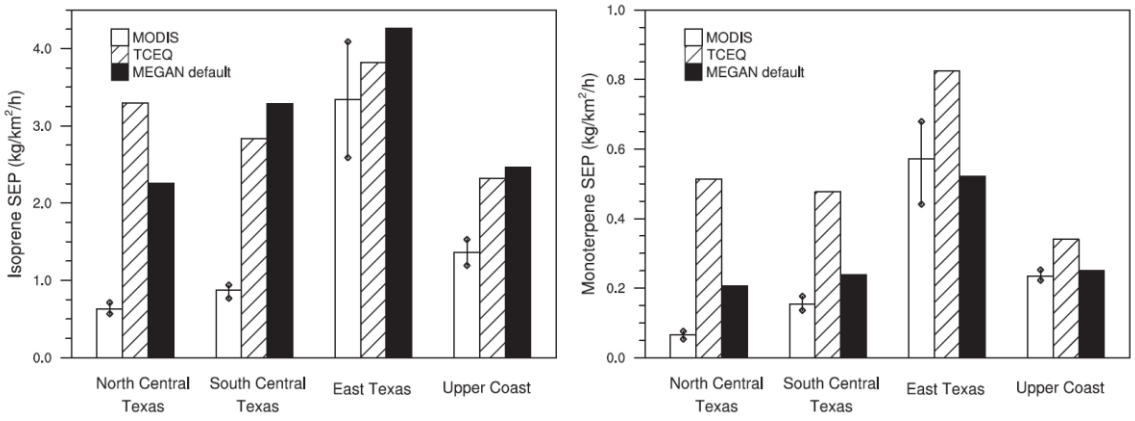

Figure 5-4: Area-averaged isoprene (left) and monoterpene (right) SEPs (kg/km^2/h) generated by the MODIS (averaged over 2006-2011) and TCEQ land cover products and MEGAN's default emission factor maps (results from SM1). Black lines confine the maximum and minimum range during 2006-2011.

Isoprene and monoterpene SEPs from the MODIS land cover product were lower by 13% and 41%, respectively, in East Texas than from the TCEQ data. The relatively better agreement between the area-averaged SEPs between the two land cover datasets in East Texas than in North and South Central Texas was attributed to the higher tree and shrub coverage in the MODIS data (Figure 5-3). In the Upper Coast, isoprene and monoterpene SEPs generated with the MODIS data were approximately 40% and 30% lower than with the TCEQ data. Among the four climate regions, East Texas exhibited the greatest interannual variations in SEPs generated from the MODIS land cover data (as indicated by Figure 5-4); the maximum isoprene SEP over the six-year-period (i.e., year 2007) even exceeded that generated from the TCEQ data. The substantial variations in the East Texas SEPs were associated with interannual fluctuations in the coverage of

trees (ranging from 28% to 40%; including all tree PFTs) and broadleaf deciduous temperate shrubs (ranging from 4% to 20%) during 2006 through 2011.

Emission activity factor (γ). In the MEGAN canopy environment model, land cover characterization is associated with the calculations of light and temperature distributions within the canopy and consequently the overall activity factor (Guenther et al., 2012). The overall emission activity factors (γ) generated from the second set of MEGAN simulations (SM2) were averaged by month and climate region for comparison. As an example, Figure D-3 contrasts the spatial distributions of monthly averaged activity factors for isoprene and monoterpenes (using α-pinene) generated from the MODIS and the TCEQ land cover products for June 2011; the relative differences in emission activity factors between the two scenarios were within 10% for most grid cells. Differences in area-averaged emission activity factors associated with different land cover data were generally negligible (< 5%; Table D-4). Results were similar when MEGAN's default PFT data were used. Most PFT-dependent canopy parameters, such as leaf length and light scattering and reflecting coefficients that are associated with the canopy environment model calculation, exhibit little or no difference among PFTs; only three parameters, canopy depth, canopy height, and leaf width differed significantly between trees and the low-growing PFTs (ref. MEGAN source codes). The canopy environment model is more sensitive to external inputs such as LAI and temperature (Tawfik et al., 2012; Huang et al., 2015), which have no differentiation among PFTs. Moreover, averaging the emission activity factors over climate regions could also mitigate the differences caused by different PFT distributions; differences could be larger at a finer spatial scale. For example, the maximum relative difference between the two land cover scenarios during June 2011 was 20%. In this particular grid cell of maximum

relative difference, the MODIS data indicated 100% coverage of broadleaf deciduous temperate trees while TCEQ data indicated 96% crop coverage.

Estimation of isoprene and monoterpene emissions. The isoprene and monoterpene emissions from SM2 were compared to examine the impact of land cover characterization on modeled emissions through the differences in both the SEP and emission activity factor. Table 5-1 shows the estimated isoprene and monoterpene emissions (sum of four climate regions for March through October) using the two land cover products as well as MEGAN's default input data (i.e. MEGAN default PFT and emission factor maps). The TCEQ and MEGAN land cover data resulted in similar isoprene emissions (differences <5%), while emission estimates from the MODIS land cover data were, on average, ~50% lower. Interannual variability associated with the MODIS data was also weaker (~10%) compared to the other cases. For monoterpenes, the TCEQ land cover data resulted in the highest emissions. The spatial distributions of the SEPs determined the spatial distribution of estimated isoprene and monoterpene emissions, as illustrated in Figure 5-5.

Table 5-1: Isoprene and monoterpene emissions (Tg) for different land cover scenarios during March through October of 2006-2011.

Isoprene	**2006**	**2007**	**2008***	**2009**	**2010**	**2011**	**Mean**	**IAV****
MODIS	0.86	0.80	0.82	0.85	1.04	1.05	0.90	10.6%
TCEQ	1.76	1.28	1.60	1.53	1.97	2.34	1.75	15.9%
MEGAN default	1.72	1.23	1.55	1.49	1.91	2.34	1.71	16.6%
Monoterpenes	**2006**	**2007**	**2008***	**2009**	**2010**	**2011**	**Mean**	**IAV****
MODIS	0.18	0.19	0.21	0.23	0.24	0.26	0.22	11.4%
TCEQ	0.45	0.41	0.40	0.40	0.50	0.52	0.45	9.2%
MEGAN default	0.25	0.23	0.22	0.23	0.28	0.29	0.25	9.7%

*October 2008 is unavailable due to missing PAR data.

**Interannual variability (IAV) was determined as the average absolute percent departure from the 2006 through 2011 mean according to the approach of Tawfik et al. (2012).

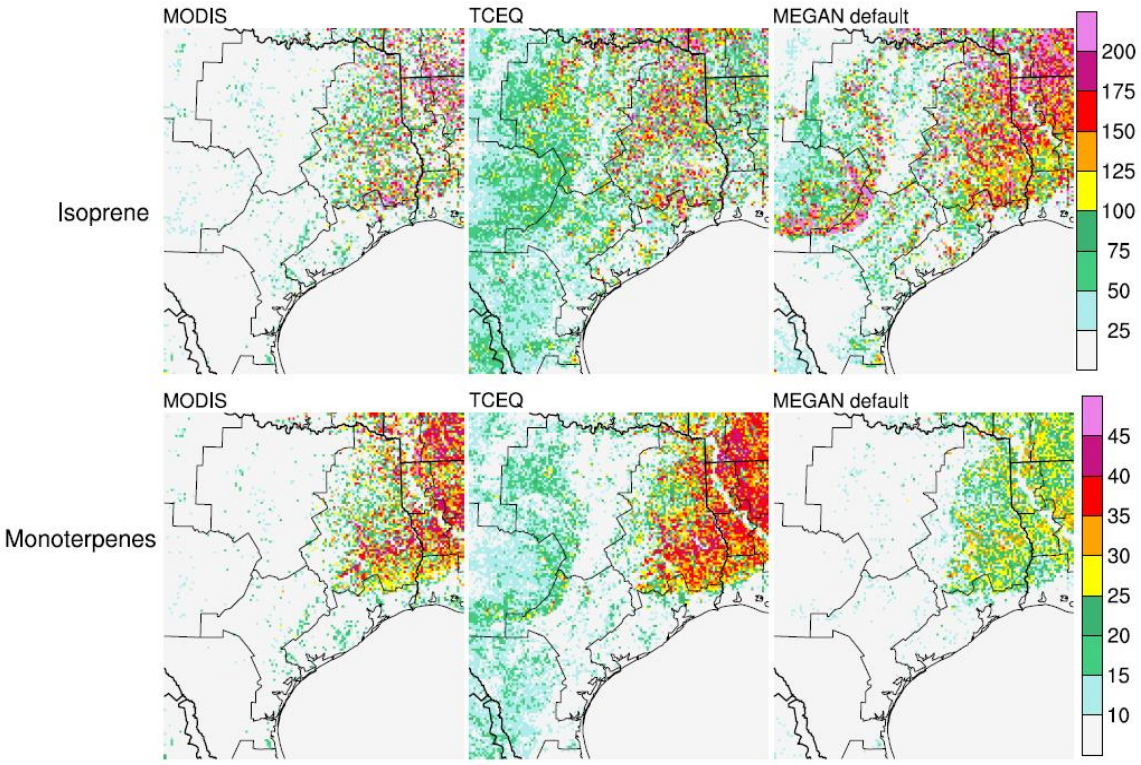

Figure 5-5: Spatial distributions of summer-averaged (June-July-August) isoprene (top) and monoterpene (bottom) emissions (kg/km^2/day) generated using the MODIS and TCEQ land cover products for 2011 (results from SM2). Results generated from MEGAN's default input data are also shown.

Figure 5-6 contrasts monthly area-averaged isoprene and monoterpene emissions generated using the MODIS and TCEQ land cover products for March through October of 2006-2011. Although correlation coefficients between the two scenarios were high (0.93-0.98), substantial differences in the magnitude of emission estimates were apparent. MODIS-based estimates for both isoprene and monoterpenes were as much as 90% lower in North Central Texas than those generated with the TCEQ land cover characterization. Similar trends were evident in South Central Texas and the Upper Coast. Relative differences between monthly isoprene emissions in East Texas ranged from -32% (underestimated by MODIS in 2011 relative to TCEQ estimates) to 19% (overestimated

by MODIS in 2007 relative to TCEQ estimates); monoterpene emission estimates obtained with the MODIS land cover were consistently lower by 16% to 46% than with the TCEQ land cover. MODIS-based estimates for monoterpenes were in better agreement with estimates from the MEGAN default input data.

Similarities between the results from SM1 and SM2 suggested that the influences of different land cover characterizations on isoprene and monoterpene emissions were primarily associated with differences in the standard emission potentials; differences in emission activity factors due to differences in PFT distribution had a negligible contribution to the overall differences in emission estimates in this study. It should also be noted that even when the two land cover products predicted similar monthly emissions for a region, substantial differences could exist spatially. For example, total isoprene emissions from East Texas generated using the MODIS and TCEQ land cover products were within 5% (i.e., 158 Gg/month versus 164 Gg/month) during July of 2009. However, large discrepancies were observed spatially (Figure D-4) with the maximum difference exceeding 100 kg/km^2/day.

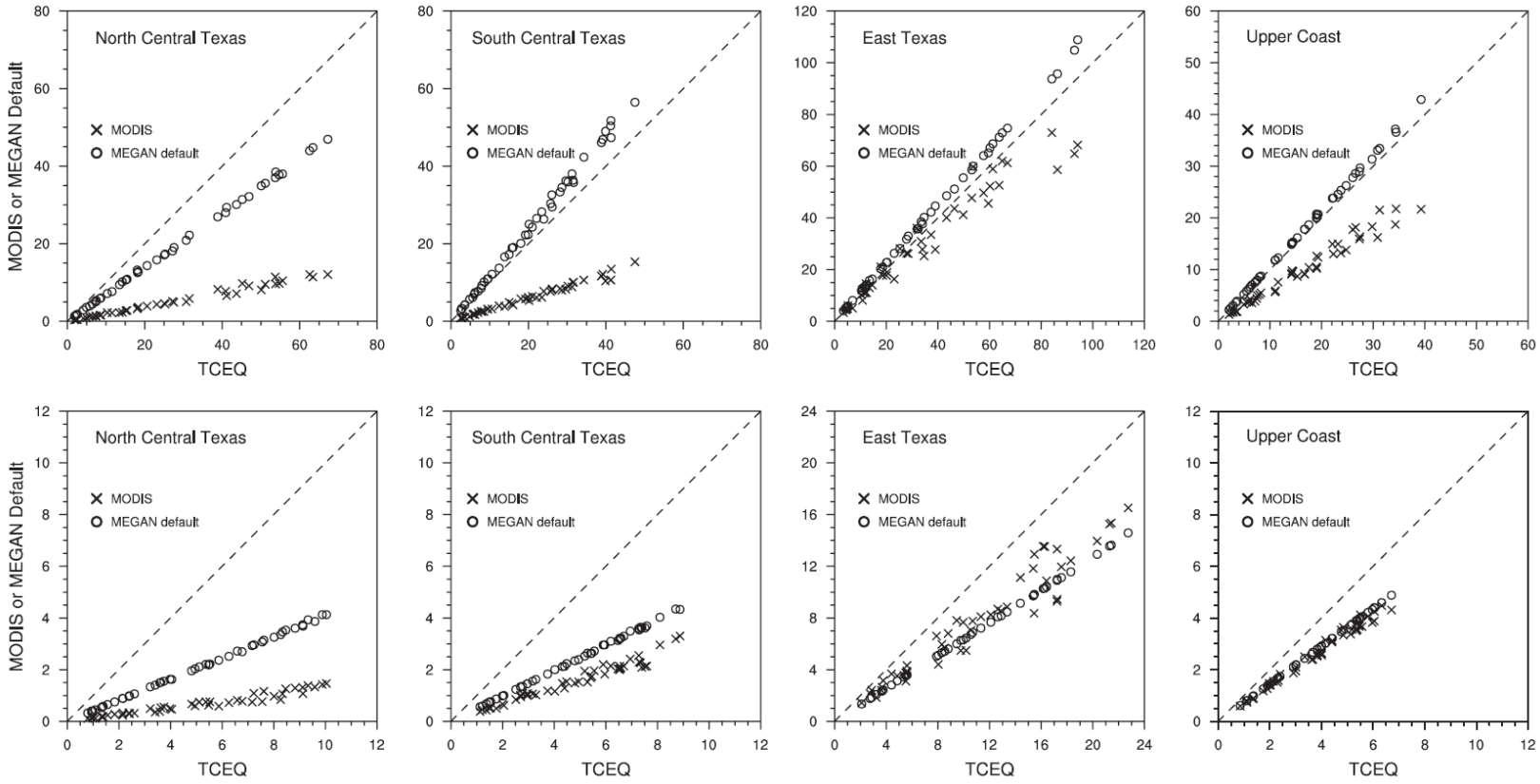

Figure 5-6: Comparison of monthly averaged isoprene (top) and monoterpene (bottom) emissions (kg/km^2/day) generated from the TCEQ and MODIS land cover data and MEGAN default input data for March through October of 2006-2011 (results from SM2). October 2008 was not shown due to missing data.

When prescribed emission factor maps such as MEGAN's default emission factor maps (Figure D-2) were utilized to replace the PFT-dependent emission factors (i.e. MEGAN simulation SM3), the relative differences in monthly isoprene and monoterpene emissions generated from the MODIS and TCEQ land cover data decreased substantially (Figure D-5), again demonstrating that the major uncertainties in isoprene and monoterpene emissions associated with uncertainties in land cover data were associated with the SEPs. For isoprene, average relative differences (with respect to the TCEQ product) were less than 15% for all climate regions. Relative differences between monthly monoterpene emissions were approximately 25% and 17% in North and South Central Texas; differences were less than 15% in East Texas and Upper Coast. Previous studies have also reported differences in biogenic emissions caused by different PFT distributions at global or regional scales (Kim et al., 2014; Pfister et al., 2008), but are smaller than those observed in this study. For example, Kim et al. (2014) reported differences in biogenic emission estimates over a 3 km x 3 km domain covering the Seoul, Gyeonggi, and Incheon metropolitan areas of 4.2 Gg (corresponding to a 15% relative difference) for May-June in 2008, between three PFT scenarios. Pfister et al. (2008) examined the MEGAN sensitivity to three sets of satellite-derived LAI and PFT input data on global and regional scales and reported a factor of two or more difference in monthly isoprene emissions. The much higher spatial resolution (1 km x 1 km) and temporal LAI resolution (4 day) employed in this study could have resulted in more significant differences in isoprene and monoterpene emissions between the two land cover products in the central regions of Texas.

5.3.3 Impact of land cover characterization on predicted ozone concentrations

Parallel CAMx simulations were implemented to estimate the impact of land cover characterization on ozone concentrations through differences in biogenic

emissions. Figure 5-7 shows the spatial distributions of mean and maximum differences in maximum daily average 8-hour (MDA8) ozone concentrations, respectively, between the two land cover scenarios (shown as C_{MODIS} minus C_{TCEQ}) during June 2006. MDA8 ozone concentrations from the MODIS land cover data were lower than with the TCEQ data with mean differences of 2 to 6 ppb, while maximum differences exceeded 20 ppb. The most substantial differences were near highly developed urban areas, including Austin and San Antonio in South Central Texas, Dallas/Fort Worth in North Central Texas, and Houston in the Upper Coast; NO_x emissions were relatively abundant, typical of most urban areas. Figure 5-8 shows differences in MDA8 ozone concentrations at ambient monitoring sites surrounding the three metropolitan areas. MDA8 ozone concentrations with the MODIS land cover data were generally lower than with the TCEQ data by approximately 2 ppb; however, maximum differences in the Houston area reached 30 ppb. These results indicated that differences in biogenic emission estimates due to different land cover representations have the potential to lead to substantial differences in predicted ozone concentrations.

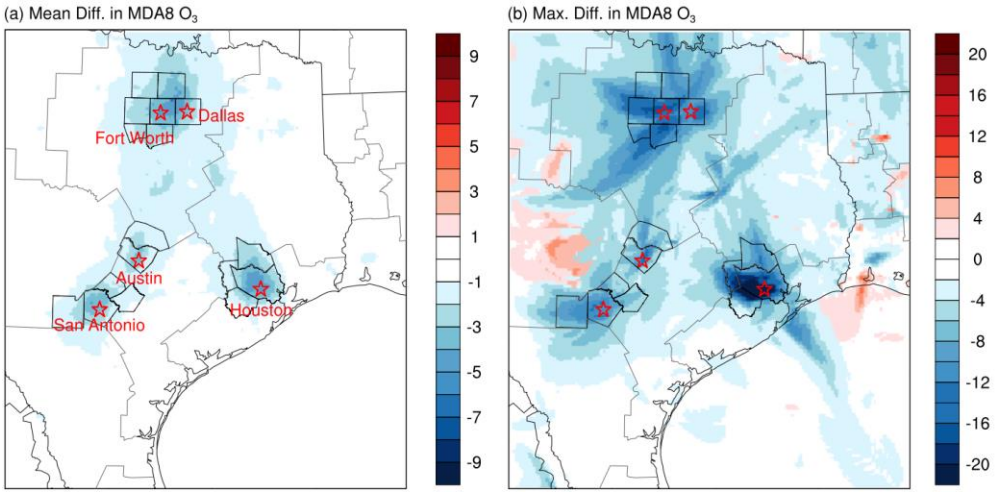

Figure 5-7: Spatial distributions of (a) mean and (b) maximum differences in MDA8 ozone concentrations (ppb) between the MODIS and TCEQ land cover scenarios (as C_{MODIS} minus C_{TCEQ}) during June 2006. Major cities and counties in close proximity are highlighted.

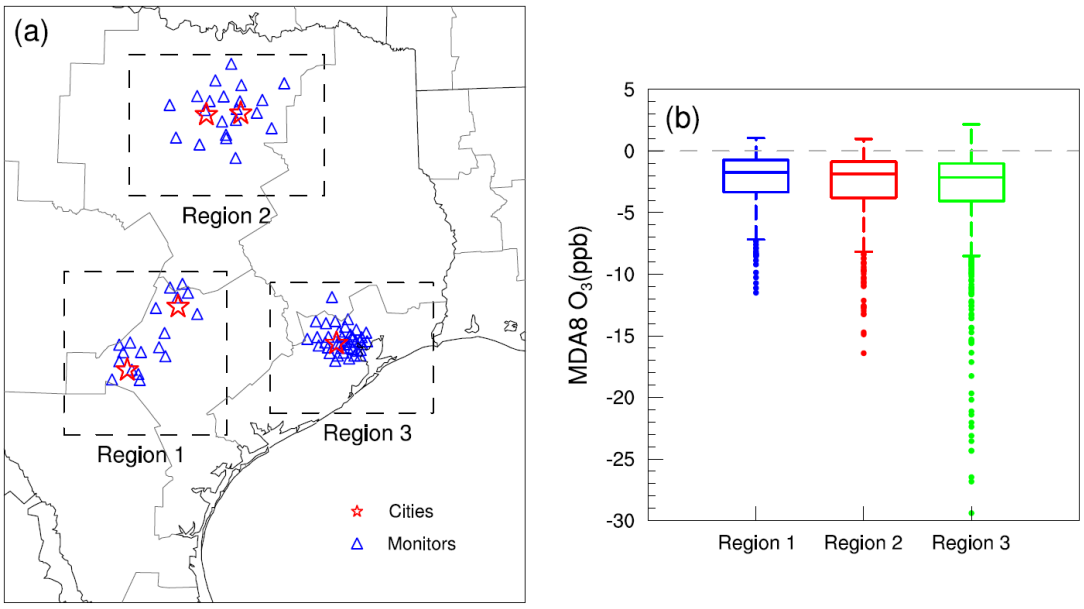

Figure 5-8: (a) Locations of selected ambient monitors near major metropolitan areas in eastern Texas and (b) box and whisker plot of differences in MDA8 ozone concentrations (ppb) between the MODIS and TCEQ land cover scenarios (as C_{MODIS} minus C_{TCEQ}) during June 2006. In the box and whisker plot, the box represents the 25th and 75th quartiles with the central horizontal line as the median value. The top and bottom whiskers extend to 1.5 times the interquartile range from the box. Values that lie outside the whiskers are plotted as individual points.

5.4 CONCLUSIONS

Uncertainties in land cover characterization could lead to uncertainties in modeled biogenic emissions and consequently predictions of air quality. This work investigated the influence of two eastern Texas land cover products on isoprene and monoterpene emission estimates from MEGAN. In addition, estimates generated using MEGAN's default PFT distribution and gridded emission factor maps were included for comparison. In general, forest coverage was significantly lower in the global MODIS land cover product compared to the regional TCEQ product in Central Texas, which resulted in lower estimated monthly isoprene and monoterpene emissions by as much as 90%. Predicted isoprene emissions generated from MEGAN's default input data agreed more

closely with those obtained using the TCEQ data; in contrast, predicted monoterpene emissions were in closer agreement with those based on the MODIS product. The influences of land cover characterization on isoprene and monoterpene emissions were dominated by contributions to differences in the standard emission potential that are dependent on PFT-distribution; differences in the MEGAN overall emission activity factor associated with different land cover data were generally negligible in this analysis.

Photochemical modeling was conducted to investigate the effects of differences in estimated biogenic emissions associated with land cover characterization on predicted ozone concentrations. Mean differences in MDA8 ozone concentrations were 2 to 6 ppb with maximum differences exceeding 20 ppb. Overall, these findings suggested that the uncertainties associated with land cover data could lead to significant uncertainties in modeled biogenic emissions that could be even greater than using different biogenic emission models (e.g., Hogrefe et al., 2011). Land cover in Texas is highly diverse, varying from dense forest in East Texas to grasses and croplands towards the central regions. Misclassification between trees and grasses/crops has the potential to lead to large differences in biogenic emission estimates. This could also be of particular importance in other regions of the world where rapid land cover change is occurring, such as deforestation due to an expansion in agricultural operations (e.g. South America, Geist and Lambin, 2002). Continued focus should be on reducing uncertainties in the representation of land cover through field validation and in the basal emission factors assigned for each PFT.

5.5 REFERENCES

Atkinson, R. (2000). Atmospheric chemistry of VOCs and NOx. *Atmospheric Environment*, *34*(12), 2063-2101.

Bonan, G. B., Oleson, K.W., Vertenstein, M., Levis, S., Zeng, X., Dai, Y., & Yang, Z.L. (2002). The land surface climatology of the community land model coupled to the NCAR community climate model. *Journal of Climate*, *15*(22), 3123–3149.

Byun, D. W., Kim, S., Czader, B., Nowak, D., Stetson, S., & Estes, M. (2005). Estimation of biogenic emissions with satellite-derived land use and land cover data for air quality modeling of Houston-Galveston ozone nonattainment area.*Journal of environmental management*, *75*(4), 285-301.

Carlton, A. G., Wiedinmyer, C., & Kroll, J. H. (2009). A review of Secondary Organic Aerosol (SOA) formation from isoprene. *Atmospheric Chemistry and Physics*, *9*(14), 4987-5005.

Chameides, W. L., Lindsay, R. W., Richardson, J., & Kiang, C. S. (1988). The role of biogenic hydrocarbons in urban photochemical smog: Atlanta as a case study. *Science*, *241*(4872), 1473-1475.

Claeys, M., Graham, B., Vas, G., Wang, W., Vermeylen, R., Pashynska, V., ... & Maenhaut, W. (2004). Formation of secondary organic aerosols through photooxidation of isoprene. *Science*, *303*(5661), 1173-1176.

Drewniak, B. A., Snyder, P. K., Steiner, A. L., Twine, T. E., & Wuebbles, D. J. (2014). Simulated changes in biogenic VOC emissions and ozone formation from habitat expansion of Acer Rubrum (red maple). *Environmental Research Letters*, *9*(1), 014006.

ENVIRON. (2014). User's guide Comprehensive Air Quality Model with Extension (CAMx), version 6.10. Retrieved April 17, 2015, from http://www.camx.com/files/camxusersguide_v6-10.txt

EPA. (2014). 2011 National Emission Inventory, version 1 Technical Support Document Draft. Retrieved Febrary 19, 2015, from http://www.epa.gov/ttn/chief/net/2011nei/2011_nei_tsdv1_draft2_june2014.pdf

Fehsenfeld, F., Calvert, J., Fall, R., Goldan, P., Guenther, A. B., Hewitt, C. N., ... & Zimmerman, P. (1992). Emissions of volatile organic compounds from vegetation and the implications for atmospheric chemistry. *Global Biogeochemical Cycles*, *6*(4), 389-430.

Friedl, M. A., McIver, D. K., Hodges, J. C., Zhang, X. Y., Muchoney, D., Strahler, A. H., ... & Schaaf, C. (2002). Global land cover mapping from MODIS: algorithms and early results. *Remote Sensing of Environment*, *83*(1), 287-302.

Friedl, M. A., Sulla-Menashe, D., Tan, B., Schneider, A., Ramankutty, N., Sibley, A., & Huang, X. (2010). MODIS Collection 5 global land cover: Algorithm refinements and characterization of new datasets. *Remote Sensing of Environment*, *114*(1), 168-182.

Geist, H. J., & Lambin, E. F. (2002). Proximate Causes and Underlying Driving Forces of Tropical Deforestation Tropical forests are disappearing as the result of many pressures, both local and regional, acting in various combinations in different geographical locations. *BioScience*, *52*(2), 143-150.

Guenther, A., Geron, C., Pierce, T., Lamb, B., Harley, P., & Fall, R. (2000). Natural emissions of non-methane volatile organic compounds, carbon monoxide, and oxides of nitrogen from North America. *Atmospheric Environment*, *34*(12), 2205-2230.

Guenther, A. B., Jiang, X., Heald, C. L., Sakulyanontvittaya, T., Duhl, T., Emmons, L. K., & Wang, X. (2012). The Model of Emissions of Gases and Aerosols from Nature version 2.1 (MEGAN2. 1): an extended and updated framework for modeling biogenic emissions.

Guenther, A., Karl, T., Harley, P., Wiedinmyer, C., Palmer, P. I., & Geron, C. (2006). Estimates of global terrestrial isoprene emissions using MEGAN (Model of Emissions of Gases and Aerosols from Nature). *Atmospheric Chemistry and Physics Discussions*, *6*(1), 107-173.

Guenther, A., Zimmerman, P., & Wildermuth, M. (1994). Natural volatile organic compound emission rate estimates for US woodland landscapes. *Atmospheric Environment*, *28*(6), 1197-1210.

Gulden, L. E., Yang, Z. L., & Niu, G. Y. (2008). Sensitivity of biogenic emissions simulated by a land-surface model to land-cover representations. *Atmospheric Environment*, *42*(18), 4185-4197.

Hoffmann, T., Odum, J. R., Bowman, F., Collins, D., Klockow, D., Flagan, R. C., & Seinfeld, J. H. (1997). Formation of organic aerosols from the oxidation of biogenic hydrocarbons. *Journal of Atmospheric Chemistry*. *26*(2), 189-222.

Hogrefe, C., Isukapalli, S. S., Tang, X., Georgopoulos, P. G., He, S., Zalewsky, E. E., ... & Sistla, G. (2011). Impact of biogenic emission uncertainties on the simulated

response of ozone and fine particulate matter to anthropogenic emission reductions. *Journal of the Air & Waste Management Association*, *61*(1), 92-108.

Homer, C., Dewitz, J., Fry, J., Coan, M., Hossain, N., Larson, C., ... & Wickham, J. (2007). Completion of the 2001 national land cover database for the counterminous United States. *Photogrammetric Engineering and Remote Sensing*, *73*(4), 337.

Huang, L., McDonald-Buller, E. C., McGaughey, G., Kimura, Y., & Allen, D. T. (2014). Annual variability in leaf area index and isoprene and monoterpene emissions during drought years in Texas. *Atmospheric Environment, 92*, 240–249. doi:10.1016/j.atmosenv.2014.04.016.

Huang, L., McGaughey, G., McDonald-Buller, E., Kimura, Y., & Allen, D. T. (2015). Quantifying regional, seasonal and interannual contributions of environmental factors on isoprene and monoterpene emissions estimates over eastern Texas. *Atmospheric Environment, 106*, 120-128.

Kavouras, I.G., Mihalopoulos, N., & Stephanou, E. G. (1998). Formation of atmospheric particles from organic acids produced by forests. *Nature. 395*(6703), 683-686.

Kim, H. K., Woo, J. H., Park, R. S., Song, C. H., Kim, J. H., Ban, S. J., & Park, J. H. (2014). Impacts of different plant functional types on ambient ozone predictions in the Seoul Metropolitan Areas (SMAs), Korea. *Atmospheric Chemistry and Physics, 14*(14), 7461–7484. doi:10.5194/acp-14-7461-2014.

Knyazikhin, Y., Glassy, J., Privette, J. L., Tian, Y., Lotsch, A., Zhang, Y., … Running, S. W. (1999). MODIS leaf area index (LAI) and fraction of photosynthetically active radiation absorbed by vegetation (FPAR) product (MOD15): Algorithm theoretical basis document. Retrieved December 1, 2014, from http://modis.gsfc.nasa.gov/data/atbd/atbd_mod15.pdf

McCallum, I., Obersteiner, M., Nilsson, S., & Shvidenko, A. (2006). A spatial comparison of four satellite derived 1km global land cover datasets. *International Journal of Applied Earth Observation and Geoinformation, 8*(4), 246–255.

Myneni, R.B., Ramakrishna, R., Nemani, R., & Running, S. W. (1997). Estimation of global leaf area index and absorbed PAR using radiative transfer models. *IEEE Transactions on Geoscience and Remote Sensing, 35*(6), 1380–1393. doi:10.1109/36.649788.

Pacifico, F., Harrison, S. P., Jones, C. D., & Sitch, S. (2009). Isoprene emissions and climate. *Atmospheric Environment, 43*(39): 6121-6135

Pfister, G. G., Emmons, L. K., Hess, P. G., Lamarque, J. F., Orlando, J. J., Walters, S., ... & Lawrence, P. J. (2008). Contribution of isoprene to chemical budgets: A model tracer study with the NCAR CTM MOZART-4. *Journal of Geophysical Research: Atmospheres (1984–2012)*, *113*(D5).

Popescu, S. C., Stukey, J., Mutlu, M., Zhao, K., Sheridan, R., Ku, N. W., … Harper, C. (2011). Expansion of Texas land use/land cover through class crosswalking and Lidar parameterization of arboreal vegetation. Retrieved December 1, 2014, from https://www.tceq.texas.gov/assets/public/implementation/air/am/contracts/reports/oth/5820564593FY0925-20110419-tamu-expension_tx_lulc_arboreal_vegetation.pdf

Potosnak, M. J., LeStourgeon, L., Pallardy, S. G., Hosman, K. P., Gu, L., Karl, T., … Guenther, A. B. (2014). Observed and modeled ecosystem isoprene fluxes from an oak-dominated temperate forest and the influence of drought stress. *Atmospheric Environment*, *84*, 314–322.

Pouliot, D., Latifovic, R., Zabcic, N., Guindon, L., & Olthof, I. (2014). Development and assessment of a 250m spatial resolution MODIS annual land cover time series (2000–2011) for the forest region of Canada derived from change-based updating. *Remote Sensing of Environment, 140,* 731–743. doi:10.1016/j.rse.2013.10.004.

Quaife, T., Quegan, S., Disney, M., Lewis, P., Lomas, M., & Woodward, F. I. (2008). Impact of land cover uncertainties on estimates of biospheric carbon fluxes. *Global Biogeochemical Cycles, 22*(4), GB4016. doi:10.1029/2007GB003097.

Rollins, M.G. (2009). LANDFIRE: a nationally consistent vegetation, wildland fire, and fuel assessment. *International Journal of Wildland Fire, 18*(3), 235-249.

Ruiz, L.H, & Yarwood, G. (2013). Interactions between organic aerosol and NOy: Influence on oxidant production. Prepared for the Texas AQRP (Project 12-012), by the University of Texas at Austin, and ENVIRON International Corporation, Novato, CA. Retrieved April 17, 2015 from http://aqrp.ceer.utexas.edu/projectinfoFY12_13/12-012/12-012%20Final%20Report.pdf

Running, S.W., Nemani, R., Glassy, J. M., & Thornton, P. E. (1999). MODIS daily photosynthesis (PSN) and annual net primary production (NPP) product (MOD17) algorithm theoretical basis document. http://modis.gsfc.nasa.gov/data/atbd/atbd_mod16.pdf (accessed on December 1, 2014).

Sanderson, M.G., Jones, C.D., Collins, W.J., Johnson, C.E., & Derwent, R. G. (2003). Effect of climate change on isoprene emissions and surface ozone levels. *Geophysical Research Letters, 30*(18).

Sindelarova, K., Granier, C., Bouarar, I., Guenther, A., Tilmes, S., Stavrakou, T., … Knorr, W. (2014). Global dataset of biogenic VOC emissions calculated by the MEGAN model over the last 30 Years. *Atmospheric Chemistry and Physics, 14*, 9317-9341.

Song, J., Vizuete, W., Chang, S., Allen, D., Kimura, Y., Kemball-Cook, S., …McDonald-Buller, E. (2008). Comparisons of modeled and observed isoprene concentrations in southeast Texas. *Atmospheric Environment, 42*(8), 1922-1940.

Steinbrecher, R., Smiatek, G., Köble, R., Seufert, G., Theloke, J., Hauff, K., … Curci, G. (2009). Intra- and inter-annual variability of VOC emissions from natural and semi-natural vegetation in Europe and neighbouring countries. *Atmospheric Environment, 43*(7), 1380–1391. doi:10.1016/j.atmosenv.2008.09.072.

Tawfik, A.B., Stöckli, R., Goldstein, A., Pressley, S., & Steiner, A. L. (2012). Quantifying the contribution of environmental factors to isoprene flux interannual variability. *Atmospheric Environment, 54*, 216–224. doi:10.1016/j.atmosenv.2012.02.018.

Texas A&M Forest Service, (2012). Texas A&M Forest Service survey shows 301 million trees killed by drought. Retrieved February 19, 2015, from http://texasforestservice.tamu.edu/main/popup.aspx?id=16509

Tsigaridis, K, & Kanakidou, M. (2003). Global modelling of secondary organic aerosol in the troposphere : a sensitivity analysis. *Atmospheric Chemistry and Physics, 3*(5), 1849–1869.

Yarwood, G., Gookyoung, H., Carter, W. P. L., & Whitten, G.Z. (2012). Environmental Chamber Experiments to Evaluate NOx Sinks and Recycling in Atmospheric Chemical Mechanisms. Final report prepared for the Texas Air Quality Research Program, University of Texas, Austin, Texas. Retrieved April 17, 2015, from http://aqrp.ceer.utexas.edu/projectinfo%5C10-042%5C10-042%20Final%20Report.pdf

Zhang, L., Brook, J. R., & Vet, R. (2003). A revised parameterization for gaseous dry deposition in air-quality models. *Atmospheric Chemistry and Physics*, *3*, 2067–2082.

Chapter 6: The Impact of Drought on Ozone Dry Deposition over Eastern Texas

(to be submitted to Atmospheric Environment)

6.1 INTRODUCTION

Dry deposition is broadly defined as the transport of gaseous and particulate species from the atmosphere by turbulent transfer to surfaces in the absence of precipitation (Seinfeld and Pandis, 2012). Dry deposition is estimated to account for 20-25% of total ozone removal from the troposphere globally (Lelieveld and Dentener, 2000; Wild, 2007). On a regional level in Texas, dry deposition represents the most important physical removal mechanism for ozone during the warm spring through early fall seasons (McDonald-Buller et al., 2001); therefore, accurate estimates of ozone dry deposition are required for air quality modeling and management. The magnitude of ozone dry deposition is controlled by the combined effects of all removal pathways, which include the stomatal and non-stomatal uptake, e.g. deposition to soils, cuticles or any other external surface (Hogg et al., 2007; Fares et al., 2010, 2012). The relative importance of stomatal and non-stomatal removal varies with vegetation types and changes diurnally and seasonally (Lamaud et al., 2009; Rannik et al., 2012; Fares et al., 2012; Neirynck et al., 2012). Stomatal uptake is considered to be the main mechanism through which ozone-associated damage occurs within plants (UNECE, 2004). Exposure to elevated ozone concentrations leads to biochemical and physiological changes including inhibition of carbon assimilation from photosynthesis that can result in reduced agricultural yields (Wittig et al., 2009; Mills et al., 2011; Fares et al., 2013). Understanding ozone deposition, especially stomatal uptake, is thus important for risk assessment in order to protect vegetation and ecosystems from ozone damage (Pleijel et al., 2007; Mills et al., 2011). However, despite its importance in various applications, dry

deposition remains one of the major uncertainties in modeling ozone in the troposphere (Wild, 2007).

Dry deposition can be measured directly or indirectly. The eddy covariance (EC) method is the most commonly used direct technique to measure dry deposition flux (Wesely et al., 1982), where the vertical flux is calculated from the covariance of the vertical wind speed and concentration fields. Currently, the EC method is being used as a standard technique for measuring fluxes of heat, water vapor and air pollutants (Ingwersen et al., 2011). The gradient method is a representative indirect method, where gradient transport theory is used to infer the deposition flux (Seinfeld and Pandis, 2012). Long-term flux measurements over relatively large areas remains difficult (Wesely and Hicks, 2000) and a suitable model parameterization is needed. Dry deposition is often treated as a first-order removal mechanism, where a characteristic dry deposition velocity V_d (ratio of deposition flux and concentration) is used to describe the process. A number of models available to estimate V_d employ a resistance approach analogous to Ohm's law in electrical circuits. For example, the widely used Wesely scheme (Wesely, 1989) and the more recently developed Zhang scheme (Zhang et al., 2003), both treat the canopy as a single layer (or big leaf model). Other models apply a multilayer approach to account for the vertical distribution of leaf area within the canopy (Finkelstein et al. 2000; Meyers et al., 1998). For example, the Clean Air Status and Trends Network (CASTNET) is a U.S. national air quality monitoring work that uses a multi-layer model (MLM) to simulate dry deposition velocities (Clarke et al., 1997). Validation of dry deposition models against observations, as well as inter-comparisons between models, have been conducted in numerous studies (Zhang et al., 2002; Michou et al., 2005; Schwede et al., 2011; Park et al., 2014; Val Martin et al., 2014; Wu et al., 2011), yet significant uncertainties remain (Pleim and Ran, 2011).

Drought is a recurring phenomenon in many regions of the world (Sheffield and Wood, 2012; Melillo et al., 2014). Within the United States, Texas is among the regions that have faced tremendous challenges from recent droughts, for example, in 2011 with record agricultural losses and high numbers of wildfires (Fannin et al., 2011). Drought associated high temperatures and soil moisture deficits have the potential to suppress stomatal conductance, and thus lead to reductions in dry deposition and higher surface ozone concentrations (Pio et al., 2000; Solberg et al., 2008). Concurrent effects of ozone and drought on vegetation can be synergistic or antagonistic, depending on the sequence of the events and various environmental and phenotypical factors (Bohler et al., 2015). It is critical to understand the effects of drought on ozone dry deposition in Texas and other regions where drought is a frequent occurrence and requirements to achieve and maintain attainment with the National Ambient Air Quality Standard (NAAQS) in large metropolitan areas exist.

The purpose of this study was to investigate the impacts of drought on ozone dry deposition during the daytime by exploring interannual variations in predicted dry deposition velocities and associated component resistances in eastern Texas. The Comprehensive Air Quality Model with Extensions (CAMx, ENVRION, 2014) is a photochemical dispersion model that is currently being used by the state of Texas for attainment demonstrations. The dry deposition sub-module within CAMx was utilized offline to simulate ozone dry deposition velocities during years with extreme to exceptional droughts as well as years with above average precipitation patterns. Due to its advantages in characterizing the non-stomatal resistance, Zhang's dry deposition scheme was chosen for this study.

6.2 METHODOLOGY

6.2.1 Zhang's dry deposition algorithm

Zhang's dry deposition algorithm (Zhang et al., 2003) adopts the common resistance method to simulate dry deposition velocity V_d, which is determined as the reciprocal of the sum for aerodynamic resistance (R_a), quasi-laminar resistance (R_b), and overall canopy resistance (R_c) as follows:

$$V_d = (R_a + R_b + R_c)^{-1} \quad \text{Eq. 6-1}$$

The parameterizations of R_a and R_b are generally similar among different models. Daytime deposition is mainly limited by the overall canopy resistance R_c in Zhang's algorithm, which is parameterized as:

$$\frac{1}{R_c} = \underbrace{\frac{1 - W_{st}}{R_{st} + R_m}}_{G_{st}} + \underbrace{\frac{1}{R_{cut}} + \frac{1}{R_{ac} + R_g}}_{G_{ns}} \quad \text{Eq. 6-2}$$

The first term of the right side of Eq. 6-2 represents the stomatal deposition pathway; G_{st} is defined as the stomatal conductance. It should be noted that G_{st} as defined in our study is not the simple reciprocal of the stomatal resistance (R_{st}); instead, it accounts for the mesophyll resistance (R_m) and the stomatal blocking (W_{st}) under wet conditions. For ozone, R_m is negligible and R_{st} controls the stomatal pathway. R_{st} is affected by various environmental factors including temperature, solar radiation, relative humidity and is simulated as:

$$R_{st} = 1/[G_S(PAR) f(T) f(VPD) f(\psi) D_i / D_v] \quad \text{Eq. 6-3}$$

The functions G_s (PAR), f (T), f (D), f (ψ) represent the stomatal response to photosynthetically active radiation (PAR), air temperature T, leaf-air vapor pressure deficit VPD, and water stress ψ (correlated with solar radiation). Figure E-1 demonstrates the latter three functions for four selected land use categories – deciduous broadleaf tree, deciduous shrubs, long grass, and crops. f (T) is a bell-shape function with maximum

stomatal opening at the optimum temperature, below or above which would cause stomatal closure. f (D) and f (ψ) are linear functions and stomatal resistance (conductance) starts to increase (decrease) above a certain level of VPD (for forest and shrubs only) or water stress.

The last two terms of the right side of Eq. 6-2 together represent the non-stomatal deposition pathways; G_{ns} represents the non-stomatal conductance. One of the advantages that Zhang's algorithm shows over Wesely's is the utilization of the leaf area index (LAI) in the calculation of the in-canopy aerodynamic resistance R_{ac} and cuticle resistance R_{cut} as followings:

$$R_{ac} = R_{ac0} LAI^{0.25} / u_*^2 \qquad \text{Eq. 6-4}$$

$$R_{cutd} = R_{cutd0} / (e^{0.03RH} LAI^{0.25} u_*) \quad \text{(dry condition)} \qquad \text{Eq. 6-5}$$

$$R_{cutw} = R_{cutw0} / (LAI^{0.5} u_*) \quad \text{(wet condition)} \qquad \text{Eq. 6-6}$$

where the resistances with zero in the subscript are reference values. Higher LAI values would increase the in-canopy transport resistance but provide greater leaf area for cuticle deposition. Friction velocity (u_*) is negatively correlated with both R_{ac} and R_{cut}.

6.2.2 WRF configuration

Meteorological inputs are essential for estimating dry deposition. In this study, the Weather Research and Forecasting (WRF) Model (version 3.4.1) was used to simulate meteorological conditions over eastern Texas during the growing seasons (April-October) for 2006, 2007 and 2011. These years represent both extreme to exceptional drought conditions (e.g. 2006, 2011) as well as periods with above average precipitation (e.g. 2007; Huang et al., 2014). The WRF modeling domain follows an existing CAMx episode developed by the Texas Commission on Environmental Quality (TCEQ) in support of air quality planning for Texas, which includes 36-km, 12-km, and 4-km

horizontal grid domains shown in Figure 6-1a (http://www.tceq.texas.gov/airquality/airmod/rider8/rider8Modeling.html). The vertical grid consists of 43 vertical layers with the first layer midpoint at 16.9 m. The National Centers for Environmental Prediction Eta (NCEP) Eta/NAM reanalysis data product at 3-hr temporal and 40-km spatial resolution was utilized as the initial and boundary conditions. Physics options of the WRF simulations include Yonsei University (YSU) boundary layer physics (Hong et al., 2006), Noah land surface model (Chen and Dudhia, 2001), MM5 surface layer scheme (Skamarock et al. 2005), WRF single moment (WSM) 5-class for the 36/12-km domain and WSM 6-class for the 4-km domain (Hong and Lim, 2006), analysis nudging of winds, temperature and moisture with two-way feedback. Model performance was evaluated against observations (see details in Supplemental Information) and demonstrated reasonable agreement sufficient to support dry deposition simulations for the purposes of this study.

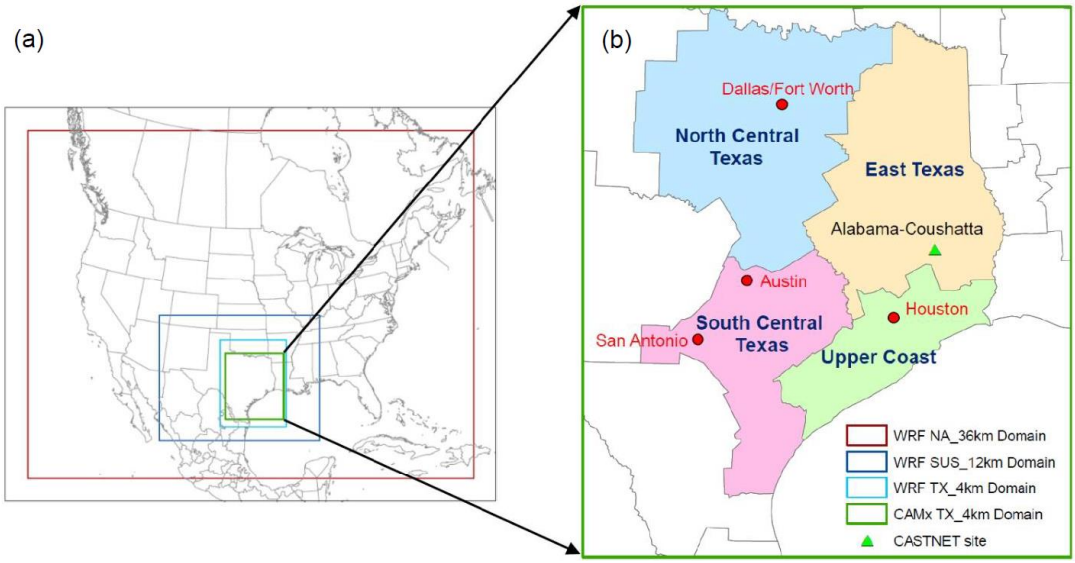

Figure 6-1: (a) WRF nested grid domains (Red: 36-km North America domain; Dark-blue: 12-km south U.S. domain; light-blue: 4-km eastern Texas domain). (b) CAMx 4-km eastern Texas domain with boundaries of four climate regions and locations of major metropolitan areas. Domain structures were adopted from the TCEQ (https://www.tceq.texas.gov/airquality/airmod/data/domain).

6.2.3 Dry deposition configuration

CAMx version 6.10 ((ENVRION, 2014) is a photochemical grid model that is currently being used by the State of Texas for air quality modeling and attainment demonstrations. For the purposes of our study, which specifically focuses on ozone dry deposition, the dry deposition sub-module of CAMx was extracted as an offline program to calculate hourly dry deposition velocities based on meteorological conditions and other inputs. In addition to the output of ozone dry deposition velocities, the original module was modified to generate associated component resistances for each land cover category. The WRFCAMx preprocessor was used to prepare CAMx meteorological input files using WRF output files. As shown in Figure 6-1b, the 4-km CAMx modeling domain covers the eastern part of Texas and by design is slightly smaller than the WRF 4-km domain to minimize the impacts of boundary artifacts in the meteorological fields. Four climate regions located in eastern Texas, North Central Texas, South Central Texas, East Texas and Upper Coast, were the focus of this study. The default WRFCAMx applies the WRF skin surface temperature as the temperature to adjust stomatal conductance (i.e. $f(T)$ in Eq. 6-3). However, this skin surface temperature caused complete stomatal closure during midday hours. Instead, the 2-m air temperature generated by WRF was in closer agreement with the leaf temperature obtained using the leaf energy balance within the Model of Emissions of Gases and Aerosols from Nature (MEGAN; Guenther et al., 2012) and was considered to be more appropriate.

An existing regional land cover database was used, which was developed by the TCEQ based on the combination of three products including the 2001 National Land Cover Dataset, Biogenic Emission Landuse Data (BELD) version 3, and a land cover dataset developed by the Texas A&M Spatial Sciences Laboratory (Popescu et al., 2011; Harper, 2012). Of the 26 land cover categories adopted by the Zhang scheme, seven

vegetation categories (plus water and urban) existed (>1% area percentage) in the four eastern Texas climate regions (Figure 6-2). For simplicity, the seven vegetation categories were further condensed into four simplified land cover categories – forest, shrubs, crops and grass (see Table 6-1). For example, evergreen needleleaf trees, deciduous broadleaf trees, and mixed wood forest share the same or similar parameters for calculating various component resistances (see Table 1 in Zhang et al. 2003) so are together referred to as forest. Figure 6-3 shows the area coverage of each simplified land cover category in the four climate regions of interest. For all climate regions except East Texas, grasses covered approximately one-third of the area; forest had slightly lower coverage followed by crops and shrubs. In East Texas, forest was the dominant land cover category with area coverage of 67%, and negligible coverage by shrubs.

Table 6-1: Simplification of Zhang's land cover categories

No.	Zhang's land cover categories in eastern Texas	Simplified land cover categories
4	Evergreen needleleaf trees	Forest
7	Deciduous broadleaf trees	Forest
11	Deciduous shrubs	Shrubs
13	Short grass and forbs	Grass
14	Long grass	Grass
15	Crops	Crops
25	Mixed wood forest	Forest

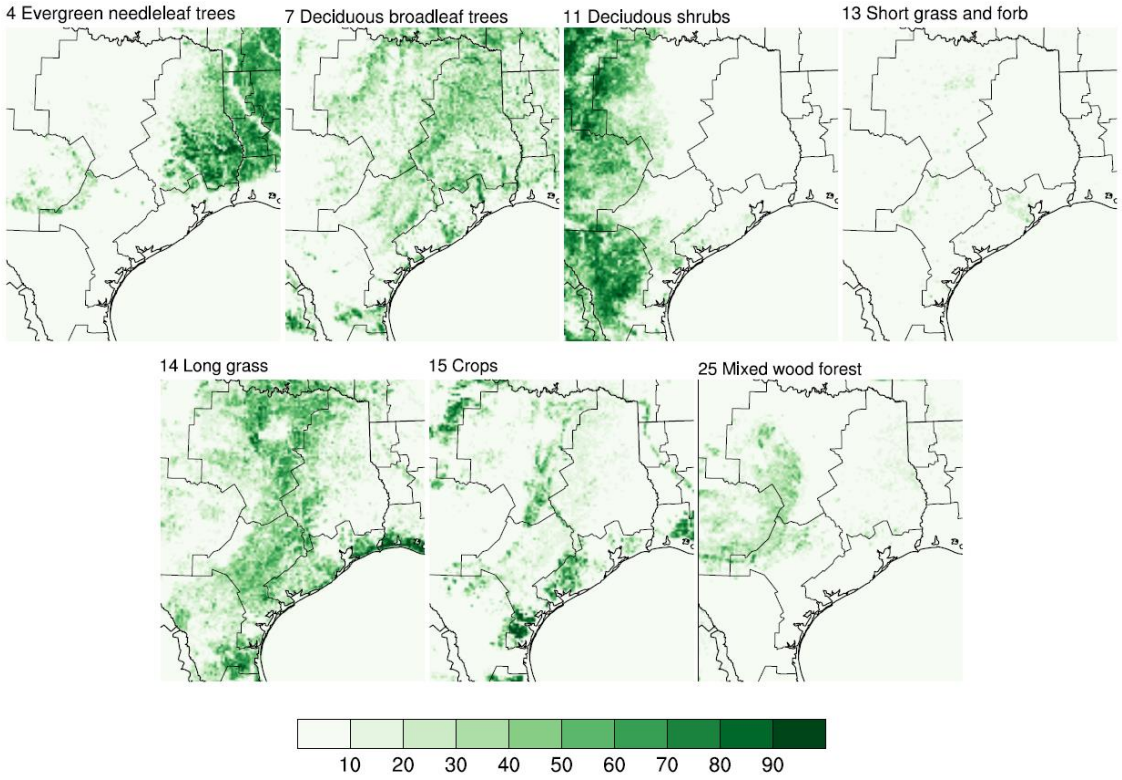

Figure 6-2: Spatial distributions of area coverage of seven vegetation land cover categories in eastern Texas.

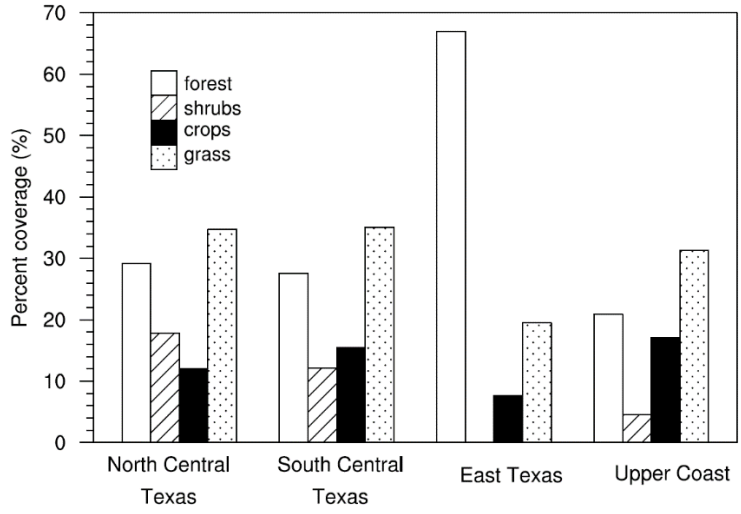

Figure 6-3: Area percentages of simplified land cover categories in eastern Texas climate regions.

Other inputs included the Moderate Resolution Imaging Spectroradiometer (MODIS) 4-day LAI product (MCD15A3) that was regridded to a 4-km resolution. Offline dry deposition simulations were conducted at 4-km horizontal resolution over eastern Texas during April-October of years 2006, 2007 and 2011. Hourly ozone dry deposition velocities as well as component resistances for each land cover category were generated. Results were averaged by climate region, simplified land cover category, and month/season (spring: April/May; summer: June/July/August; fall: September/October) for further analysis. Values during CST 0800-1800 were used to calculate daytime averages.

6.3 RESULTS AND DISCUSSIONS

6.3.1 Seasonal patterns of ozone deposition over eastern Texas

Daytime ozone dry deposition velocities (V_d) were mainly limited by the surface resistance (R_c) when the aerodynamic (R_a) and sub-layer (R_b) resistances were relatively small. Seasonal patterns of daytime V_d reflected the combined seasonal variations in the non-stomatal conductance (G_{ns}, shown in Figure E-2) and the stomatal conductance (G_{st}, shown in Figure E-3). Non-stomatal removal included two parallel pathways – deposition to ground surfaces and leaf cuticles with the cuticle resistances generally much larger than the surface resistances (combination of the in-canopy aerodynamic resistance and ground resistance). For example, the ratio of cuticle to surface resistance for crops ranged between 3.2-17.9 for all years/seasons/climate regions, indicating only 5-24% of non-stomatal deposition occurred through cuticle deposition. Two factors contributed to the imbalance between cuticle and surface deposition. First, the reference resistance assigned for the cuticle pathway was much higher than the ground surface pathway (see Table 1 in

Zhang et al. 2003). For instance, the reference resistance for in-canopy aerodynamic resistance (R_{ac0}) was 10-40 s/m for crops; the corresponding reference value for cuticle resistance was 4000 s/m under dry conditions. Second, for low-growing vegetation such as crops and grass, LAI values were generally small (<2 m^2/m^2, Figure E-4); cuticle resistance was relatively large simply due to less available leaf surface area. On the other hand, smaller LAI values indicate better turbulent mixing within the canopy and thus more deposition to the ground. For forest with relatively high LAI values (2~4 m^2/m^2), cuticle resistance decreased and became comparable to the surface resistance, especially under wet conditions when a much lower reference resistance was assigned for the cuticle resistance.

For all climate regions and land cover categories, non-stomatal conductance G_{ns} generally peaked in the spring season with lower values during the summer and fall seasons (Figure E-2). This pattern was attributed to changes in the estimated friction velocity u_* (Figure E-5), which was positively correlated with wind speed. Strong winds facilitate the turbulent transport of ozone within the canopy and thus deposition. The magnitudes of simulated daytime wind speeds were considerably larger in the spring (as is also reported by Klink, 1999), especially during the drought years (Figure E-6). For crops, G_{ns} showed a notable rebound in the fall season, which was associated with the substantial LAI reductions as shown in Figure E-4. Compared with other land cover categories, crops exhibited significant LAI reductions (~90%) during the fall season, which is expected due to agricultural harvesting activities.

The stomatal conductance G_{st} (Figure E-3) exhibited different seasonal patterns from the non-stomatal component. Forests and shrubs exhibited similar seasonal G_{st} variations with the highest values during the spring and lowest during the summer. Vapor pressure deficit (VPD) was the major contributor to the G_{st} variations. VPD reached a

maximum in the summertime (Figure E-7) and suppressed the stomatal conductance via f (D) in the model. During the summer of the two dry years (2006 and 2011), f (D) reached the minimum value (0.1) set by the model, implying a stomatal resistance that was a factor of 10 greater compared with conditions when the VPD was zero; thus G_{st} was at a minimum during the summer season. In contrast, f (D) was always set to one for crops and grass, suggesting no suppression of stomatal conductance. For both crops and grass, variations of G_{st} followed closely with the LAI values (Figure E-4). LAI values for croplands were generally higher during the summer and dropped drastically in the fall. Grass, on the other hand, showed an increase in the late summer and fall seasons.

Seasonal variations of daytime V_d were influenced by both the stomatal and non-stomatal pathways. Figure 6-4 shows predicted monthly averaged V_d values by simplified land cover category in the four climate regions during the modeling period. For forest and shrubs, G_{ns} and G_{st} showed similar seasonal variations; V_d showed a minimum during the summer season. For crops, monthly averaged G_{ns} and G_{st} varied in opposing directions, and the overall V_d showed a gradual decreasing trend over the growing season. The deposition velocities of grasses exihibited minimal seasonal variations compared with other land cover cateogries likely due to offsetting variations in G_{ns} and G_{st}. Previous studies have described the seasonality of observed or modeled ozone deposition velocities for different regions and land cover categories (e.g. Pio and Feliciano, 1996; Pio et al., 2000; Sickles and Shadwick, 2007; Fares et al., 2014; Val Martin et al., 2014). Some studies show similar seasonal patterns as discussed in this study (Pio and Feliciano, 1996; Pio et al., 2000) while others do not. For example, estimation of deposition velocities at 34 CASTNET sites in the eastern U.S. suggested highest values in summer and lowest in winter with a summer/winter ratio of approximately three (Sickles and Shadwick, 2007).

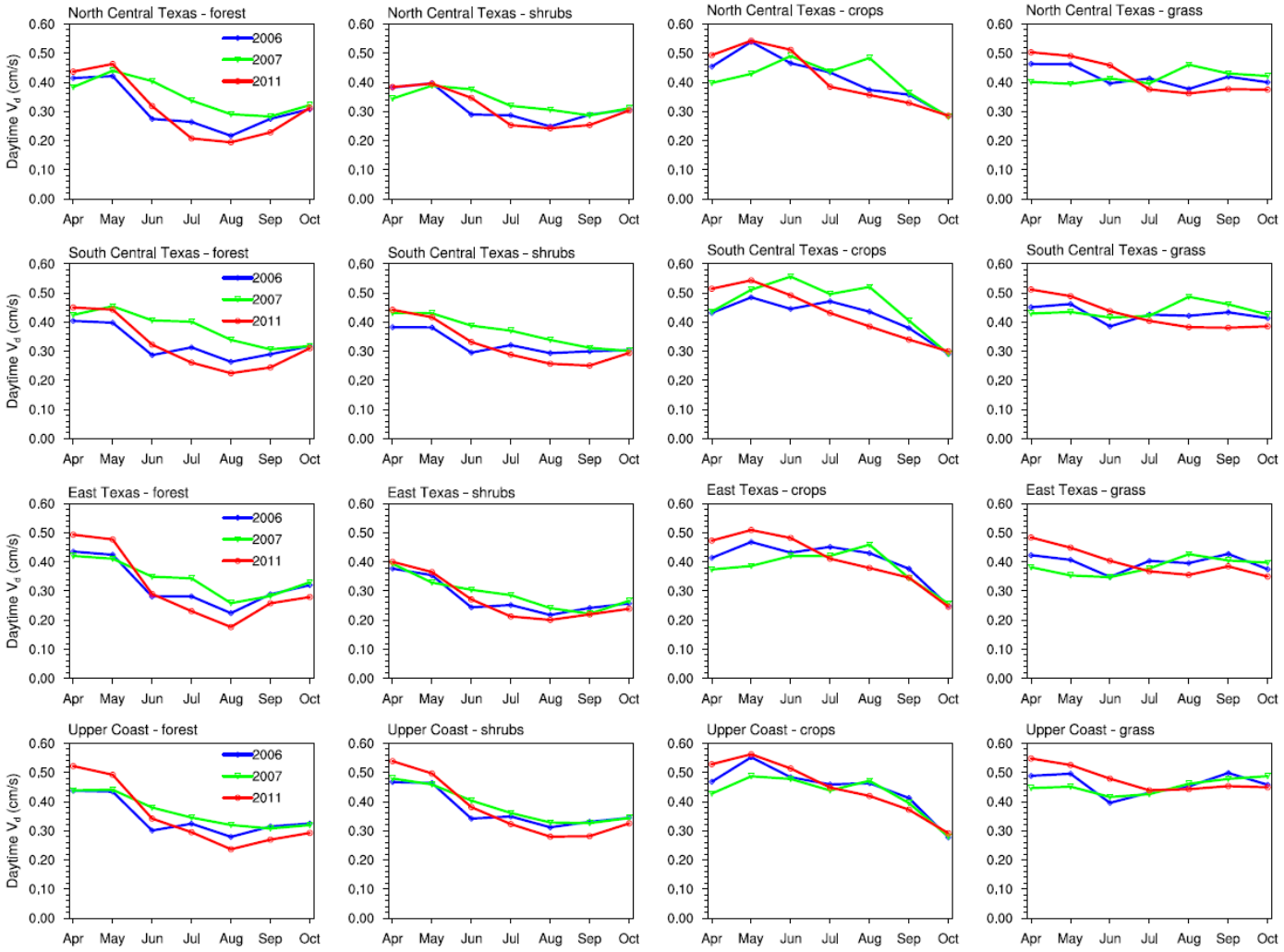

Figure 6-4: Monthly averaged ozone daytime V_d (cm/s) by climate region and simplified land cover category during April-October of 2006, 2007 and 2011.

6.3.2 Comparisons with observations and other model estimates

Land cover-specific V_d values (including non-vegetated surfaces) were aggregated to the overall V_d for each modeling grid based on the fraction of each land cover category. Table 6-2 shows the seasonal mean daytime V_d for each land cover category as well as the overall V_d by climate region of the three years. The maximum and minimum daytime V_d is estimated to be 0.46 (spring) and 0.27 (summer) cm/s during 2011 over East Texas. Variations of the overall V_d across climate regions during the same season were generally small (<10%). Observations of ozone dry deposition velocities are extremely limited in Texas, making it difficult to evaluate model estimates. To the authors' knowledge, only one study (Kawa, 1986) has reported ozone V_d in the range of 1.1 to 1.2 cm/s determined using an eddy covariance technique over the Big Thicket National Preserve (forest) located in East Texas around 13:00 CST on June 23rd, 1982. The reported V_d was much higher than the modeled values in this study, which may be attributable to two causes. First, the V_d values presented in Table 6-2 represent values averaged over large areas instead of a single location; we were not able to discern the specific location and meteorological conditions under which the measurement took place. Second, several studies have found the relative importance of ozone reactions with the biogenic volatile organic compounds (VOCs) or NO emissions from the crown or forest floor contributing to non-stomatal removal (Neirynck et al., 2012; Fares et al., 2012), which is not considered in the current dry deposition algorithm. Val Martin et al. (2014) summarized observed V_d values for major land cover categories reported by a number of studies. Measured V_d values ranged from as low as 0.15 cm/s for grassland in Sacramento, CA to 1.8 cm/s for tropical forest in Amazon. Substantial differences were also observed between high and low LAI conditions (Val Martin et al., 2014).

Table 6-2: Simulated seasonal average daytime V_d (cm/s; ± standard deviation) by climate region and land cover category.

Climate region	2006			2007			2011		
	spring	**summer**	**fall**	**spring**	**summer**	**fall**	**spring**	**summer**	**fall**
North Central Texas	**0.42** ± 0.08	**0.32** ± 0.07	**0.33** ± 0.08	**0.38** ± 0.09	**0.37** ± 0.08	**0.34** ± 0.08	**0.45** ± 0.09	**0.32** ± 0.08	**0.30** ± 0.09
forest	0.42	0.25	0.29	0.41	0.34	0.30	0.45	0.24	0.27
shrubs	0.39	0.27	0.30	0.37	0.33	0.30	0.39	0.28	0.28
crops	0.50	0.42	0.32	0.41	0.47	0.32	0.52	0.42	0.31
grass	0.46	0.39	0.41	0.40	0.42	0.43	0.50	0.40	0.38
South Central Texas	**0.40** ± 0.07	**0.34** ± 0.07	**0.33** ± 0.08	**0.41** ± 0.09	**0.40** ± 0.08	**0.34** ± 0.08	**0.45** ± 0.08	**0.33** ± 0.07	**0.30** ± 0.08
forest	0.40	0.29	0.30	0.44	0.38	0.31	0.45	0.27	0.28
shrubs	0.38	0.30	0.30	0.43	0.37	0.31	0.43	0.29	0.27
crops	0.46	0.45	0.34	0.47	0.52	0.35	0.53	0.44	0.32
grass	0.46	0.41	0.42	0.43	0.44	0.44	0.50	0.41	0.38
East Texas	**0.41** ± 0.08	**0.29** ± 0.08	**0.31** ± 0.09	**0.39** ± 0.10	**0.33** ± 0.08	**0.31** ± 0.08	**0.46** ± 0.10	**0.27** ± 0.07	**0.28** ± 0.10
forest	0.43	0.26	0.30	0.42	0.32	0.31	0.49	0.23	0.27
shrubs	na*	na	na	na	na	na	na	na	na
crops	0.44	0.44	0.31	0.38	0.43	0.30	0.49	0.42	0.30
grass	0.42	0.38	0.40	0.37	0.38	0.40	0.47	0.38	0.37
Upper Coast	**0.38** ± 0.06	**0.32** ± 0.06	**0.32** ± 0.06	**0.36** ± 0.08	**0.33** ± 0.07	**0.32** ± 0.06	**0.42** ± 0.08	**0.32** ± 0.06	**0.29** ± 0.07
forest	0.43	0.30	0.32	0.44	0.35	0.31	0.51	0.29	0.28
shrubs	0.47	0.33	0.34	0.47	0.36	0.34	0.52	0.33	0.31
crops	0.51	0.47	0.34	0.46	0.46	0.34	0.55	0.46	0.33
grass	0.49	0.43	0.48	0.45	0.43	0.48	0.54	0.45	0.45

CASTNET is a national air quality monitoring network that determines dry deposition velocities for various compounds including ozone based on the MLM. Estimated hourly ozone deposition velocities from this study were contrasted with the results at one of the CASTNET monitoring sites located in the East Texas climate region (Figure 6-1b; site name: Alabama-Coushatta; 30.70ºN, 94.67ºW). This monitoring site is located in a 4-km grid cell characterized as 55% of evergreen needleleaf trees, 36% of deciduous broadleaf trees and 7.4% of mixed wood forest. Scatter plot of paired results are shown in Figure 6-5. Mean difference (MD), mean absolute difference (MAD) and the Pearson correlation coefficient (R) were calculated for each year using the method of Schwede et al. (2011). Generally, the calculated MD, MAD and R values were comparable with values reported by Schwede et al. (2011) for four other CASTNET sites in the eastern U.S. and Canada. Nighttime deposition exhibited better agreements between the two models than daytime deposition.

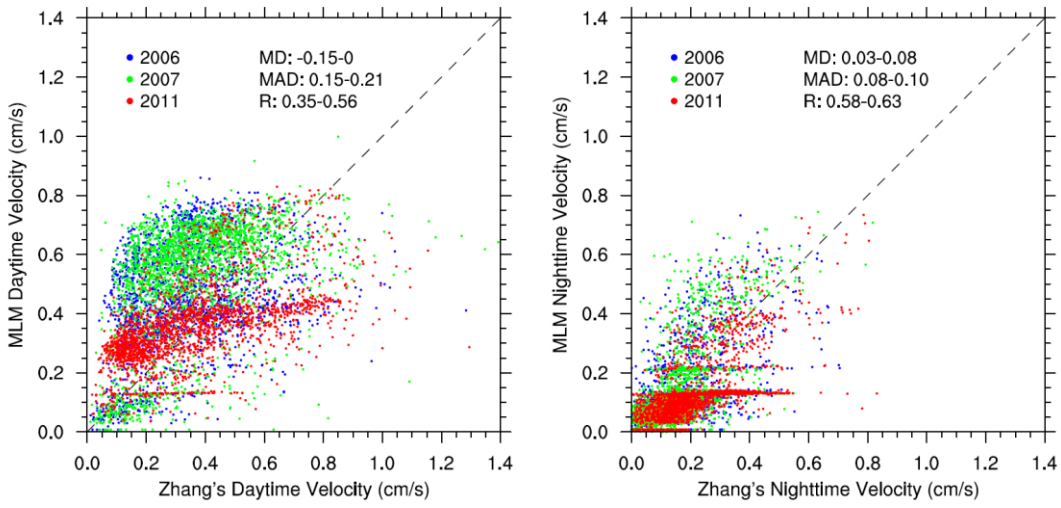

Figure 6-5: Scatter plot of daytime (left) and nighttime (right) hourly ozone V_d predicted by the MLM and Zhang's algorithm at the Alabama-Coushatta monitoring site during April-October of 2006, 2007 and 2011. Values for the mean difference (MD), mean absolute difference (MAD) and Pearson correlation coefficient (R) are shown as a range for the three years.

6.3.3 Impact of drought on ozone dry deposition

The impact of drought on predicted ozone dry deposition velocities was examined by contrasting 2007, a year with greater than average precipitation, with 2011, a historical drought year. Similar to the seasonal patterns, the drought response in predicted deposition velocities was a reflection of the combined drought responses of the stomatal and non-stomatal conductances. Interannual differences in daytime deposition velocity and associated component resistances were examined in this work. As described earlier, stomatal and non-stomatal conductances were simulated as functions of temperature (T), vapor pressure deficit (VPD), solar radiation (SRAD), LAI, and friction velocity (u_*, or wind speed). Table 6-3 compares the absolute differences of the aforementioned input variables (as well as the overall V_d values) between drought and non-drought conditions (calculated as 2011 minus 2007) by season and climate region; a *t*-test was performed to determine the significance levels of differences.

Table 6-3: Absolute differences (calculated as 2011 minus 2007) of temperature, vapor pressure deficit (VPD), solar radiation (SRAD), wind speed, LAI (by land cover category), friction velocity (u_*, by land cover category) and overall daytime V_d between drought (2011) and non-drought (2007) conditions by season and climate region. Values with ** indicate significant a difference between the two years (p<0.05).

Season	Climate region	Temp. (K)	VPD (kPa)	SRAD (W/m^2)	Wind speed (m/s)	LAI (m^2/m^2)				u_* (cm/s)				V_d (cm/s)
						forest	shrubs	crops	grass	forest	shrubs	crops	grass	
Spring	North Central Texas	3.5**	0.8**	21.1	2.0**	-0.2**	-0.4**	-0.2**	-0.1**	0.24**	0.10**	0.14**	0.12**	0.07**
	South Central Texas	3.3**	0.7**	43.3**	1.6**	-0.4**	-0.4**	-0.2**	-0.1**	0.19**	0.08**	0.10**	0.09**	0.04**
	East Texas	2.6**	0.4**	19.5	2.0**	0.1	na*	-0.03	-0.07**	0.25**	na	0.14**	0.12**	0.07**
	Upper Coast	2.2**	0.3**	26	1.7**	0.01	-0.2**	-0.2**	-0.05**	0.22**	0.13**	0.12**	0.10**	0.06**
Summer	North Central Texas	5.6**	2.1**	26.0**	0.6**	-0.5**	-0.6**	-0.6**	-0.2**	0.05	0.02	0.02	0.02	-0.05**
	South Central Texas	3.2**	1.2**	39.8**	0.3	-0.5**	-0.6**	-0.8**	-0.2**	0.02	-0.01	0.01	0.0	-0.07**
	East Texas	4.3**	1.5**	26.8**	0.5**	-0.1**	na	-0.5**	-0.2**	0.06**	na	0.03**	0.03**	-0.06**
	Upper Coast	2.3**	0.8**	37.7**	0.6**	-0.2**	-0.4**	-0.4**	-0.1**	0.08**	0.04**	0.04**	0.03**	-0.01
Fall	North Central Texas	-0.1	0.5**	5.2	0.3	-0.3**	-0.2**	-0.2**	-0.3**	0.03	0.0	0.01	0.0	-0.04**
	South Central Texas	0.4	0.5**	15.6	0.2	-0.3**	-0.4**	-0.2**	-0.3**	0.03	-0.01	0.01	-0.01	-0.04**
	East Texas	0.2	0.6**	12	0.4	-0.1**	na	-0.2	-0.3**	0.04	na	0.02	0.01	-0.03
	Upper Coast	0.2	0.4**	12.2	0.4	-0.2**	-0.4**	-0.2**	-0.3**	0.05	0.01	0.02	0.01	-0.03

As shown by Table 6-3, regional averaged daytime air temperatures were significantly higher (p<0.05) during the spring and summer seasons of the drought year; the maximum temperature increases reached 5.6 K in North Central Texas during the summer. For major land cover categories present in eastern Texas, the temperature for maximum stomatal opening ranges between 288~300 K (Figure E-1a); temperatures below or above this range suppress stomatal opening in the model. Summer daytime average temperatures were well above this optimal range (e.g., ~303 K during 2007) in eastern Texas, and the even higher temperatures during the drought year would be predicted to impose greater stress on stomatal conductance. Higher temperatures and lower humidity associated with the drought conditions also resulted in larger VPD during 2011. For all seasons, VPD was significantly larger during the drought year with a maximum increase by 2.1 kPa. In Zhang's algorithm, the stomatal conductance of low growing vegetation such as crops and grass are unaffected by VPD; but for trees and shrubs, an increase of 1 kPa in VPD could reduce the stomatal conductance by 27-36% compared to conditions with no VPD stress. Solar radiation (SRAD) was also greater during the drought year. The change in solar radiation had two opposing effects on the stomatal conductance. First, the canopy stomatal conductance G_s (PAR) in Eq. 6-3 is positively correlated with the incoming solar radiation, which is responsible for the diurnal cycle of stomatal opening and closure. However, the increase in canopy stomatal conductance quickly saturates when the incoming solar radiation reaches a certain level (e.g. 400 W/m^2). Thus this positive impact of stronger solar radiation associated with drought conditions on stomatal conductance was expected to be negligible. On the other hand, very high solar radiation lowers the leaf water potential (ψ) and causes stomatal closure through the $f(\psi)$ function (Figure E-1c). The minimum solar radiation that causes stomatal suppression for forest and shrubs was approximately 900 W/m^2 (corresponding

to ψ_{c1} of -1.9 kPa) compared to 600 W/m^2 (ψ_{c1}=-1.5 kPa) for crops and grasses, suggesting stronger suppression for the low-growing vegetation. The drought year was also associated with stronger wind speeds, especially during the spring season. As a result, simulated friction velocity (u_*) was significantly larger in 2011 for all land cover categories and climate regions in the spring. The differences in u_* became smaller during the summer and fall seasons. LAI is an important parameter for modeling both stomatal and non-stomatal conductances; lower values were observed during the drought year by as much as 0.8 m^2/m^2. Reductions in LAI were greater in North and South Central Texas than East Texas. In summary, temperature, VPD, solar radiation, wind speed and friction velocity generally exhibited increases, albeit to different extents, while LAI decreased during the drought year.

Figure 6-6 illustrates the absolute change in seasonal daytime non-stomatal conductance (G_{ns}), stomatal conductance (G_{st}) and deposition velocity (V_d) between the drought (2011) and non-drought (2007) years (calculated as 2011 minus 2007). Under drought conditions, non-stomatal conductance (G_{ns}) increased across climate regions and land cover categories, with the exception of forests. Surface deposition was the dominant contribution to non-stomatal deposition, except for forests, for which cuticle deposition also played a role. The changes in G_{ns} between drought and non-drought years were closely related to the changes in the friction velocity. As friction velocity increased substantially during the spring of 2011, simulated G_{ns} also exhibited a maximum increase (>0.1 cm/s). This increase of non-stomatal deposition under drought conditions became weaker during the summer and fall seasons when friction velocity was only slightly higher during the drought year. For forests with relatively high LAI values, cuticle deposition was comparable to surface deposition. Reductions in the cuticle deposition due to the LAI reductions exceeded the increase in the surface deposition thus leading to an

overall decrease in non-stomatal deposition for forests during the summer of 2011 (Figure 6-6a).

As opposed to the general increase of G_{ns} during the drought year, stomatal conductances (G_{st}) were suppressed (with one exception) under the drier and hotter conditions in 2011. For forest and shrubs, substantial decreases in G_{st} occurred during the spring in response to the increased VPD and decreased LAI. In contrast, for crops and grasses that were not affected by VPD, the spring G_{st} changed slightly during the spring of the drought year; the direction of the change depended on the relative magnitudes in the LAI reduction versus temperature increase. For all land cover categories except grass, maximum G_{st} reductions occurred during the summer season as the factors that suppressed stomatal conductance became most significant. For crops in South Central Texas, G_{st} decreased by as much as 0.18 cm/s, corresponding to a relative reduction of 44%. Because forest and shrubs have relative lower G_{st} compared with crops and grass (due to the VPD impact), the relative G_{st} reductions associated with drought were larger, reaching 84% for shrubs in North Central Texas. During the fall season, grasses exhibited the largest G_{st} decrease (>0.1 cm/s) when LAI reductions during the drought year were most substantial (Table 6-3), while other land cover categories exhibited smaller G_{st} reductions. Due to the opposing drought responses of G_{st} and G_{ns}, the ratio of $G_{st}/(G_{ns} + G_{st})$ was smaller under drought conditions. For instance, the ratio ranged between 29%-67% in 2007 and 7%-58% in 2011.

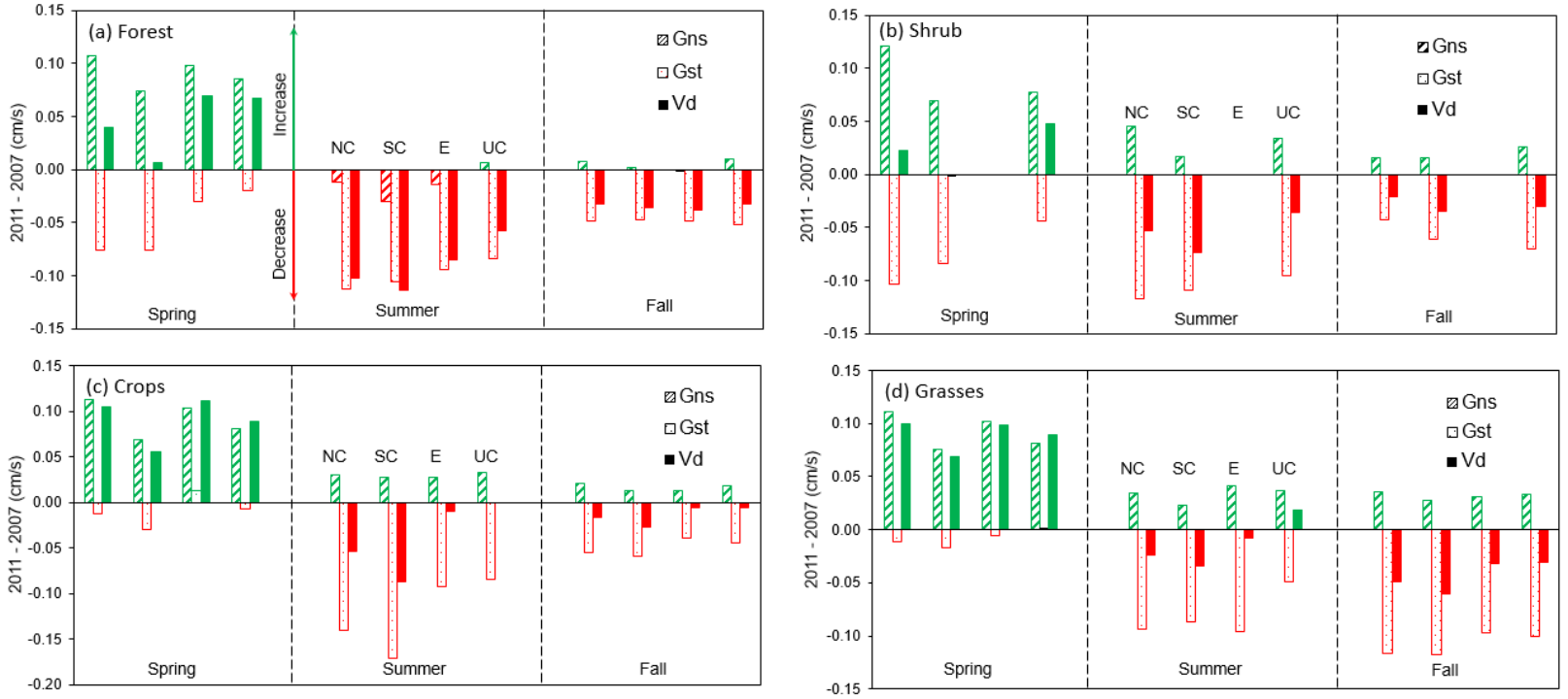

Figure 6-6: Absolute changes in seasonal mean daytime non-stomatal conductances (G_{ns}, cm/s), stomatal conductances (G_{st}, cm/s) and dry deposition velocities (V_d, cm/s) between drought (2011) and non-drought (2007) years (calculated as 2011 minus 2007) by land cover category and climate region – North Central Texas (NC), South Central Texas (SC), East Texas (E), and Upper Coast (UC). Green indicates an increase and red indicates a decrease in 2011. Because East Texas had negligible coverage of shrubs, results are not shown.

The impact of drought on daytime deposition velocity V_d depends on the relative magnitudes of changes in G_{ns} and G_{st}. In spring, the increase in G_{ns} exceeded the decrease in G_{st}, resulting in an overall increase in V_d during 2011. Crops and grass showed stronger increases in V_d than forest and shrubs during the drought year. The opposite trend was predicted during the summer and fall seasons when G_{st} reductions overwhelmed the increases in G_{ns}. Forest had the largest reductions in V_d during the drought year summer compared to other land cover categories, as both G_{ns} and G_{st} decreased; for example, the maximum decrease in V_d in South Central Texas was 0.11 cm/s (corresponding to a relative reduction of 30%). Figure E-8 compares area-averaged daytime V_d between 2007 and 2011. In general, all climate regions show the same directional change in V_d associated with drought but the magnitudes differs. The increase in V_d during the spring of the drought year was most significant in the Upper Coast (by 28%), but minimal reductions in V_d (<4%) were observed during the summer. Forest covers almost 70% of East Texas; thus East Texas experienced the most substantial relative reductions (~18%) in V_d associated with the drought conditions.

Previous studies have measured/modeled ozone deposition and/or stomatal/non-stomatal removal at various locations and for different land cover categories (e.g. Park et al., 2014; Neirynck et al., 2012; Tuzet et al., 2011; Rannik et al., 2012; Fares et al., 2013; Val Martin et al., 2014;). The relative contributions of stomatal and non-stomatal deposition differed by location (i.e. canopy types) and climate regime. For example, non-stomatal deposition was reported to account for 20-63% of total ozone deposition by Rannik et al., (2012) and Tuzet et al. (2011). Driving variables controlling ozone dry deposition processes include LAI, vapor pressure deficit, gas-phase chemistry, etc. Although it is a general consensus that stomatal conductance will decrease under drought conditions, few studies have specifically examined the impacts of drought on deposition

velocity and the associated component resistances simultaneously. As found in this study, non-stomatal conductances under drought conditions actually exhibited increases due to larger simulated friction velocities and lower LAI values, which facilitates the mechanical mixing of ozone into the air space of the canopy. Several studies have also reported that gas-phase ozone reactions with biogenic VOCs are an important contribution to ozone uptake (e.g. Kurpius and Goldstein, 2003; Goldstein et al., 2004; Neirynck et al., 2012). As drought is expected to enhance the emissions of most biogenic VOCs due to higher temperatures, ozone scavenging by BVOCs, which is not included in the current dry deposition algorithm, could also lead to more ozone uptake through the chemical reactions within the canopy air space.

6.4 CONCLUSIONS

Drought is a recurring phenomenon in Texas with the potential for increases in frequency and intensity under future climate change (Melillo et al., 2014). Understanding impacts on ozone dry deposition is critical for regional air quality modeling and management. This work quantified seasonal and interannual variations of ozone daytime dry deposition velocities estimated by Zhang's dry deposition algorithm over eastern Texas. This work is the first to examine changes in ozone deposition velocity and associated component resistances (e.g. stomatal and non-stomatal conductance) simultaneously in response to drought conditions. Drought-induced changes in meteorological fields (including temperature, wind speed, vapor pressure deficit, etc.) and leaf area index (LAI) resulted in opposing responses of stomatal and non-stomatal conductances: stomatal conductances generally decreased under drought conditions while non-stomatal conductances showed increases associated with higher wind speeds and smaller LAI values. The overall deposition velocities increased during the spring of the drought year but decreased during the summer (>0.1 cm/s) and fall seasons. Forests

exhibited the most significant reductions in ozone dry deposition velocities. Results from this study emphasize the need for field measurements and the importance of understanding the spatial distribution of impacts on ozone dry deposition over eastern Texas and other regions of the world subject to recurring drought.

6.5 REFERENCES

Bohler, S., Cuypers, A., & Vangronsveld, J. (2015). *Combined Stresses in Plants*. (pp. 147–157). Springer International Publishing.

Chen, F., & Dudhia, J. (2001). Coupling an advanced land surface-hydrology model with the Penn State-NCAR MM5 modeling system. Part I: Model implementation and sensitivity. *Monthly Weather Review*, *129*(4), 569-585.

Clarke, J. F., Edgerton, E. S., & Martin, B. E. (1997). Dry deposition calculations for the clean air status and trends network. *Atmospheric Environment*, *31*(21), 3667–3678.

ENVIRON. (2014). User's Guide Comprehensive Air Quality Model with Extensions version 6.1. Retrieved June 8, 2015 from http://www.camx.com/files/camxusersguide_v6-10.pdf

Fannin, B. (2011). Texas agricultural drought losses reach record $5.2 billion. AgriLife Today. Retrieved June 8, 2015, from http://today.agrilife.org/2011/08/17/texas-agricultural-drought-losses-reach-record-5-2-billion

Fares, S., McKay, M., Holzinger, R., & Goldstein, A. H. (2010). Ozone fluxes in a Pinus ponderosa ecosystem are dominated by non-stomatal processes: Evidence from long-term continuous measurements. *Agricultural and Forest Meteorology*, *150*(3), 420–431. doi:10.1016/j.agrformet.2010.01.007

Fares, S., Savi, F., Muller, J., Matteucci, G., & Paoletti, E. (2014). Simultaneous measurements of above and below canopy ozone fluxes help partitioning ozone deposition between its various sinks in a Mediterranean Oak Forest. *Agricultural and Forest Meteorology*, 198-199, 181–191. doi:10.1016/j.agrformet.2014.08.014

Fares, S., Vargas, R., Detto, M., Goldstein, A. H., Karlik, J., Paoletti, E., & Vitale, M. (2013). Tropospheric ozone reduces carbon assimilation in trees: estimates from analysis of continuous flux measurements. *Global Change Biology*, *19*(8), 2427–43. doi:10.1111/gcb.12222

Fares, S., Weber, R., Park, J.-H., Gentner, D., Karlik, J., & Goldstein, A. H. (2012). Ozone deposition to an orange orchard: Partitioning between stomatal and non-stomatal sinks. *Environmental Pollution*, *169*, 258–266. doi:10.1016/j.envpol.2012.01.030

Finkelstein, P. L., Ellestad, T. G., Clarke, J. F., Meyers, T. P., Schwede, D. B., Hebert, E. O., & Neal, J. A. (2000). Ozone and sulfur dioxide dry deposition to forests:

Observations and model evaluation. *Journal of Geophysical Research: Atmospheres (1984–2012)*, *105*(D12), 15365-15377.

Goldstein, A. H., McKay, M., Kurpius, M. R., Schade, G. W., Lee, A., Holzinger, R., & Rasmussen, R. A. (2004). Forest thinning experiment confirms ozone deposition to forest canopy is dominated by reaction with biogenic VOCs. *Geophysical research letters*, *31*(22).

Guenther, A. B., Jiang, X., Heald, C. L., Sakulyanontvittaya, T., Duhl, T., Emmons, L. K., & Wang, X. (2012). The Model of Emissions of Gases and Aerosols from Nature version 2.1 (MEGAN2. 1): an extended and updated framework for modeling biogenic emissions.

Harper, C., Personal Communication, Nov. 2012

Hogg, A., Uddling, J., Ellsworth, D., Carroll, M. A., Pressley, S., Lamb, B., & Vogel, C. (2007). Stomatal and non-stomatal fluxes of ozone to a northern mixed hardwood forest. *Tellus B*, *59*(3), 514-525.

Hong, S. Y., & Lim, J. O. J. (2006). The WRF single-moment 6-class microphysics scheme (WSM6). *Asia-Pacific Journal of Atmospheric Sciences*, *42*(2), 129-151.

Hong, S. Y., Noh, Y., & Dudhia, J. (2006). A new vertical diffusion package with an explicit treatment of entrainment processes. *Monthly Weather Review*, *134*(9), 2318-2341.

Huang, L., McDonald-Buller, E. C., McGaughey, G., Kimura, Y., & Allen, D. T. (2014). Annual variability in leaf area index and isoprene and monoterpene emissions during drought years in Texas. *Atmospheric Environment*, *92*, 240–249. doi:10.1016/j.atmosenv.2014.04.016

Ingwersen, J., Steffens, K., Högy, P., Warrach-Sagi, K., Zhunusbayeva, D., Poltoradnev, M., ... & Streck, T. (2011). Comparison of Noah simulations with eddy covariance and soil water measurements at a winter wheat stand. *Agricultural and Forest Meteorology*, *151*(3), 345-355.

Kawa, S. R. (1986). *Ozone deposition, scalar budgets and radiative heating over Texas coastal forest and ocean*. Department of Atmospheric Science, Colorado State University.

Klink, K. (1999). Climatological mean and interannual variance of United States surface wind speed, direction and velocity. *International Journal of Climatology*, *19*(5), 471-488.

Kurpius, M. R., & Goldstein, A. H. (2003). Gas-phase chemistry dominates O_3 loss to a forest, implying a source of aerosols and hydroxyl radicals to the atmosphere. *Geophysical Research Letters*, *30*(7).

Lamaud, E., Loubet, B., Irvine, M., Stella, P., Personne, E., & Cellier, P. (2009). Partitioning of ozone deposition over a developed maize crop between stomatal and non-stomatal uptakes, using eddy-covariance flux measurements and modelling. *Agricultural and Forest Meteorology*, *149*(9), 1385–1396. doi:10.1016/j.agrformet.2009.03.017

Lelieveld, J., & Dentener, F. J. (2000). What controls tropospheric ozone ? *Journal of Geophysical Research: Atmospheres* (1984–2012), *105*(1999), 3531–3551.

McDonald-Buller, E., Wiedinmyer, C., Kimura, Y., & Allen, D. (2001). Effects of land use data on dry deposition in a regional photochemical model for eastern Texas. *Journal of the Air & Waste Management Association*, *51*(8), 1211–1218. doi:10.1080/10473289.2001.10464340

Melillo, J. M., Richmond, T. T., & Yohe, G. W. (2014). Climate change impacts in the United States. *Third National Climate Assessment*.

Meyers, T. P., Finkelstein, P., Clarke, J., Ellestad, T. G., & Sims, P. F. (1998). A multilayer model for inferring dry deposition using standard meteorological measurements. *Journal of Geophysical Research*, *103*(D17), 22645–22661.

Michou, M., Laville, P., Serça, D., Fotiadi, A., Bouchou, P., & Peuch, V.H. (2005). Measured and modeled dry deposition velocities over the ESCOMPTE area. *Atmospheric Research*, *74*(1-4), 89–116. doi:10.1016/j.atmosres.2004.04.011

Mills, G., Hayes, F., Simpson, D., Emberson, L., Norris, D., Harmens, H., & Büker, P. (2011). Evidence of widespread effects of ozone on crops and (semi-) natural vegetation in Europe (1990–2006) in relation to AOT40-and flux-based risk maps. *Global Change Biology*, *17*(1), 592–613.

Neirynck, J., Gielen, B., Janssens, I. A, & Ceulemans, R. (2012). Insights into ozone deposition patterns from decade-long ozone flux measurements over a mixed temperate forest. *Journal of Environmental Monitoring*, *14*(6), 1684–1695. doi:10.1039/c2em10937a

Park, R. J., Hong, S. K., Kwon, H. A., Kim, S., Guenther, a., Woo, J.H., & Loughner, C. P. (2014). An evaluation of ozone dry deposition simulations in East Asia. *Atmospheric Chemistry and Physics*, *14*(15), 7929–7940. doi:10.5194/acp-14-7929-2014

Pio, C. A., & Feliciano, M. S. (1996). Dry deposition of ozone and sulphur dioxide over low vegetation in moderate southern European weather conditions. Measurements and modelling. *Physics and Chemistry of the Earth*, *21*(5), 373–377.

Pio, C. A., Feliciano, M. S., Vermeulen, A. T., & Sousa, E. C. (2000). Seasonal variability of ozone dry deposition under southern European climate conditions, in Portugal. *Atmospheric Environment*, *34*, 195–205.

Pleijel, H., Danielsson, H., Emberson, L., Ashmore, M. R., & Mills, G. (2007). Ozone risk assessment for agricultural crops in Europe: Further development of stomatal flux and flux–response relationships for European wheat and potato. *Atmospheric Environment*, *41*(14), 3022–3040. doi:10.1016/j.atmosenv.2006.12.002

Pleim, J., & Ran, L. (2011). Surface flux modeling for air quality applications. *Atmosphere*, *2*(4), 271–302. doi:10.3390/atmos2030271

Popescu, S. C., Stukey, J., Mutlu, M., Zhao, K., Sheridan, R., Ku, N. W. (2011). Expansion of Texas Land Use/Land Cover through Class Crosswalking and Lidar Parameterization of Arboreal Vegetation Secondary Investigators. Retrieved June 8, 2015 from https://www.tceq.texas.gov/assets/public/implementation/air/am/contracts/reports/oth/5820564593FY0925-20110419-tamu-expension_tx_lulc_arboreal_vegetation.pdf

Rannik, Ü., Altimir, N., Mammarella, I., Bäck, J., Rinne, J., Ruuskanen, T. M., et al. (2012). Ozone deposition into a boreal forest over a decade of observations: evaluating deposition partitioning and driving variables. *Atmospheric Chemistry and Physics*, *12*(24), 12165–12182. doi:10.5194/acp-12-12165-2012

Schwede, D., Zhang, L., Vet, R., & Lear, G. (2011). An intercomparison of the deposition models used in the CASTNET and CAPMoN networks. *Atmospheric Environment*, *45*(6), 1337–1346. doi:10.1016/j.atmosenv.2010.11.050

Seinfeld, J. H., & Pandis, S. N. (2012). *Atmospheric chemistry and physics: from air pollution to climate change*. John Wiley & Sons.

Sheffield, J., & Wood, E. F. (2012). Major drought events of the 20th century. *Drought: Past Problems and Future Scenarios* (pp. 123–164). Routledge.

Sickles, J. E., & Shadwick, D. S. (2007). Seasonal and regional air quality and atmospheric deposition in the eastern United States. *Journal of Geophysical Research*, *112*(D17), D17302. doi:10.1029/2006JD008356

Skamarock, W. C., Klemp, J. B., Dudhia, J., Gill, D. O., Barker, D. M., Wang, W., & Powers, J. G. (2005). *A description of the advanced research WRF version 2* (No.

NCAR/TN-468+ STR). National Center For Atmospheric Research Boulder Co Mesoscale and Microscale Meteorology Div.

Solberg, S., Hov, Ø., Søvde, A., Isaksen, I. S. A., Coddeville, P., De Backer, H., et al. (2008). European surface ozone in the extreme summer 2003. *Journal of Geophysical Research*, 113(D7), D07307. doi:10.1029/2007JD009098.

Tuzet, A., Perrier, A., Loubet, B., Cellier, P. (2011). Modelling ozone deposition fluxes: the relative roles of deposition and detoxification processes. *Agricultural and Forest Meteorology*, *151*(4), 480-492.

UNECE. (2004). Revised Manual on Methodologies and Criteria for Mapping Critical Levels/loads and Geographical Areas where they are Exceeded. www.icpmapping.org.

Val Martin, M., Heald, C. L., & Arnold, S. R. (2014). Coupling dry deposition to vegetation phenology in the Community Earth System Model: Implications for the simulation of surface O_3. *Geophysical Research Letters*, *41*(8), 2988–2996. doi:10.1002/2014GL059651.Received

Wesely, M. L. (1989). Parameterization of surface resistances to gaseous dry deposition in regional-scale numerical models. *Atmospheric Environment*, *23*(6), 1293–1304.

Wesely, M. L., Eastman, J. A., Stedman, D. H., & Yalvac, E. D. (1982). An eddy-correlation measurement of NO_2 flux to vegetation and comparison to O_3 flux. *Atmospheric Environment*, *16*(4), 815–820.

Wesely, M. L., & Hicks, B. B. (2000). A review of the current status of knowledge on dry deposition. *Atmospheric Environment*, *34*(12), 2261–2282.

Wild, O. (2007). Modelling the global tropospheric ozone budget : exploring the variability in current models. *Atmospheric Chemistry and Physics*, *7*(10), 2643–2660.

Wittig, V. E., Ainsworth, E. A., Naidu, S. L., Karnosky, D. F., & Long, S. P. (2009). Quantifying the impact of current and future tropospheric ozone on tree biomass, growth, physiology and biochemistry: a quantitative meta-analysis. *Global Change Biology*, *15*(2), 396–424. doi:10.1111/j.1365-2486.2008.01774.x

Wu, Z., Wang, X., Chen, F., Turnipseed, A. A., Guenther, A. B., Niyogi, D., ... & Alapaty, K. (2011). Evaluating the calculated dry deposition velocities of reactive nitrogen oxides and ozone from two community models over a temperate deciduous forest. *Atmospheric Environment*, *45*(16), 2663-2674.

Zhang, L., Brook, J. R., & Vet, R. (2002). On ozone dry deposition — with emphasis on non-stomatal uptake and wet canopies. *Atmospheric Environment*, *36*(30), 4787–4799.

Zhang, L., Brook, J. R., & Vet, R. (2003). A revised parameterization for gaseous dry deposition in air-quality models. *Atmospheric Chemistry and Physics*, *3*(6), 2067–2082.

Chapter 7: Process Analysis of Ozone Formation under Drought Conditions

7.1 INTRODUCTION

Ground-level ozone is a well-known air pollutant that has adverse impacts on public health (e.g. Brook et al., 2002; Ruidavets et al., 2005; Gryparis et al., 2004) and ecosystems (e.g. Ashmore 2002; Fuhrer and Booker, 2003). Tropospheric ozone is formed via photochemical reactions involving nitrogen oxides (NO_x) and volatile organic compounds (VOCs) (Atkinson et al., 2000) and is removed by chemical destruction and dry deposition to the Earth's surface. As described in previous chapters, biogenic emissions (the dominant source of VOCs) and ozone dry deposition in eastern Texas are subject to the impacts of drought. For biogenic emissions, specifically isoprene and monoterpenes, higher temperatures associated with drought conditions could lead to higher emissions estimates while reductions in the leaf area index (LAI) and soil moisture could result in lower emissions, although large uncertainties exist in the soil moisture impact (Chapter 3 and 4). For ozone dry deposition, stomatal conductances were substantially suppressed under drought conditions due to higher temperatures, larger vapor pressure deficits and reduced LAI values, resulting in lower daytime dry deposition velocities during the summer and fall seasons (Chapter 6).

Ground-level ozone concentrations are influenced by complex chemical and physical processes, anthropogenic/biogenic emissions, and meteorological conditions. This chapter utilizes the process analysis diagnostic tool in the Comprehensive Air Quality Model with Extension (CAMx) to explore the relative contributions of different physical and chemical processes on predicted ground-level ozone concentrations during representative wet and dry periods, thereby providing valuable information for

understanding the impact of drought on ground-level ozone concentrations over eastern Texas.

7.2 CAMx CONFIGURATION

CAMx simulations were conducted during August 2007 and August 2011 as representative wet and dry periods, respectively. The CAMx modeling domain follows an existing CAMx episode developed by the Texas Commission on Environmental Quality (TCEQ; 2012 June episode, https://www.tceq.texas.gov/airquality/airmod/data/tx2012), which includes 36-km, 12-km, and 4-km horizontal grid domains (Figure 7-1a). The latest CAMx version 6.20 was used with Carbon Bond 6 revision 2 (CB6r2; Yarwood et al, 2012; Ruiz and Yarwood, 2013) as the gas-phase chemistry mechanism and the Zhang algorithm for dry deposition (Zhang et al., 2003). Meteorological fields were provided by simulation results from the Weather Research and Forecasting (WRF) model (see details in Section 6.2.2). Initial and boundary conditions were generated by the three-dimensional chemical transport Model for Ozone and Related Chemical Tracers (MOZART; Brasseur et al., 1998). Landuse data developed by the TCEQ were based on the combination of three products including the 2001 National Land Cover Dataset, Biogenic Emission Landuse Data (BELD) version 3, and a land cover dataset developed by the Texas A&M Spatial Sciences Laboratory (Popescu et al., 2011; Harper, 2012); land use data were mapped to Zhang's 26 categories used in the deposition algorithm in CAMx. The MODIS 8-day (MCD15A2) and 4-day (MCD15A3) LAI products were used for the 36/12-km and 4-km domains, respectively. Biogenic emissions were generated by MEGAN2.10 for all three horizontal grid domains. For the 36/12-km domains, MEGAN simulations were driven by the WRF generated meteorological fields, including Photosynthetically Active Radiation (PAR) that was converted from WRF predicted

surface shortwave radiation. For the 4-km domain, MEGAN simulations followed the same settings described in Chapter 3 and Chapter 4 (see details in Section 3.2.3 and Section 4.2.2). The soil moisture algorithm was only applied to the 4-km domain, using soil moisture data generated by the Noah land surface model (Ek et al., 2003). Anthropogenic emissions from point sources, mobile sources, and area sources provided by the TCEQ (reg3a scenario) were averaged over June 2012 to generate episode means by weekdays (Monday-Thursday), Fridays, Saturdays, and Sundays. These episode mean values were then combined with daily specific biogenic emissions to form daily emissions profiles for August 2007 and 2011.

Process analysis (PA) has been widely used to investigate the formation of ozone and particulate matter (e.g. Hogrefe et al., 2007; Kimura et al., 2008; Wang et al., 2010; Liu et al., 2010). The integrated process rate (IPR) method is one of the three components of the process analysis diagnostic tool implemented in CAMx. The IPR analysis calculates the hourly contributions of each physical process (i.e., advection, diffusion, deposition, and chemistry) on ozone formation (ENVIRON, 2014) and was activated over the 4-km domain for this work. Results including dry deposition velocity, deposition flux, surface ozone concentrations, and IPR rates were analyzed by eastern Texas climate regions (North Central Texas, South Central Texas, East Texas, and Upper Coast) and/or three urban regions – Austin/San Antonio (AUS/SA), Dallas/Fort Worth (DFW) and Houston/Galveston/Brazoria (HGB) as shown in Figure 7-1b. These urban areas are currently designated as 8-hour ozone non-attainment or near non-attainment regions.

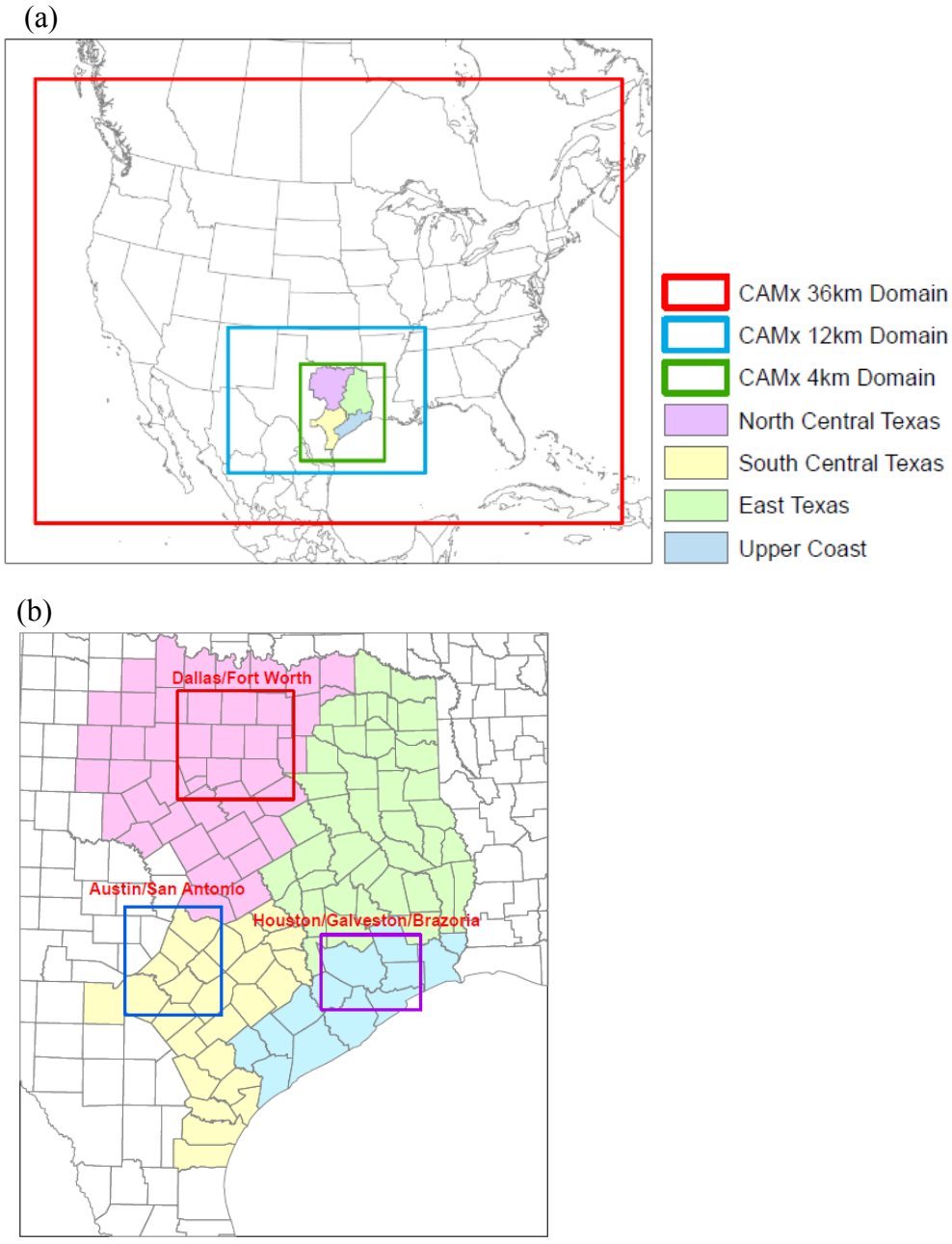

Figure 7-1: (a) CAMx nested grid domains (Red: 36 km; Blue: 12 km; Green: 4 km) with eastern Texas climate regions highlighted. Source: https://www.tceq.texas.gov/airquality/airmod/data/domain). (b) Boundaries of Austin/San Antonio, Dallas/Fort Worth and Houston/Galveston/Brazoria urban regions for process analysis.

7.3 RESULTS AND DISCUSSIONS

7.3.1 Analysis of integrated process rates (IPR)

The ozone IPR rates of the surface layer (~17m) were analyzed for the three urban regions as shown in Figure 7-1b. Five processes including chemistry, Plume-in-Grid change, horizontal/vertical transport, and dry deposition were considered. Horizontal transport includes horizontal advection and diffusion, and vertical transport includes vertical advection and diffusion at the top and bottom boundary. Figure 7-2 shows the daily-mean hourly contributions of individual processes to surface ozone concentrations over AUS/SA urban regions during August 2007 and 2011 as an example. Similar plots for DFW and HGB are shown in Figure F-1 and Figure F-2. For all regions, vertical transport and dry deposition represented the dominant mechanism for surface ozone production and removal during both wet and drought periods. Dry deposition exhibited substantial contributions for ozone removal with averaged values of ~10 ppb/hr in AUS/SA and DFW and slight lower (~8 ppb/hr) in HGB. Portions of the large contributions from the vertical transport could be interpreted as the ozone formed by chemical reactions in higher layers (above 17m) entrained down to the surface layer. Horizontal transport was negligible as the regions for IPR analysis were relatively large compared to typical wind speeds.

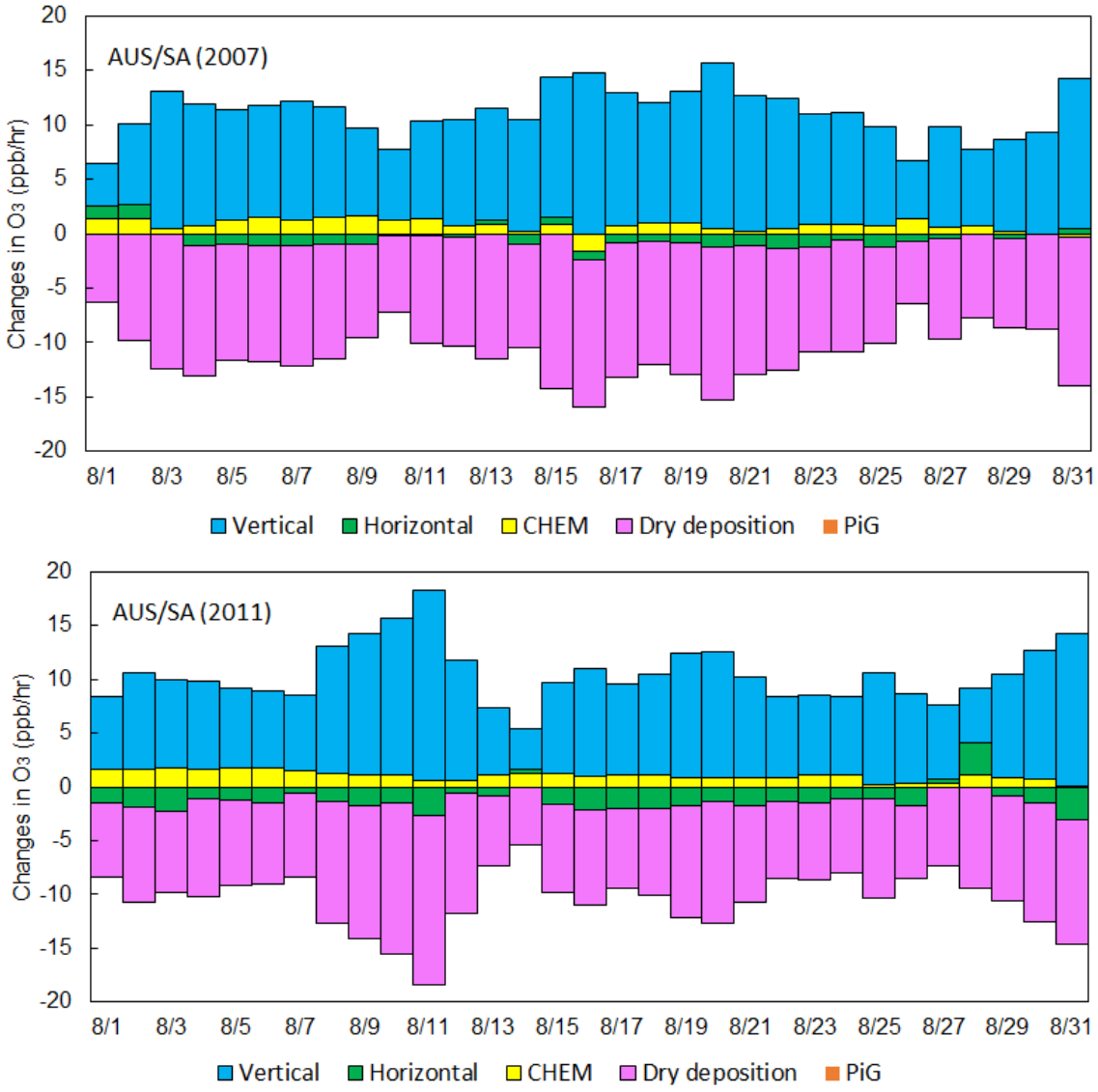

Figure 7-2: Daily-mean hourly contributions of vertical transport, horizontal transport, chemistry (CHEM), dry deposition, and Plume-in-Grid change (PiG) over Austin/San Antonio (AUS/SA) during August 2007 (upper) and 2011 (bottom). (Note that different meteorological inputs were used for 2007 and 2011, so individual days should not be compared across years)

Figure 7-3 shows the diurnal profile of monthly-averaged IPR rates in AUS/SA (similar plots for DFW and HGB are shown in Figure F-3 and Figure F-4). Daytime dry

deposition could result in ozone removal of as much as 20 ppb/hr. Chemistry contributed to ozone formation during the daytime and destruction during the nighttime.

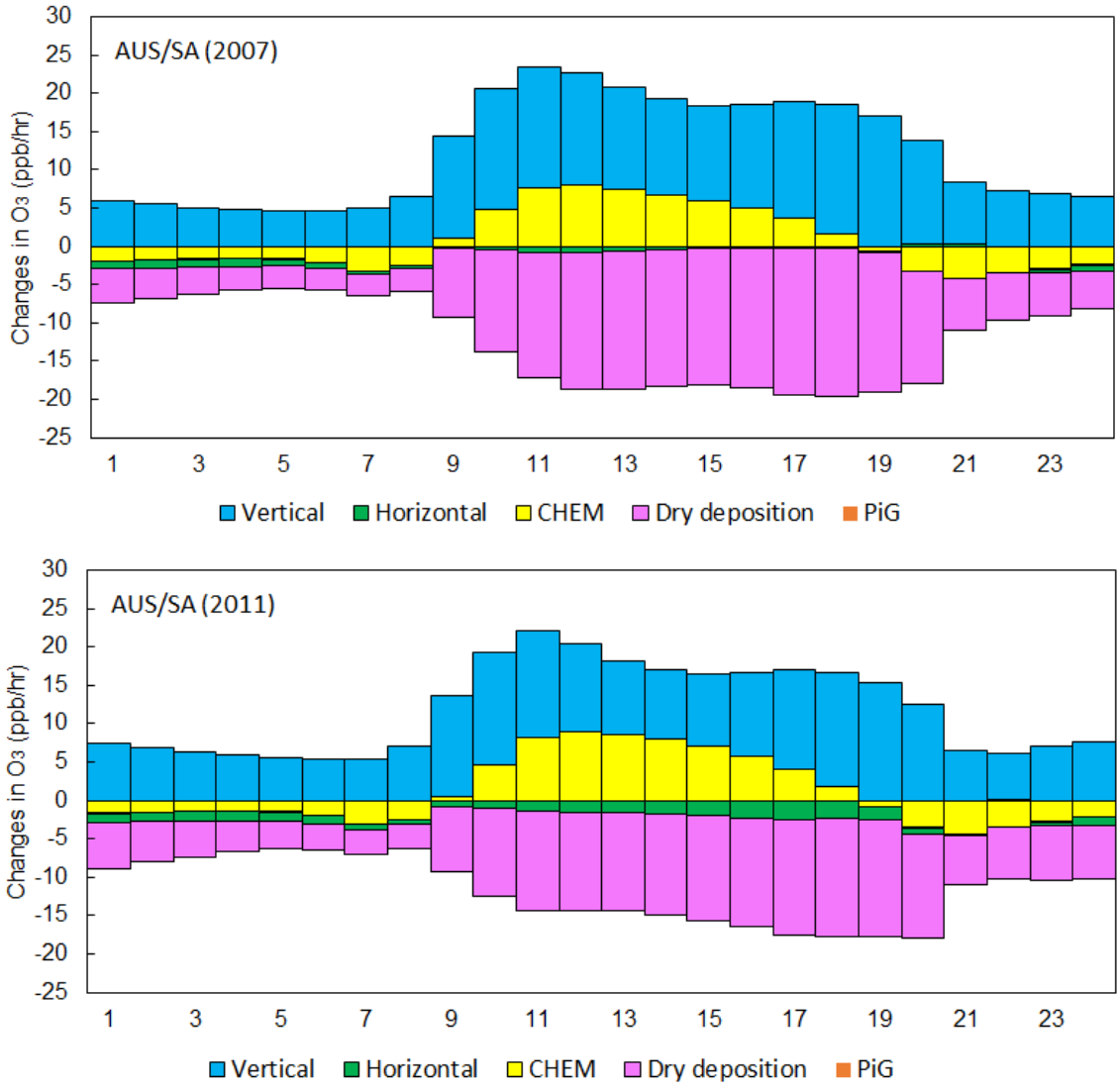

Figure 7-3: Diurnal profile of monthly-mean contributions of vertical transport, horizontal transport, chemistry (CHEM), dry deposition, and Plume-in-Grid change (PiG) over Austin/San Antonio (AUS/SA) during August 2007 (upper) and 2011 (bottom).

7.3.2 The impact of drought on ozone deposition flux

Figure 7-4 shows the spatial differences in simulated monthly-mean daytime (CST 0600-1800) ozone dry deposition velocities, deposition mass, and ozone concentrations over eastern Texas between August 2007 and 2011 (calculated as 2011 – 2007). Ozone deposition velocities showed ubiquitous reductions under drought conditions, as described in Chapter 6. Ozone deposition mass also decreased during 2011 while surface ozone concentrations generally increased, especially over the urban regions with maximum increases of approximately 8 ppb. Figure 7-5 contrasts daytime deposition velocities and deposition masses by climate regions during 2007 and 2011. Reductions in area-averaged daytime deposition velocity and mass during the drought period were substantial: relative changes in the deposition velocity ranged from -10.9% to -24.2%; ozone deposition mass was reduced by -13.6% to -23.5%.

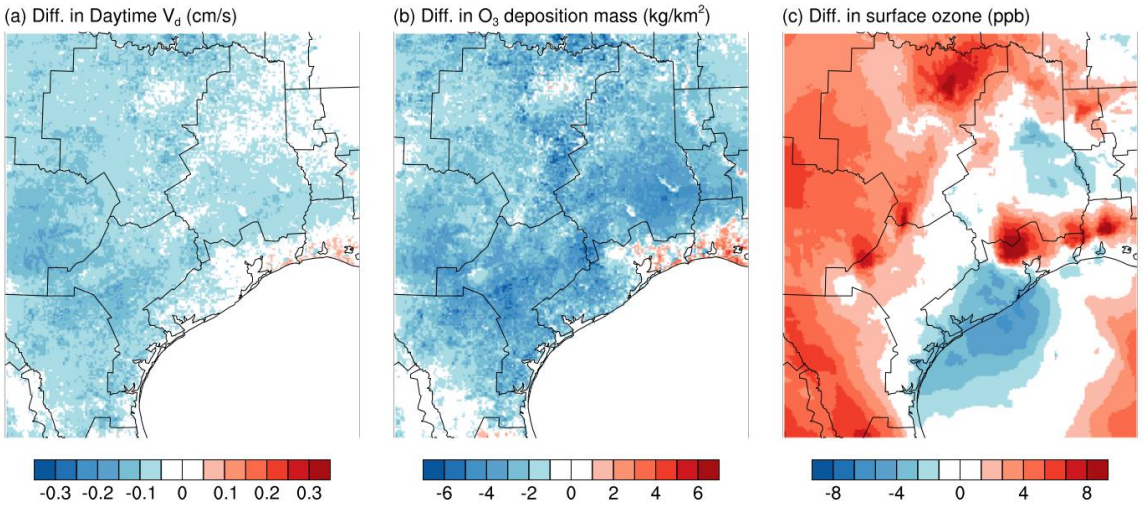

Figure 7-4: Spatial differences in monthly-mean daytime (a) ozone dry deposition velocities (V_d, cm/s), (b) deposition masses (kg/km^2), and (c) surface ozone concentrations (ppb) between August 2007 and 2011 over eastern Texas. Daytime deposition mass is accumulated over CST 0600-1800.

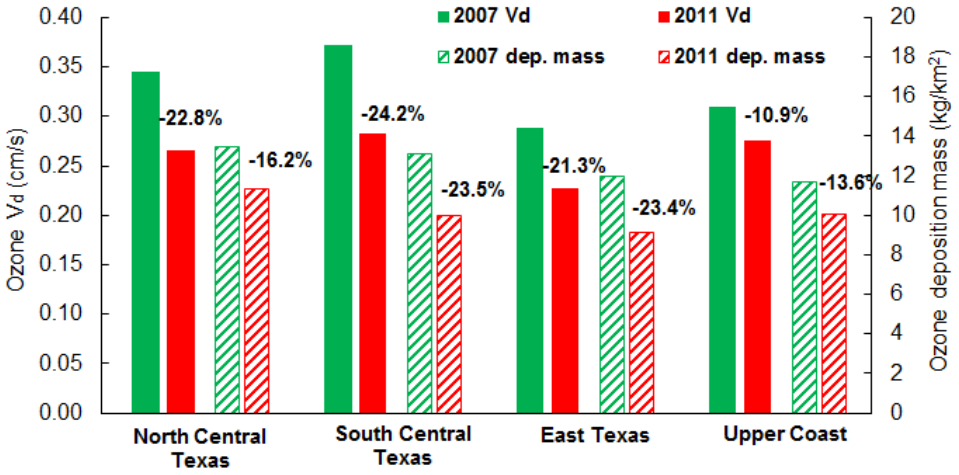

Figure 7-5: Monthly-mean daytime (CST 0600-1800) ozone dry deposition velocities (V_d, in cm/s) and deposition masses (in kg/km^2) by climate region during August 2007 and 2011. Relative changes calculated as (2011-2007)/2007 were also shown.

Similar analyses were also performed for the three urban regions. Figure 7-6 contrasts the diurnal profiles of monthly-averaged ozone deposition velocities, deposition fluxes, and surface ozone concentrations over the three urban regions. Reductions of deposition velocity and flux during the drought period were substantial during daytime hours while nighttime deposition slightly increased. Averaged daytime ozone concentrations increased by ~5 ppb during 2011. Figure 7-7 shows the distribution of maximum daily 8-hour average (MDA8) ozone concentrations over the three urban regions during August 2007 and 2011. DFW exhibited the highest median MDA8 ozone concentrations while HGB had more days that were predicted to exceed the 75 ppb standard. Monthly-averaged MDA8 ozone concentrations increased by 5.3, 4.2, and 2.6 ppb in AUS/SA, DFW, and HGB urban regions during the drought period.

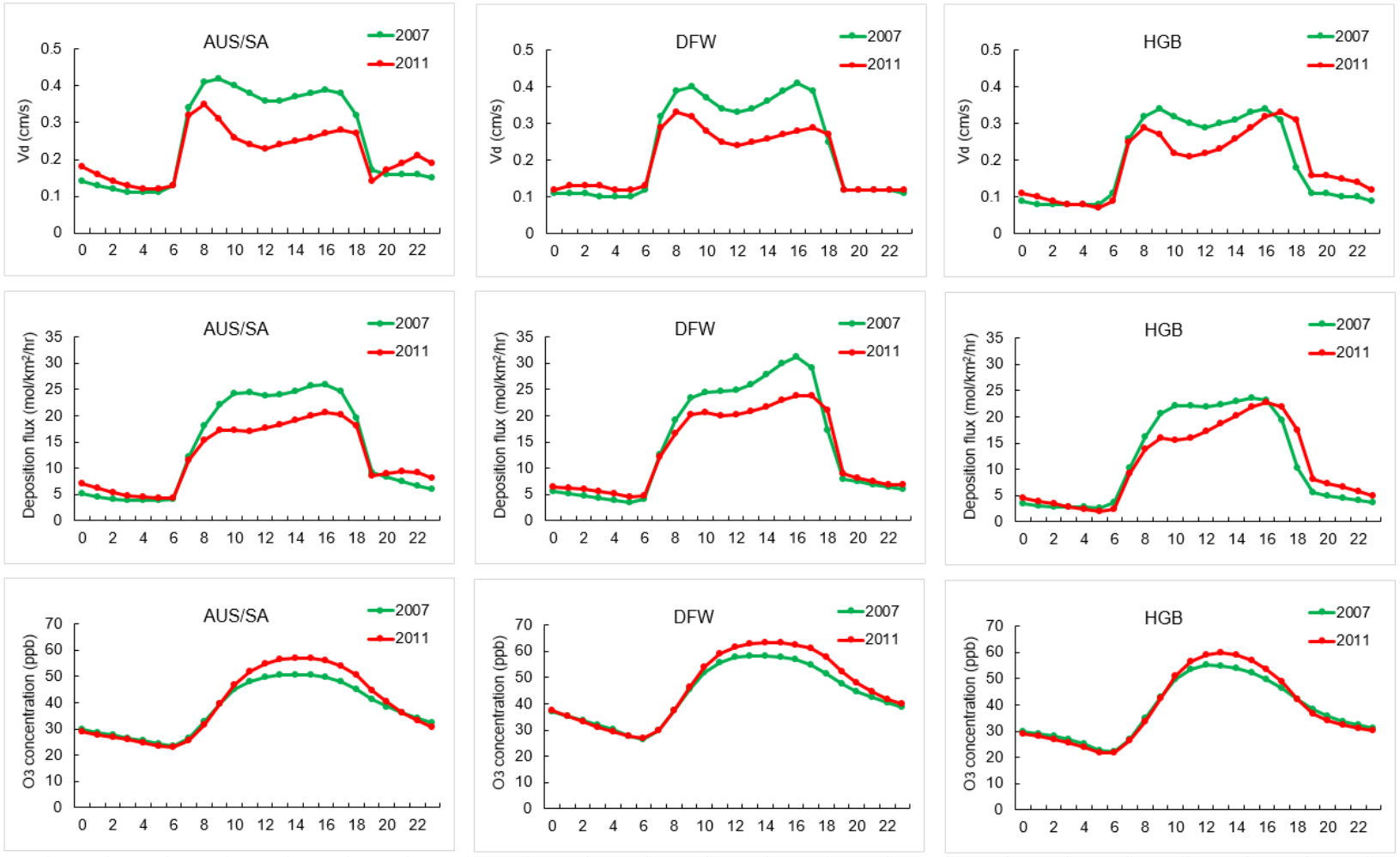

Figure 7-6: Diurnal profile of monthly-averaged ozone deposition velocities (in cm/s), deposition fluxes (mol/km^2/hr), and surface ozone concentrations (ppb) for AUS/SA, DFW and HGB urban regions during August 2007 and 2011.

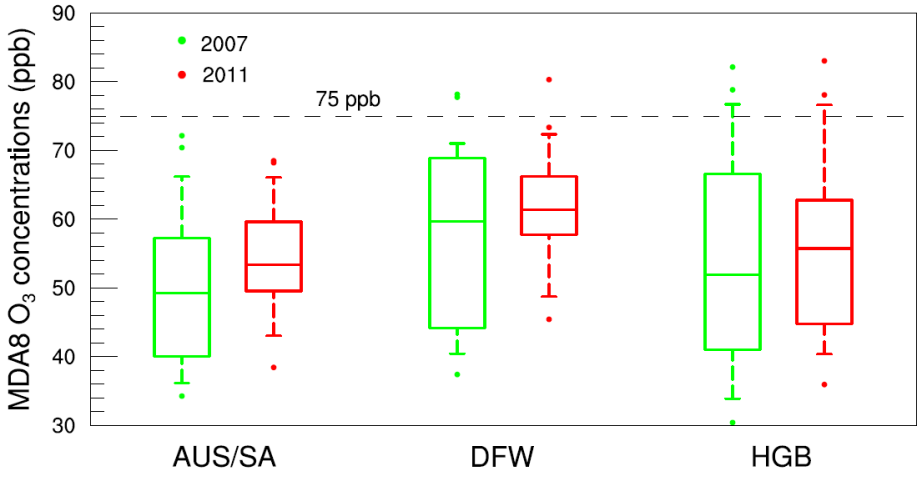

Figure 7-7: Box and whisker plot of MDA8 ozone concentrations (ppb) over the AUS/SA, DFW, and HGB urban regions during August 2007 and 2011. The box and whiskers represent the 5, 25, 50, 75 and 95 percentiles. Values that lie outside the whiskers are plotted as individual points.

To specifically focus on high ozone days, days with the top 20% (i.e. 6 days) of predicted MDA8 ozone concentrations during August 2007 and 2011 over the three urban regions were selected for further analysis. Figure 7-8 contrasts the daytime deposition velocities and deposition masses during the selected high ozone days. Similar results were observed as above where both deposition velocity and mass showed substantial reductions during the drought period. Relative changes in deposition velocities ranged from -12.8% to -20.4% and deposition mass from -14.6% to -26.5%. Reductions in dry deposition velocities were associated with the suppressed stomatal conductances in response to higher temperatures, larger vapor pressure deficits and lower LAI values under drought conditions.

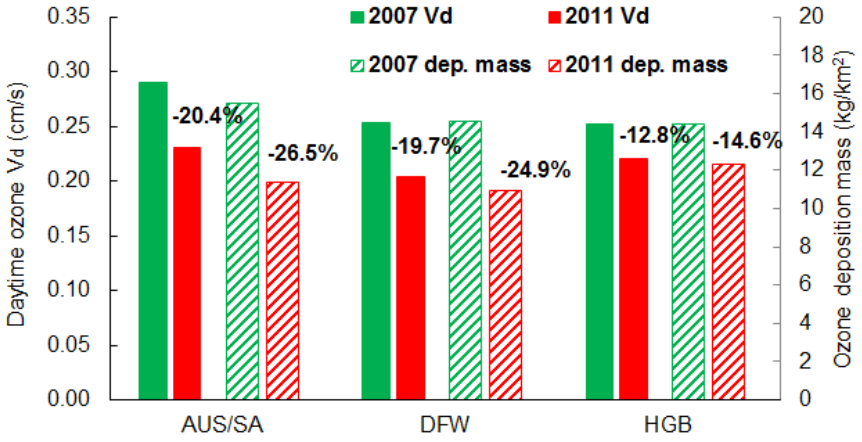

Figure 7-8: Daytime (CST 0600-1800) ozone dry deposition velocities (V_d, in cm/s) and deposition masses (in kg/km^2) for 6 days with the highest predicted MDA8 ozone concentrations during August 2007 and 2011 over AUS/SA, DFW and HGB. Relative changes calculated as (2011-2007)/2007 were also shown.

7.4 CONCLUSIONS

The IPR analyses implemented in CAMx were applied to quantify the contributions of individual chemical and physical processes to the formation of ground-level ozone over eastern Texas during representative wet and dry periods. Results from the IPR analyses suggested that dry deposition was the dominant ozone removal mechanism during both wet and dry periods. Averaged daily ozone removal through dry deposition ranged 8~10 ppb/hr over selected urban regions. Both ozone daytime dry deposition velocities and deposition masses were substantially reduced under drought conditions. Relative changes in daytime ozone deposition masses over the urban regions ranged -14.6% to -26.5% on high ozone days. Results from this study emphasize the importance of accurate characterizations of the spatial distributions as well as magnitudes of the drought impacts on dry deposition for regional air quality planning and management in eastern Texas.

7.5 REFERENCES

Ashmore, M. R. (2002). Effects of oxidants at the whole plant and community level. *Air Pollution and Plant Life*, 89-118. John Wiley, Chichester, UK

Atkinson, R. (2000). Atmospheric chemistry of VOCs and NOx. *Atmospheric Environment*, 34(12), 2063-2101.

Brasseur, G. P., Hauglustaine, D. A., Walters, S., Rasch, P. J., Müller, J. F., Granier, C., & Tie, X. X. (1998). MOZART, a global chemical transport model for ozone and related chemical tracers: 1. Model description. *Journal of Geophysical Research*: *Atmospheres* (1984–2012), 103(D21), 28265-28289.

Brook, R. D., Brook, J. R., Urch, B., Vincent, R., Rajagopalan, S., & Silverman, F. (2002). Inhalation of fine particulate air pollution and ozone causes acute arterial vasoconstriction in healthy adults. *Circulation*, 105(13), 1534-1536.

Ek, M. B., Mitchell, K. E., Lin, Y., Rogers, E., Grunmann, P., Koren, V., ... & Tarpley, J. D. (2003). Implementation of Noah land surface model advances in the National Centers for Environmental Prediction operational mesoscale Eta model. *Journal of Geophysical Research: Atmospheres (1984–2012)*, *108*(D22).

ENVIRON. (2014). User's guide Comprehensive Air Quality Model with Extension (CAMx), version 6.10. Retrieved April 17, 2015, from http://www.camx.com/files/camxusersguide_v6-10.txt

Fuhrer, J., & Booker, F. (2003). Ecological issues related to ozone: agricultural issues. *Environment International*, 29(2), 141-154.

Gryparis, A., Forsberg, B., Katsouyanni, K., Analitis, A., Touloumi, G., Schwartz, J., ... & Dörtbudak, Z. (2004). Acute effects of ozone on mortality from the "air pollution and health: a European approach" project. *American journal of respiratory and critical care medicine*, *170*(10), 1080-1087.

Harper, C., Personal Communication, Nov. 2012

Hogrefe, C., Werth, D., Avissar, R., Lynn, B., Rosenzweig, C., Goldberg, R., ... & Kinney, P. L. (2007). .2 Analyzing the impacts of climate change on ozone and particulate matter with tracer species, process analysis, and multiple regional climate scenarios. *Developments in Environmental Science*, *6*, 648-660.

Kimura, Y., McDonald-Buller, E., Vizuete, W., & Allen, D. T. (2008). Application of a Lagrangian process analysis tool to characterize ozone formation in Southeast Texas. *Atmospheric Environment*. 42(23), 5743-5759.

Liu, X. H., Zhang, Y., Xing, J., Zhang, Q., Wang, K., Streets, D. G., ... & Hao, J. M. (2010). Understanding of regional air pollution over China using CMAQ, part II. Process analysis and sensitivity of ozone and particulate matter to precursor emissions. *Atmospheric Environment*. 44(30), 3719-3727.

Popescu, S.C., J. Stukey, M. Mutlu, K. Zhao, R. Sheridan, N.W. Ku, … C. Harper. (2011). Expansion of Texas land use/land cover through class crosswalking and Lidar parameterization of arboreal vegetation. Retrieved December 1, 2014, from https://www.tceq.texas.gov/assets/public/implementation/air/am/contracts/reports/oth/5820564593FY0925-20110419-tamu-expension_tx_lulc_arboreal_vegetation.pdf

Ruidavets, J. B., Cournot, M., Cassadou, S., Giroux, M., Meybeck, M., & Ferrières, J. (2005). Ozone air pollution is associated with acute myocardial infarction. *Circulation.* 111(5), 563-569.

Ruiz, L.H, and G. Yarwood. (2013). Interactions between organic aerosol and NOy: Influence on oxidant production. Prepared for the Texas AQRP (Project 12-012), by the University of Texas at Austin, and ENVIRON International Corporation, Novato, CA. Retrieved April 17, 2015, from http://aqrp.ceer.utexas.edu/projectinfoFY12_13/12-012/12-012%20Final%20Report.pdf

Wang, X., Zhang, Y., Hu, Y., Zhou, W., Lu, K., Zhong, L., ... & Russell, A. G. (2010). Process analysis and sensitivity study of regional ozone formation over the Pearl River Delta, China, during the PRIDE-PRD2004 campaign using the Community Multiscale Air Quality modeling system. *Atmospheric Chemistry and Physics*, *10*(9), 4423-4437.

Yarwood, G., H. Gookyoung, W.P.L. Carter, G.Z. Whitten. (2012). Environmental Chamber Experiments to Evaluate NOx Sinks and Recycling in Atmospheric Chemical Mechanisms. Final report prepared for the Texas Air Quality Research Program, University of Texas, Austin, Texas. Retrieved April 17, 2015, from http://aqrp.ceer.utexas.edu/projectinfo%5C10-042%5C10-042%20Final%20Report.pdf

Zhang, L., J.R. Brook, & R. Vet. (2003). A revised parameterization for gaseous dry deposition in air-quality models. *Atmospehric Chemistry and Physics*. 3, 2067–2082.

Chapter 8: Conclusions and Recommendations

8.1 CONCLUSIONS

This dissertation investigated the impacts of drought on regional air quality in eastern Texas by exploring changes in biogenic emissions, meteorological conditions, and dry deposition rates, individually as well as simultaneously. The primary objectives were accomplished by series of simulations and sensitivity studies during representative drought and wet periods with widely applied global and regional models. Major conclusions of this dissertation are listed as follows:

- Leaf area index (LAI) is a key parameter for estimating biogenic emissions. Drought-induced reductions in LAI values could result in lower biogenic emissions estimates by as much as -24% in central Texas.
- Temperature is a primary driver of seasonal and interannual variations of predicted biogenic emissions. Higher temperatures associated with drought conditions more than compensate for the reductions associated with lower LAI and soil moisture values generated by the Noah-MP land surface model, thereby promoting biogenic emissions during drought periods.
- Reductions in soil moisture under drought conditions could result in lower isoprene emissions yet large uncertainties remain in the soil moisture and wilting point data employed from land surface models, as well as the soil moisture algorithm in MEGAN to fully represent short and long-term responses of vegetation to drought.
- Uncertainties in land cover characterizations affect modeled biogenic emissions, primarily associated with the standard emission potentials that are dependent on land cover distributions. Differences between regional and global land cover products resulted in substantially different biogenic

emissions estimates (by as much as a factor of 10) and predicted ground-level ozone concentrations (mean differences of 2-6 ppb in maximum daily 8-hour average ozone concentrations) for eastern Texas.

- Stomatal conductances were substantially suppressed under drought conditions due to higher temperatures, larger vapor pressure deficits, and lower LAI values, while non-stomatal conductances increased due to higher simulated friction velocities. Ozone daytime deposition velocities increased during spring and decreased during the summer and fall seasons under drought conditions.
- Dry deposition represents the dominant physical removal mechanism for ozone with averaged daily ozone removal of 8~10 ppb/hr over urban regions during August. On selected high ozone days, reductions in dry deposition associated with drought conditions ranged from -14.6% to -26.5%.

8.2 CONTRIBUTIONS FROM THIS WORK

- This work is the first comprehensive analysis of drought impacts on ground-level ozone concentrations, simultaneously addressing emissions, deposition, and meteorological effects in eastern Texas.
- This study investigated in detail the MEGAN model source codes and quantified the relative contributions of various environmental factors on predicted biogenic emissions while maintaining an environmentally consistent set of model inputs.
- This study was the first to examine the changes in ozone dry deposition velocities and associated stomatal/non-stomatal conductances simultaneously in response to drought conditions.

- The findings of this work (i.e. changes in magnitudes and spatial distribution of biogenic emissions, dry deposition, and ground-level ozone concentrations) could be used to inform future air quality planning and management strategies and guide the design of measurement campaigns at the surface and aloft.

8.3 RECOMMENDATIONS

Recommendations for future work are listed as the follows:

- Accurate estimations of biogenic emissions are essential for regional air quality modeling. Future work regarding biogenic emissions modeling include improving the drought stress (both short- and long-term) parameterizations (not only limited to isoprene) in the current MEGAN modeling framework, conducting additional ecosystem-level studies of biogenic emissions in response to natural drought conditions, reducing uncertainties in the land cover representations through field validation, and improving the representation of basal emission factors from in-situ or aircraft measurements.
- Dry deposition is the most important ozone removal mechanism in eastern Texas yet observations are extremely limited. Future work should include field measurements of ozone dry deposition velocities/fluxes, particularly in forested regions under drought conditions and validation of modeled deposition velocities as well as stomatal conductances against observations.
- Simulations should continue to be conducted to reflect the state of the science and quantify the relative sensitivities of ground-level ozone concentrations to drought-induced changes in biogenic emissions, deposition, and meteorological conditions.
- Future work should also investigate the effects of drought on particular matter (PM) concentrations over eastern Texas. Changes in the magnitudes and

spatial distributions of both ground-level ozone and PM concentrations should be considered in the development of emission reduction strategies in Texas cities to attain air quality standards.

Appendix A: Supporting Information for Chapter 2

Table A-1: Descriptions of MEGAN2.1 activity factors (Guenther et al., 2006, 2012; MEGAN2.1 offline source codes)

Activity factors	Descriptions	Algorithm/Value
γ_{age}	Leaf age activity factor accounts for different emission rates at different foliage age. For isoprene, mature and old leaves emit more than new and growing leaves; opposite is true for monoterpenes.	$\gamma_{age} = F_{new} \cdot A_{new} + F_{gro} \cdot A_{gro} + F_{mat} \cdot A_{mat} + F_{old} \cdot A_{old}$ (Eq. A-1) $F_{new/gro/mat/old}$: fraction of new/growing/mature/old leaves; depends on the LAI at current and previous time step $A_{new/gro/mat/old}$: relative emission rate of new/growing/mature/old leaves
γ_{SM}	Soil moisture activity factor accounts for the impact of water stress on biogenic emissions; only applied to isoprene.	$\gamma_{SM} = \sum_{j=1}^{4} f_{root}^{j} \max(0, \min(1, (\theta^{j} - \theta_{wilt})/0.04))$ (Eq. A-2) θ^{j}: volumetric soil moisture (m^3/m^3) at each soil layer j θ_{wilt}: wilting point data (m^3/m^3) f_{root}^{j}: root fraction at each soil layer j
γ_{CE}	Canopy environment activity factor accounts for variations due to LAI, light, temperature, humidity and wind conditions within the canopy environment	$\gamma_{CE} = 0.56 \cdot \sum_{j=1}^{5} [(\gamma_T^j)_{sun}(\gamma_P^j)_{sun} f_{sun}^{j} + (\gamma_T^j)_{shade}(\gamma_P^j)_{shade} f_{shade}^{j}] \cdot LAI^{j}$ (Eq. A-3) γ_T^j: temperature activity factor at each canopy layer level j γ_P^j: light activity factor at each canopy layer level j f^j: sun/shaded fraction at each canopy layer level j LAI^j: LAI at each canopy layer level j (based on Gaussian distribution) Both temperature and light activity factor are first calculated for sun and shaded leaves respectively then summed up over 5 canopy layers. See Guenther et al. (2006, 2012) for detailed calculations of γ_T and γ_P.
γ_{LAI}	Light-independent LAI activity factor; applied to biogenic emissions that are not dependent on light.	$\gamma_{LAI} = 0.49LAI/(1+0.2LAI^2)^{0.5}$ (Eq. A-4)
γ_{T_LIF}	Light-independent temperature activity factor; applied to biogenic emissions that are not dependent on light.	$\gamma_{T\_LIF} = \sum_{j=1}^{5} [(\gamma_{T\_LIF}^{j})_{sun} f_{sun}^{j} + (\gamma_{T\_LIF}^{j})_{shade} f_{shade}^{j}]$ (Eq. A-5) $\gamma_{T\_LIF}^{j}$: light-independent temperature activity factor at each canopy layer j See Guenther et al. (2006, 2012) for detailed calculations of γ_{T_LIF}

Table A-2: Compound Classes used in MEGAN2.1 and CLM Plant Functional Types

Compound Class Number	Compound Class	CLM PFT Number	PFT Description
1	Isoprene		Bare
2	Myrcene	1	Needleleaf Evergreen Temperature Tree
3	Sabinene	2	Needleleaf Evergreen Boreal Tree
4	Limonene	3	Needleleaf Deciduous Boreal Tree
5	3-Carene	4	Broadleaf Evergreen Tropical Tree
6	*t*-β-Ocimene	5	Broadleaf Evergreen Temperate Tree
7	β-Pinene	6	Broadleaf Deciduous Tropical Tree
8	α-Pinene	7	Broadleaf Deciduous Temperate Tree
9	Other Monoterpenes	8	Broadleaf Deciduous Boreal Tree
10	α-Farnesene	9	Broadleaf Evergreen Temperate Shrub
11	β-Caryophyllene	10	Broadleaf Deciduous Temperate Shrub
12	Other Sesquiterpenes	11	Broadleaf Deciduous Boreal Shrub
13	232-MBO	12	Arctic C3 Grass
14	Methanol	13	Cool C3 Grass
15	Acetone	14	Warm C4 Grass
16	CO	15	Crop1
17	Bidirectional VOC		
18	Stress VOC		
19	Other VOC		

Table A-3: MEGAN2.1 input variables (Guenther et al., 2006, 2012) and example datasets used in this work

Input Variables	Mandatory/ Optional	Descriptions	Dataset used in this work
Emission factor	Mandatory	· Geogridded emission factor maps · Generated from PFT distribution dataset and PFT-dependent emission factors (provided by MEGAN) · or can use global emission maps	Global emission factor input files provided by MEGAN (http://www.acd.ucar.edu/webt/MEGAN/GlobalEmissionFactor/, accessed June 23, 2014).
Plant Functional Type (PFT)	Mandatory	· Obtained from satellite observations, vegetation inventories, ecosystem maps or ecosystem model output	Regional land cover dataset developed by Texas Commission on Environmental Quality (referred as "TCEQLC_2010") covering eastern Texas (Popescu et al., 2011).
Leaf Area Index (LAI)	Mandatory	· Obtained from satellite observations or field measurements	MODIS 4-day LAI product (MCD15A3, https://lpdaac.usgs.gov/products/modis_products_table/mcd15a3).
Temperature Humidity Wind Speed	Mandatory	· Generated from global weather models with assimilated observations (e.g. Weather Research and Forest (WRF), MM5)	NCEP North American Regional Reanalysis (NARR) product with spatial resolution of 32 km and temporal resolution of 3 hour (http://rda.ucar.edu/datasets/ds608.0/).
Photosynthetically Active Radiation (PAR)	Mandatory	· Can be generated by satellite (e.g. Global Energy and Water Cycle Experiment Continental Scale International Project) or from global weather models (e.g. WRF) · Or converted from shortwave radiation by a conversion factor (usually 0.45)	Converted from hourly surface insolation (4 km) from the Geostationary Operational Environmental Satellite (GOES) generated by University of Alabama in Huntsville (http://satdas.nsstc.nasa.gov/data.html, accessed June 23, 2014).
Soil moisture and wilting point dataset	Optional	· Soil moisture can be derived from a land surface model (e.g. CLM4, Noah-MP) or from a global weather model (NCEP-DOE) · Recommend using consistent wilting point used to generate soil moisture data. · global wilting point dataset exists (Chen and Dudhia, 2001)	Soil moisture generated by Noah land surface model with multiparameterization options (Noah-MP, Cai et al., 2014) and corresponding wilting point data.
CO_2 concentration	Optional	· can be generated from coupled atmospheric model (e.g. CESM) or use fixed value	N/A

Table A-4: Comparison between the Wesely (1989) and Zhang (2003) algorithms

Algorithm	**Wesely (1989)**			**Zhang et al. (2003)**		
Dry deposition velocity	$v_d = (R_a + R_b + R_c)^{-1}$			$v_d = (R_a + R_b + R_c)^{-1}$		
Overall canopy resistance (R_c)	$\frac{1}{R_c} = \frac{1}{R_{st} + R_m} + \frac{1}{R_{lu}} + \frac{1}{R_{dc} + R_{cl}} + \frac{1}{R_{ac} + R_g}$			$\frac{1}{R_c} = \frac{1 - W_{st}}{R_{st} + R_m} + \frac{1}{R_{cut}} + \frac{1}{R_{ac} + R_g}$		
Stomatal Resistance						
Stomatal resistance (R_{st})	$R_{st} = f(LUC, season, G, T, D_i)$ $= R_i\{1 + [200(G + 0.1)^{-1}]^2\}\{400[T(40 - T)]^{-1}\} \cdot D_{H_2O} / D_i$			$R_{st} = f(LUC, PAR, T, D, \psi, D_i) = 1/[G_s(PAR) f(T) f(D) f(\psi)] \cdot D_{H_2O} / D_i$		
Mesophyll resistance (R_m)	$R_m = f(H^*, f_0) = (H^* / 3000 + 100 f_0)^{-1}$			Species-dependent		
Non-stomatal Resistance						
In-canopy aerodynamic resistance (R_{ac})	$R_{ac} = f(LUC, season)$			$R_{ac} = f(LUC, LAI, u_*) = \frac{R_{ac0}(LUC, LAI) \cdot LAI^{1/4}}{u_*^2}$		
Species	**O_3**	**SO_2**	**Other**	**O_3**	**SO_2**	**Other**
Ground resistance (R_g):	$R_g = f(LUC, season)$		Scales based on R_g values for O_3 and SO_2: $R_{g,i} = [H^* / (10^5 R_{g,SO_2}) + f_0 / R_{g,O_3}]^{-1}$	Considered separately for different surface types (water, ice, snow and soil)		
for water				2000 s/m	20 s/m	Scales based on O_3 and SO_2: $\frac{1}{R_{g,i}} = \frac{\alpha_i}{R_{g,SO_2}} + \frac{\beta_i}{R_{g,O_3}}$
for ice/snow				2000 s/m	$R_{g,SO_2,snow/ice} = 70(2 - T)$	
for soil				200 s/m (vegetated) 500 s/m (non-vegetated or wet surface)	dry: $f(LUC)$ rain: 50 s/m dew: 100 s/m	
Cuticle resistance (R_{cut})	$R_{dc} = 100[1 + 1000(G + 10)^{-1}](1 + 1000\theta)^{-1}$			dry conditions: $R_{cut} = \frac{R_{cutd0}}{e^{0.03RH} LAI^{1/4} u_*}$		Scales based on O_3 and SO_2: $\frac{1}{R_{cut,i}} = \frac{H^*}{R_{cut,SO_2}} + \frac{f_0}{R_{cut,O_3}}$
	$R_{cl} = f(LUC, season)$		Scales based on R_{cl} values for O_3 and SO_2: $R_{cl,i} = [H^* / (10^5 R_{cl,SO_2}) + f_0 / R_{g,O_3}]^{-1}$	wet conditions: $R_{cut} = \frac{R_{cutw0}}{LAI^{1/2} u_*}$		
	$R_{lu,i} = R_{lu}(LUC, season) \cdot (10^{-5} H^* + f_0)^{-1}$			$R_{cutd0}, R_{cutw0} = f(LUC)$	$R_{cutd0} = f(LUC)$ R_{cutw0} = 50 s/m (rain) or 100 s/m (dew)	
Modifications						
Response to temperature	$R_{lu}, R_{cl}, R_g : 1000\exp(-T - 4)$			$R_g, R_{cut} : \exp(0.2(-1 - T))$		
Modification for stomatal blocking	Assume two-thirds of leaves are covered. R_{st} and R_{lu} are multiplied by 3.			Use of W_{st} to represent fraction of stomatal blocking $W_{st} = f(SR)$		
In case of snow	Specified values through season			R_g and R_{cut} are adjusted based on snow fraction f_{snow}		

Table A-5: Nomenclature for Table A-4

α	parameter for cuticle and soil resistance scaling to SO_2 (0.0-10.0)
β	Parameter for cuticle and soil resistance scaling to O_3 (0.0-10.0)
ψ	leaf water potential (MPa)
D	water vapor pressure deficit (MPa)
D_{H_2O}	molecular diffusivity for water vapor (m^2/s)
D_i	molecular diffusivity for species i (m^2/s)
f_0	reactivity factor (0-1)
G	solar radiation (W/m^2)
H^*	effective Henry's constant (M/atm)
LAI	leaf area index (m^2/m^2)
LUC	land use categories, 11 for Wesely (1989), 26 for Zhang (2003)
PAR	photosynthetically active radiation (W/m^2)
R_a	aerodynamic resistance (s/m). Sam unit for all resistance parameters listed below.
R_{ac}, R_{ac0}	in-canopy aerodynamic resistance
R_b	quasilaminar sublayer resistance
R_c	canopy resistance
R_{cl}	resistance for leaves, twig, bark or other exposed surfaces in the lower canopy
R_{cut}	cuticle resistance
R_{cutd}, R_{cutd0}	dry cuticle resistance
R_{cutw}, R_{cutw0}	wet cuticle resistance
R_{dc}	resistance for a gas-phase transfer affected by buoyant convection in canopies
R_g	ground resistance
RH	relative humidity (0-100%)
R_{lu}	resistance for upper canopy
R_m	mesophyll resistance
R_{st}	stomatal resistance
SR	solar radiation (W/m^2)
T	surface air temperature (°C)
u_*	friction velocity (m/s)
v_d	dry deposition velocity (m/s)
W_{st}	fraction of stomatal blocking (0.0-0.5)
θ	slope of local terrain (radians)

Appendix B: Supporting Information for Chapter 3

B.1 Climatology during 2006 through 2011 over Texas

The following descriptions are summarized based on the "Texas Climatic Bulletins" provided by Office of the State Climatologist (http://climatexas.tamu.edu/index.php/monthly-reports/texas-climatic-bulletins).

2006

Texas began the year with record high temperatures and numerous locations had top ten (e.g., Austin, College Station, Houston) or top five (DFW, Wichita Falls, Waco) mean January temperatures. Precipitation was below average with the exception of North Central Texas; however, the warmer than normal temperatures enhanced drought conditions; the USDM indicated drought throughout Texas with extreme drought extending from deep South Texas northward through Central and North Texas. Record heat continued into the first half of February followed by average temperature conditions for the remainder of the month; rainfall was limited to North Central and East Texas and the drought intensified to exceptional over much of eastern Texas. A series of cold fronts brought much cooler temperatures to Texas during the latter half of March as well as heavy rainfall in northern portions of the state (e.g., DFW, Waco, and Austin). In contrast, areas along the coast were, on average, 4°F above normal and received 34% of normal rainfall. The generally warm and dry weather pattern continued into April and May; the USDM indicated drought throughout the state with the lower third of Texas in severe to exceptional drought. Heavy rainfall along the Texas coast occurred in association with an upper-level trough during the final days of May followed by continued wet conditions during June while precipitation remained well below average elsewhere in the state. The USDM in late June had moderate drought throughout Texas

(with the exception of no drought in extreme southeast Texas) with extreme/exceptional drought limited to South Texas. In contrast, the PDSI indicated moderate drought in southeast Texas with severe to extreme drought over the remainder of the state. The trend of cooler and wetter coastal conditions continued during July and August while interior Texas was much warmer and drier than normal; for example, Waco/Austin/San Antonio received <10% of normal rainfall. As of August 29th, the USDM had most of the state under extreme drought with some areas, including DFW and Wichita Falls, listed under exceptional drought conditions. In contrast, the Upper Coast and other Texas coastal areas were not listed under any drought category. Cooler temperatures and much needed rainfall affected much of Texas during September although rainfall remained below normal in parts of Central Texas. DFW received average precipitation for the first time since April and San Antonio reported above average precipitation for the first month during 2006. October was wetter than normal for the eastern half of Texas, with the Upper Coast having the most rainfall (e.g., 14.53 inches in Houston); however, North Central Texas remained in conditions of extreme drought. During November, most locations in Texas had precipitation <50% of normal (with the exception of DFW that had normal rainfall) accompanied by much warmer than normal temperatures. Although rainfall returned to portions of eastern Texas during December, drought conditions continued outside of the coastal regions.

2007

Consistent with a weak El Nino, Texas had below average temperatures and above average precipitation during January. Much of Texas had precipitation totals twice the average values; Victoria and Austin had three times normal rainfall. With the exception of the Edwards Plateau, the rains greatly improved the on-going drought conditions throughout Texas. In contrast, February was exceptionally dry for most of

Texas; for example, College Station, San Antonio, and Galveston had record or near-record low rainfall. Conditions turned wetter and much warmer than normal during March for most of the state with the exception of drier than normal conditions for East and South Texas. The USDM indicated great improvements in drought conditions with North Texas indicated at abnormally dry and moderate/extreme drought limited to the Edwards Plateau; PDSI indicated no occurrence of drought within Texas. April turned drier and cooler compared to normal, with portions of South Central and Upper Coast regions having above average precipitation while the rest of the state reported below average totals. May-July brought very wet conditions to Texas ending the drought that had persisted throughout much of Texas since autumn of 2005. May had a series of upper level disturbances that resulted in prolonged periods of excessive rain especially in North and Central Texas with relatively drier conditions in the Upper Coast. The PDSI indicated moderately moist to very moist conditions in most of Texas with the exception of normal in East Texas. By July, a persistent upper level trough was associated with copious amounts of rain across the state and the PDSI indicated very moist conditions for East Texas with extremely moist conditions for the remainder of the state. The development of high pressure over Texas during late July and early August produced more summer-like warmer and drier weather; however, the landfall of Tropical Storm Erin near Lamar, Texas, on August 16th brought heavy rain to parts of southeast and Central Texas. Mostly warmer and drier conditions occurred during September; for example, the monthly mean temperatures were in the top 10 for DFW and Houston. Higher than normal precipitation was mostly limited to North Texas; the Upper Coast also had slightly more than normal rainfall in association with Hurricane Humberto that made landfall near High Island, Texas, on September 13th. A return to La Nina conditions

was associated with much warmer and drier than normal conditions over much of Texas during October through December but not yet initiate a return to drought conditions.

2008

Consistent with a strong La Nina event (sea surface temperatures in the equatorial Pacific were as much as 2°F below normal), January was characterized by average temperatures and below average rainfall; only coastal Texas had above average precipitation. February had much warmer temperatures with relatively dry conditions except for above normal precipitation in the East and Upper Coast regions. Temperatures remained above normal during March with above average rainfall throughout the northern half of eastern Texas. Moderate drought conditions (USDM) were limited to South Texas as well as the Edwards Plateau. April had slightly above average temperatures with average rainfall in Central and North Texas. With the exception of northeast Texas, May and June were quite dry resulting in drought conditions for most of the state. The USDM showed extreme drought in the southern third of Texas and moderate drought in Central and North Texas. During July, substantial rainfall impacted South Texas in association with a category 2 hurricane (Dolly) that made landfall in southern Texas on July 23rd. In contrast, the northern half of Texas had little rain; for example, Austin had only 20% of normal rainfall. The USDM indicated extreme drought in the region north of Corpus Christi extending east-west across all of Texas along a line between Houston and San Antonio; much of the remainder of eastern Texas was characterized as moderate drought. Conditions turned cooler and wetter during August for most of Texas, resulting in an improvement in drought conditions, though severe to extreme drought continued over portions of the South Central and Edwards Plateau regions. Tropical Storm Edouard, a relatively weak system that moved ashore in Houston in early August, as well a strong low pressure system over Texas during mid-August,

were associated with much needed precipitation in many parts of Texas. September had a return to exceptionally dry conditions resulting in extreme drought over portions of South Central Texas and the Edwards Plateau (e.g., Victoria northwestward to Austin and Texas regions to the west). Cooler than normal temperatures and moderate rainfall over the East and Upper Coast regions occurred following the landfall of catastrophic Hurricane Ike in Galveston on September 13th. Several cold fronts pushed their way through Texas during October, but were associated with little rain over the eastern half of Texas. Continued mostly warmer and much drier conditions persisted during November and December; the USDM continued to indicate exceptional drought conditions in portions of South Central Texas.

2009

Following the trend of late 2008, Texas had an extraordinary dry January with less than half of normal monthly precipitation recorded. Temperatures were also abnormal with an unusual positive departure of average maximum temperature of 5°F to 6°F degree. These precipitation deficits and warm temperatures continued in February although a significant rainfall over portion of Texas happened due to severe storms in the middle of the month. In March, rainfall was brought by a stalled system that soaked Texas over a few days and drought conditions over East Texas were much mitigated. However, much more precipitation was needed to end the drought. April separated Texas into two opposite climate conditions in different parts. Severe drought conditions persisted in extreme southern portion of Texas (Brownsville, Corpus Christi, Victoria) while East Texas experienced torrential rainfall events with almost 6 inches of rainfall in 1 hour reported. Conditions in May turned back to warm temperatures with only the Panhandle of Texas stayed cooler than average. Although a cold front during the middle of May brought several inches of rain to various parts of Texas in a few hours, the

majority of the state was dry. Records for many area of Texas were broken in June. Houston and Galveston reached the dries May and June in recorded history with 5% of normal precipitation for the two months. Southeast Texas and Gulf Coast region was the driest parts of Texas receiving only a quarter of normal June precipitation. July continued to break records of the hottest month ever recorded for several cities in Central and South Texas. Bastrop, Caldwell and Lee counties in Central Texas, and Victoria, Bee, San Patricio, Live Oak, Jim Wells and Duval counties were reported to be in the worst drought since precipitation records kept in 1895. According to USDM, about 20% of Texas remains in exceptional drought. Abnormal temperature and precipitation continued in August across most of the state. The South Central, Coastal Bend and Lower Valley regions were in exceptional drought for entire summer, which significantly affects the agriculture and forced water conservation. September had brought some much needed rain to many parts of Texas and improved the drought situation in the South. October became fairly wet for the eastern part. However the exceptional drought conditions in Corpus Christi and much of the Coastal Bend could not be broken without enough rainfall. Cold fronts in November caused temperature fluctuations all month with several showers seen in eastern Texas. December was unusually cold across the entire state. However, abundant precipitation along the Gulf Coast was finally able to end the drought conditions in the Coastal Bend region. By the end of December, drought situations had improved all over Texas with most severe (D2) drought conditions in Kinney, Maverick and Nueces counties.

2010

As the El Nino continued to build over the Pacific Ocean, Texas began the year with a cold and wet January and February with the latter even seeing a heavy snowfall in North Texas. Monthly temperatures were much below the normal all across the entire

state. This cold weather continued in March but with less precipitation compared to the first two months. Several storms pushed through the state and became even more frequently for many parts of Texas in April. The National Weather Service (NWS) confirmed that Texas Panhandle experienced 8 tornadoes on the 23rd alone. In contrast, little precipitation fell in Southeast Texas, indicating the beginning of a drought. Most of Texas was drier than normal throughout May except isolated locations experiencing excessive amounts of rainfall, including Del Rio, Victoria and Galveston. However, rainfall became sparse across most of the state in the latter half of May and moderate drought conditions developed in East Texas. This drier than normal condition continued in June with above normal temperatures for most of Texas. By the end of June, a tropical system led to the formation of Hurricane Alex in the Gulf of Mexico which caused significant rainfall in South Padre Island. Following Hurricane Alex, precipitation was abundant during the first half of July and became spottier during the second half of the month. Temperatures were close to normal across the state and continued in August. However, rainfall was sharply reduced in August with only several places (Amarillo, Corpus Christi, Houston, Lubbock, Port Arthur, Wichita Falls and San Angelo) receiving more than an inch of rain. Weather elements became much more various in September, from heat to tropical storms. Tropical Storm Hermine was most notable bringing tornadoes to the Dallas area as well as impressive rain to Austin, Brownsville, Corpus Christi, San Antonio, Victoria and Waco. October was back to precipitation shortage with the exception in West Central Texas and the southern Panhandle. The lack of rain left East Texas under increased threat of wild fires with 190 fires in just one week. By the end of the month, portions of East Texas and the Big Bend area were depicted in moderate and severe drought by USDM. Consistent with La Nina, drier and warmer conditions prevailed across the majority of Texas in November and December, leading to an

increase of drought conditions in terms of severity and spatial coverage with South Texas designated as extreme drought conditions (D3) by USDM.

2011

2011 of Texas started from a wet and cold January with at least five tornadoes in East Texas confirmed by the NWS. Temperatures were below normal for most of the state with several absolute minimum temperatures records being broken in Austin. February began with a so called the "Big Freeze of February 2011", which hit all of Texas and caused a lot of problems, including crop damages, power shutoff. The temperature recovered a little bit for the rest of the month but precipitation was sparse leading to several wildfires in the Big Country. According to USDM, the entire state was under drought conditions except some areas in the Coastal Bend and the Panhandle. The drought conditions got worsen in March and April as precipitation became even sparser, especially in West Texas, and temperatures rebounded to be warmer than normal. By the end of April, areas that were classified as exceptional drought (D4) increased from 4.81% to 17.16% by USDM. Wildfires started active as a result of the extreme dryness as well as the newly growing vegetation during last wet winter, damaging thousands of acres of Texas land. Temperatures kept above normal as May started and several storm events brought some precipitation to the North Central Texas. However, excessive heat continued to hit Texas in June and July, exacerbating the drought conditions. Most of the state was depicted in exceptional drought and over 75% of Texas was suffering possibly the worst drought scenario on July 26th. August witnessed the average high temperature exceeding 100 degree at all observation stations except Amarillo, Lubbock and El Paso. D4 drought was still dominant over the state, and according to USDM, D4 condition exceeded 85% of the state by September 27th. Everywhere in Texas was experiencing some form of drought in September with only Waco saw above normal precipitation.

Situations got better as Texas had a much cooler and wetter October. Significant precipitation was brought by a storm system to Central Texas and North Texas over the weekend of the 8th and 9th. In November, temperatures kept above normal all over the state. Although precipitation were brought by several powerful fronts at many parts of Texas, it was still not enough to pull the region out of severe drought. In December 2011, all of Texas was under at least severe drought conditions although most of Texas received at least normal precipitation in December and temperatures dropped below normal.

B.2 COMPARISONS BETWEEN MODIS 8-DAY (MCD15A2) AND 4-DAY LAI PRODUCTS (MCD15A3)

The Land Processes Distributed Active Archive Center (LP DAAC) is currently providing two versions of the Level-4 combined Terra and Aqua Moderate Resolution Imaging Spectroradiometer (MODIS) LAI products: an 8-day LAI composite (MCD15A2) and a 4-day LAI composite (MCD15A3). The MODIS 8-day and 4-day LAI product retrievals are based on a biome dependent radiative transfer (RT) model and a Look-Up Table (LUT), which is referred to as the main algorithm (Myneni et al., 2002). An empirical backup algorithm based on the relationship between LAI and Normalized Difference Vegetation Index (NDVI) is used when the main RT algorithm fails. The retrieval of LAI values is subject to cloud contamination, which can reduce data quality and lead to a negative bias (Wang, 2009). Similar to other MODIS products, detailed Quality Control (QC) information is provided with the LAI values. Four cloud states were indicated by the QC flag: (1) significant clouds were not present (i.e. clear sky); (2) significant clouds were present; (3) mixed clouds were present in pixel and (4) cloud state not defined, assume clear (LP DAAC, 2012). Only LAI pixels designated as cloud-free and retrieved using the main algorithm were considered for the analysis. The LAI products were obtained for the time period spanning January 1, 2006 to December 31, 2011 (http://reverb.echo.nasa.gov/reverb). Data were converted to integer GeoTIFF format that were projected from the MODIS sinusoidal grid into a geographic coordinate system based on the WGS84 datum. Data were re-projected on the Lambert Conformal Conic projection and the EMEP sphere for eastern Texas and gridded to 1-km resolution by nearest neighbor resampling. Data were parsed into three separate sets as integer LAI values, general quality flags and detailed quality flags per date.

The filtered 8-day LAI and 4-day LAI products were compared for the 2006-2011 time periods for four eastern Texas climate regions: North Central Texas, South Central Texas, East Texas, and Upper Coast. Figure B-1 and Figure B-2 contrast time series of 8-day LAI and 4-day LAI values for grasses and broadleaf forest in North Central Texas and East Texas, respectively. Overall, the 8-day and 4-day LAI datasets were directionally consistent and exhibited reasonable agreement, with the 4-day LAI values showing greater fluctuations between composite periods. Variability between 4-day composite periods could exceed a factor of eight, due to cloud interference. Figure B-3 shows the relative differences between temporally-paired LAI values for grasses, crops, broadleaf forest, and shrubs in North Central Texas and indicates that approximately 90% of the differences in LAI values were within 20%. Similar results were observed in other climate regions.

Although agreement was generally reasonable, large differences did exist between the LAI datasets at times. For instance, relative differences in LAI for grasses, crops and broadleaf forest on December 11, 2007 exceeded 60% in North Central Texas. In this case, discrepancies between the 8-day and 4-day LAI products could be explained by the presence of clouds (Figure B-4). Significant clouds were present over much of eastern Texas, except parts of North Central Texas (Figure B-4a), for the 4-day LAI product on December 11, 2007. However, for the 8-day LAI on the same day, little cloud cover was present over most of the region (Figure B-4b). Areas with lower LAI values (either in the 8-day or 4-day LAI dataset) corresponded to areas with cloud cover and vice versa. Shabanov et al. (2007) compared 8-day and 4-day LAI values on July 20, 2003 grouped by MODIS land cover product (MOD12Q1). LAI values retrieved by the main algorithm were highly consistent; however, use of back-up algorithm resulted in differences

associated with contaminated input surface reflectance from the presence of clouds and aerosols.

We speculate that another cause of differences between the 4-day and 8-day LAI products is the compositing logic employed in their processing (Knyazikhin et al., 1999). After daily tiles are produced, a set of up to 4 or 8 candidate tiles are composited based on a simple selection rule, whereby the pixel with the maximum fPAR (fraction of Photosynthetically Active Radiation) across the 4 or 8 days is selected as the output pixel value, and the day with the maximum fPAR value is identified. LAI values and relevant quality assurance metadata for the day identified are chosen as the composited 4-day or 8-day LAI and quality control values. Since fPAR values are positively correlated with LAI values, the 8-day LAI dataset consists of the maximum LAI value for the eight consecutive days, while the 4-day LAI dataset is the maximum value of either the first- or second-half of the 8 consecutive days. Therefore, it may be more reasonable to compare 8-day LAI values with the larger value of the two 4-day LAI values over the same period. Figure B-5 is modified from Figure B-4 accordingly, and indicates that relative differences decrease substantially with only three days exceeding 20% for North Central Texas.

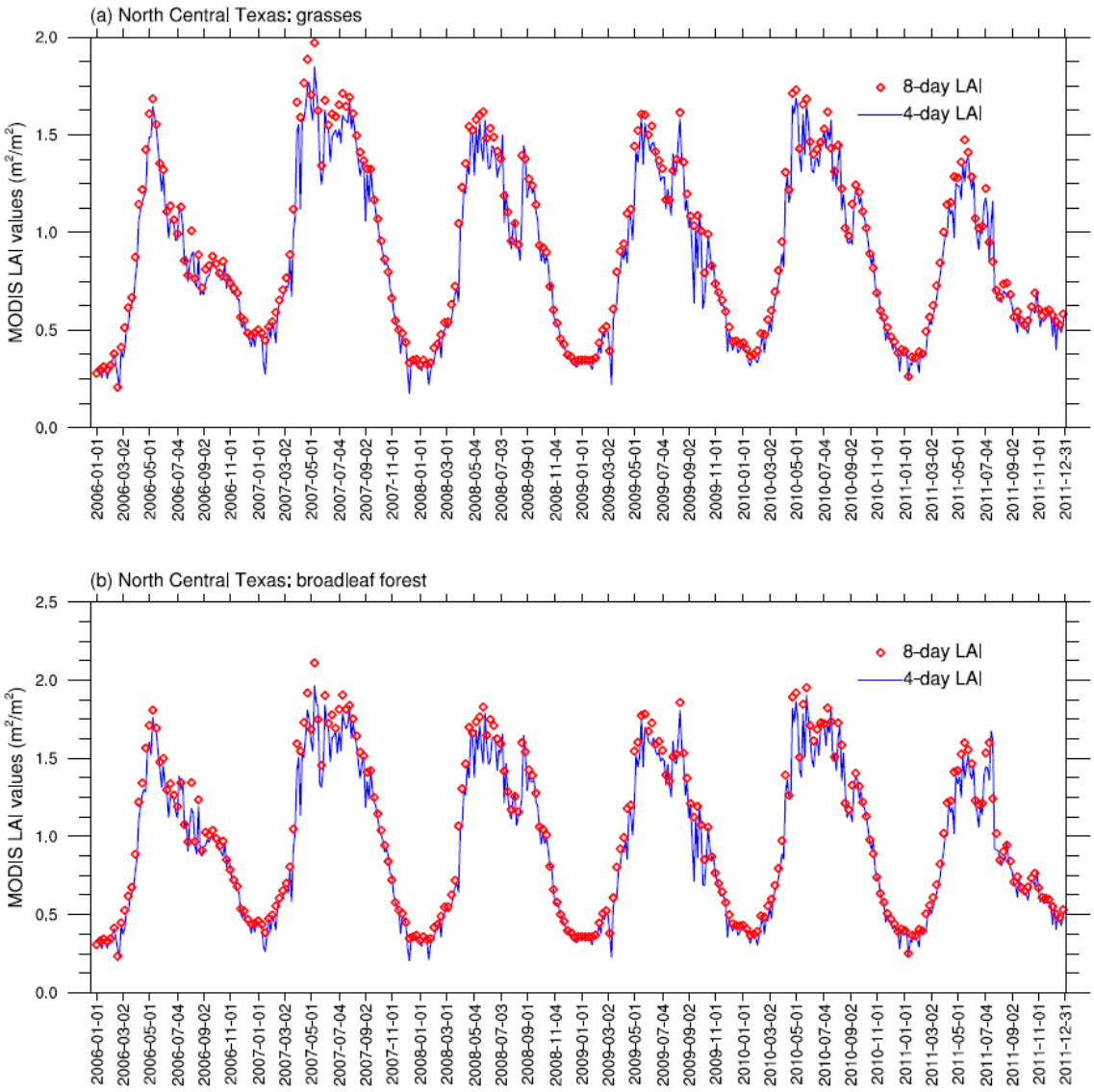

Figure B-1: Time series of 8-day LAI and 4-day LAI values for (a) grasses, and (b) broadleaf forest in North Central Texas during 2006-2011.

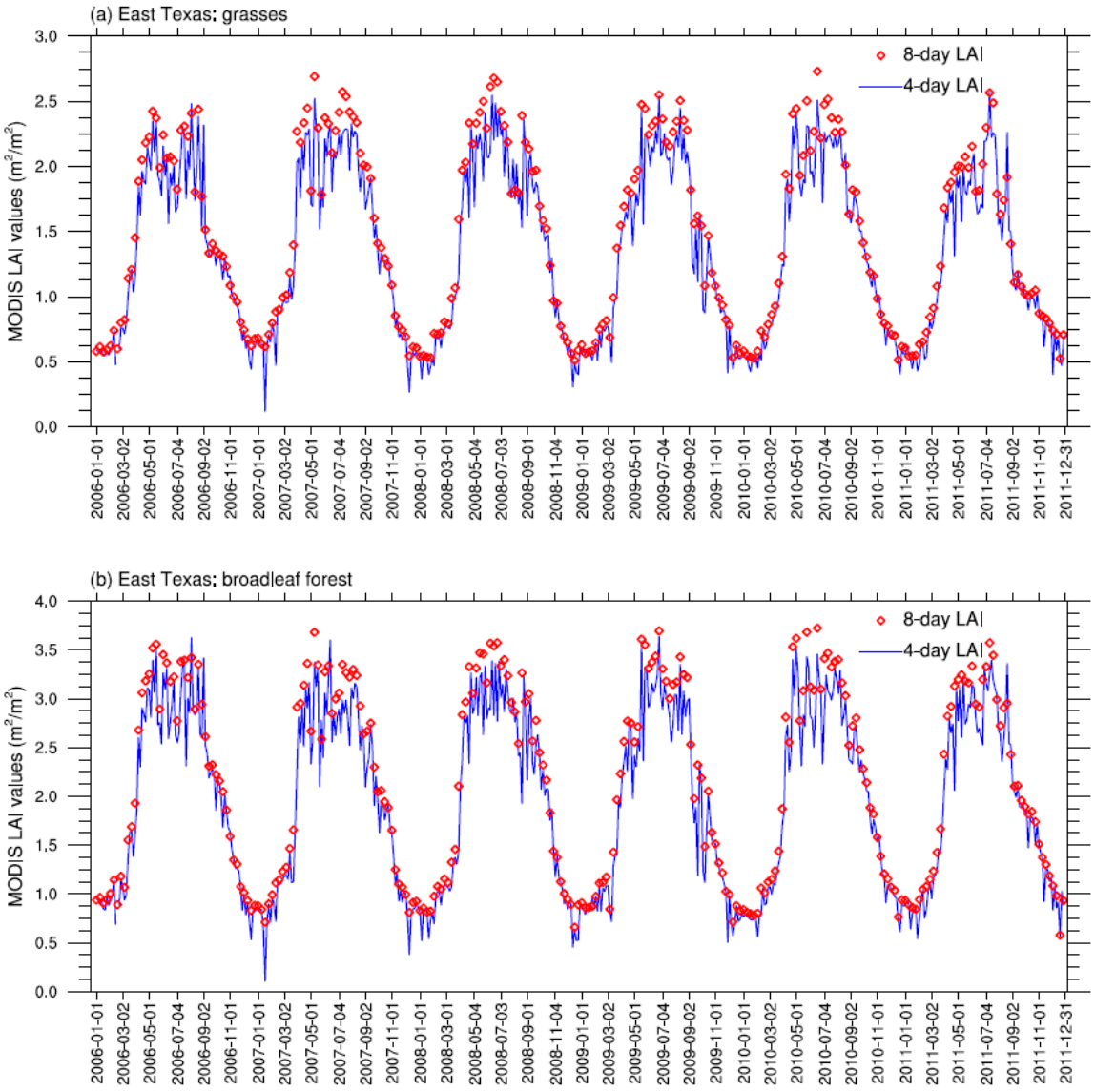

Figure B-2: Time series of 8-day LAI values and 4-day LAI values for (a) grasses and (b) broadleaf forest in East Texas

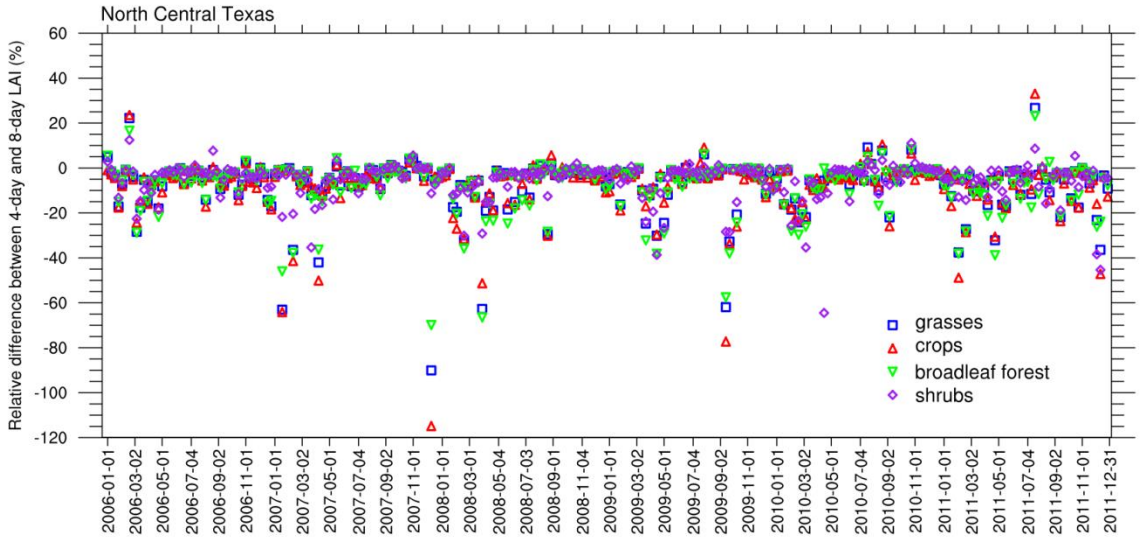

Figure B-3: Relative differences* between temporally paired 4-day LAI and 8-day LAI values for grasses, crops, broadleaf forest, and shrubs in North Central Texas for 2006-2011.

*Relative differences are calculated as $\frac{4\text{-day LAI} - 8\text{-day LAI}}{4\text{-day LAI}} \times 100\%$, where the 4-day LAI and 8-day LAI values are temporally paired.

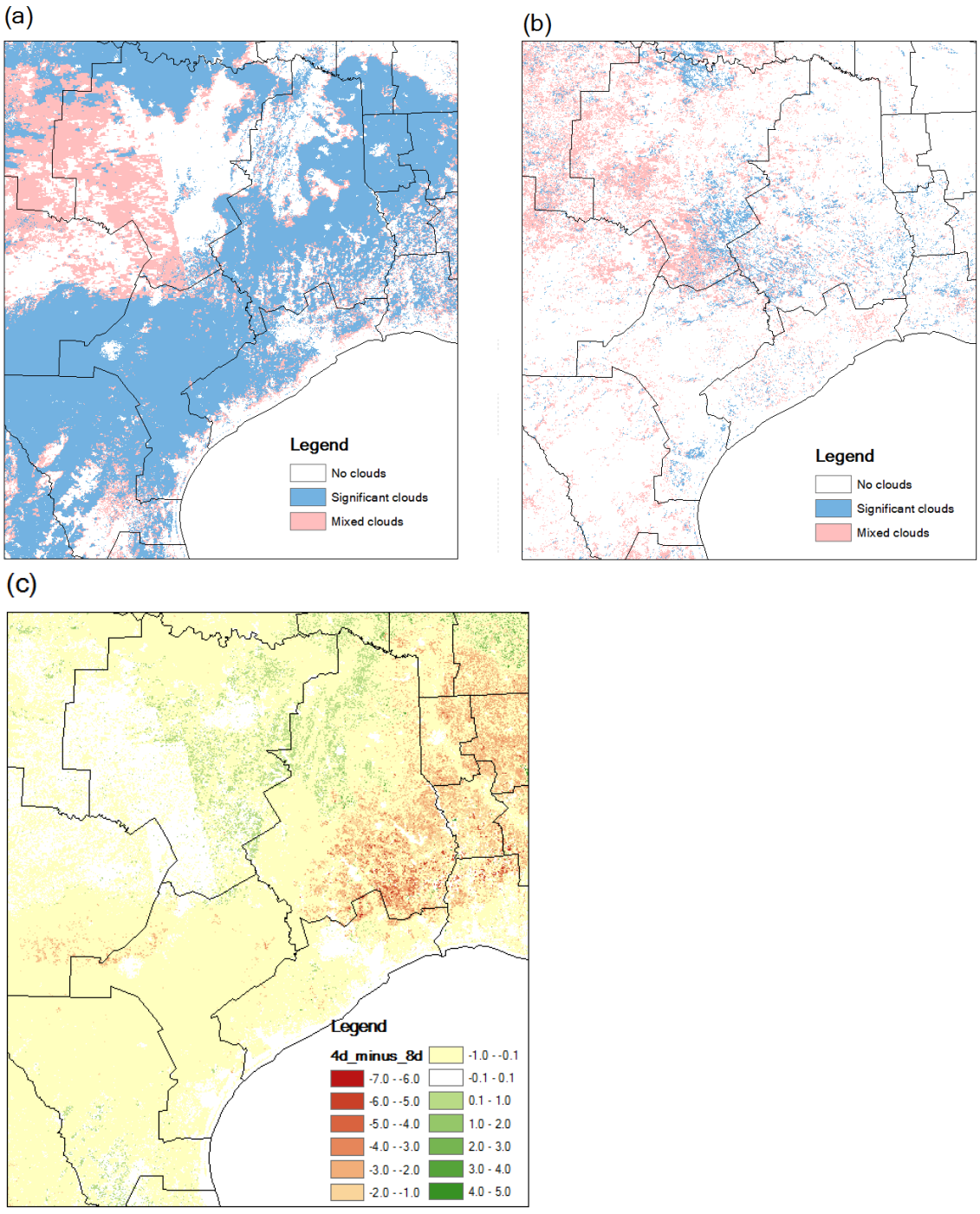

Figure B-4: Cloud state maps for the (a) 4-day and (b) 8-day LAI products on December 11, 2007 in eastern Texas; (c) Absolute differences between the 4-day and 8-day LAI products on December 11, 2007.

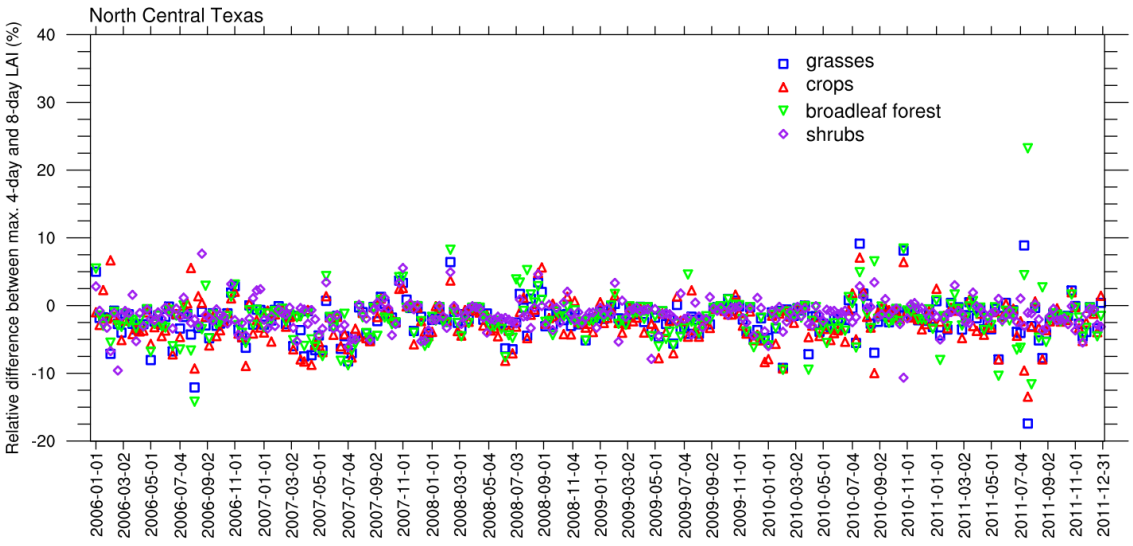

Figure B-5: Relative differences* between maximum 4-day and 8-day LAI values for grasses, crops, broadleaf forest, and shrubs over North Central Texas based on the selection of the day with the largest fPAR during the two 4-day LAI periods that are temporally coincident with the 8-day period. Note differences in scale from Figure B-3.

*Relative differences are calculated as

$$\frac{\max(4\text{-day LAI}_1, 4\text{-day LAI}_2) - 8\text{-day LAI}}{\max(4\text{-day LAI}_1, 4\text{-day LAI}_2)} \times 100\%$$

where 4-day LAI_1 and 4-day LAI_2 are the 4-day LAI value of the first- and second-half of the corresponding 8-day period.

B.3 MODIFICATIONS TO MEGAN2.1 TO INCLUDE SOIL MOISTURE

MEGAN2.1 sets the default soil moisture activity factor to a value of one. The MEGAN2.1 source codes were modified to include the impact of soil moisture based on the algorithm proposed by Guenther et al. (2006, 2012). Estimates of soil moisture were provided by Cai et al. (2014) from the newly developed Noah Land Surface Model (LSM) with multiparameterization options (Noah-MP) driven by the North American Land Data Assimilation System Phase 2. Root fraction distributions were based on the International Geosphere-Biosphere Programme (IGBP) classifications from Zeng (2001) were converted to the default MEGAN PFTs.

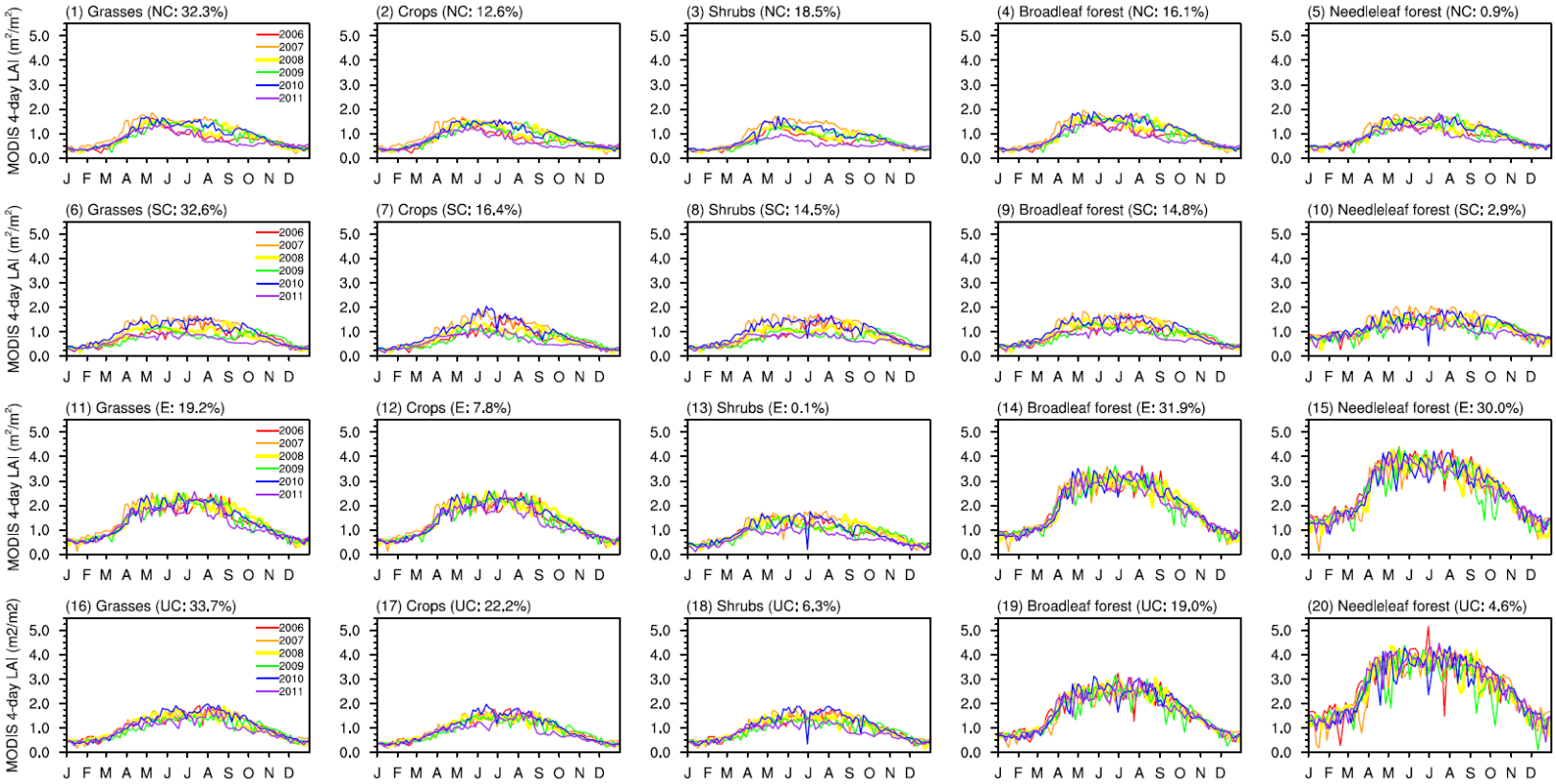

Figure B-6: Area-averaged MODIS 4-day LAI (MCD15A3) during 2006-2011 for major land cover types in North Central Texas (NC, 1st row), South Central Texas (SC, 2nd row), East Texas (E, 3rd row) and Upper Coast (UC, 4th row). Value in brackets indicates the area percentage of each land cover type within each climate division.

Table B-1: Monthly interannual variations (in m^2/m^2) in MODIS 4-day LAI for major land cover types (with areal coverage percentages >10%) by climate region during 2006-2011. Normalized monthly interannual variations are in brackets. Maximum values are highlighted in bold. The last column shows averaged interannual variations during April through to October.

Climate Division	Land Cover Type	Jan	Feb	Mar	Apr	May	Jun	Jul	Aug	Sep	Oct	Nov	Dec	Avg. (Apr - Oct)
North Central Texas	grasses	0.05 (15%)	0.08 (19%)	0.13 (20%)	0.21 (17%)	0.09 (6%)	0.18 (14%)	0.25 (21%)	**0.30 (28%)**	0.25 (26%)	0.12 (15%)	0.06 (11%)	0.07 (18%)	0.20 (18%)
	crops	0.06 (17%)	0.09 (21%)	0.13 (19%)	0.18 (15%)	0.11 (8%)	0.19 (15%)	0.23 (21%)	**0.27 (27%)**	0.22 (26%)	0.10 (15%)	0.07 (14%)	0.07 (19%)	0.19 (18%)
	broadleaf forest	0.03 (8%)	0.06 (14%)	0.11 (16%)	0.19 (15%)	0.09 (6%)	0.18 (12%)	0.20 (14%)	**0.28 (22%)**	**0.23 (22%)**	0.11 (12%)	0.05 (8%)	0.05 (13%)	0.18 (15%)
	shrubs	0.02 (7%)	0.03 (8%)	0.09 (18%)	0.23 (25%)	0.22 (18%)	0.26 (23%)	**0.31 (31%)**	0.25 (28%)	0.20 (24%)	0.10 (14%)	0.05 (9%)	0.04 (12%)	0.23 (23%)
South Central Texas	grasses	0.03 (10%)	0.07 (15%)	0.15 (22%)	0.27 (26%)	0.21 (19%)	0.22 (20%)	**0.31 (26%)**	0.29 **(27%)**	0.24 (26%)	0.16 (19%)	0.12 (20%)	0.04 (11%)	0.24 (23%)
	crops	0.03 (10%)	0.06 (15%)	0.12 (22%)	0.21 (24%)	0.22 (19%)	**0.33 (26%)**	**0.33** (27%)	0.28 **(28%)**	0.20 (25%)	0.13 (19%)	0.09 (19%)	0.04 (12%)	0.24 (24%)
	broadleaf forest	0.04 (9%)	0.06 (11%)	0.12 (16%)	**0.25 (22%)**	0.20 (16%)	0.18 (14%)	0.23 (18%)	0.24 (19%)	0.23 **(22%)**	0.13 (15%)	0.10 (15%)	0.04 (9%)	0.21 (18%)
	shrubs	0.03 (10%)	0.06 (13%)	0.15 (25%)	0.28 **(29%)**	0.25 (23%)	0.23 (20%)	0.28 (24%)	**0.30** (26%)	0.25 (25%)	0.15 (17%)	0.11 (18%)	0.04 (10%)	0.25 (23%)
East Texas	grasses	0.04 (7%)	0.07 (10%)	0.10 (10%)	0.17 (9%)	0.11 (5%)	0.16 (8%)	0.10 (5%)	0.19 (9%)	**0.25 (17%)**	0.14 (12%)	0.05 (6%)	0.04 (7%)	0.16 (9%)
	broadleaf forest	0.08 **(10%)**	0.05 (5%)	0.07 (6%)	0.15 (6%)	0.12 (4%)	0.10 (4%)	0.14 (5%)	0.12 (4%)	**0.21** (9%)	0.17 (9%)	0.06 (5%)	0.07 (8%)	0.14 (6%)
	needleleaf forest	0.15 **(12%)**	0.06 (4%)	0.11 (6%)	0.14 (4%)	0.15 (4%)	0.15 (4%)	0.15 (4%)	0.13 (4%)	0.25 (8%)	**0.26** (10%)	0.11 (6%)	0.11 (9%)	0.17 (5%)
Upper Coast	grasses	0.04 (10%)	0.04 (8%)	0.08 (10%)	0.14 (12%)	0.14 (10%)	0.14 (9%)	0.15 (10%)	0.15 (10%)	**0.20 (15%)**	0.12 (12%)	0.08 (11%)	0.06 (12%)	0.15 (11%)
	crops	0.03 (10%)	0.03 (7%)	0.07 (11%)	0.11 (11%)	0.13 (11%)	0.16 (11%)	0.12 (8%)	0.09 (6%)	**0.18 (17%)**	0.10 (12%)	0.08 (13%)	0.03 (9%)	0.13 (11%)
	broadleaf forest	0.08 **(11%)**	0.05 (6%)	0.11 (9%)	0.16 (7%)	0.15 (6%)	0.14 (5%)	0.09 (4%)	0.09 (4%)	**0.17** (8%)	0.08 (5%)	0.03 (3%)	0.06 (8%)	0.13 (6%)

Table B-2: Monthly averaged temperature (in K) and precipitation (in mm) by climate division during 2006-2011. Standard deviations are in brackets. Source: National Climatic Data Center.

Climate division	Temperature /Precipitation	Jan	Feb	Mar	Apr	May	Jun	Jul	Aug	Sep	Oct	Nov	Dec
North Central Texas	Temperature (K)	280.4	282.3	288.1	291.7	295.9	301.0	302.4	303.2	297.7	291.9	287.2	280.9
		(2.4)	(2.7)	(1.8)	(2.1)	(0.6)	(1.5)	(1.8)	(1.8)	(1.2)	(1.2)	(0.4)	(1.3)
	Precipitation (mm)	54.9	43.3	104.4	81.1	104.3	88.6	60.0	47.8	105.1	97.0	40.0	54.4
		(35.8)	(25.3)	(57.2)	(25.2)	(61.4)	(83.3)	(49.6)	(32.1)	(74.8)	(75.0)	(6.1)	(32.0)
South Central Texas	Temperature (K)	284.5	286.5	291.3	294.6	298.5	301.6	302.1	303.0	299.6	294.8	290.4	285.2
		(1.9)	(2.6)	(1.7)	(2.0)	(0.6)	(0.9)	(1.4)	(1.1)	(0.9)	(0.5)	(0.5)	(1.6)
	Precipitation (mm)	68.0	28.9	62.2	52.6	68.6	65.1	113.7	47.1	110.4	69.6	44.6	51.6
		(55.2)	(34.4)	(50.8)	(33.5)	(34.9)	(48.0)	(109.8)	(46.1)	(89.1)	(65.9)	(33.6)	(36.9)
East Texas	Temperature (K)	281.1	282.9	288.4	292.1	296.2	300.8	301.8	302.7	297.9	292.0	287.5	282.0
		(2.1)	(2.5)	(1.9)	(1.9)	(0.8)	(1.2)	(1.4)	(1.7)	(1.3)	(1.1)	(0.5)	(1.5)
	Precipitation (mm)	101.1	76.8	108.5	78.9	103.0	87.5	107.8	69.6	88.3	133.9	80.0	101.2
		(59.4)	(35.8)	(53.6)	(34.6)	(49.2)	(50.1)	(77.6)	(58.7)	(49.2)	(128.4)	(18.3)	(51.6)
Upper Coast	Temperature (K)	284.9	286.6	291.0	294.3	298.2	301.3	301.8	302.6	299.6	295.1	290.5	286.1
		(1.8)	(2.5)	(1.6)	(1.5)	(0.5)	(0.8)	(1.1)	(0.9)	(0.8)	(0.6)	(0.4)	(1.5)
	Precipitation (mm)	93.7	48.9	71.2	74.2	84.4	92.7	190.2	89.2	125.3	128.7	73.7	82.5
		(63.9)	(31.2)	(39.2)	(66.3)	(51.9)	(58.4)	(121.9)	(63.4)	(46.4)	(121.9)	(28.0)	(43.8)

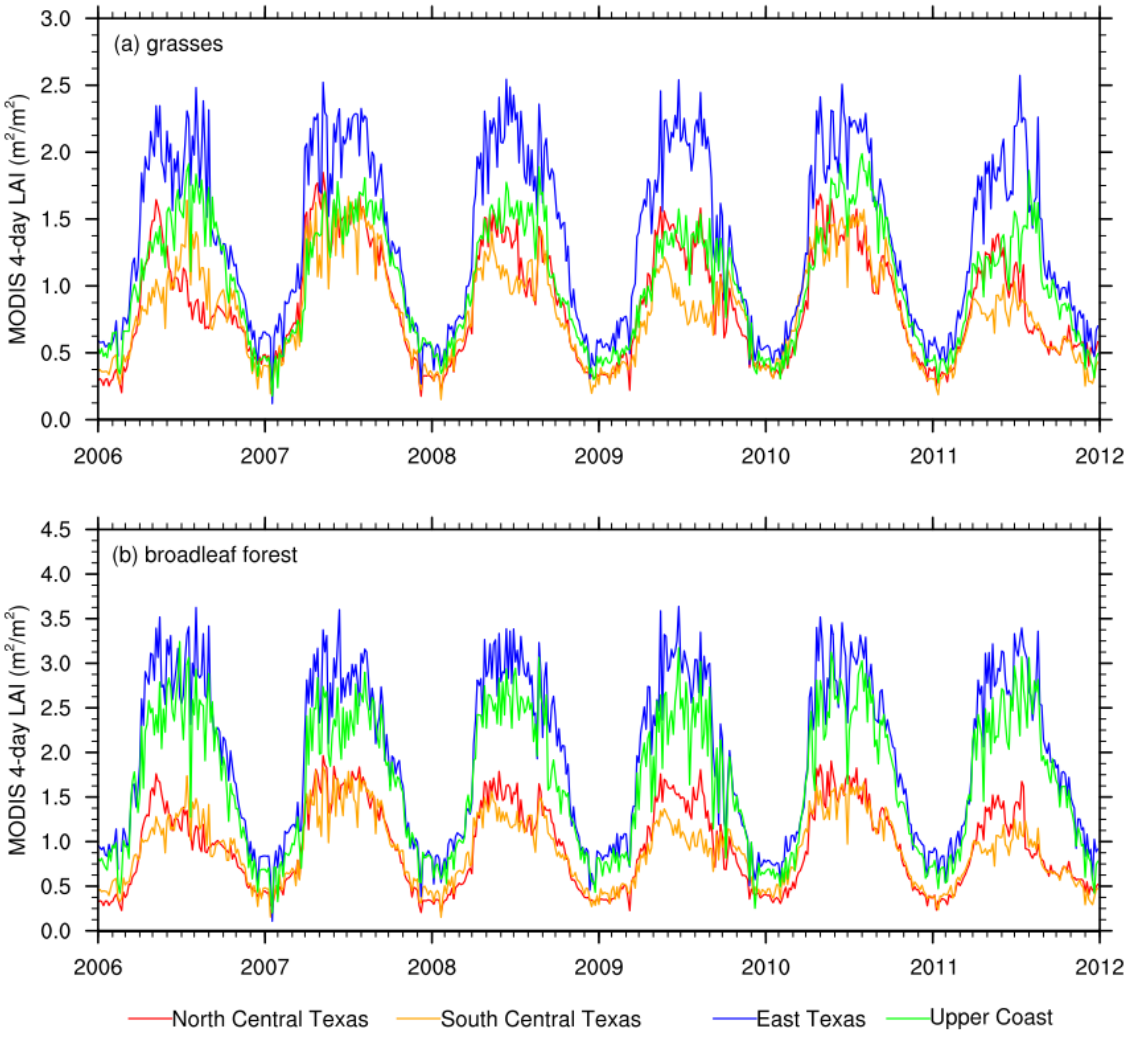

Figure B-7: Time series of area-averaged 4-day LAI for (a) grasses and (b) broadleaf forest by eastern Texas climate division during 2006-2011. Note differences in scale for LAI between plots.

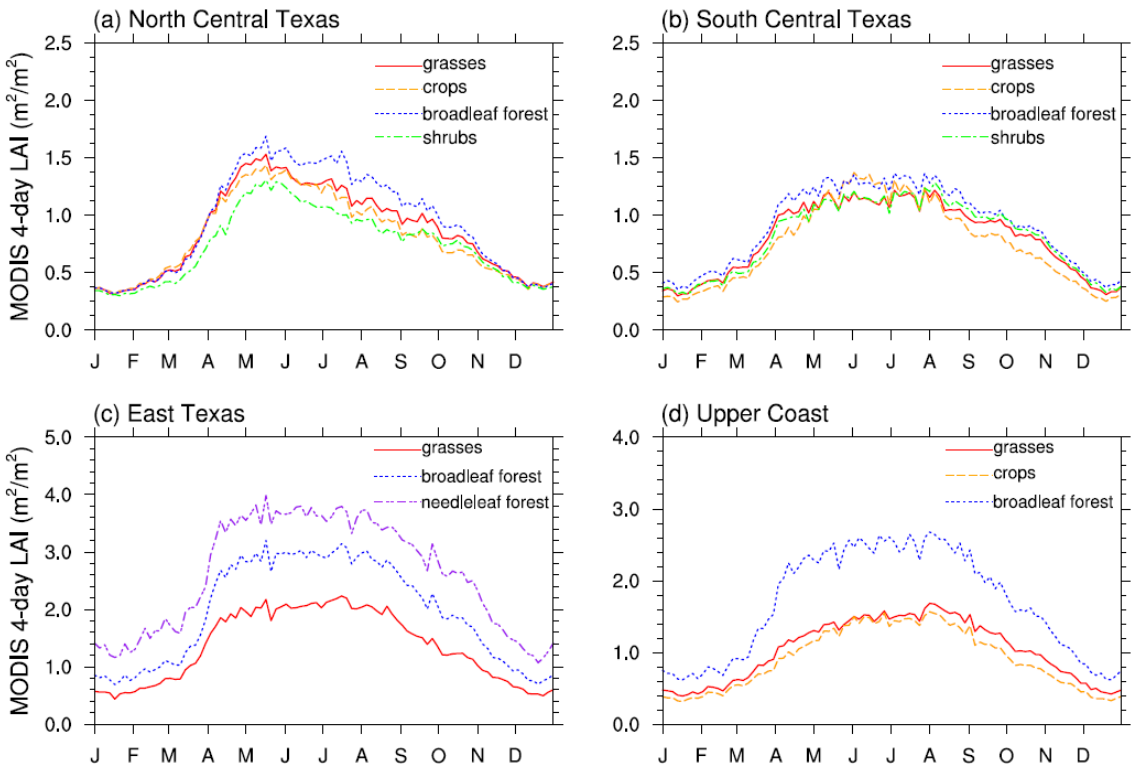

Figure B-8: Time-series of six-year-averaged (2006-2011) LAI for major land cover types (with areal coverage percentages >10%) in (a) North Central Texas, (b) South Central Texas, (c) East Texas and (d) Upper Coast. Note differences in scales for LAI between plots.

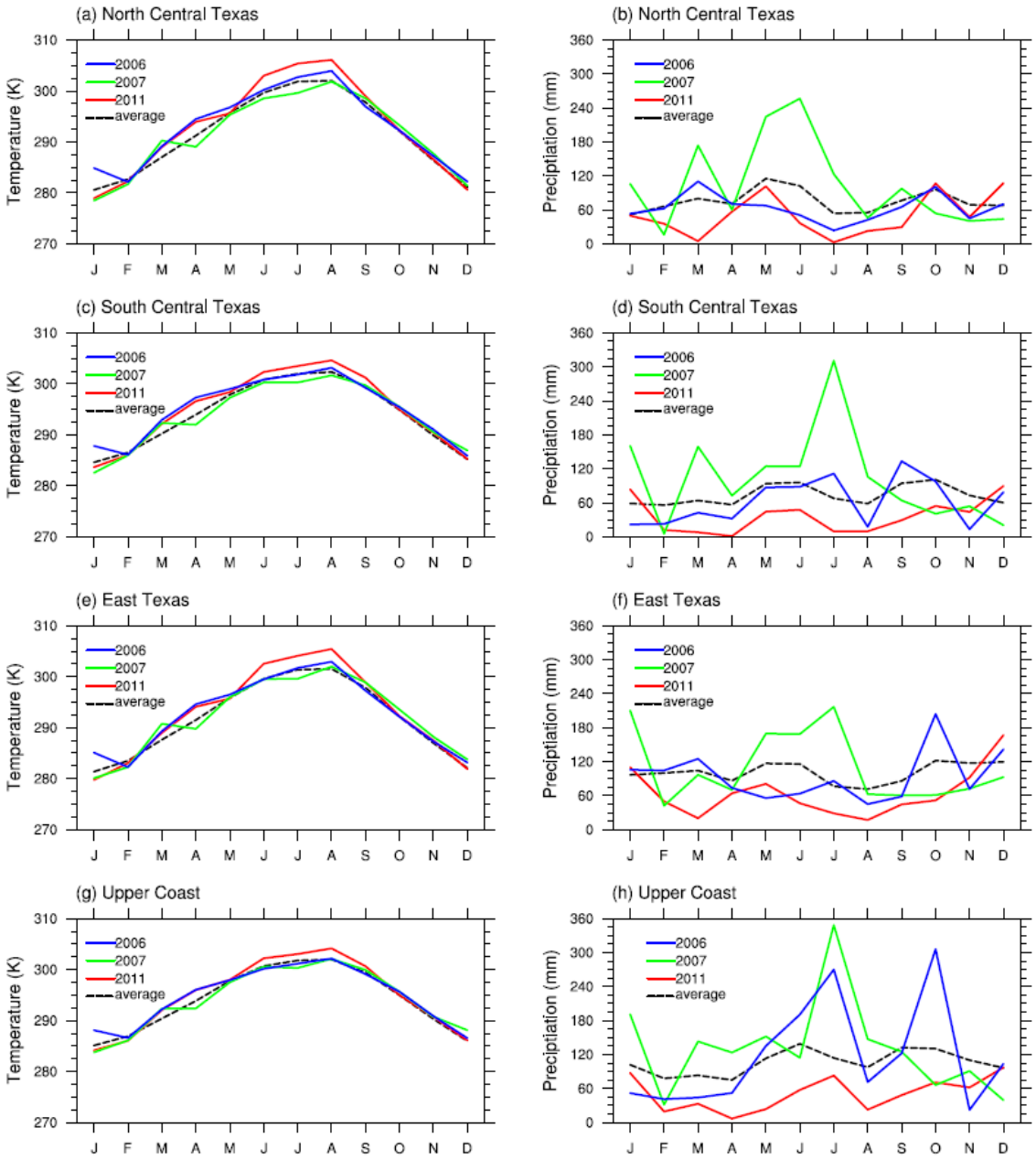

Figure B-9: Time series of monthly temperature (K; left) and precipitation (mm; right) for North Central Texas, South Central Texas, East Texas and the Upper Coast during 2006, 2007, and 2011. The climatological mean (from 1982 to 2011) is shown by the black dashed line. Source: National Climatic Data Center.

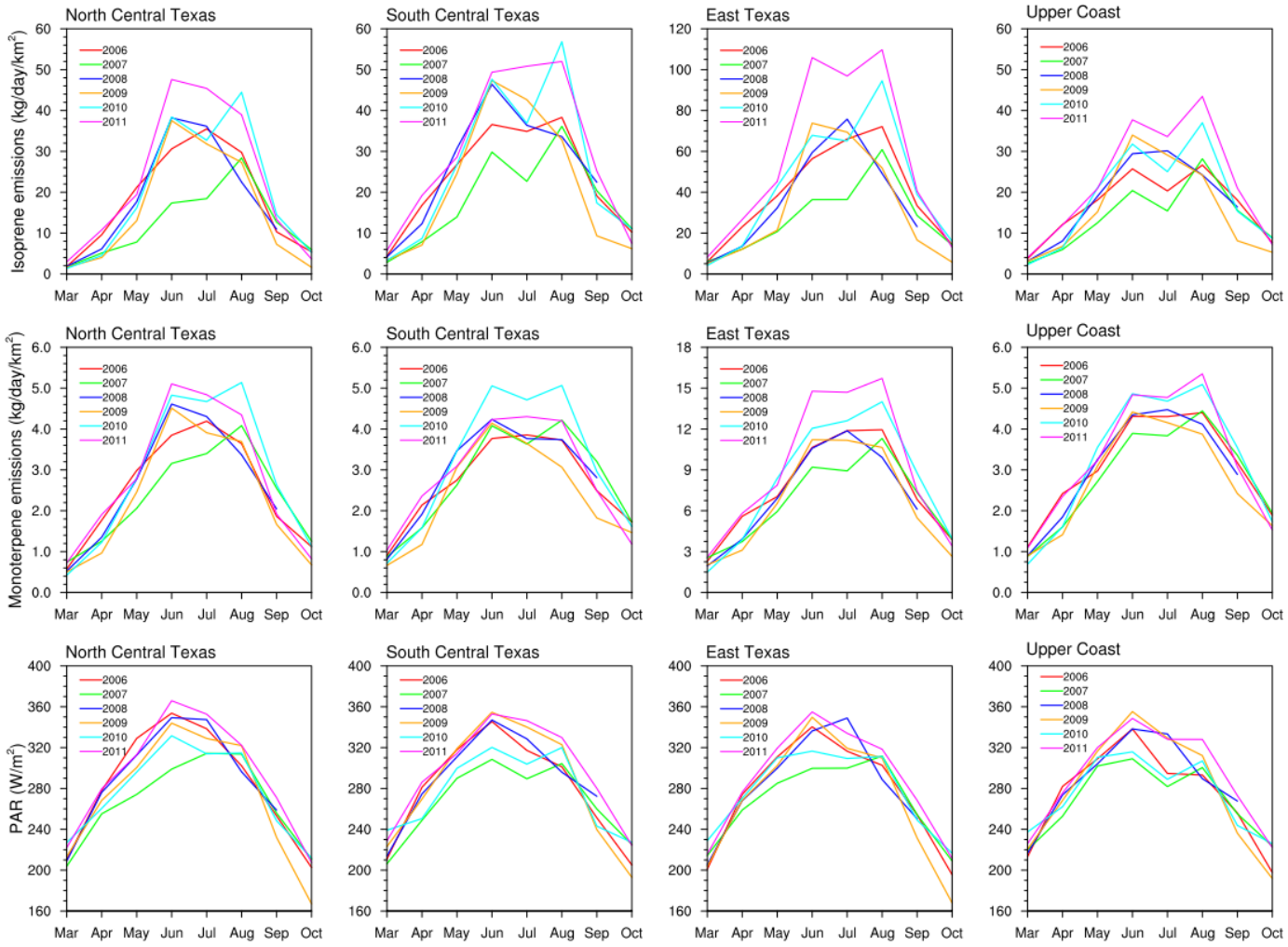

Figure B-10: Time series of area-averaged isoprene and monoterpene emissions (kg/day/km^2) and PAR (W/m^2) for 2006-2011 with consistent annual LAI and meteorological fields (SM1). October 2008 PAR data were not available. Note differences in scales between plots.

Appendix C: Supporting Information for Chapter 4

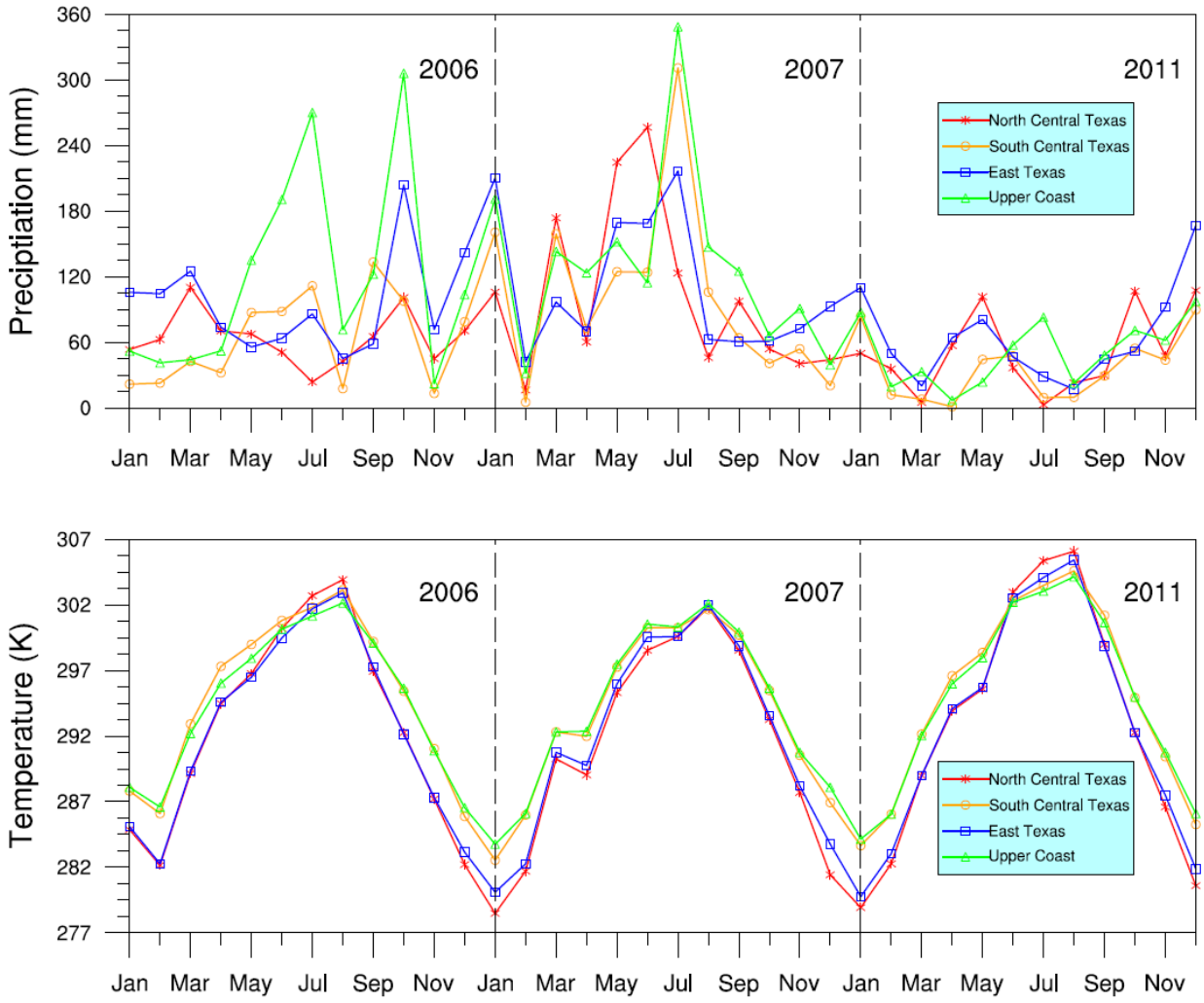

Figure C-1: Monthly precipitation (mm; top) and temperature (K; bottom) for North Central Texas, South Central Texas, East Texas and the Upper Coast during 2006, 2007, and 2011. Source: National Climatic Data Center.

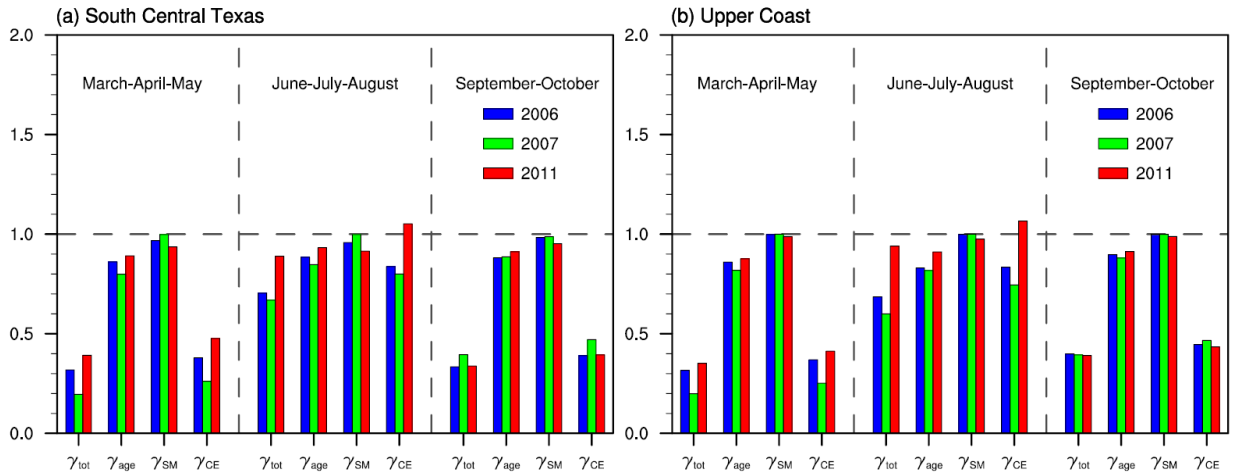

Figure C-2: Area- and season- averaged MEGAN activity factors for isoprene during 2006, 2007, and 2011 in (a) South Central Texas and (b) Upper Coast.

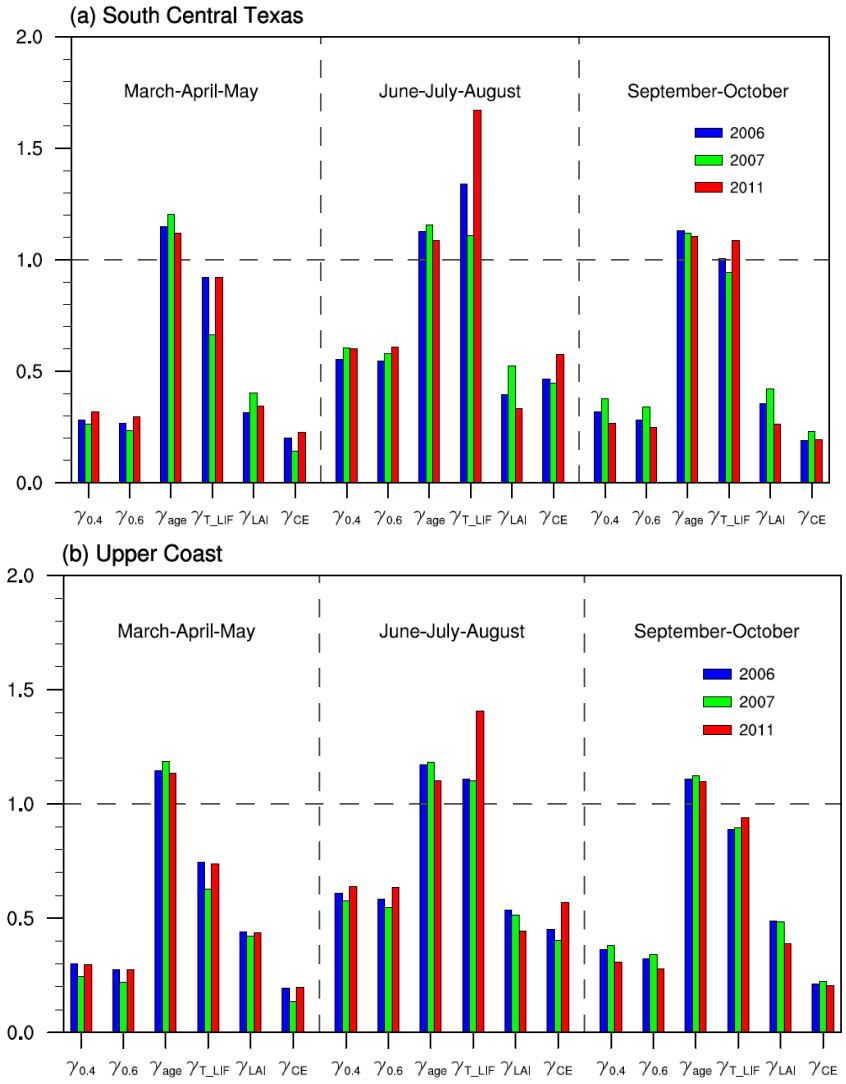

Figure C-3: Area- and season- averaged MEGAN activity factors for monoterpenes during 2006, 2007, and 2011 in (a) South Central Texas and (b) Upper Coast.

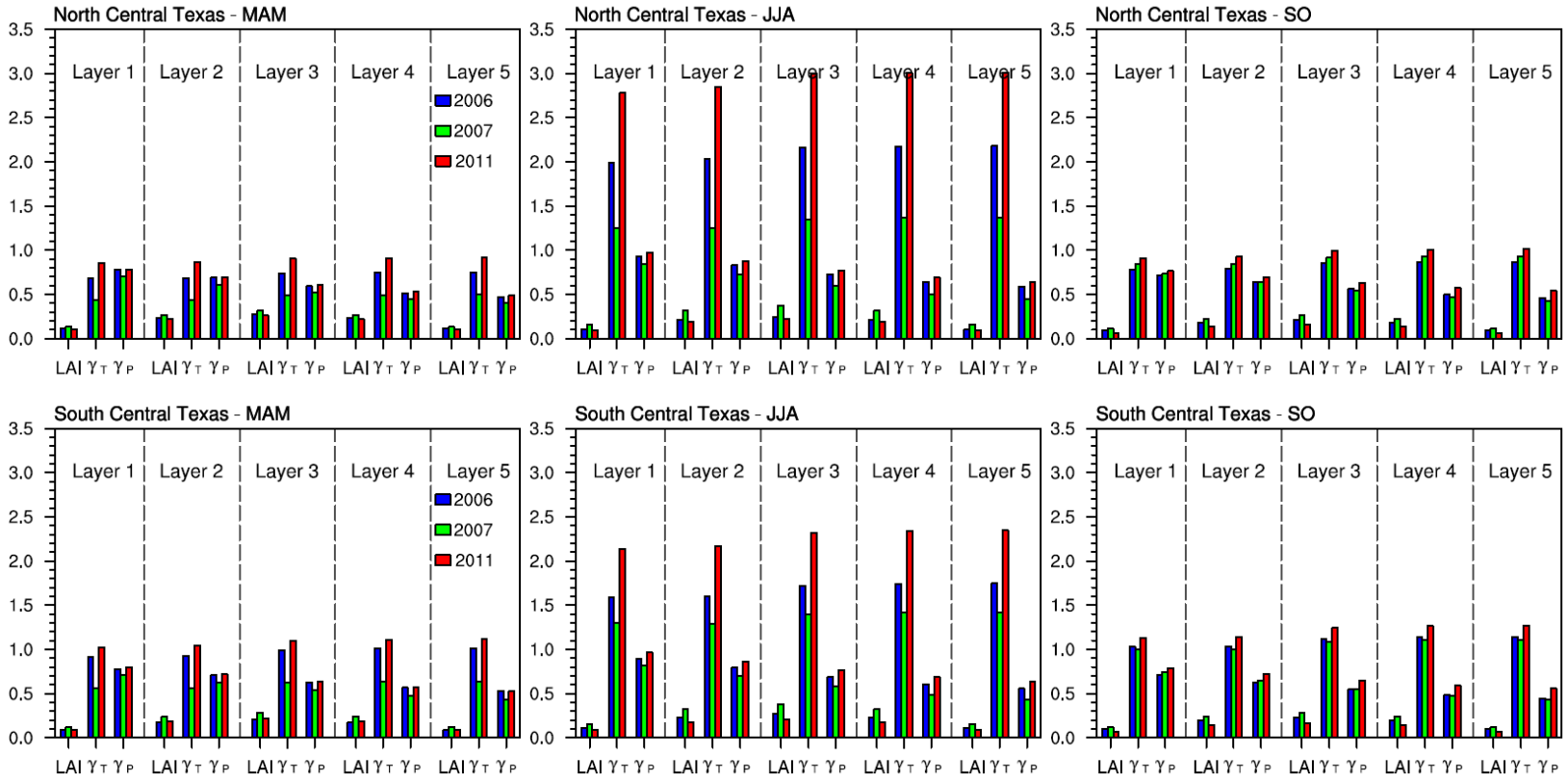

Figure C-4: Area- and season-averaged layer-level activity factors for isoprene during 2006, 2007 and 2011 in North Central Texas (1st row), South Central Texas (2nd row), East Texas (3rd row) and Upper Coast (4th row).

(Figure C-4 continued)

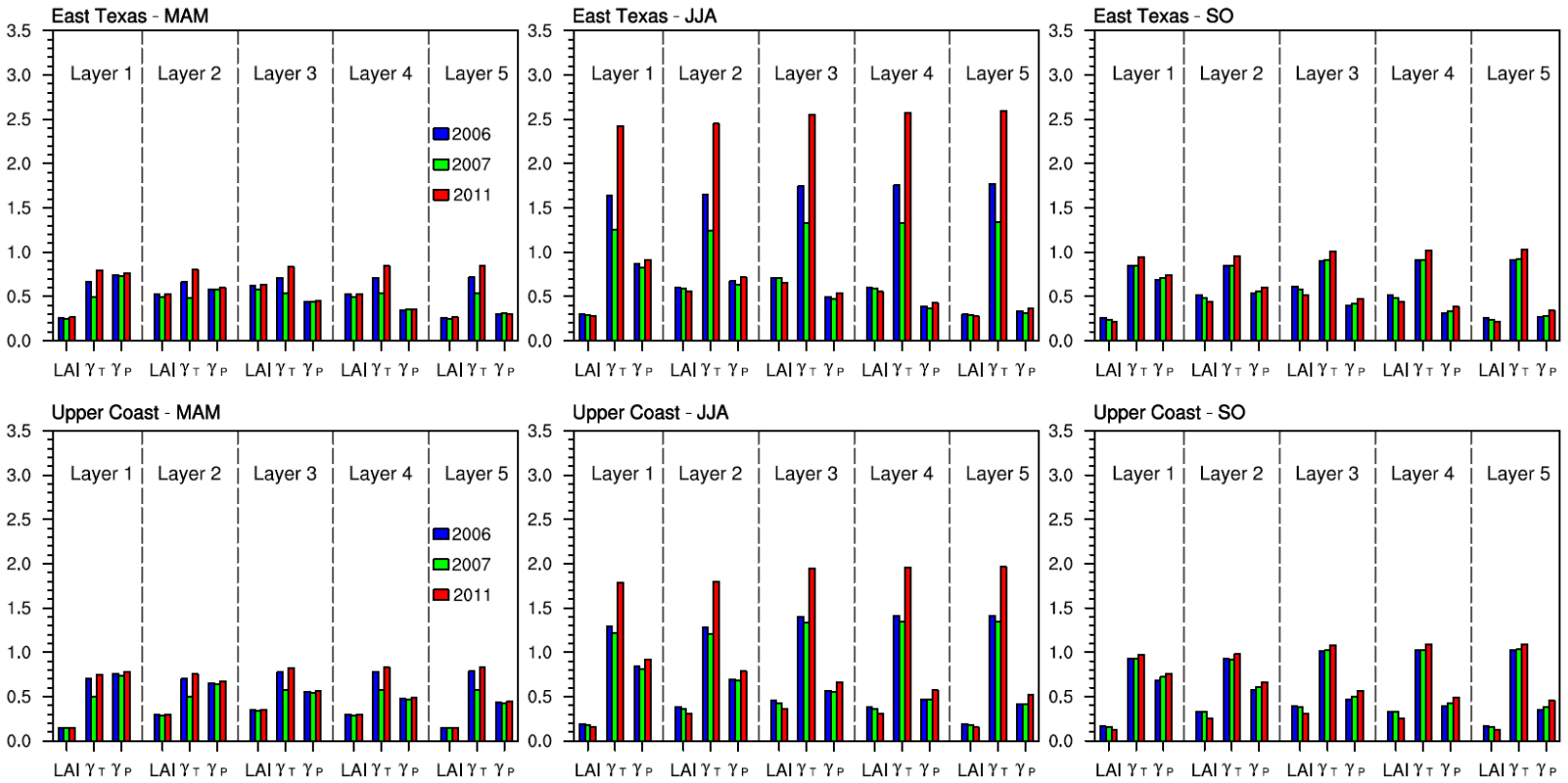

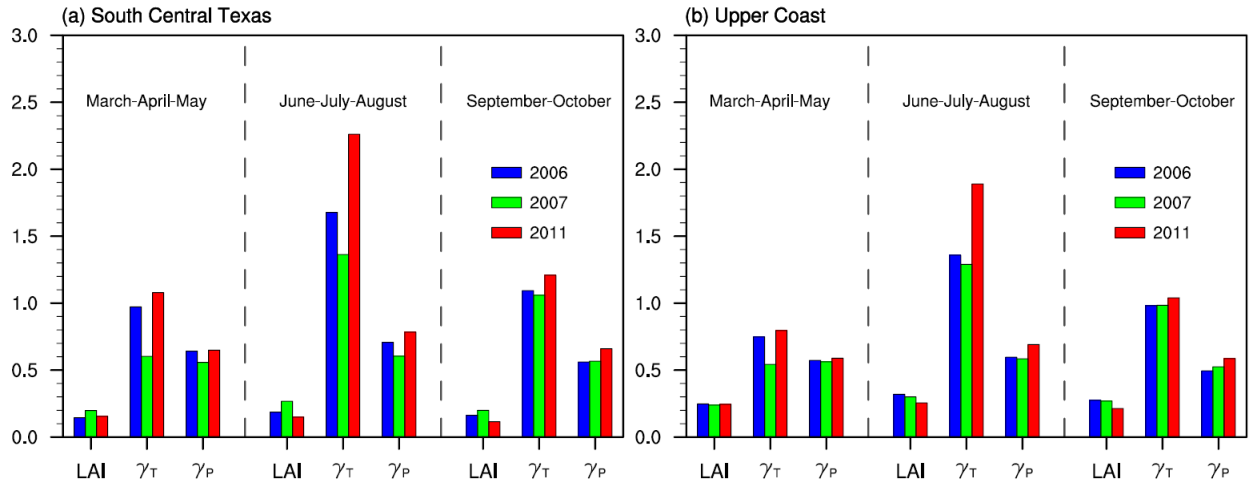

Figure C-5: Layer-averaged LAI, temperature and light activity factors for isoprene during 2006, 2007, and 2011 by season and region – (a) South Central Texas and (b) Upper Coast.

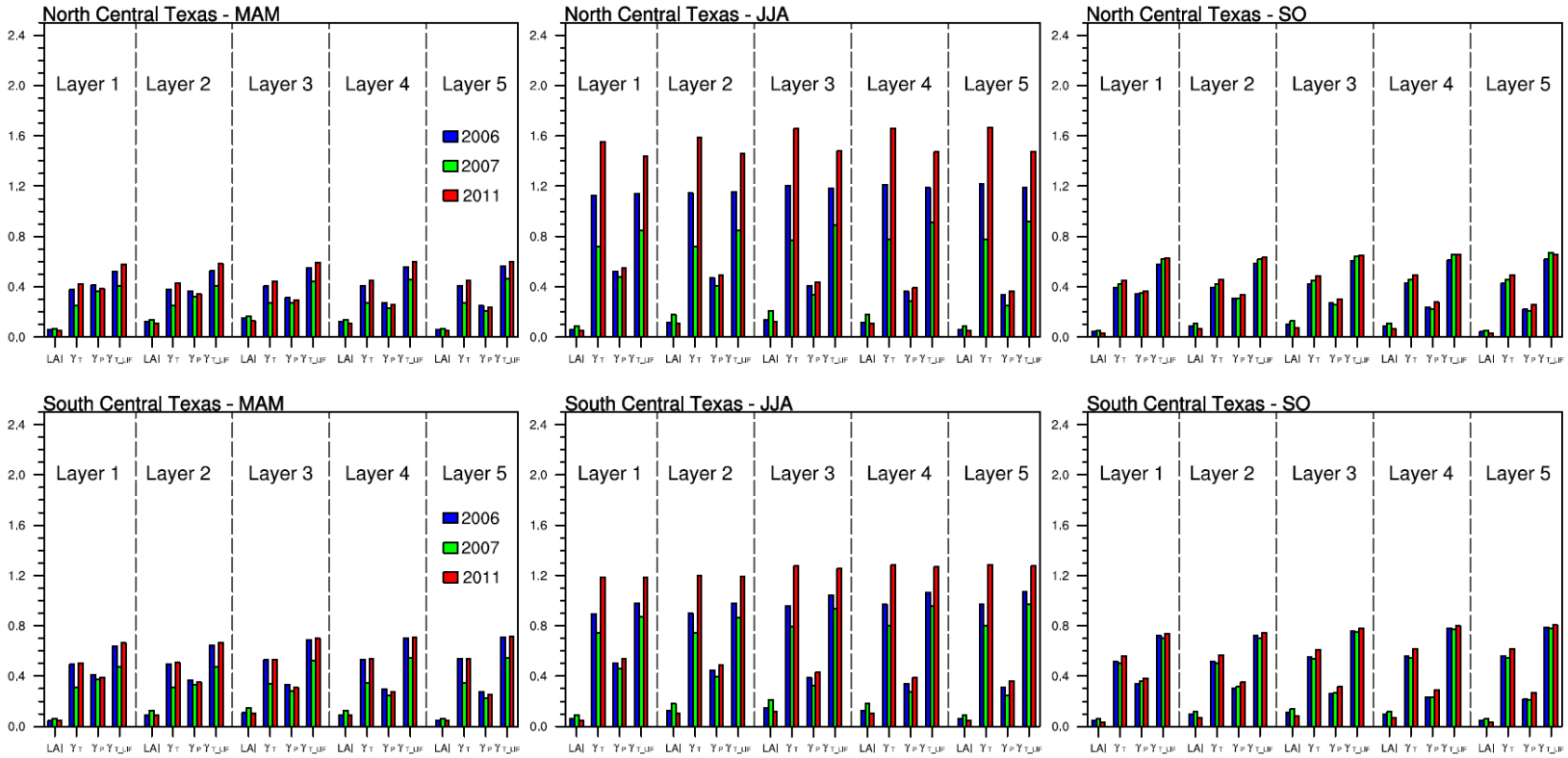

Figure C-6: Area- and season-averaged layer-level activity factors for monoterpenes during 2006, 2007 and 2011 in North Central Texas (1st row), South Central Texas (2nd row), East Texas (3rd row) and Upper Coast (4th row).

(Figure C-6 continued)

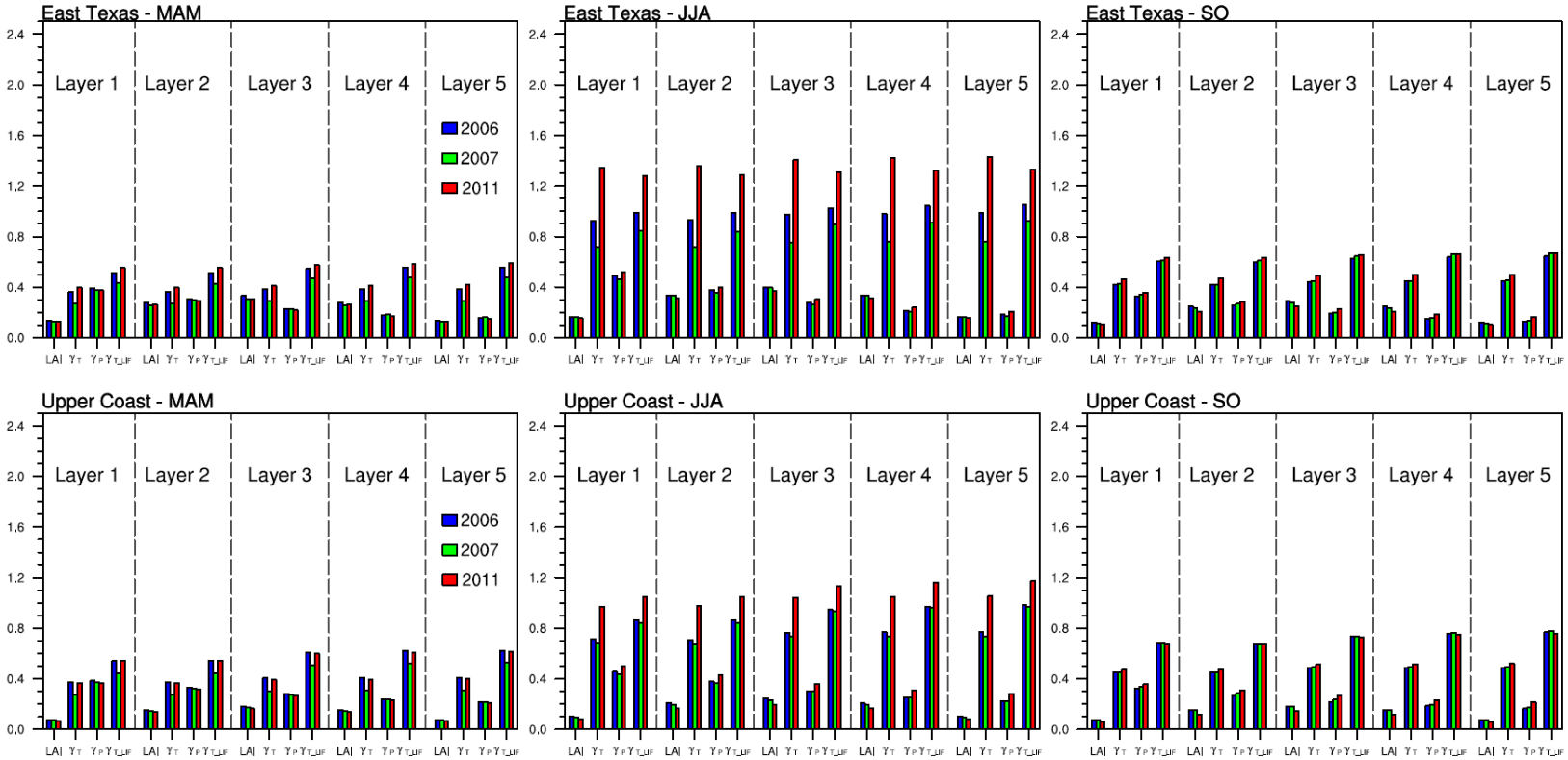

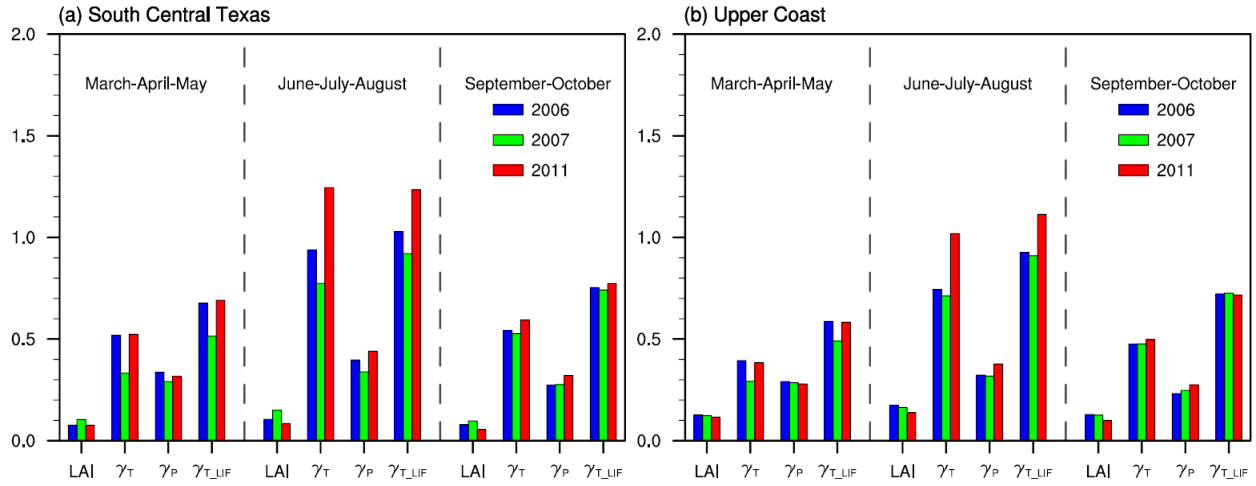

Figure C-7: Layer-averaged LAI, temperature and light activity factors for monoterpenes during 2006, 2007, and 2011 by season and region – (a) South Central Texas and (b) Upper Coast.

Appendix D: Supporting Information for Chapter 5

Table D-1: Mapping of the MODIS Land Cover (MCD12Q1) Type 5 classification to the MEGAN PFT scheme. Basal emission factors for isoprene and monoterpenes (sum of all classes of monoterpenes) are also shown (Guenther et al., 2012).

MODIS PFT scheme	**MEGAN PFT scheme**	**Basal emission factor (µg/m^2/h)**	
		Isoprene	Monoterpenes
Water	Water	n/a	n/a
1 Evergreen needleleaf trees	1 Needleleaf evergreen temperate tree	600	1270
2 Evergreen broadleaf trees	5 Broadleaf evergreen temperate tree	10000	840
3 Deciduous needleleaf trees	2 Needleleaf deciduous boreal tree	1	1080
4 Deciduous broadleaf trees	7 Broadleaf deciduous temperate tree	10000	840
5 Shrub	10 Broadleaf deciduous temperate shrub	4000	920
6 Grass	13 Cool C3 grass / 14 Warm C4 grass[a]	800 / 200	7.5
7 Cereal crops	15 Other crops / 16 Corn[b]	50 / 1	7.5
8 Broad-leaf crops			
9 Urban and built-up	Non-vegetated	n/a	n/a
10 Snow and ice			
11 Barren or sparse vegetation			

[a] The MODIS product does not differentiate between grass types. The distributions of C3/C4 grass were determined by MEGAN's default PFT distribution for North America. The C3/C4 ratio was averaged over each climate region for eastern Texas and applied to the MODIS grassland characterization.
[b] The distributions of other crops and corn were determined by MEGAN's default PFT distribution for North America. The ratio was averaged by each county for eastern Texas and applied to the MODIS cropland data

Table D-2: Mapping of the TCEQ land cover product to MEGAN PFT scheme.

ID	Description	Needleleaf evergreen temperate tree (PFT1)	Needleleaf deciduous boreal tree (PFT2)	Broadleaf evergreen temperate tree (PFT5)	Broadleaf evergreen temperate tree (PFT7)	Broadleaf deciduous temperate shrub (PFT10)	Cool C3 grass (PFT13) / Warm C4 grass (PFT14)[a]	Crops (PFT15) / Corn (PFT16)[b]	Non-Veg
1	Open Water								100
2	Developed Open Space	x*	x*	x*	x*	x*	x*	x*	
3	Developed Low Intensity	x*	x*	x*	x*	x*	x*	x*	35
4	Developed Medium Intensity	x*	x*	x*	x*	x*	x*	x*	65
5	Developed High Intensity								100
6	Barren Land (Rock/Sand/Clay/ Unconsolidated Shore)								100
7	Herbaceous Natural						100		
8	Herbaceous Cultivated							100	
9	Riparian Forested Wetland				100				
10	Swamp Forested Wetland		50		50				
27	Western Swamp Forested Wetland		50		50				
11	Shrub Wetland					100			

Table D-2 continued

ID	Description	Needleleaf evergreen temperate tree (PFT1)	Needleleaf deciduous boreal tree (PFT2)	Broadleaf evergreen temperate tree (PFT5)	Broadleaf evergreen temperate tree (PFT7)	Broadleaf deciduous temperate shrub (PFT10)	Cool C3 grass (PFT13) / Warm C4 grass (PFT14)[a]	Crops (PFT15) / Corn (PFT16)[b]	Non-Veg
28	Western Shrub Wetland					100			
12	Herbaceous Emergent Wetland						100		
13	Cold-Deciduous Forest				100				
29	Western Cold-Deciduous Forest				100				
14	Broad-Leafed Evergreen Forest			100					
30	Western Broad-Leafed Evergreen Forest			100					
15	Needle-Leafed Evergreen Forest	100							
31	Western Needle-Leafed Evergreen Forest	100							
16	Mixed Forest	50			50				
32	Western Mixed Forest	50			50				
17	Cultivated Woody Vegetation	18			18	36			28
18	Cold-Deciduous Woodland				50		50		

Table D-2 Continued

ID	Description	Needleleaf evergreen temperate tree (PFT1)	Needleleaf deciduous boreal tree (PFT2)	Broadleaf evergreen temperate tree (PFT5)	Broadleaf evergreen temperate tree (PFT7)	Broadleaf deciduous temperate shrub (PFT10)	Cool C3 grass (PFT13) / Warm C4 grass (PFT14)[a]	Crops (PFT15) / Corn (PFT16)[b]	Non-Veg
33	Western Cold-Deciduous Woodland				50		50		
19	Broad-Leafed Evergreen Woodland			50			50		
34	Western Broad-Leafed Evergreen Woodland			50			50		
20	Needle-Leafed Evergreen Woodland	50					50		
35	Western Needle-Leafed Evergreen Woodland	50					50		
21	Mixed Woodland	25			25		50		
36	Western Mixed Woodland	25			25		50		
22	Cold-Deciduous Shrub					100			
23	Broad-Leafed Evergreen Shrub					100			
24	Needle-Leafed Evergreen Shrub					100			
25	Mixed Shrub					100			
26	Desert Shrub					100			

[a] TCEQ land cover data do not differentiate between different grass types. The distributions of C3 and C4 grasses were determined by MEGAN's default PFT distribution.
[b] The distributions of other crops and corn were determined by MEGAN's default PFT distribution. The ratio was averaged by each county for eastern Texas and applied to the TCEQ data.
[*] Pixels with developed land cover (e.g. "Developed Open Space", "Developed Low Intensity", and "Developed Medium Intensity" greater than 75% usually occurred in the center of urban regions and in clusters within a 5-km range of the urban center. All natural vegetation within an individual urban/suburban cluster was averaged to determine the PFT distribution that is unique to that cluster. Thus the vegetation portion of developed land cover within the cluster was assumed to represent the locally determined PFT distribution.

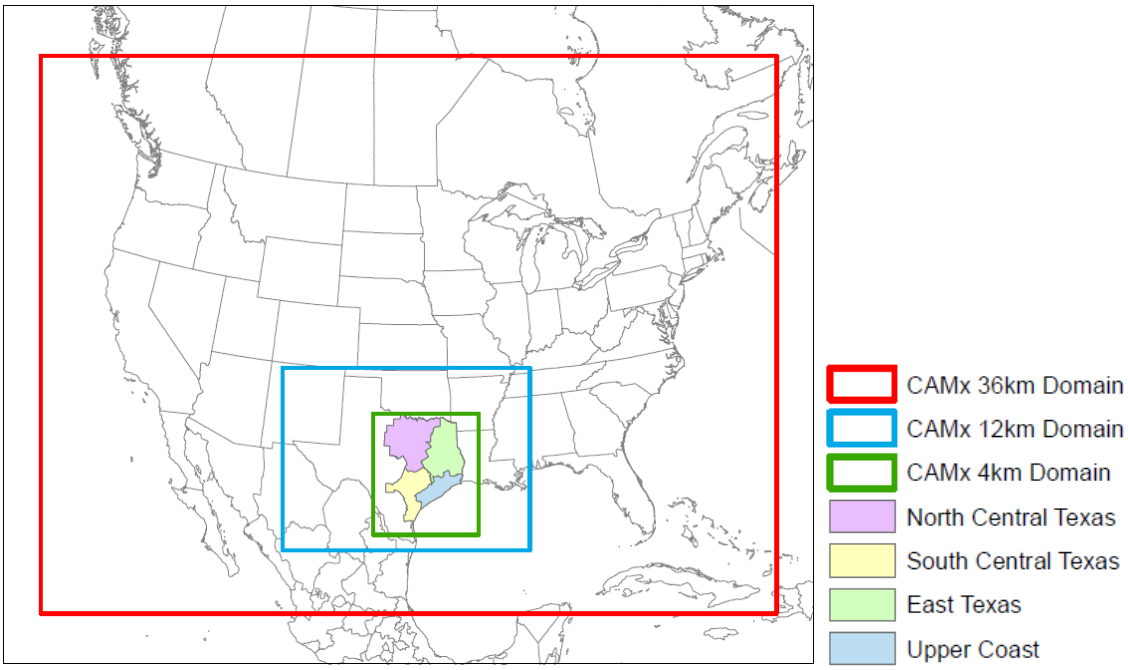

Figure D-1: CAMx nested grid domains (Red: 36 km; Blue: 12 km; Green: 4 km) with eastern Texas climate regions highlighted. Source: https://www.tceq.texas.gov/airquality/airmod/data/domain).

Table D-3: Percent coverage of PFTs mapped from the MODIS (averaged over 2006-2011) and TCEQ land cover products and MEGAN default PFT distribution by climate region.

Climate Region	Land Cover	Needleleaf evergreen temperate tree (PFT1)	Needleleaf deciduous boreal tree (PFT2)	Broadleaf evergreen temperate tree (PFT5)	Broadleaf deciduous temperate tree (PFT7)	Broadleaf deciduous temperate shrub (PFT10)	Cool C3 grass (PFT13)	Warm C4 grass (PFT14)	Crop (PFT15)	Corn (PFT16)
North Central Texas	TCEQ	5.0%	0.0%	0.9%	22.4%	18.1%	21.3%	15.4%	10.2%	1.8%
	MODIS	0.4%	0.0%	0.2%	0.7%	2.1%	48.9%	35.4%	7.3%	1.4%
	MEGAN	1.6%	0.0%	0.1%	10.9%	11.8%	20.2%	14.7%	14.7%	2.3%
South Central Texas	TCEQ	7.1%	0.0%	1.2%	19.0%	14.6%	17.4%	18.1%	14.7%	0.8%
	MODIS	0.4%	0.0%	0.4%	0.9%	10.1%	33.5%	34.9%	13.3%	0.6%
	MEGAN	3.1%	0.1%	2.6%	11.6%	12.5%	5.4%	5.7%	32.3%	1.3%
East Texas	TCEQ	32.6%	0.0%	0.0%	35.1%	0.1%	11.4%	8.6%	7.5%	0.1%
	MODIS	11.3%	0.0%	13.7%	11.4%	13.6%	23.1%	17.4%	7.3%	0.1%
	MEGAN	18.4%	0.1%	0.0%	23.4%	7.8%	5.1%	3.9%	25.4%	0.2%
Upper Coast	TCEQ	5.1%	0.0%	0.2%	18.8%	6.0%	14.3%	16.1%	15.3%	1.8%
	MODIS	1.6%	0.1%	4.2%	3.9%	10.4%	10.5%	11.8%	31.3%	3.0%
	MEGAN	6.3%	0.5%	0.1%	11.2%	4.8%	4.0%	4.4%	32.0%	3.1%

Table D-4: Monthly-averaged emission activity factors (averaged over 2006-2011) for isoprene and monoterpenes (using α-pinene) generated from the MODIS and TCEQ land cover products as well as MEGAN's default PFT data.

Isoprene									
Climate Region	**PFT case**	**Mar**	**Apr**	**May**	**Jun**	**Jul**	**Aug**	**Sep**	**Oct**
North Central Texas	MODIS	0.08	0.25	0.51	1.04	0.97	0.95	0.40	0.17
	TCEQ	0.09	0.26	0.53	1.08	1.00	0.99	0.41	0.16
	MEGAN	0.08	0.25	0.52	1.06	0.98	0.97	0.40	0.16
South Central Texas	MODIS	0.10	0.26	0.53	0.85	0.68	0.82	0.43	0.26
	TCEQ	0.10	0.27	0.54	0.88	0.70	0.85	0.44	0.23
	MEGAN	0.10	0.26	0.53	0.85	0.68	0.82	0.43	0.22
East Texas	MODIS	0.13	0.33	0.59	1.08	1.10	1.25	0.57	0.27
	TCEQ	0.13	0.34	0.60	1.09	1.12	1.26	0.57	0.24
	MEGAN	0.13	0.33	0.58	1.07	1.09	1.24	0.56	0.24
Upper Coast	MODIS	0.10	0.25	0.49	0.77	0.65	0.82	0.46	0.25
	TCEQ	0.11	0.26	0.51	0.80	0.68	0.86	0.48	0.23
	MEGAN	0.10	0.25	0.50	0.78	0.66	0.83	0.47	0.22
Monoterpenes									
Climate Regions	**PFT case**	**Mar**	**Apr**	**May**	**Jun**	**Jul**	**Aug**	**Sep**	**Oct**
North Central Texas	MODIS	0.08	0.21	0.40	0.69	0.66	0.63	0.31	0.14
	TCEQ	0.08	0.21	0.41	0.70	0.68	0.64	0.32	0.13
	MEGAN	0.08	0.21	0.41	0.69	0.67	0.63	0.31	0.13
South Central Texas	MODIS	0.11	0.25	0.44	0.62	0.57	0.57	0.37	0.21
	TCEQ	0.11	0.25	0.44	0.63	0.58	0.58	0.37	0.19
	MEGAN	0.11	0.24	0.44	0.62	0.57	0.57	0.36	0.19
East Texas	MODIS	0.13	0.28	0.49	0.82	0.84	0.86	0.46	0.22
	TCEQ	0.13	0.29	0.49	0.82	0.85	0.86	0.46	0.20
	MEGAN	0.13	0.28	0.49	0.81	0.84	0.85	0.46	0.20
Upper Coast	MODIS	0.11	0.24	0.42	0.61	0.59	0.61	0.41	0.22
	TCEQ	0.11	0.24	0.43	0.62	0.60	0.62	0.41	0.21
	MEGAN	0.11	0.24	0.42	0.61	0.59	0.61	0.41	0.20

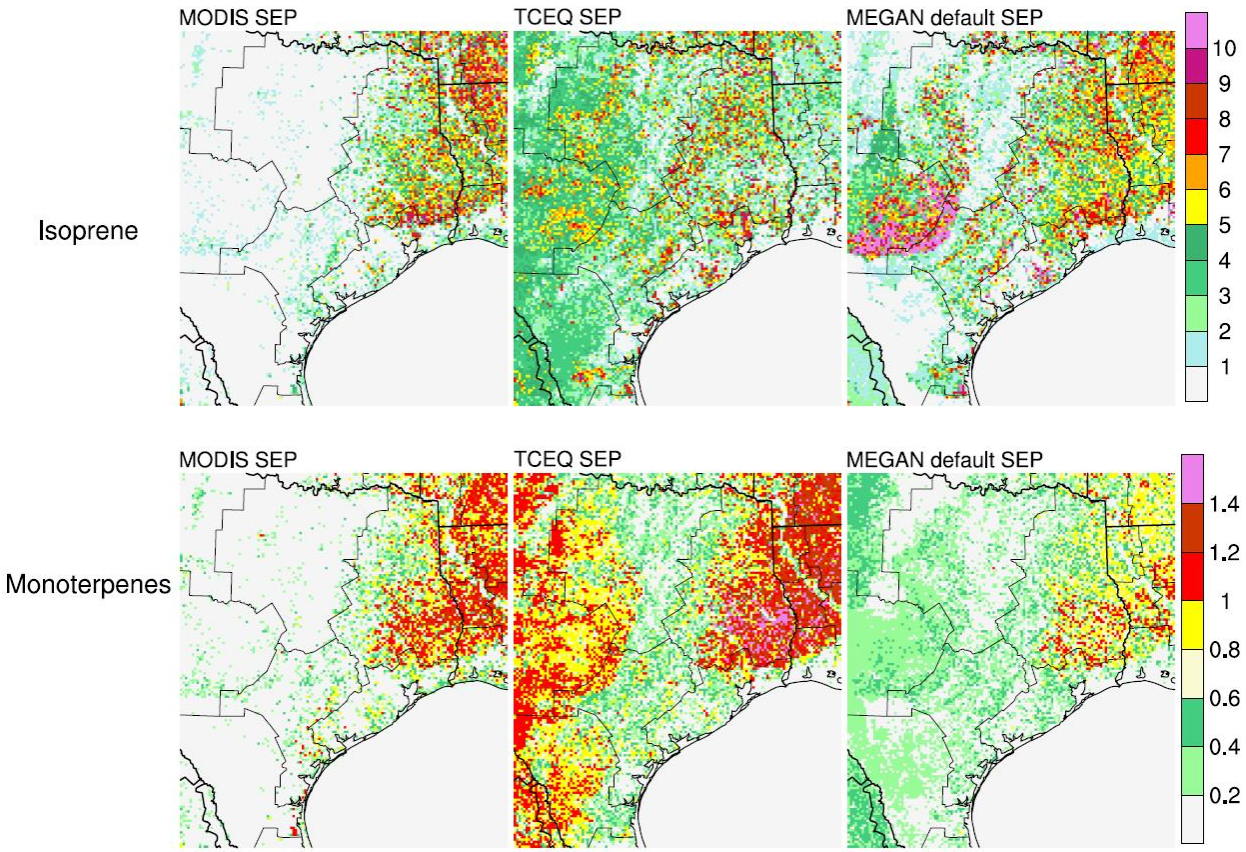

Figure D-2: Isoprene and monoterpene standard emission potentials (kg/km^2/h) generated using the MODIS (averaged over 2006-2011) and TCEQ land cover products and MEGAN's default emission factor maps over eastern Texas (results from SM1). Note differences in scales between plots.

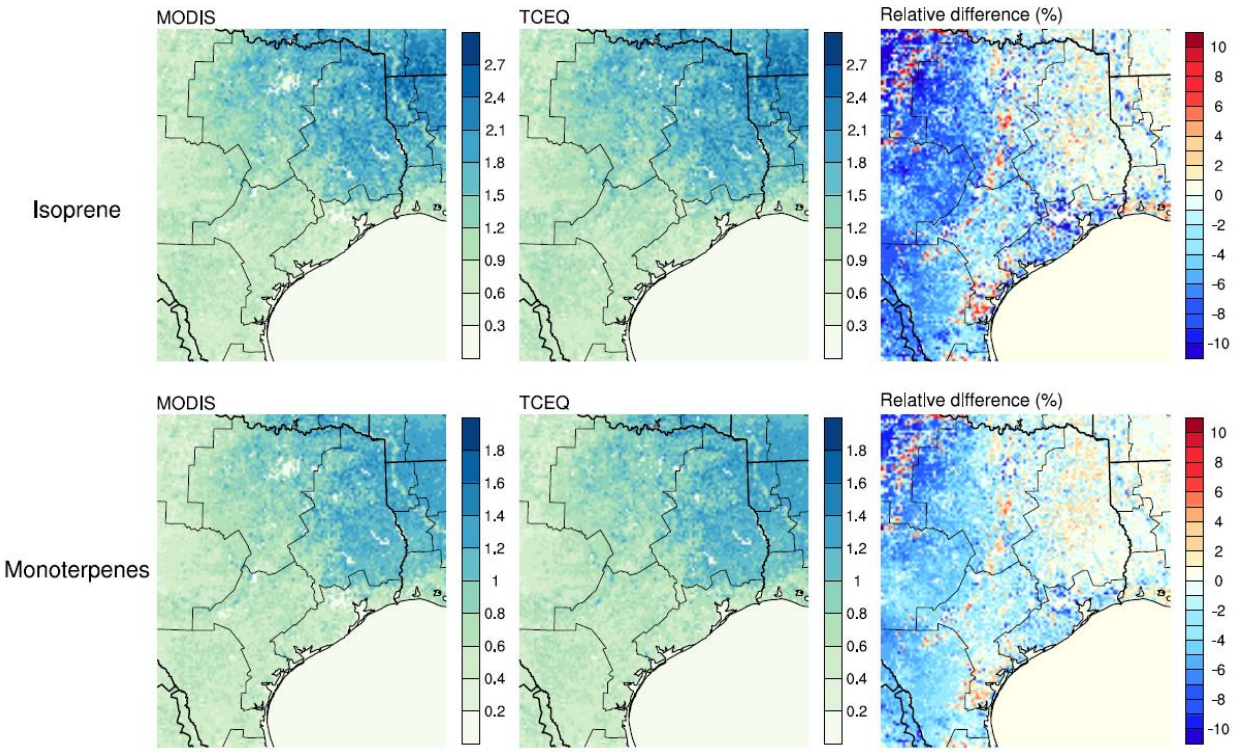

Figure D-3: Spatial distributions of monthly-averaged emission activity factors for isoprene (top) and monoterpenes (using α-pinene, bottom) generated from the MODIS and TCEQ land cover products for June 2011 (results from SM2). Relative percent differences are also shown.

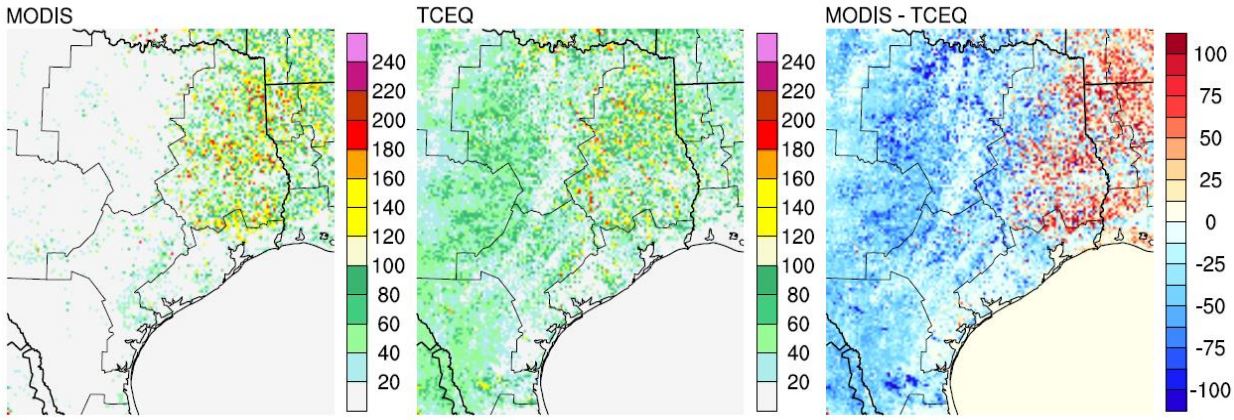

Figure D-4: Spatial distributions of isoprene emissions (kg/km^2/day) for July 2009 generated using the MODIS and TCEQ land cover products (results from SM2); absolute differences between the two scenarios are also shown. Note differences in scales between plots.

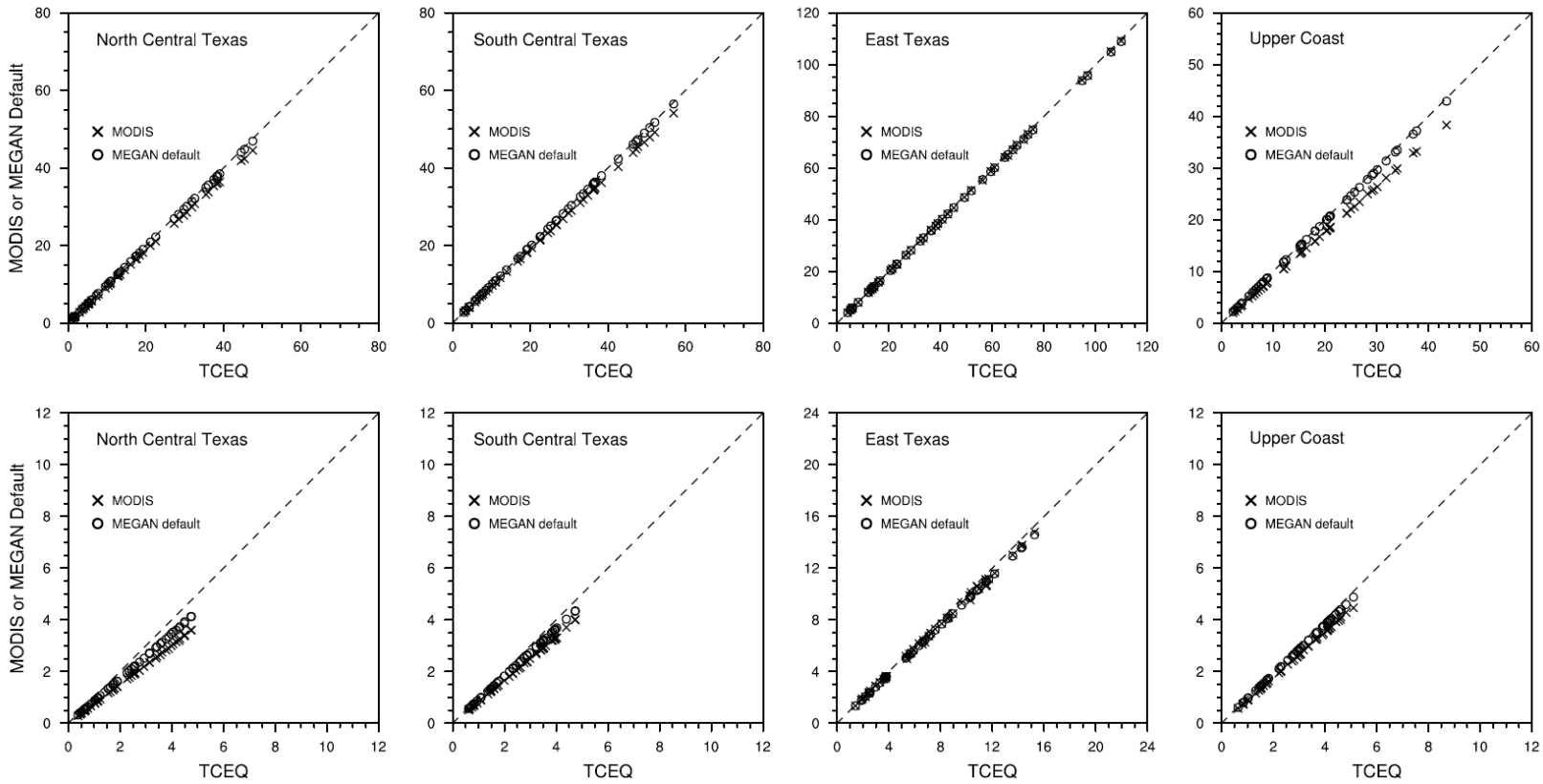

Figure D-5: Comparison of monthly averaged isoprene (top) and monoterpene (bottom) emissions (kg/km^2/day) generated using MEGAN's default emission factor maps (results from SM3). October 2008 was not shown due to missing data.

Appendix E: Supporting Information for Chapter 6

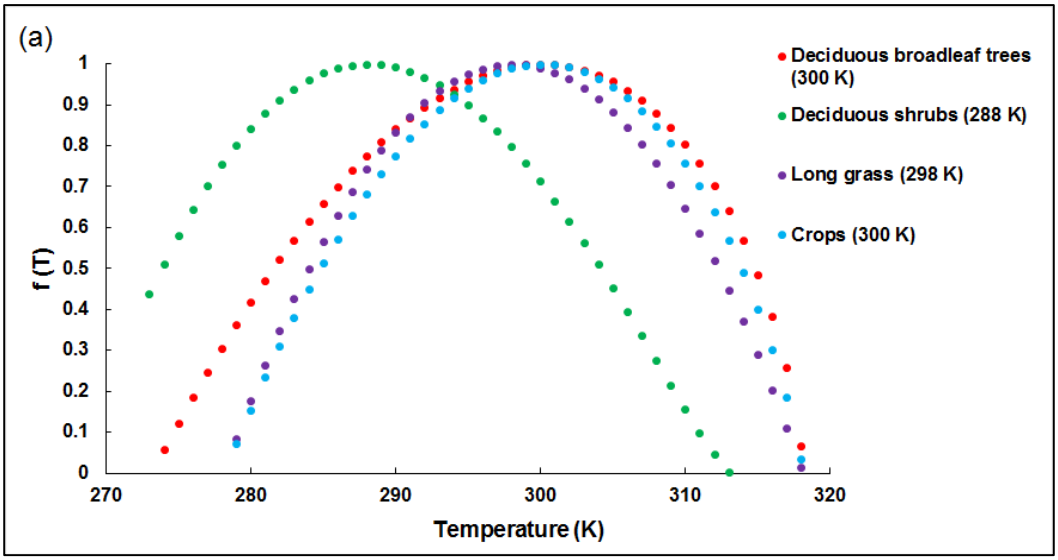

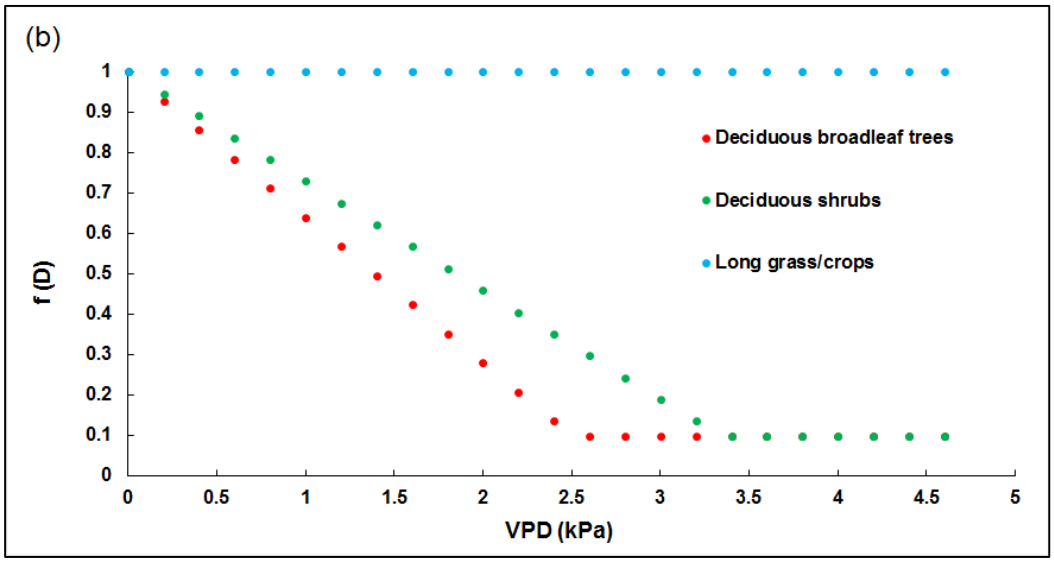

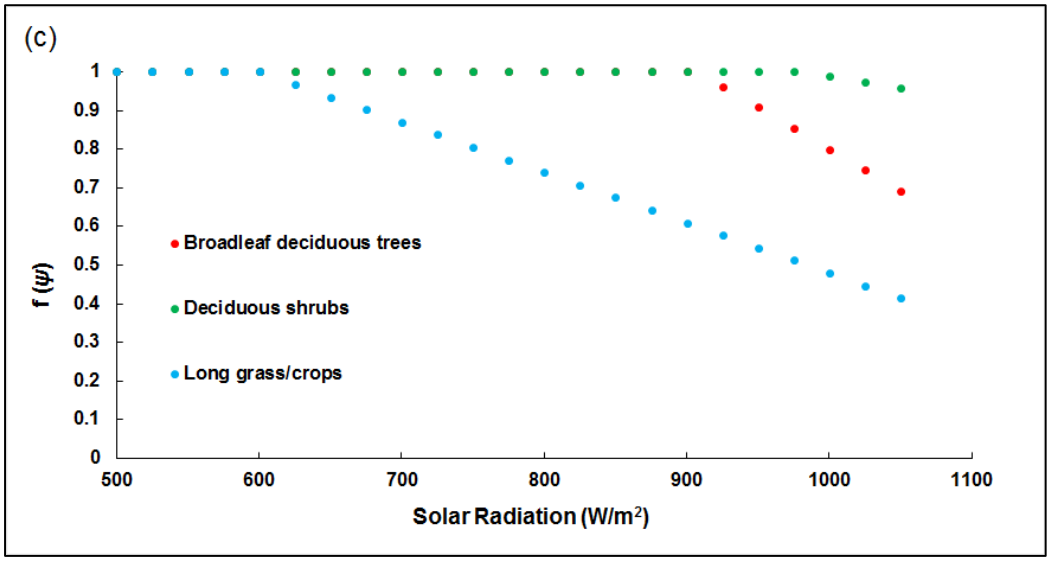

Figure E-1: Stomatal response to (a) temperature, (b) vapor pressure deficit (VPD) and (c) solar radiation for four land cover categories – broadleaf deciduous trees, deciduous shrubs, long grass and crops as modeled in Zhang's dry deposition algorithm. The optimum temperatures of maximum stomatal opening for each land cover category are shown in (a).

E.1 WRF MODEL PERFORMANCE EVALUATION

WRF model performance was evaluated on a monthly basis using both quantitative and qualitative analysis during April-October for year 2006, 2007 and 2011 within each of the four eastern Texas climate regions – North Central Texas, South Central Texas, East Texas, and Upper Coast (Figure 6-1). The quantitative analysis calculated statistical metrics for selected surface variables (e.g. temperature, specific humidity, winds) against observations collected at National Weather Service (NWS) stations (retrieved from the National Climatic Data Center Integrated Surface Database, http://www.ncdc.noaa.gov/oa/climate/isd/) throughout the eastern half of Texas. Performance benchmarks developed by Emery et al. (2001) were used for the purpose of overall performance evaluation. In addition to the surface variables, qualitative analysis compared the predicted downwelling shortwave radiation with satellite-based observations provided by the University of Alabama at Huntsville (UAH) (Pour-Biazar, et al, 2007) and total monthly precipitation with NWS observed precipitation. Overall, the performance evaluation demonstrated good results for surface variables and acceptable results for downwelling shortwave radiation across all months and years. Predicted monthly precipitation patterns were under-predicated but with reasonable magnitude and spatial coverage. Therefore, it was reasonable to use the WRF outputs, including temperature, wind speed, specific humidity, clouds, precipitation and other fields, to drive CAMx dry deposition simulations during the growing season in eastern Texas for the selected three years.

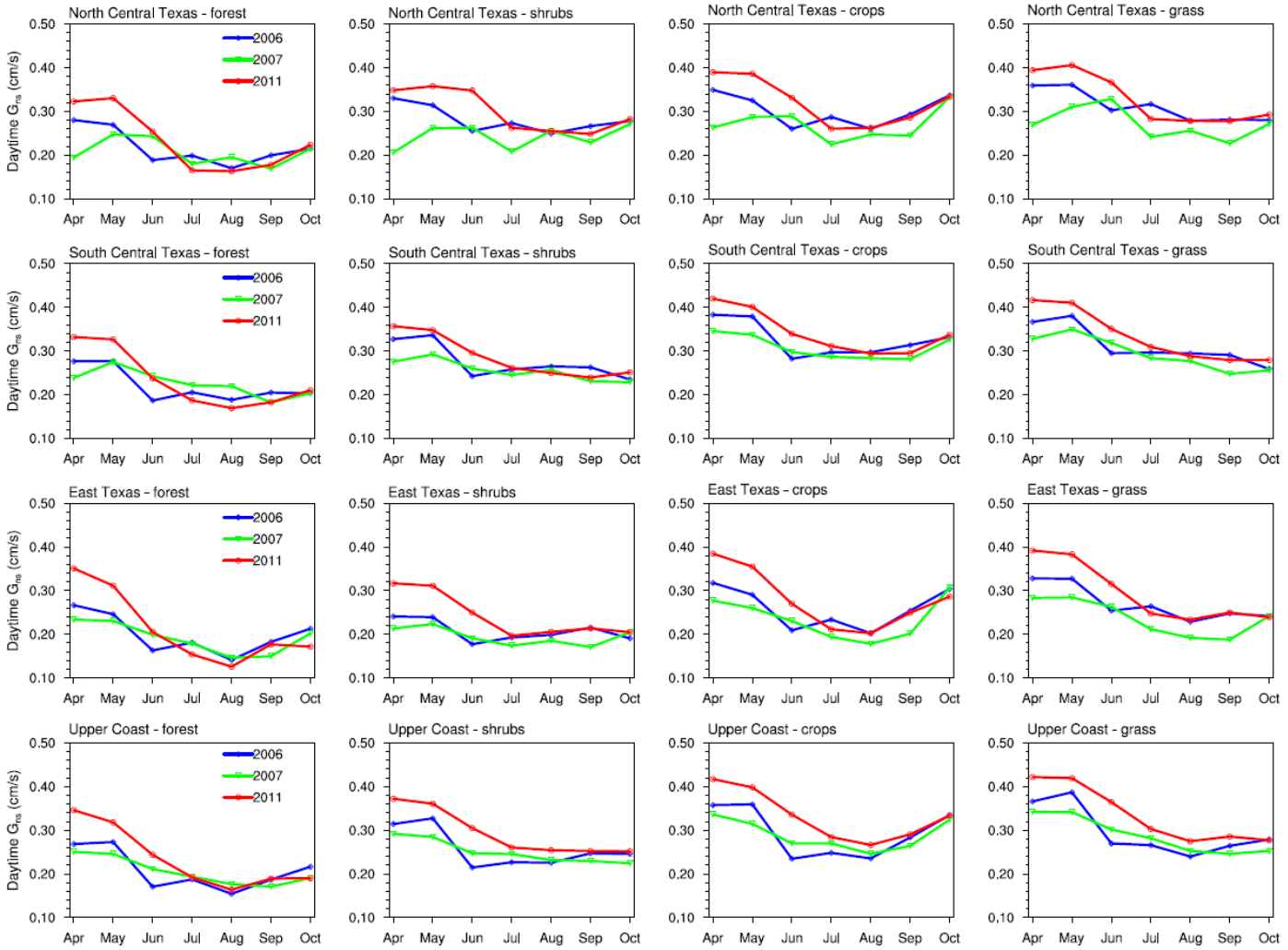

Figure E-2: Monthly averaged ozone daytime non-stomatal conductances G_{ns} (cm/s) by climate region and land cover category during April-October of 2006, 2007 and 2011.

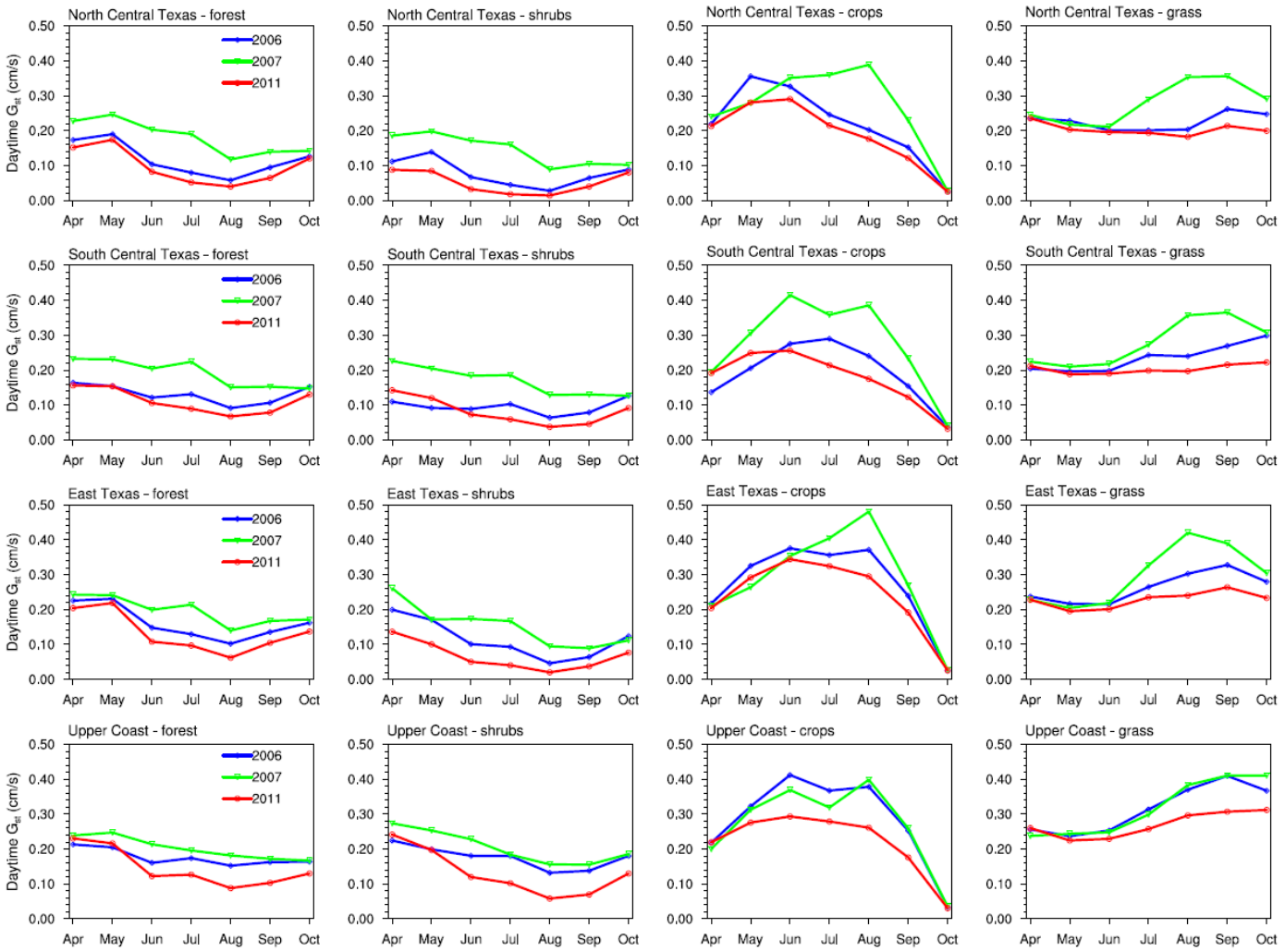

Figure E-3: Monthly averaged ozone daytime stomatal conductances G_{st} (cm/s) by climate region and land cover category during April-October of 2006, 2007 and 2011.

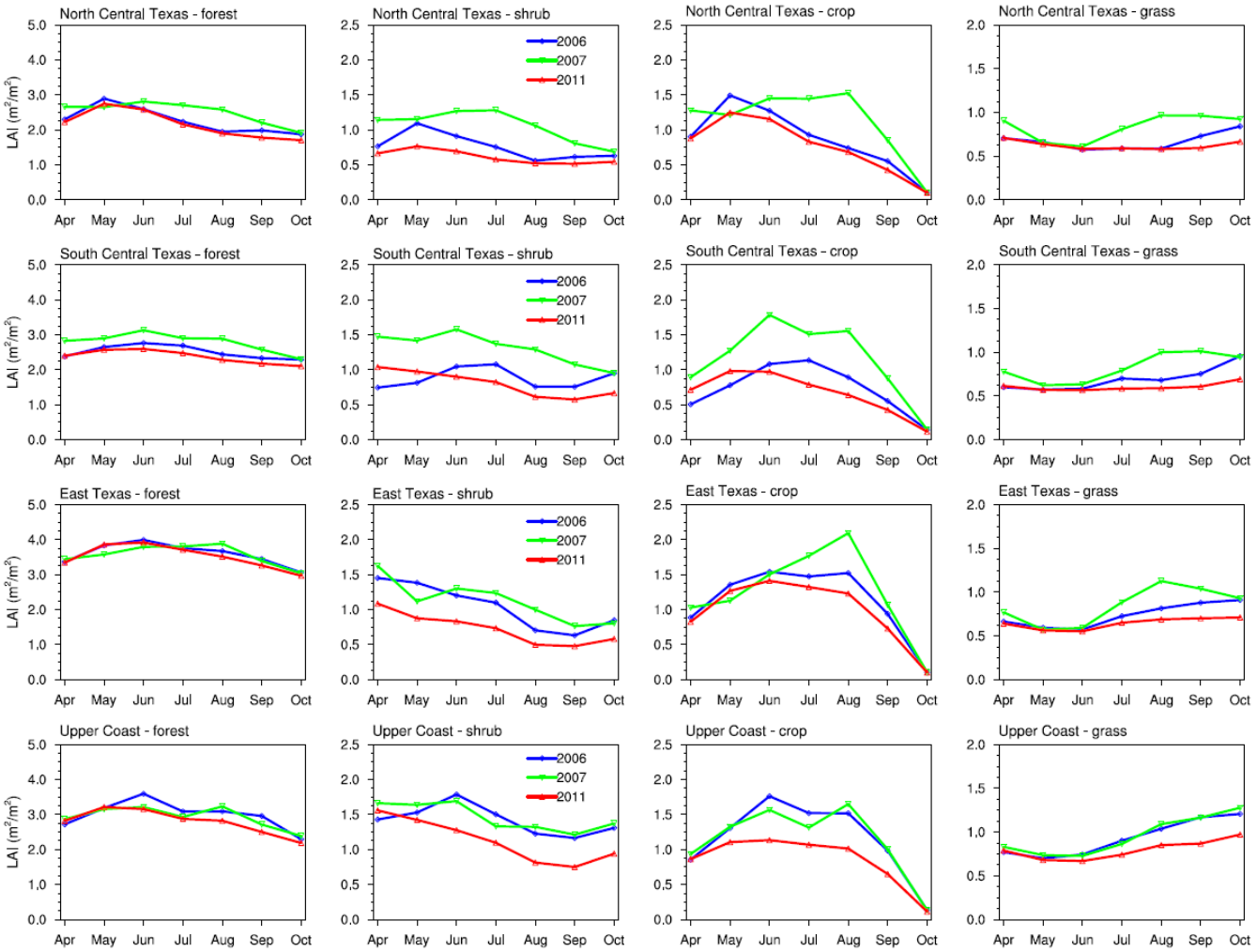

Figure E-4: Monthly averaged LAI (m^2/m^2) by climate region and land cover category during April-October of 2006, 2007 and 2011.

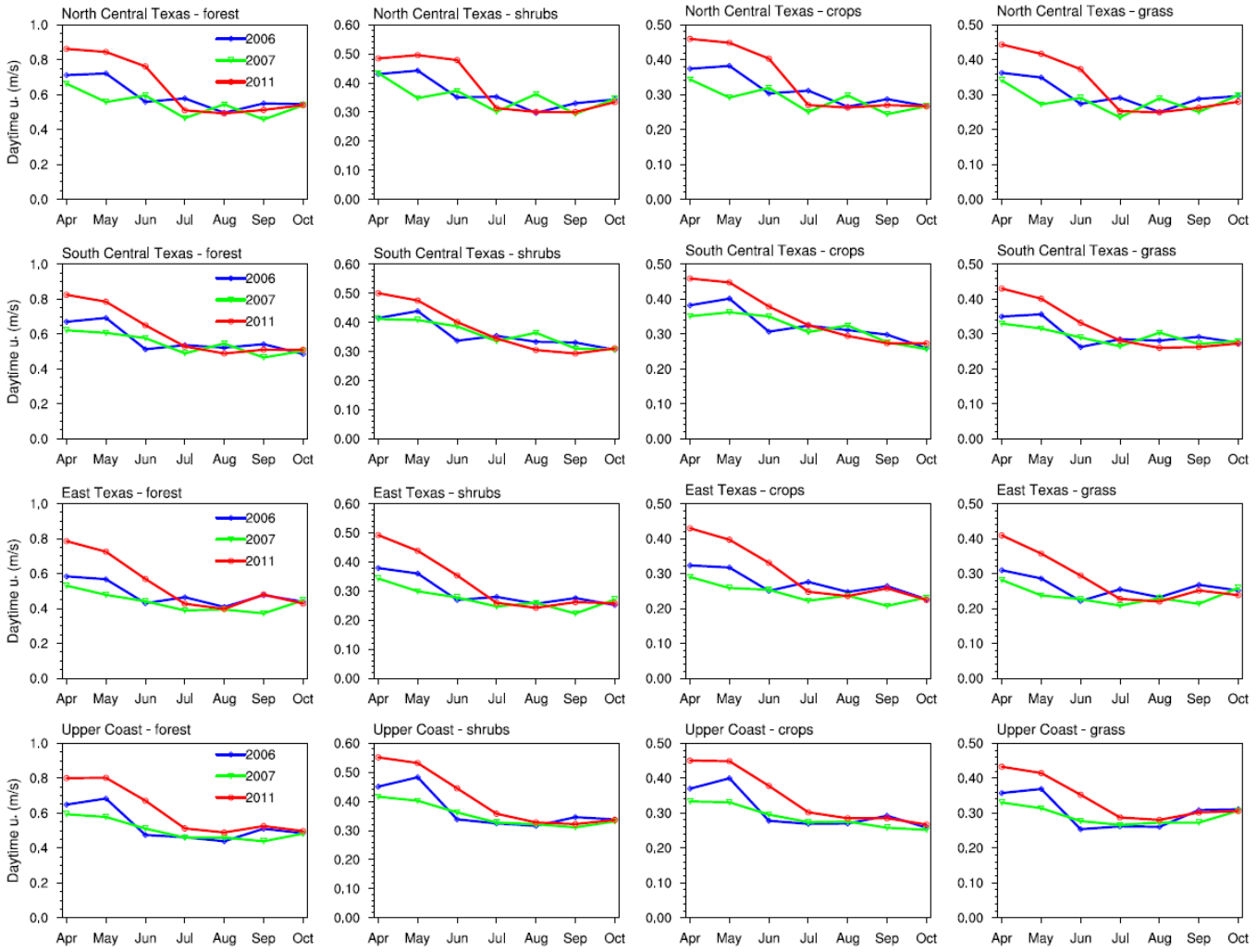

Figure E-5: Monthly averaged friction velocities (u_*, m/s) by climate region and land cover category during April-October of 2006, 2007 and 2011.

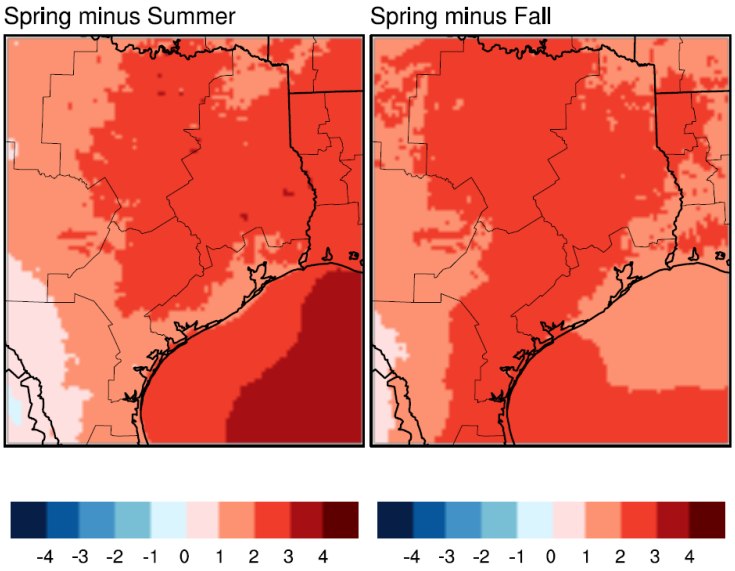

Figure E-6: Spatial distribution of differences in seasonal mean daytime wind speeds (m/s) over eastern Texas during 2011.

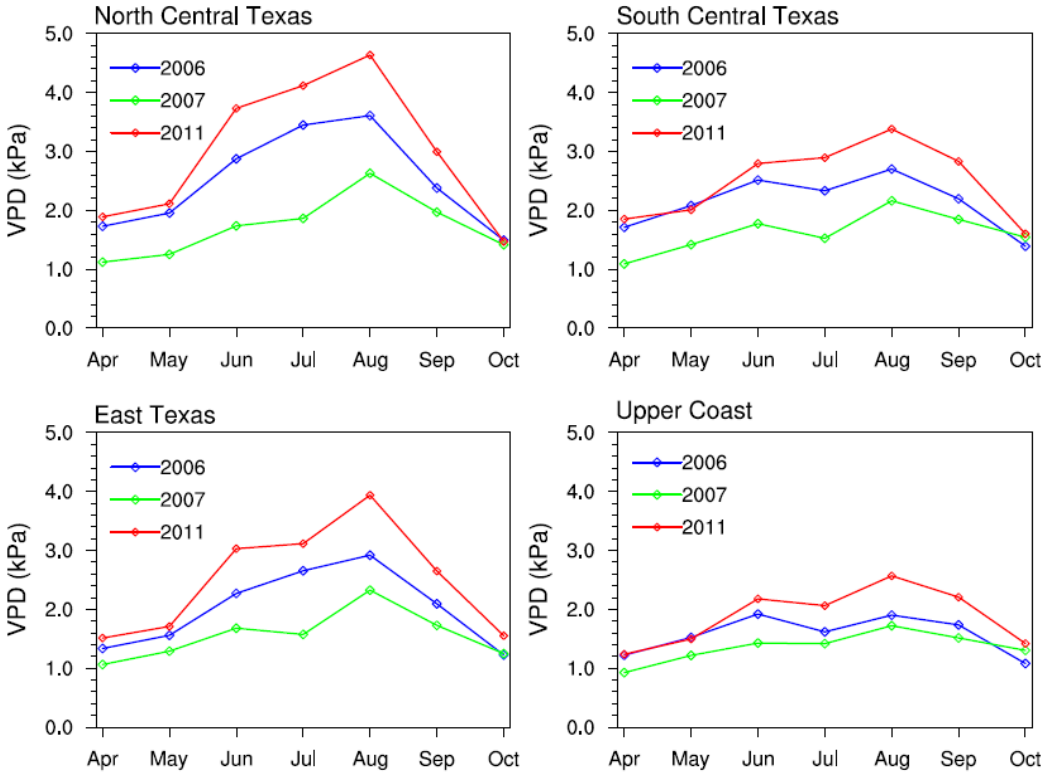

Figure E-7: Monthly averaged daytime vapor pressure deficits (VPD, in kPa) by climate region.

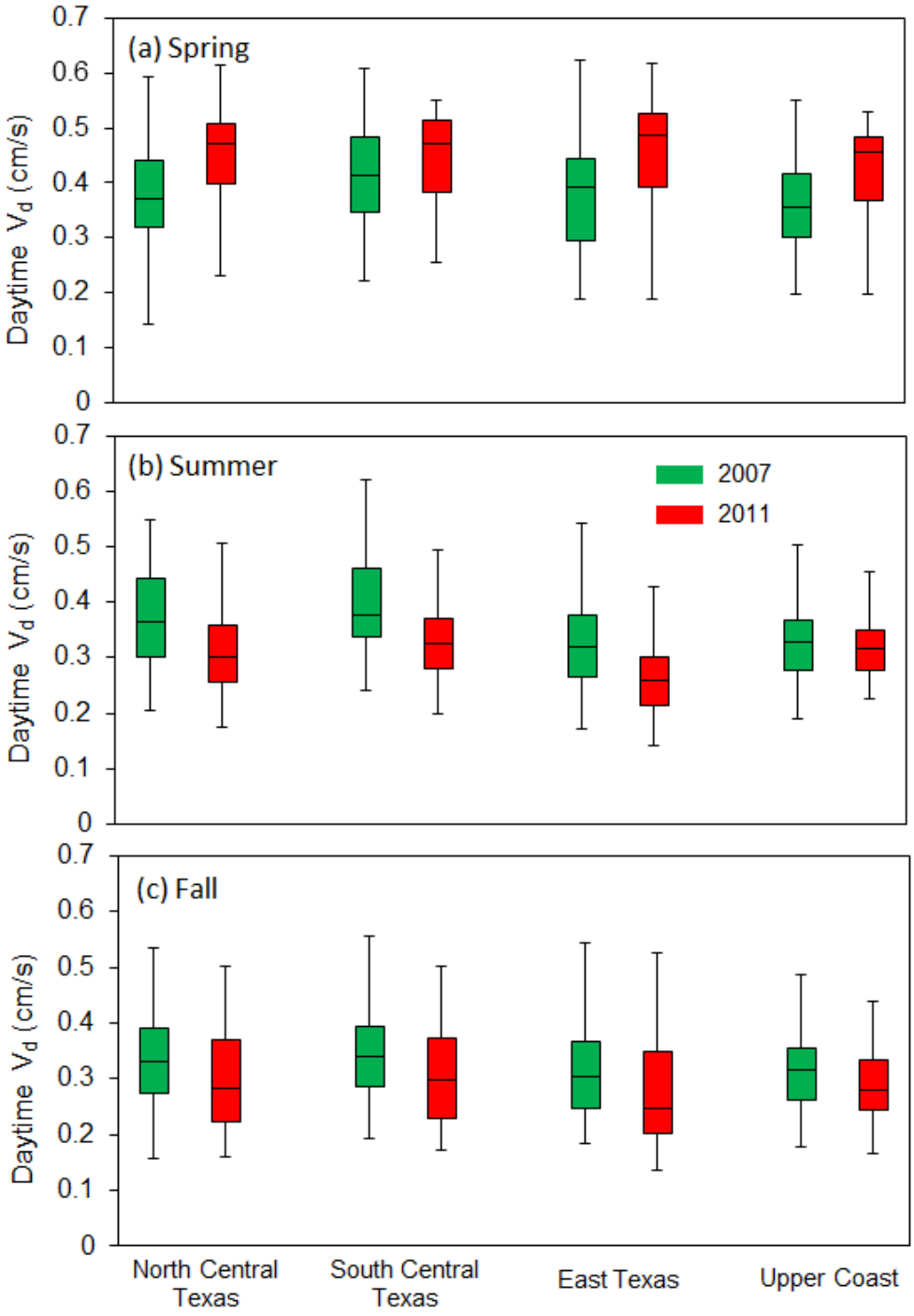

Figure E-8: Box and whisker plot of seasonal- and area-averaged daytime V_d during 2007 and 2011 by climate region. The box represents the 25th and 75th quartiles with the central horizontal line as the median value. The top and bottom whiskers extend to minimum and maximum values.

Appendix F: Supporting information for Chapter 7

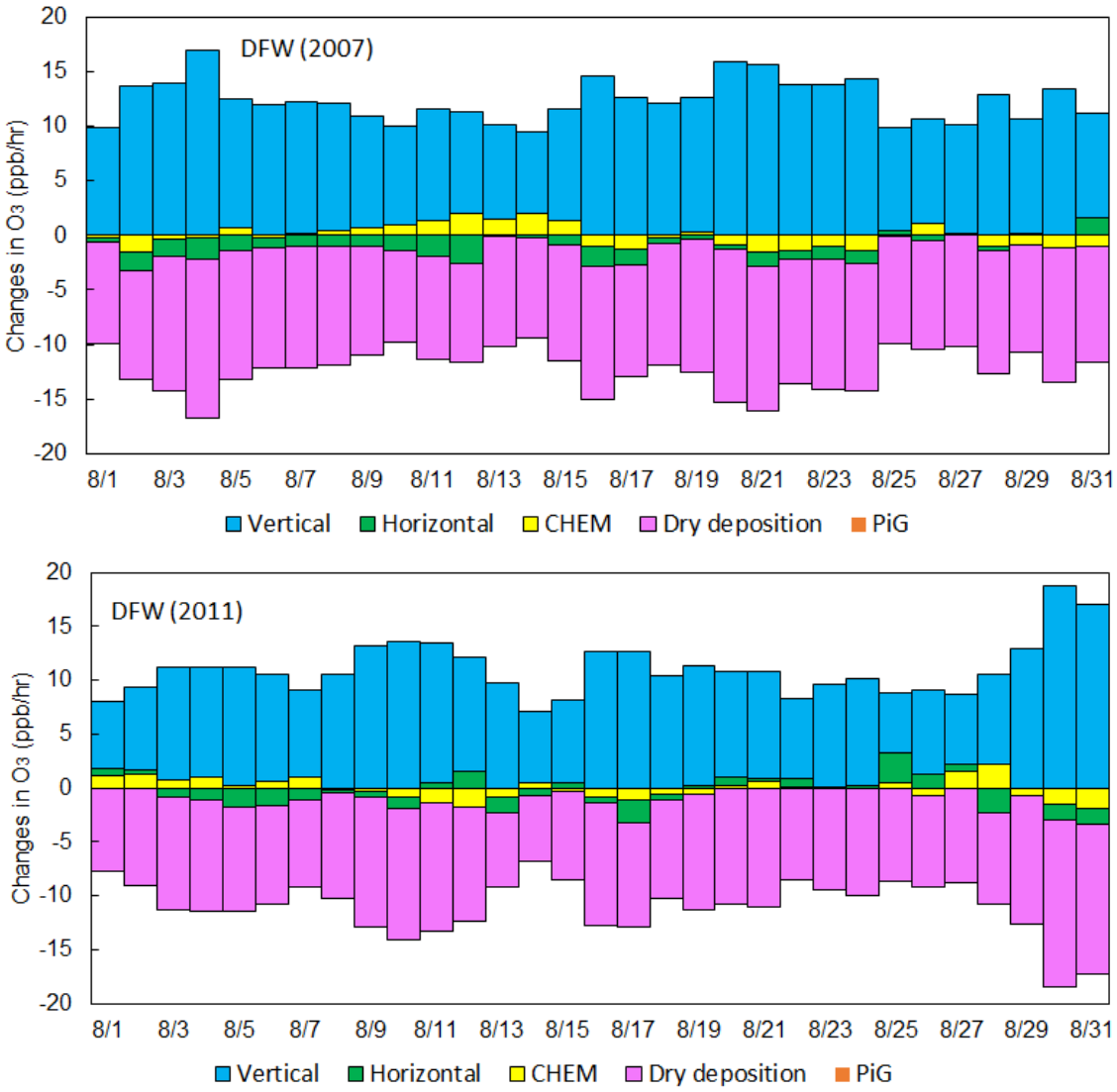

Figure F-1: Daily-mean hourly contributions of vertical transport, horizontal transport, chemistry (CHEM), dry deposition, and Plume-in-Grid change (PiG) over Dallas/Fort Worth (DFW) during August 2007 (upper) and 2011 (bottom).

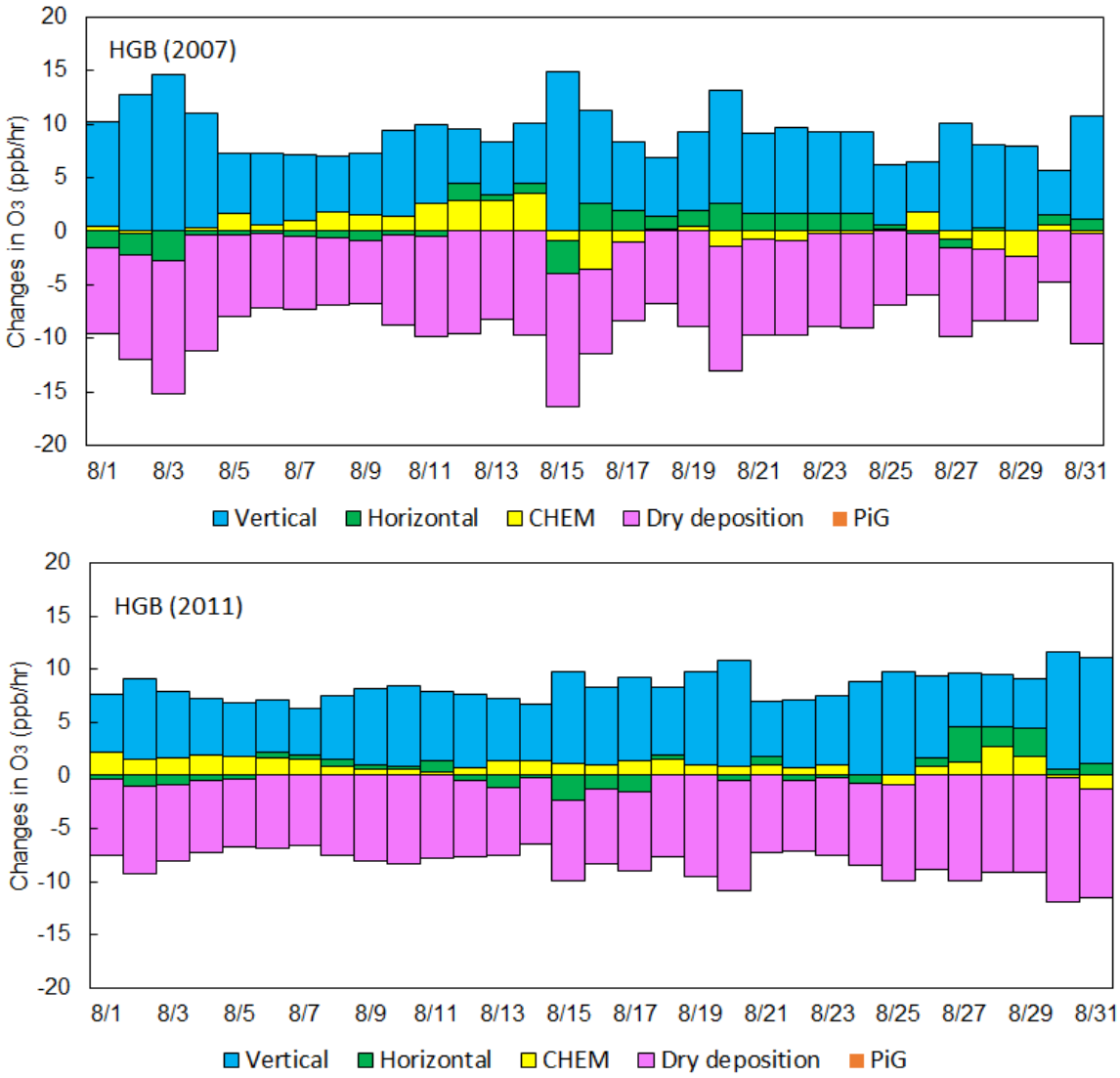

Figure F-2: Daily-mean hourly contributions of vertical transport, horizontal transport, chemistry (CHEM), dry deposition, and Plume-in-Grid change (PiG) over Houston/Galveston/ Brazoria (HGB) during August 2007 (upper) and 2011 (bottom).

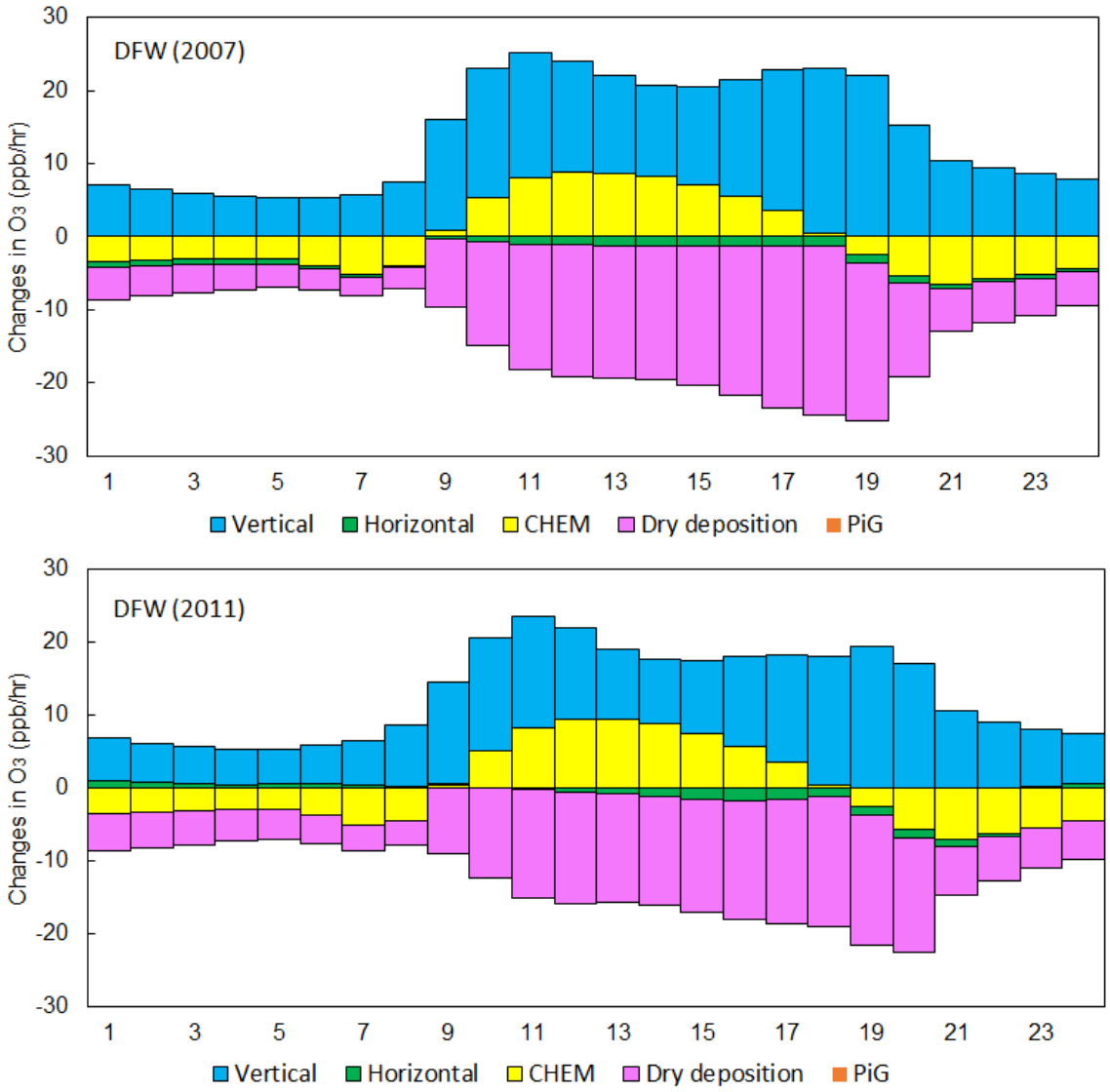

Figure F-3: Diurnal profile of monthly-mean contributions of vertical transport, horizontal transport, chemistry (CHEM), dry deposition, and Plume-in-Grid change (PiG) over Dallas/Fort Worth (DFW) during August 2007 (upper) and 2011 (bottom).

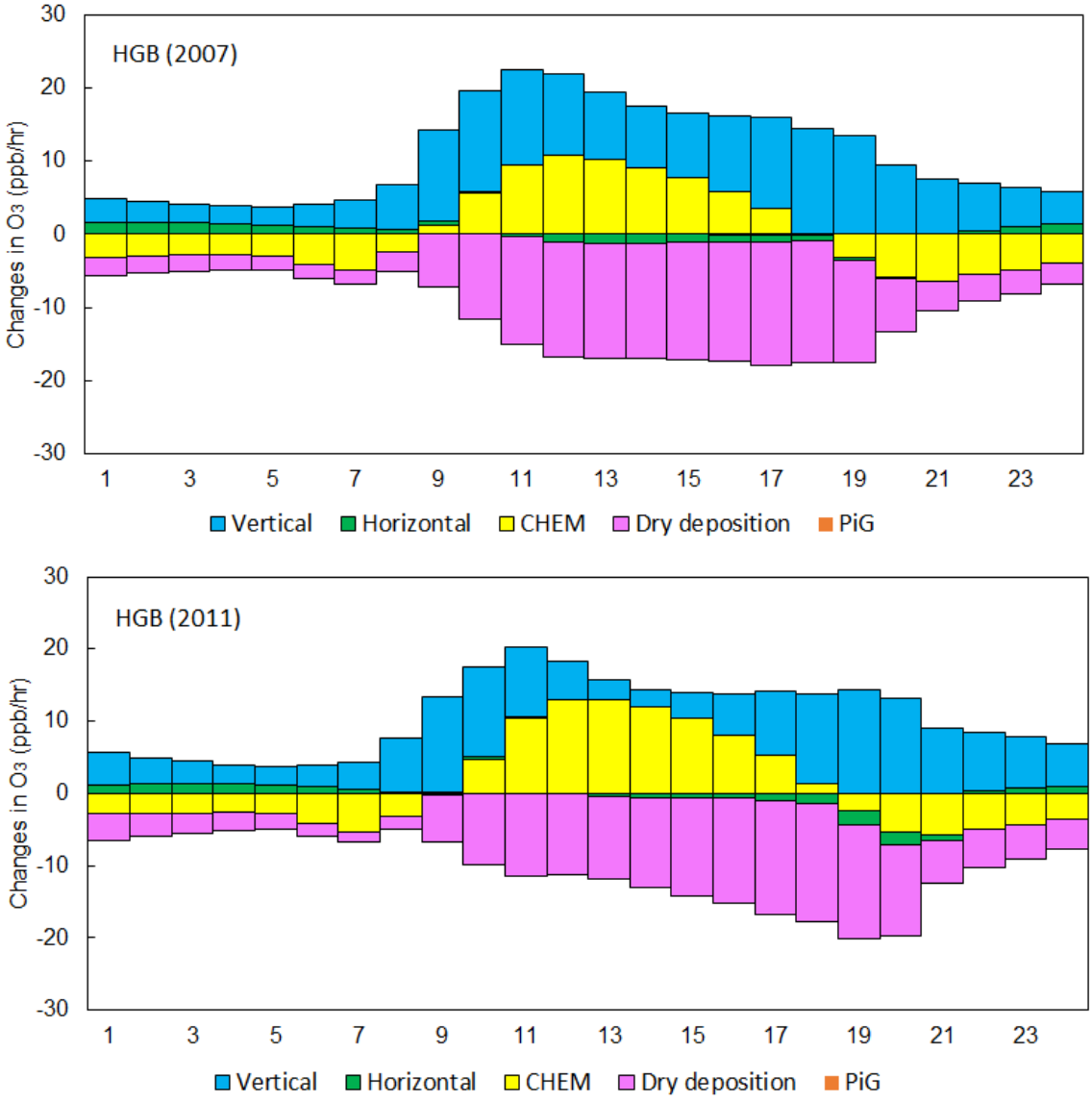

Figure F-4: Diurnal profile of monthly-mean contributions of vertical transport, horizontal transport, chemistry (CHEM), dry deposition, and Plume-in-Grid change (PiG) over Houston/Galveston/ Brazoria (HGB) during August 2007 (upper) and 2011 (bottom).

References

Abbot, D. S., Palmer, P. I., Martin, R. V., Chance, K. V., & Jacob, D. J. (2003). Seasonal and interannual variability of North American isoprene emissions as determined by formaldehyde column measurements from space. *Geophysical Research Letters*, *30*(17). doi:10.1029/2003GL017336

Adams, H. D., Macalady, A. K., Breshears, D. D., Allen, C. D., Stephenson, N. L., Saleska, S. R., & Huxman, T. E. (2010). Climate-Induced Tree Mortality: Earth System Consequences. *Eos, Transactions American Geophysical Union*, *91*(17), 153-154.

Ainsworth, E. A., & Rogers, A. (2007). The response of photosynthesis and stomatal conductance to rising [CO_2]: mechanisms and environmental interactions. *Plant, Cell & Environment*, *30*(3), 258-270.

Allen, C. D., & Breshears, D. D. (2007). Climate-induced forest dieback as an emergent global phenomenon. *Eos, Transactions American Geophysical Union*, *88*(47), 504.

Allen, C. D., Macalady, A. K., Chenchouni, H., Bachelet, D., McDowell, N., Vennetier, M., … Cobb, N. (2010). A global overview of drought and heat-induced tree mortality reveals emerging climate change risks for forests. *Forest Ecology and Management*, *259*(4), 660–684. doi:10.1016/j.foreco.2009.09.001

Alley, W. M. (1984). The Palmer drought severity index: limitations and assumptions. *J. Climate Appl. Meteorol.*, 23(7), pp. 1100-1109

Alonso, R., Elvira, S., González-Fernández, I., Calvete, H., García-Gómez, H., & Bermejo, V. (2014). Drought stress does not protect Quercus ilex L. from ozone effects: results from a comparative study of two subspecies differing in ozone sensitivity. *Plant Biology*, *16*(2), 375-384.

Altimir, N., Kolari, P., Tuovinen, J. P., Vesala, T., Bäck, J., Suni, T., & Hari, P. (2006). Foliage surface ozone deposition: a role for surface moisture? *Biogeosciences Discussions*, *2*(6), 1739-1793.

American Meteorological Society (AMS). (1997). Meteorological drought—policy statement. *Bullutin of the American Meteorological Society*, *78*, 847–849. Retrieved from http://www.ametsoc.org/policy/drought2.html

Anderson, M. C., & Kustas, W. P. (2008). Mapping evapotranspiration and drought at local to continental scales with a thermal-based surface energy balance model. In *Meeting Abstract*.

Anderegg, W. R., Berry, J. A., Smith, D. D., Sperry, J. S., Anderegg, L. D., & Field, C. B. (2012). The roles of hydraulic and carbon stress in a widespread climate-induced forest die-off. *Proceedings of the National Academy of Sciences*, *109*(1), 233-237.

Andreae, M. O., & Crutzen, P. J. (1997). Atmospheric aerosols: Biogeochemical sources and role in atmospheric chemistry. *Science*, *276*(5315), 1052-1058.

Arneth, A., Schurgers, G., Lathiere, J., Duhl, T., Beerling, D. J., Hewitt, C. N., ... & Guenther, A. (2011). Global terrestrial isoprene emission models: sensitivity to variability in climate and vegetation. *Atmospheric Chemistry and Physics*, *11*(15), 8037-8052.

Ashmore, M. R. (2002). Effects of oxidants at the whole plant and community level. *Air Pollution and Plant Life*, 89-118. John Wiley, Chichester, UK

Ashmore, M. R. (2005). Assessing the future global impacts of ozone on vegetation. *Plant, Cell & Environment*, *28*(8), 949-964.

Ashworth, K., Boissard, C., Folberth, G., Lathière, J., & Schurgers, G. (2013). Global modelling of volatile organic compound emissions. In *Biology, controls and models of tree volatile organic compound emissions* (pp. 451-487). Springer Netherlands.

Atkinson, R. (2000). Atmospheric chemistry of VOCs and NO_x. *Atmospheric Environment*, *34*(12), 2063-2101.

Atkinson, R., & Arey, J. (2003). Gas-phase tropospheric chemistry of biogenic volatile organic compounds: a review. *Atmospheric Environment*, *37*, 197-219.

Bayarjargal, Y., Karnieli, A, Bayasgalan, M., Khudulmur, S., Gandush, C., & Tucker, C. (2006). A comparative study of NOAA–AVHRR derived drought indices using change vector analysis. *Remote Sensing of Environment*, *105*(1), 9–22. doi:10.1016/j.rse.2006.06.003

Beckett, M., Loreto, F., Velikova, V., Brunetti, C., Di Ferdinando, M., Tattini, M., ... & Farrant, J. M. (2012). Photosynthetic limitations and volatile and non-volatile isoprenoids in the poikilochlorophyllous resurrection plant Xerophyta humilis during dehydration and rehydration. *Plant, cell & environment*, *35*(12), 2061-2074.

Bergamaschi, P., Hein, R., Heimann, M., & Crutzen, P. J. (2000). Inverse modeling of the global CO cycle: 1. Inversion of CO mixing ratios. *Journal of Geophysical Research: Atmospheres (1984–2012)*, *105*(D2), 1909-1927.

Biswas, D. K., & Jiang, G. M. (2011). Differential drought-induced modulation of ozone tolerance in winter wheat species. *Journal of Experimental Botany*, doi: 10.1093/jxb/err104

Bohler, S., Cuypers, A., & Vangronsveld, J. (2015). *Combined Stresses in Plants.* (pp. 147–157). Springer International Publishing.

Bohler, S., Sergeant, K., Jolivet, Y., Hoffmann, L., Hausman, J. F., Dizengremel, P., & Renaut, J. (2013). A physiological and proteomic study of poplar leaves during ozone exposure combined with mild drought. *Proteomics*,*13*(10-11), 1737-1754.

Bonan, G. B., Oleson, K.W., Vertenstein, M., Levis, S., Zeng, X., Dai, Y., & Yang, Z.L. (2002). The land surface climatology of the community land model coupled to the NCAR community climate model. *Journal of Climate*, *15*(22), 3123–3149.

Bond, N. R., Lake, P. S., & Arthington, A. H. (2008). The impacts of drought on freshwater ecosystems: an Australian perspective. *Hydrobiologia*, *600*(1), 3–16. doi:10.1007/s10750-008-9326-z

Brantley, S. T., Zinnert, J. C., & Young, D. R. (2011). Application of hyperspectral vegetation indices to detect variations in high leaf area index temperate shrub thicket canopies. *Remote Sensing of Environment*, *115*(2), 514–523. doi:10.1016/j.rse.2010.09.020

Brasseur, G. P., Hauglustaine, D. A., Walters, S., Rasch, P. J., Müller, J. F., Granier, C., & Tie, X. X. (1998). MOZART, a global chemical transport model for ozone and related chemical tracers: 1. Model description. *Journal of Geophysical Research*: *Atmospheres* (1984–2012), 103(D21), 28265-28289.

Breshears, D. D., Cobb, N. S., Rich, P. M., Price, K. P., Allen, C. D., Balice, R. G., … Meyer, C. W. (2005). Regional vegetation die-off in response to global-change-type drought. *Proceedings of the National Academy of Sciences of the United States of America*, 102, 15144–15148. doi:10.1073/pnas.0505734102

Brilli, F., Barta, C., Fortunati, A., Lerdau, M., Loreto, F., & Centritto, M. (2007). Response of isoprene emission and carbon metabolism to drought in white poplar (*Populus alba*) saplings. *New Phytologist*, *175*(2), 244-254.

Brook, R. D., Brook, J. R., Urch, B., Vincent, R., Rajagopalan, S., & Silverman, F. (2002). Inhalation of fine particulate air pollution and ozone causes acute arterial vasoconstriction in healthy adults. *Circulation*, 105(13), 1534-1536.

Brüggemann, N., & Schnitzler, J. P. (2002). Comparison of isoprene emission, intercellular isoprene concentration and photosynthetic performance in water-limited

oak (*Quercus pubescens* Willd. and *Quercus robur* L.) saplings. *Plant Biology*, *4*(4), 456-463.

Buermann, W., Wang, Y., Dong, J., Zhou, L., Zeng, X., Dickinson, R. E., ... & Myneni, R. B. (2002). Analysis of a multiyear global vegetation leaf area index data set. *Journal of Geophysical Research: Atmospheres (1984–2012)*,*107*(D22), ACL-14.

Burnash, R. J. C., Ferral, R. L., & McGuire, R. A. (1973), A generalized streamflow simulation system: Conceptual models for digital computer. Technical report, joint Federal-State River Forecast Center, Sacramento, Calif.

Byun, D. W., Kim, S., Czader, B., Nowak, D., Stetson, S., & Estes, M. (2005). Estimation of biogenic emissions with satellite-derived land use and land cover data for air quality modeling of Houston-Galveston ozone nonattainment area.*Journal of environmental management*, *75*(4), 285-301.

Byun, H. R., & Wilhite, D. A. (1999). Objective quantification of drought severity and duration. *Journal of Climate*, *12*(9), 2747-2756.

Cai, X., Yang, Z. L., David, C. H., Niu, G. Y., & Rodell, M. (2014a). Hydrological evaluation of the Noah-MP land surface model for the Mississippi River Basin. *Journal of Geophysical Research: Atmospheres*.119, doi:10.1002/2013JD020792

Cai, X., Yang, Z.-L., Xia, Y., Huang, M., Wei, H., Leung, L. R. & Ek, M. B. (2014b). Assessment of simulated water balance from Noah, Noah-MP, CLM, and VIC over CONUS using the NLDAS test bed. *Journal of Geophysical Research: Atmospheres*, *119*.

Cape, J. N., Hamilton, R., & Heal, M. R. (2009). Reactive uptake of ozone at simulated leaf surfaces: implications for 'non-stomatal'ozone flux. *Atmospheric Environment*, *43*(5), 1116-1123.

Carlton, A. G., Wiedinmyer, C., & Kroll, J. H. (2009). A review of Secondary Organic Aerosol (SOA) formation from isoprene. *Atmospheric Chemistry and Physics*, *9*(14), 4987-5005.

Centritto, M., Brilli, F., Fodale, R., & Loreto, F. (2011). Different sensitivity of isoprene emission, respiration and photosynthesis to high growth temperature coupled with drought stress in black poplar (*Populus nigra*) saplings. *Tree Physiology*, tpq112.

Chameides, W. L., Lindsay, R. W., Richardson, J., & Kiang, C. S. (1988). The role of biogenic hydrocarbons in urban photochemical smog: Atlanta as a case study. *Science*, *241*(4872), 1473-1475.

Chavez-Figueroa, E. M., Cohan, D. S., Aghedo, A. M., Lash, B., Bi, J., & Myneni, R. (October, 2012). Impact of vegetation variability on biogenic emissions. Unpublished paper presented at the 11th Annual CMAS Conference, Chapel Hill, NC.

Chen, J., Avise, J., Guenther, A., Wiedinmyer, C., Salathe, E., Jackson, R. B., & Lamb, B. (2009). Future land use and land cover influences on regional biogenic emissions and air quality in the United States. *Atmospheric Environment*, *43*(36), 5771-5780.

Chen, F., & Dudhia, J. (2001). Coupling an advanced land surface-hydrology model with the Penn State-NCAR MM5 modeling system. Part I: Model implementation and sensitivity. *Monthly Weather Review*, *129*(4), 569-585.

Cieslik, S. A. (2004). Ozone uptake by various surface types: a comparison between dose and exposure. *Atmospheric Environment*, *38*(15), 2409-2420.

Claeys, M., Graham, B., Vas, G., Wang, W., Vermeylen, R., Pashynska, V., … Maenhaut, W. (2004). Formation of secondary organic aerosols through photooxidation of isoprene. *Science*, *303*(5661), 1173-1176.

Clarke, J. F., Edgerton, E. S., & Martin, B. E. (1997). Dry deposition calculations for the clean air status and trends network. *Atmospheric Environment*, *31*(21), 3667–3678.

Cohen, W. B., Maiersperger, T. K., Turner, D. P., Ritts, W. D., Pflugmacher, D., Kennedy, R. E., ... & Gower, S. T. (2006). MODIS land cover and LAI collection 4 product quality across nine sites in the western hemisphere.*Geoscience and Remote Sensing, IEEE Transactions on*, *44*(7), 1843-1857.

Curci, G., Beekmann, M., Vautard, R., Smiatek, G., Steinbrecher, R., Theloke, J., & Friedrich, R. (2009). Modelling study of the impact of isoprene and terpene biogenic emissions on European ozone levels. *Atmospheric Environment*, *43*(7), 1444-1455.

Dai, A. (2011). Drought under global warming: a review. *Wiley Interdisciplinary Reviews: Climate Change*, *2*(1), 45–65. doi:10.1002/wcc.81

Dai, A. (2013). Increasing drought under global warming in observations and models. *Nature Climate Change*, *3*(1), 52-58.

De Kauwe, M. G., Disney, M. I., Quaife, T., Lewis, P., & Williams, M. (2011). An assessment of the MODIS collection 5 leaf area index product for a region of mixed coniferous forest. *Remote Sensing of Environment*, *115*(2), 767–780. doi:10.1016/j.rse.2010.11.004

Dockery, D. W., Pope, C. A., Xu, X., Spengler, J. D., Ware, J. H., Fay, M. E., … Speizer, F. E. (1993). An association between air pollution and mortality in six US cities. *New England Journal of Medicine*, *329*(24), 1753-1759.

Drewniak, B. A., Snyder, P. K., Steiner, A. L., Twine, T. E., & Wuebbles, D. J. (2014). Simulated changes in biogenic VOC emissions and ozone formation from habitat expansion of Acer Rubrum (red maple). *Environmental Research Letters*, *9*(1), 014006.

Duncan, B. N., Yoshida, Y., Damon, M. R., Douglass, A. R., & Witte, J. C. (2009). Temperature dependence of factors controlling isoprene emissions. *Geophysical Research Letters*, *36*(5), L05813.

Ek, M. B., Mitchell, K. E., Lin, Y., Rogers, E., Grunmann, P., Koren, V., ... & Tarpley, J. D. (2003). Implementation of Noah land surface model advances in the National Centers for Environmental Prediction operational mesoscale Eta model. *Journal of Geophysical Research: Atmospheres (1984–2012)*, *108*(D22).

Emberson, L. D., Büker, P., Ashmore, M. R., Mills, G., Jackson, L. S., Agrawal, M., ... & Wahid, A. (2009). A comparison of North American and Asian exposure–response data for ozone effects on crop yields. *Atmospheric Environment*, *43*(12), 1945-1953.

Emberson, L. D., Kitwiroon, N., Beevers, S., Büker, P., & Cinderby, S. (2013). Scorched Earth: how will changes in the strength of the vegetation sink to ozone deposition affect human health and ecosystems? *Atmospheric Chemistry and Physics*, *13*(14), 6741-6755.

Emery, C., Tai, E., & Yarwood, G. (2001). "Enhanced Meteorological Modeling and Performance Evaluation for Two Texas Ozone Episodes." Prepared for the Texas Natural Resource Conservation Commission, prepared by ENVIRON International Corporation, Novato, CA. 31-August. http://www.tceq.texas.gov/assets/public/implementation/air/am/contracts/reports/mm/EnhancedMetModelingAndPerformanceEvaluation.pdf

ENVIRON. (2014). User's guide Comprehensive Air Quality Model with Extension (CAMx), version 6.10. Retrieved April 17, 2015, from http://www.camx.com/files/camxusersguide_v6-10.txt

ENVIRON International Corporation (2011). Project status updates and isoprene comparisons from using different sources of PAR [PowerPoint Slides]. Retrieved February 19, 2014, from http://www.wrapair2.org/pdf/MGN210_sat_vs_wrf_DecCall14.Final2.ppt

EPA. (2013). 2008 National Emission Inventory, version 3 Technical Support Document Draft, Retrived July 8, 2015, from http://www.epa.gov/ttn/chief/net/2008neiv3/2008_neiv3_tsd_draft.pdf

EPA. (2014). 2011 National Emission Inventory, version 1 Technical Support Document Draft. Retrieved Febrary 19, 2015, from http://www.epa.gov/ttn/chief/net/2011nei/2011_nei_tsdv1_draft2_june2014.pdf

Fang, C., Monson, R. K., & Cowling, E. B. (1996). Isoprene emission, photosynthesis, and growth in sweetgum (*Liquidambar styraciflua*) seedlings exposed to short-and long-term drying cycles. *Tree Physiology*, *16*(4), 441-446.

Fang, H., Jiang, C., Li, W., Wei, S., Baret, F., & Chen, J. M. (2013a). Characterization and intercomparison of global moderate resolution leaf area index (LAI) products: Analysis of climatologies and theoretical uncertainties. *Journal of Geophysical Research: Biogeosciences*, *118*, 1–20.

Fang, H., Li, W., & Myneni, R. (2013b). The impact of potential land cover misclassification on MODIS leaf area index (LAI) estimation: A statistical perspective. *Remote Sensing*, *5*(2), 830–844. doi:10.3390/rs5020830

Fang, X., & Pomeroy, J. W. (2008). Drought impacts on Canadian prairie wetland snow hydrology. *Hydrological Processes*, *22*(15), 2858–2873.

Fannin, B. (2011). Texas agricultural drought losses reach record $5.2 billion. *AgriLife Today*. Retrieved May 28, 2013, from http://today.agrilife.org/2011/08/17/texas-agricultural-drought-losses-reach-record-5-2-billion/

Fannin, B. (2012). Updated 2011 Texas agricultural drought losses total $7.62 billion. Retrieved July 5, 2015, from http://today.agrilife.org/2012/03/21/updated-2011-texas-agricultural-drought-losses-total-7-62-billion/

Fares, S., McKay, M., Holzinger, R., & Goldstein, A. H. (2010). Ozone fluxes in a Pinus ponderosa ecosystem are dominated by non-stomatal processes: evidence from long-term continuous measurements. *Agricultural and Forest Meteorology*, *150*(3), 420-431.

Fares, S., Savi, F., Muller, J., Matteucci, G., & Paoletti, E. (2014). Simultaneous measurements of above and below canopy ozone fluxes help partitioning ozone deposition between its various sinks in a Mediterranean Oak Forest. *Agricultural and Forest Meteorology*, 198-199, 181–191. doi:10.1016/j.agrformet.2014.08.014

Fares, S., Vargas, R., Detto, M., Goldstein, A. H., Karlik, J., Paoletti, E., & Vitale, M. (2013). Tropospheric ozone reduces carbon assimilation in trees: estimates from

analysis of continuous flux measurements. *Global Change Biology*, *19*(8), 2427–43. doi:10.1111/gcb.12222

Fares, S., Weber, R., Park, J.-H., Gentner, D., Karlik, J., & Goldstein, A. H. (2012). Ozone deposition to an orange orchard: Partitioning between stomatal and non-stomatal sinks. *Environmental Pollution*, *169*, 258–266. doi:10.1016/j.envpol.2012.01.030

Fehsenfeld, F., Calvert, J., Fall, R., Goldan, P., Guenther, A. B., Hewitt, C. N., ... & Zimmerman, P. (1992). Emissions of volatile organic compounds from vegetation and the implications for atmospheric chemistry. *Global Biogeochemical Cycles*, *6*(4), 389-430.

Fensham, R. J., Fairfax, R. J., & Ward, D. P. (2008). Drought-induced tree death in savanna. *Global Change Biology*, *15*(2), 380–387.

Ferreira, J., Reeves, C. E., Murphy, J. G., Garcia-Carreras, L., Parker, D. J., & Oram, D. E. (2010). Isoprene emissions modelling for West Africa: MEGAN model evaluation and sensitivity analysis. *Atmospheric Chemistry and Physics*,*10*(17), 8453-8467.

Finkelstein, P. L., Ellestad, T. G., Clarke, J. F., Meyers, T. P., Schwede, D. B., Hebert, E. O., & Neal, J. A. (2000). Ozone and sulfur dioxide dry deposition to forests: Observations and model evaluation. *Journal of Geophysical Research: Atmospheres (1984–2012)*, *105*(D12), 15365-15377.

Fischbach, R. J., Staudt, M., Zimmer, I., Rambal, S., & Schnitzler, J. P. (2002). Seasonal pattern of monoterpene synthase activities in leaves of the evergreen tree Quercus ilex. *Physiologia Plantarum*, *114*(3), 354-360.

Fortunati, A., Barta, C., Brilli, F., Centritto, M., Zimmer, I., Schnitzler, J. P., & Loreto, F. (2008). Isoprene emission is not temperature-dependent during and after severe drought-stress: a physiological and biochemical analysis. *The Plant Journal*, 55(4), 687-697.

Frédéric, A., & Volkmar, W. (2006). Impact of summer drought on forest biodiversity : what do we know ? *Annals of Forest Science*, *63*(6), 645–652.

Friedl, M. A., McIver, D. K., Hodges, J. C., Zhang, X. Y., Muchoney, D., Strahler, A. H., ... & Schaaf, C. (2002). Global land cover mapping from MODIS: algorithms and early results. *Remote Sensing of Environment*, *83*(1), 287-302.

Friedl, M. A., Sulla-Menashe, D., Tan, B., Schneider, A., Ramankutty, N., Sibley, A., & Huang, X. (2010). MODIS Collection 5 global land cover: Algorithm refinements

and characterization of new datasets. *Remote Sensing of Environment*, *114*(1), 168–182. doi:10.1016/j.rse.2009.08.016

Fu, Y., & Liao, H. (2012). Simulation of the interannual variations of biogenic emissions of volatile organic compounds in China: Impacts on tropospheric ozone and secondary organic aerosol. *Atmospheric Environment*, *59*, 170-185.

Fuhrer, J., & Booker, F. (2003). Ecological issues related to ozone: agricultural issues. *Environment International*, 29(2), 141-154.

Funk, J. L., Jones, C. G., Gray, D. W., Throop, H. L., Hyatt, L. A., & Lerdau, M. T. (2005). Variation in isoprene emission from *Quercus rubra*: sources, causes, and consequences for estimating fluxes. *Journal of Geophysical Research: Atmospheres (1984–2012)*, *110*(D4).

Geist, H. J., & Lambin, E. F. (2002). Proximate Causes and Underlying Driving Forces of Tropical Deforestation Tropical forests are disappearing as the result of many pressures, both local and regional, acting in various combinations in different geographical locations. *BioScience*, *52*(2), 143-150.

Geng, F., Tie, X., Guenther, A., Li, G., Cao, J., & Harley, P. (2011). Effect of isoprene emissions from major forests on ozone formation in the city of Shanghai, China. *Atmospheric Chemistry and Physics*, *11*(20), 10449-10459.

Gerosa, G., Vitale, M., Finco, A., Manes, F., Denti, A. B., & Cieslik, S. (2005). Ozone uptake by an evergreen Mediterranean forest (Quercus ilex) in Italy. Part I: Micrometeorological flux measurements and flux partitioning. *Atmospheric Environment*, *39*(18), 3255-3266.

Goldstein, A. H., McKay, M., Kurpius, M. R., Schade, G. W., Lee, A., Holzinger, R., & Rasmussen, R. A. (2004). Forest thinning experiment confirms ozone deposition to forest canopy is dominated by reaction with biogenic VOCs. *Geophysical research letters*, *31*(22).

Gryparis, A., Forsberg, B., Katsouyanni, K., Analitis, A., Touloumi, G., Schwartz, J., ... & Dörtbudak, Z. (2004). Acute effects of ozone on mortality from the "air pollution and health: a European approach" project. *American journal of respiratory and critical care medicine*, *170*(10), 1080-1087.

Guenther, A., Geron, C., Pierce, T., Lamb, B., Harley, P., & Fall, R. (2000). Natural emissions of non-methane volatile organic compounds, carbon monoxide, and oxides of nitrogen from North America. *Atmospheric Environment*, *34*(12), 2205-2230.

Guenther, A., Hewitt, C. N., Erickson, D., Fall, R., Geron, C., Graedel, T., ... & Zimmerman, P. (1995). A global model of natural volatile organic compound emissions. *Journal of Geophysical Research: Atmospheres (1984–2012),100*(D5), 8873-8892.

Guenther, A. B., Jiang, X., Heald, C. L., Sakulyanontvittaya, T., Duhl, T., Emmons, L. K., & Wang, X. (2012). The Model of Emissions of Gases and Aerosols from Nature version 2.1 (MEGAN2. 1): an extended and updated framework for modeling biogenic emissions, *Geoscientific Model Development Discussions*, 5, 1503-1560.

Guenther, A., Karl, T., Harley, P., Wiedinmyer, C., Palmer, P. I., & Geron, C. (2006). Estimates of global terrestrial isoprene emissions using MEGAN (Model of Emissions of Gases and Aerosols from Nature). *Atmospheric Chemistry and Physics*, *6*(11), 3181-3210.

Guenther, A., & Sakulyanontvittaya, T. (2011). Improved biogenic emission inventories across the West. Retrieved Februray 19, 2014, from http://www.wrapair2.org/pdf/WGA_Task1_TechnicalAnalysisReport_ImprovedBiogenicEmissionInventories.pdf

Guenther, A., Zimmerman, P., & Wildermuth, M. (1994). Natural volatile organic compound emission rate estimates for US woodland landscapes. *Atmospheric Environment*, *28*(6), 1197-1210.

Gulden, L. E., Yang, Z. L., & Niu, G. Y. (2007). Interannual variation in biogenic emissions on a regional scale. *Journal of Geophysical Research*, *112*, D14103. doi:10.1029/2006JD008231

Han, K. M., Park, R. S., Kim, H. K., Woo, J. H., Kim, J., & Song, C. H. (2013). Uncertainty in biogenic isoprene emissions and its impacts on tropospheric chemistry in East Asia. *Science of The Total Environment*, *463*, 754-771.

Hardacre, C., Wild, O., & Emberson, L. (2015). An evaluation of ozone dry deposition in global scale chemistry climate models. *Atmospheric Chemistry and Physics*, *15*(11), 6419-6436.

Harper, C., Personal Communication, Nov. 2012

Hayes, M., Svoboda, M., & Wilhite, D. A. (2000). Monitoring Drought Using the Standardized Precipitation Index. *Drought: A Global Assessment* (pp. 168–180). London/New York: Taylor and Francis Group.

Heald, C. L., Henze, D. K., Horowitz, L. W., Feddema, J., Lamarque, J. F., Guenther, A., ... & Fung, I. (2008). Predicted change in global secondary organic aerosol

concentrations in response to future climate, emissions, and land use change. *Journal of Geophysical Research: Atmospheres (1984–2012)*,*113*(D5).

Heim Jr, R. R. (2002). A review of twentieth-century drought indices used in the United States. *Bulletin of the American Meteorological Society*, *83*(8), 1149-1165.

Heiskanen, J., Rautiainen, M., Stenberg, P., Mõttus, M., Vesanto, V.-H., Korhonen, L., & Majasalmi, T. (2012). Seasonal variation in MODIS LAI for a boreal forest area in Finland. *Remote Sensing of Environment*, *126*, 104–115. doi:10.1016/j.rse.2012.08.001

Hewitt, K. (1997). *Regions of risk: A geographical introduction to disasters* (pp. 189-213). Harlow: Longman.

Hoffmann, T., Odum, J. R., Bowman, F., Collins, D., Klockow, D., Flagan, R. C., & Seinfeld, J. H. (1997). Formation of organic aerosols from the oxidation of biogenic hydrocarbons. *Journal of Atmospheric Chemistry*,*26*(2), 189-222.

Hogg, A., Uddling, J., Ellsworth, D., Carroll, M. A., Pressley, S., Lamb, B., & Vogel, C. (2007). Stomatal and non-stomatal fluxes of ozone to a northern mixed hardwood forest. *Tellus B*, *59*(3), 514–525.

Hogrefe, C., Isukapalli, S. S., Tang, X., Georgopoulos, P. G., He, S., Zalewsky, E. E., ... & Sistla, G. (2011). Impact of biogenic emission uncertainties on the simulated response of ozone and fine particulate matter to anthropogenic emission reductions. *Journal of the Air & Waste Management Association*, *61*(1), 92-108.

Hogrefe, C., Werth, D., Avissar, R., Lynn, B., Rosenzweig, C., Goldberg, R., ... & Kinney, P. L. (2007). .2 Analyzing the impacts of climate change on ozone and particulate matter with tracer species, process analysis, and multiple regional climate scenarios. *Developments in Environmental Science*, *6*, 648-660.

Holm, J. A., Jardine, K., Guenther, A. B., Chambers, J. Q., & Tribuzy, E. (2014). Evaluation of MEGAN-CLM parameter sensitivity to predictions of isoprene emissions from an Amazonian rainforest. *Atmospheric Chemistry and Physics Discussions*, *14*, 23995-24041.

Homer, C., Dewitz, J., Fry, J., Coan, M., Hossain, N., Larson, C., ... & Wickham, J. (2007). Completion of the 2001 national land cover database for the counterminous United States. *Photogrammetric Engineering and Remote Sensing*, *73*(4), 337.

Hong, S. Y., Noh, Y., & Dudhia, J. (2006). A new vertical diffusion package with an explicit treatment of entrainment processes. *Monthly Weather Review*, *134*(9), 2318-2341.

Huang, L., McDonald-Buller, E. C., McGaughey, G., Kimura, Y., & Allen, D. T. (2014). Annual variability in leaf area index and isoprene and monoterpene emissions during drought years in Texas. *Atmospheric Environment*, *92*, 240-249.

Huang, L., McGaughey, G., McDonald-Buller, E., Kimura, Y., & Allen, D. T. (2015). Quantifying regional, seasonal and interannual contributions of environmental factors on isoprene and monoterpene emissions estimates over eastern Texas. *Atmospheric Environment, 106*, 120-128.

Hummel, I., Pantin, F., Sulpice, R., Piques, M., Rolland, G., Dauzat, M., ... & Muller, B. (2010). Arabidopsis plants acclimate to water deficit at low cost through changes of carbon usage: an integrated perspective using growth, metabolite, enzyme, and gene expression analysis. *Plant Physiology*, *154*(1), 357-372.

Ingwersen, J., Steffens, K., Högy, P., Warrach-Sagi, K., Zhunusbayeva, D., Poltoradnev, M., ... & Streck, T. (2011). Comparison of Noah simulations with eddy covariance and soil water measurements at a winter wheat stand. *Agricultural and Forest Meteorology*, *151*(3), 345-355.

Iyer, N. J., Tang, Y., & Mahalingam, R. (2013). Physiological, biochemical and molecular responses to a combination of drought and ozone in Medicago truncatula. *Plant, Cell & Environment*, *36*(3), 706-720.

Jacob, D. J., Field, B. D., Jin, E. M., Bey, I., Li, Q., Logan, J. A., ... & Singh, H. B. (2002). Atmospheric budget of acetone. *Journal of Geophysical Research: Atmospheres (1984–2012)*, *107*(D10), ACH-5.

Jacob, D. J., Field, B. D., Li, Q., Blake, D. R., De Gouw, J., Warneke, C., ... & Guenther, A. (2005). Global budget of methanol: Constraints from atmospheric observations. *Journal of Geophysical Research: Atmospheres (1984–2012),110*(D8).

Jarvis, P. G. (1976). The interpretation of the variations in leaf water potential and stomatal conductance found in canopies in the field. *Philosophical Transactions of the Royal Society of London B: Biological Sciences*, *273*(927), 593-610.

Jiang, X., Wiedinmyer, C., Chen, F., Yang, Z. L., & Lo, J. C. F. (2008). Predicted impacts of climate and land use change on surface ozone in the Houston, Texas, area. *Journal of Geophysical Research: Atmospheres (1984–2012)*, *113*(D20).

Kangasjärvi, J., Jaspers, P., & Kollist, H. (2005). Signalling and cell death in ozone-exposed plants. *Plant, Cell & Environment*, *28*(8), 1021-1036.

Kavouras, I.G., Mihalopoulos, N., & Stephanou, E. G. (1998). Formation of atmospheric particles from organic acids produced by forests. *Nature. 395*(6703), 683-686.

Kawa, S. R. (1986). *Ozone deposition, scalar budgets and radiative heating over Texas coastal forest and ocean*. Department of Atmospheric Science, Colorado State University.

Keetch, J. J. & Byram, G. M. (1968). A drought index for forest fire control. US Department of Agriculture, Forest Service, Southeastern Forest Experiment Station.

Kim, H. K., Woo, J. H., Park, R. S., Song, C. H., Kim, J. H., Ban, S. J., & Park, J. H. (2014). Impacts of different plant functional types on ambient ozone predictions in the Seoul Metropolitan Areas (SMAs), Korea. *Atmospheric Chemistry and Physics, 14*(14), 7461–7484. doi:10.5194/acp-14-7461-2014.

Kimura, Y., McDonald-Buller, E., Vizuete, W., & Allen, D. T. (2008). Application of a Lagrangian process analysis tool to characterize ozone formation in Southeast Texas. *Atmospheric Environment*. 42(23), 5743-5759.

Kleindienst, T. E., Jaoui, M., Lewandowski, M., Offenberg, J. H., Lewis, C. W., Bhave, P. V., & Edney, E. O. (2007). Estimates of the contributions of biogenic and anthropogenic hydrocarbons to secondary organic aerosol at a southeastern US location. *Atmospheric Environment*, *41*(37), 8288-8300.

Klink, K. (1999). Climatological mean and interannual variance of United States surface wind speed, direction and velocity. *International Journal of Climatology*, *19*(5), 471-488.

Knyazikhin, Y., Glassy, J., Privette, J. L., Tian, Y., Lotsch, A., Zhang, Y., … Running, W. (1999). MODIS Leaf Area Index (LAI) and Fraction of Photosynthetically Active Radiation Absorbed by Vegetation (FPAR) Product (MOD15) Algorithm Theoretical Basis Document. Retrieved Feburary 19, 2014, from http://modis.gsfc.nasa.gov/data/atbd/atbd_mod15.pdf

Koster, R. D., Guo, Z., Yang, R., Dirmeyer, P. A., Mitchell, K. & Puma, M. J. (2009). On the nature of soil moisture in land surface models. *Journal of Climate*, *22*, 4322–4335.

Koster, R., & Suarez, M. (1996). Energy and water balance calculations in the Mosaic LSM. NASA Technical Memorandum, NASA TM-104606, Volume 9, 60 pp.

Kuhn, U., Andreae, M. O., Ammann, C., Araújo, A. C., Brancaleoni, E., Ciccioli, P., ... & Kesselmeier, J. (2007). Isoprene and monoterpene fluxes from Central Amazonian rainforest inferred from tower-based and airborne measurements, and implications on the atmospheric chemistry and the local carbon budget. *Atmospheric Chemistry and Physics*, *7*(11), 2855-2879.

Kuhn, U., Rottenberger, S., Biesenthal, T., Wolf, A., Schebeske, G., Ciccioli, P., & Kesselmeier, J. (2004). Strong correlation between isoprene emission and gross photosynthetic capacity during leaf phenology of the tropical tree species Hymenaea courbaril with fundamental changes in volatile organic compounds emission composition during early leaf development. *Plant, Cell & Environment*,*27*(12), 1469-1485.

Kurpius, M. R., & Goldstein, A. H. (2003). Gas-phase chemistry dominates O_3 loss to a forest, implying a source of aerosols and hydroxyl radicals to the atmosphere. *Geophysical Research Letters*, *30*(7).

Lamaud, E., Loubet, B., Irvine, M., Stella, P., Personne, E., & Cellier, P. (2009). Partitioning of ozone deposition over a developed maize crop between stomatal and non-stomatal uptakes, using eddy-covariance flux measurements and modelling. *Agricultural and Forest Meteorology*, *149*(9), 1385–1396. doi:10.1016/j.agrformet.2009.03.017

Lamb, B., Gay, D., Westberg, H., & Pierce, T. (1993). A biogenic hydrocarbon emission inventory for the USA using a simple forest canopy model. *Atmospheric Environment. Part A. General Topics*, *27*(11), 1673-1690.

Lathiere, J., Hauglustaine, D. A., Friend, A. D., Noblet-Ducoudré, N. D., Viovy, N., & Folberth, G. A. (2006). Impact of climate variability and land use changes on global biogenic volatile organic compound emissions. *Atmospheric Chemistry and Physics*, *6*(8), 2129–2146.

Lathiere, J., Hewitt, C. N., & Beerling, D. J. (2010). Sensitivity of isoprene emissions from the terrestrial biosphere to 20th century changes in atmospheric CO2 concentration, climate, and land use. *Global Biogeochemical Cycles*,*24*(1).

Lavoir, A. V., Staudt, M., Schnitzler, J. P., Landais, D., Massol, F., Rocheteau, A., ... & Rambal, S. (2009). Drought reduced monoterpene emissions from the evergreen Mediterranean oak Quercus ilex: results from a throughfall displacement experiment. *Biogeosciences*, *6*, p-1167.

Lawrence, D. M., Oleson, K. W., Flanner, M. G., Thornton, P. E., Swenson, S. C., Lawrence, P. J., ... & Slater, A. G. (2011). Parameterization improvements and functional and structural advances in version 4 of the Community Land Model. *Journal of Advances in Modeling Earth Systems*, *3*(1).

Lee, J. D., Lewis, A. C., Monks, P. S., Jacob, M., Hamilton, J. F., Hopkins, J. R., ... & Jenkin, M. E. (2006). Ozone photochemistry and elevated isoprene during the UK heatwave of August 2003. *Atmospheric Environment*, *40*(39), 7598-7613.

Lehning, A., Zimmer, I., Steinbrecher, R., Brüggemann, N., & Schnitzler, J. P. (1999). Isoprene synthase activity and its relation to isoprene emission in *Quercus robur* L. leaves. *Plant, Cell & Environment*, 22(5), 495-504.

Lelieveld, J., & Dentener, F. J. (2000). What controls tropospheric ozone ? *Journal of Geophysical Research: Atmospheres (1984–2012)*, *105*(1999), 3531–3551.

Lerdau, M., Guenther, A., & Monson, R. (1997). Plant production and emission of volatile organic compounds. *Bioscience*, 373-383.

Li, G., Zhang, R., Fan, J., & Tie, X. (2007). Impacts of biogenic emissions on photochemical ozone production in Houston, Texas. *Journal of Geophysical Research: Atmospheres (1984–2012)*, *112*(D10).

Liang, X., Lettenmaier, D. P., Wood, E. F., & Burges, S. J. (1994). A simple hydrologically based model of land surface water and energy fluxes for general circulation models. *Journal of Geophysical Research*, *99*(D7), 14415-14428.

Limousin, J. M., Rambal, S., Ourcival, J. M., Rocheteau, A., Joffre, R., & Rodriguez-Cortina, R. (2009). Long-term transpiration change with rainfall decline in a Mediterranean *Quercus ilex* forest. *Global Change Biology*, *15*(9), 2163–2175. doi:10.1111/j.1365-2486.2009.01852.x

Lippmann, M. (1989). Health effects of ozone a critical review. *Japca*, *39*(5), 672-695.

Liu, X. H., Zhang, Y., Xing, J., Zhang, Q., Wang, K., Streets, D. G., ... & Hao, J. M. (2010). Understanding of regional air pollution over China using CMAQ, part II. Process analysis and sensitivity of ozone and particulate matter to precursor emissions. *Atmospheric Environment*. 44(30), 3719-3727.

Liverman, D. M. (1990). Drought impacts in Mexico: climate, agriculture, technology, and land tenure in Sonora and Puebla. *Annals of the Association of American Geographers*, *80*(1), 49-72.

Logan, J. A., Regniere, J., & Powell, J. A. (2003). Assessing the impacts of global warming on forest pest dynamics. *Frontiers in Ecology and the Environment*, *1*(3), 130–137.

Logar, I., & van den Bergh, J. C. J. M. (2011). *Methods for assessment of the costs of droughts* (pp. 1–58). CONHAZ Report. Retrieved from http://conhaz.org/CONHAZ%20REPORT%20WP05_1_FINAL.pdf

Löw, M., Herbinger, K., Nunn, A. J., Häberle, K. H., Leuchner, M., Heerdt, C., ... & Matyssek, R. (2006). Extraordinary drought of 2003 overrules ozone impact on adult beech trees (Fagus sylvatica). *Trees*, *20*(5), 539-548.

LP DAAC (2012). *MODIS LAI_FPAR User's Guide.* Retrieved September 17, 2013, from https://lpdaac.usgs.gov/sites/default/files/public/modis/docs/MODIS-LAI-FPAR-User-Guide.pdf

Lusebrink, I., Evenden, M. L., Blanchet, F. G., Cooke, J. E., & Erbilgin, N. (2011). Effect of water stress and fungal inoculation on monoterpene emission from an historical and a new pine host of the mountain pine beetle. *Journal of chemical ecology*, *37*(9), 1013-1026.

Marsh, T. J. (2004). The UK drought of 2003: a hydrological review. *Weather*, *59*(8), 224–230. doi:10.1256/wea.79.04

McCallum, I., Obersteiner, M., Nilsson, S., & Shvidenko, A. (2006). A spatial comparison of four satellite derived 1km global land cover datasets. *International Journal of Applied Earth Observation and Geoinformation, 8*(4), 246–255.

McDonald-Buller, E., Wiedinmyer, C., Kimura, Y., & Allen, D. (2001). Effects of land use data on dry deposition in a regional photochemical model for eastern Texas. *Journal of the Air & Waste Management Association*, *51*(8), 1211–1218. doi:10.1080/10473289.2001.10464340

McDowell, N. G. (2011). Mechanisms linking drought, hydraulics, carbon metabolism, and vegetation mortality. *Plant Physiology*, *155*(3), 1051–9. doi:10.1104/pp.110.170704

McDowell, N., Pockman, W. T., Allen, C. D., Breshears, D. D., Cobb, N., Kolb, T., ... & Yepez, E. A. (2008). Mechanisms of plant survival and mortality during drought: why do some plants survive while others succumb to drought? *New phytologist*, *178*(4), 719-739.

McKee, T. B., Doesken, N. J., & Kleist, J. (1993). The relationship of drought frequency and duration to time scale. *Proceedings of 8th Conference on Applied Climatology, American Meteorological Society* (pp. 179–184). Boston.

McNider, R., personal communication, July 31, 2013

Melillo, J.M., Richmond, T.C., & Yohe, G.W. (2014). Climate Change Impacts in the United States. *Third National Climate Assessment*. US Global Change Research Program.

Meyers, T. P., Finkelstein, P., Clarke, J., Ellestad, T. G., & Sims, P. F. (1998). A multilayer model for inferring dry deposition using standard meteorological measurements. *Journal of Geophysical Research*, *103*(D17), 22645–22661.

Michou, M., Laville, P., Serça, D., Fotiadi, A., Bouchou, P., & Peuch, V.H. (2005). Measured and modeled dry deposition velocities over the ESCOMPTE area. *Atmospheric Research, 74*(1-4), 89–116. doi:10.1016/j.atmosres.2004.04.011

Mills, G., Hayes, F., Simpson, D., Emberson, L., Norris, D., Harmens, H., & Büker, P. (2011). Evidence of widespread effects of ozone on crops and (semi-) natural vegetation in Europe (1990–2006) in relation to AOT40-and flux-based risk maps. *Global Change Biology*, *17*(1), 592–613.

Mishra, A. K., & Singh, V. P. (2010). A review of drought concepts. *Journal of Hydrology*, *391*(1-2), 202–216. doi:10.1016/j.jhydrol.2010.07.012

Mitchell, K. E., Lohmann, D., Houser, P. R., Wood, E. F., Schaake, J. C., Robock, A., ... & Bailey, A. A. (2004). The multi-institution North American Land Data Assimilation System (NLDAS): Utilizing multiple GCIP products and partners in a continental distributed hydrological modeling system. *Journal of Geophysical Research: Atmospheres (1984–2012)*, *109*(D7).

Mitchell, P. J., O'Grady, A. P., Tissue, D. T., White, D. A., Ottenschlaeger, M. L., & Pinkard, E. A. (2013). Drought response strategies define the relative contributions of hydraulic dysfunction and carbohydrate depletion during tree mortality. *New Phytologist*, *197*(3), 862-872.

Monteith, J. L. (1995). A reinterpretation of stomatal responses to humidity. *Plant, Cell & Environment*, *18*(4), 357-364.

Morgan, P. B., Mies, T. A., Bollero, G. A., Nelson, R. L., & Long, S. P. (2006). Season-long elevation of ozone concentration to projected 2050 levels under fully open-air conditions substantially decreases the growth and production of soybean. *New Phytologist*, *170*(2), 333-343.

Müller, J. F., Stavrakou, T., Wallens, S., Smedt, I. D., Roozendael, M. V., Potosnak, M. J., et al. (2008). Global isoprene emissions estimated using MEGAN, ECMWF analyses and a detailed canopy environment model. *Atmospheric Chemistry and Physics*, *8*(5), 1329-1341.

Myneni, R. B., Hoffman, S., Knyazikhin, Y., Privette, J. L., & Glassy, J. (2002). Global products of vegetation leaf area and fraction absorbed PAR from year one of MODIS data. *Remote Sensing of Environment*, *83*(1-2), 214–231.

Myneni, R.B., Ramakrishna, R., Nemani, R., & Running, S. W. (1997). Estimation of global leaf area index and absorbed PAR using radiative transfer models. *IEEE Transactions on Geoscience and Remote Sensing, 35*(6), 1380–1393. doi:10.1109/36.649788.

National Climate Data Center, Retrieved September 17, 2013, from http://www1.ncdc.noaa.gov/pub/data/cirs/

National Oceanic and Atmospheric Administration, Retrieved September 17, 2013, from http://www.esrl.noaa.gov/psd/data/usclimdivs/boundaries.html

National Weather Service, Advanced Hydrologic Prediction Service, Retrieved September 17, 2013, from http://water.weather.gov/precip/

Neirynck, J., Gielen, B., Janssens, I. A, & Ceulemans, R. (2012). Insights into ozone deposition patterns from decade-long ozone flux measurements over a mixed temperate forest. *Journal of Environmental Monitoring*, *14*(6), 1684–1695. doi:10.1039/c2em10937a

Niemeyer, S. (2008). New drought indices. In *Proceedings of the 1st international conference "Drought management: Scientific and technological innovations", Zaragoza, Spain* (pp. 12-14).

Niinemets, U. (2010). Mild versus severe stress and BVOCs: thresholds, priming and consequences. *Trends in Plant Science*, *15*(3), 145–53. doi:10.1016/j.tplants.2009.11.008

Niu, G.-Y., et al. (2011). The community Noah land surface model with multiparameterization options (Noah-MP): 1. Model description and evaluation with local-scale measurements. *Journal of Geophysical Research*, *116*.

Nogués, I., Medori, M., & Calfapietra, C. (2015). Limitations of monoterpene emissions and their antioxidant role in Cistus sp. under mild and severe treatments of drought and warming. *Environmental and Experimental Botany*.

Novakov, T., & Penner, J. E. (1993). Large contribution of organic aerosols to cloud-condensation-nuclei concentrations. *Nature, 365*(6449), 823-826.

Nowak, D. J., Crane, D. E., & Stevens, J. C. (2006). Air pollution removal by urban trees and shrubs in the United States. *Urban Forestry & Urban Greening*,*4*(3), 115-123.

Ntale, H. K., & Gan, T. Y. (2003). Drought indices and their application to East Africa. *International Journal of Climatology*, *23*(11), 1335–1357. doi:10.1002/joc.931

Obasi, G. O. P. (1994). WMO's role in the international decade for natural disaster reduction. *Bulletin of the American Meteorological Society*, 75(9), 1655-1661.

Ochsner, T. E., Cosh, M. H., Cuenca, R. H., Dorigo, W. A., Draper, C. S., Hagimoto, Y., ... & Zreda, M. (2013). State of the art in large-scale soil moisture monitoring. *Soil Science Society of America Journal*, *77*(6), 1888-1919.

Ormeno, E., Mevy, J. P., Vila, B., Bousquet-Melou, A., Greff, S., Bonin, G., & Fernandez, C. (2007). Water deficit stress induces different monoterpene and sesquiterpene emission changes in Mediterranean species. Relationship between terpene emissions and plant water potential. *Chemosphere*, 67(2), 276-284.

Pacifico, F., Harrison, S. P., Jones, C. D., & Sitch, S. (2009). Isoprene emissions and climate. *Atmospheric Environment*, *43*(39), 6121-6135.

Palmer, P. I., Abbot, D. S., Fu, T. M., Jacob, D. J., Chance, K., Kurosu, T. P., ... & Sumner, A. L. (2006). Quantifying the seasonal and interannual variability of North American isoprene emissions using satellite observations of the formaldehyde column. *Journal of Geophysical Research: Atmospheres (1984–2012)*, *111*(D12).

Palmer, P. I., Jacob, D. J., Fiore, A. M., Martin, R. V., Chance, K., & Kurosu, T. P. (2003). Mapping isoprene emissions over North America using formaldehyde column observations from space. *Journal of Geophysical Research: Atmospheres (1984–2012)*, *108*(D6).

Palmer, W. C. (1965). *Meteorological Drought*. Washington, DC: US Department of Commerce, Weather Bureau.

Panek, J. A., & Goldstein, A. H. (2001). Response of stomatal conductance to drought in ponderosa pine: implications for carbon and ozone uptake. *Tree physiology*, *21*(5), 337-344.

Park, R. J., Hong, S. K., Kwon, H. A., Kim, S., Guenther, a., Woo, J.H., & Loughner, C. P. (2014). An evaluation of ozone dry deposition simulations in East Asia. *Atmospheric Chemistry and Physics*, *14*(15), 7929–7940. doi:10.5194/acp-14-7929-2014

Pegoraro, E., Potosnak, M. J., Monson, R. K., Rey, A., Barron-Gafford, G., & Osmond, C. B. (2007). The effect of elevated CO_2, soil and atmospheric water deficit and seasonal phenology on leaf and ecosystem isoprene emission. *Functional Plant Biology*, 34(9), 774-784.

Pegoraro, E., Rey, A. N. A., Abrell, L., Haren, J., & Lin, G. (2006). Drought effect on isoprene production and consumption in Biosphere 2 tropical rainforest. *Global Change Biology*, 12(3), 456-469.

Pegoraro, E., Rey, A., Barron-Gafford, G., Monson, R., Malhi, Y., & Murthy, R. (2005). The interacting effects of elevated atmospheric CO_2 concentration, drought and leaf-to-air vapour pressure deficit on ecosystem isoprene fluxes. *Oecologia*, 146(1), 120-129.

Pegoraro, E., Rey, A., Bobich, E. G., Barron-Gafford, G., Grieve, K. A., Malhi, Y., & Murthy, R. (2004a). Effect of elevated CO_2 concentration and vapour pressure deficit on isoprene emission from leaves of Populus deltoides during drought. *Functional Plant Biology*, *31*(12), 1137-1147.

Pegoraro, E., Rey, A., Greenberg, J., Harley, P., Grace, J., Malhi, Y., & Guenther, A. (2004b). Effect of drought on isoprene emission rates from leaves of *Quercus virginiana* Mill. *Atmospheric Environment*, *38*(36), 6149-6156.

Petron, G., Harley, P., Greenberg, J., & Guenther, A. (2001). Seasonal temperature variations influence isoprene emission. *Geophysical Research Letters*, *28*(9), 1707-1710.

Pfister, G. G., Emmons, L. K., Hess, P. G., Lamarque, J. F., Orlando, J. J., Walters, S., ... & Lawrence, P. J. (2008). Contribution of isoprene to chemical budgets: A model tracer study with the NCAR CTM MOZART-4. *Journal of Geophysical Research: Atmospheres (1984–2012)*, *113*(D5).

Pio, C. A., & Feliciano, M. S. (1996). Dry deposition of ozone and sulphur dioxide over low vegetation in moderate southern European weather conditions. Measurements and modelling. *Physics and Chemistry of the Earth*, *21*(5), 373–377.

Pio, C. A., Feliciano, M. S., Vermeulen, A. T., & Sousa, E. C. (2000). Seasonal variability of ozone dry deposition under southern European climate conditions, in Portugal. *Atmospheric Environment*, *34*, 195–205.

Pleijel, H., Danielsson, H., Emberson, L., Ashmore, M. R., & Mills, G. (2007). Ozone risk assessment for agricultural crops in Europe: Further development of stomatal flux and flux–response relationships for European wheat and potato. *Atmospheric Environment*, *41*(14), 3022–3040. doi:10.1016/j.atmosenv.2006.12.002

Pleim, J., & Ran, L. (2011). Surface flux modeling for air quality applications. *Atmosphere*, *2*(4), 271–302. doi:10.3390/atmos2030271

Poisson, N., Kanakidou, M., & Crutzen, P. J. (2000). Impact of non-methane hydrocarbons on tropospheric chemistry and the oxidizing power of the global troposphere: 3-dimensional modelling results. *Journal of Atmospheric Chemistry, 36*(2), 157-230.

Popescu, S. C., Stukey, J., Mutlu, M., Zhao, K., Sheridan, R., Ku, N. W., … Harper, C. (2011). Expansion of Texas land use/land cover through class crosswalking and Lidar parameterization of arboreal vegetation. Retrieved December 1, 2014, from https://www.tceq.texas.gov/assets/public/implementation/air/am/contracts/reports/oth/5820564593FY0925-20110419-tamu-expension_tx_lulc_arboreal_vegetation.pdf

Potosnak, M. J., LeStourgeon, L., Pallardy, S. G., Hosman, K. P., Gu, L., Karl, T., ... & Guenther, A. B. (2014). Observed and modeled ecosystem isoprene fluxes from an oak-dominated temperate forest and the influence of drought stress. *Atmospheric Environment, 84*, 314-322.

Pouliot, D., Latifovic, R., Zabcic, N., Guindon, L., & Olthof, I. (2014). Development and assessment of a 250m spatial resolution MODIS annual land cover time series (2000–2011) for the forest region of Canada derived from change-based updating. *Remote Sensing of Environment, 140,* 731–743. doi:10.1016/j.rse.2013.10.004.

Pour-Biazar, A., McNider, R.T., Roselle, S.J., Suggs, R., Jedlovec, G., Byun, … Cameron, R. (2007). Correcting photolysis rates on the basis of satellite observed clouds. *Journal of Geophysical Research.* 112, doi:10.1029/2006JD007422.

Pressley, S., Lamb, B., Westberg, H., & Vogel, C. (2006). Relationships among canopy scale energy fluxes and isoprene flux derived from long-term, seasonal eddy covariance measurements over a hardwood forest. *Agricultural and Forest Meteorology,* 136(3), 188-202.

Pressley, S., Lamb, B., Westberg, H., Guenther, A., Chen, J., & Allwine, E. (2004). Monoterpene emissions from a Pacific Northwest Old-Growth Forest and impact on regional biogenic VOC emission estimates. *Atmospheric Environment*, *38*(19), 3089-3098.

Prosperop, J. M., & Nees, R. T. (1986). Impact of the North African drought and El Nino on mineral dust in the Barbados trade winds. *Nature, 320,* 735 – 738.

Purves, D. W., Caspersen, J. P., Moorcroft, P. R., Hurtt, G. C., & Pacala, S. W. (2004). Human-induced changes in US biogenic volatile organic compound emissions: evidence from long-term forest inventory data. *Global Change Biology*, *10*(10), 1737-1755.

Quaife, T., Quegan, S., Disney, M., Lewis, P., Lomas, M., & Woodward, F. I. (2008). Impact of land cover uncertainties on estimates of biospheric carbon fluxes. *Global Biogeochemical Cycles, 22*(4), GB4016. doi:10.1029/2007GB003097.

Rannik, Ü., Altimir, N., Mammarella, I., Bäck, J., Rinne, J., Ruuskanen, T. M., ... & Kulmala, M. (2012). Ozone deposition into a boreal forest over a decade of observations: evaluating deposition partitioning and driving variables.*Atmospheric Chemistry and Physics, 12*(24), 12165-12182.

Rollins, M.G. (2009). LANDFIRE: a nationally consistent vegetation, wildland fire, and fuel assessment. *International Journal of Wildland Fire, 18*(3), 235-249.

Ryan, A. C., Hewitt, C. N., Possell, M., Vickers, C. E., Purnell, A., Mullineaux, P. M., ... & Dodd, I. C. (2014). Isoprene emission protects photosynthesis but reduces plant productivity during drought in transgenic tobacco (Nicotiana tabacum) plants. *New Phytologist*, *201*(1), 205-216.

Rodríguez-Calcerrada, J., Buatois, B., Chiche, E., Shahin, O., & Staudt, M. (2013). Leaf isoprene emission declines in *Quercus pubescens* seedlings experiencing drought–Any implication of soluble sugars and mitochondrial respiration? *Environmental and Experimental Botany*, 85, 36-42.

Rosenstiel, T. N., Potosnak, M. J., Griffin, K. L., Fall, R., & Monson, R. K. (2003). Increased CO_2 uncouples growth from isoprene emission in an agriforest ecosystem. *Nature*, *421*(6920), 256-259.

Ruidavets, J. B., Cournot, M., Cassadou, S., Giroux, M., Meybeck, M., & Ferrières, J. (2005). Ozone air pollution is associated with acute myocardial infarction. *Circulation.* 111(5), 563-569.

Ruiz, L.H, & Yarwood, G. (2013). Interactions between organic aerosol and NOy: Influence on oxidant production. Prepared for the Texas AQRP (Project 12-012), by the University of Texas at Austin, and ENVIRON International Corporation, Novato, CA. Retrieved April 17, 2015 from http://aqrp.ceer.utexas.edu/projectinfoFY12_13/12-012/12-012%20Final%20Report.pdf

Running, S.W., Nemani, R., Glassy, J. M., & Thornton, P. E. (1999). MODIS daily photosynthesis (PSN) and annual net primary production (NPP) product (MOD17) algorithm theoretical basis document. http://modis.gsfc.nasa.gov/data/atbd/atbd_mod16.pdf (accessed on December 1, 2014).

Sakulyanontvittaya, T., Duhl, T., Wiedinmyer, C., Helmig, D., Matsunaga, S., Potosnak, M., ... & Guenther, A. (2008). Monoterpene and sesquiterpene emission estimates for the United States. *Environmental science & technology*,*42*(5), 1623-1629.

Sala, A., Piper, F., and Hoch, G. (2010). Physiological mechanisms of drought-induced tree mortality are far from being resolved. *New Phytologist*, *186*, 274–281.

Sanderson, M.G., Jones, C.D., Collins, W.J., Johnson, C.E., & Derwent, R. G. (2003). Effect of climate change on isoprene emissions and surface ozone levels. *Geophysical Research Letters, 30*(18).

Scholes, M., & Andreae, M. O. (2000). Biogenic and pyrogenic emissions from Africa and their impact on the global atmosphere. *AMBIO: A Journal of the Human Environment*, *29*(1), 23-29.

Schwede, D., Pouliot, G., & Pierce, T. (2005). Changes to the biogenic emissions inventory system version 3 (BEIS3). In *4th Annual CMAS Models-3 Users' Conference, September* (Vol. 26, p. 28).

Schwede, D., Zhang, L., Vet, R., & Lear, G. (2011). An intercomparison of the deposition models used in the CASTNET and CAPMoN networks. *Atmospheric Environment*, *45*(6), 1337–1346. doi:10.1016/j.atmosenv.2010.11.050

Seco, R., Karl, T., Guenther, A., Hosman, K. P., Pallardy, S. G., Gu, L., ... & Kim, S. (2015). Ecosystem-scale VOC fluxes during an extreme drought in a broad-leaf temperate forest of the Missouri Ozarks (central USA). *Global change biology*.

Seinfeld, J. H., & Pandis, S. N. (2012). *Atmospheric chemistry and physics: from air pollution to climate change*. John Wiley & Sons.

Sevanto, S., McDowell, N. G., Dickman, L. T., Pangle, R., & Pockman, W. T. (2014). How do trees die? A test of the hydraulic failure and carbon starvation hypotheses.*Plant, Cell & Environment*, *37*(1), 153-161.

Shabanov, N., Samanta, A., Myneni, R. B., Knyazikhin, Y., Votava, P., & Nemani, R. (2007). Collection 5 MODIS LAI and FPAR Products, University of Maryland. Retrieved Februray 19, 2014 from http://modis.gsfc.nasa.gov/sci_team/meetings/c5meeting/pres/day1/shabanov.pdf

Sharkey, T. D. (2005). Effects of moderate heat stress on photosynthesis: importance of thylakoid reactions, rubisco deactivation, reactive oxygen species, and thermotolerance provided by isoprene. *Plant, Cell & Environment*,28(3), 269-277.

Sharkey, T. D., & Loreto, F. (1993). Water stress, temperature, and light effects on the capacity for isoprene emission and photosynthesis of kudzu leaves. *Oecologia*, 95(3), 328-333.

Sharkey, T. D., Singsaas, E. L., Vanderveer, P. J., & Geron, C. (1996). Field measurements of isoprene emission from trees in response to temperature and light. *Tree Physiology*, *16*(7), 649-654.

Shaw, J. D., Steed, B. E., & Deblander, L. T. (2005). Forest Inventory and Analysis (FIA) annual inventory answers the question: What is happening to pinyon-juniper woodlands? *Journal of Forestry*, *103*(6), 280–285.

Sheffield, J., & Wood, E. F. (2012a). Major drought events of the 20th century. *Drought: Past Problems and Future Scenarios* (pp. 123–164). Routledge.

Sheffield, J., & Wood, E. F. (2012b). What is drought? *Drought: Past Problems and Future Scenarios* (p. 12). Routledge.

Sickles, J. E., & Shadwick, D. S. (2007). Seasonal and regional air quality and atmospheric deposition in the eastern United States. *Journal of Geophysical Research*, *112*(D17), D17302. doi:10.1029/2006JD008356

Sindelarova, K., Granier, C., Bouarar, I., Guenther, A., Tilmes, S., Stavrakou, T., ... & Knorr, W. (2014). Global data set of biogenic VOC emissions calculated by the MEGAN model over the last 30 years. *Atmospheric Chemistry and Physics*, *14*(17), 9317-9341.

Situ, S., Guenther, A., Wang, X., Jiang, X., Turnipseed, A., Wu, Z., & Bai, J. (2013). Impacts of seasonal and regional variability in biogenic VOC emissions on surface ozone in the Pearl River delta region, China. *Atmospheric Chemistry and Physics*, *13*(23), 11803-11817.

Situ, S., Wang, X., Guenther, A., Zhang, Y., Wang, X., Huang, M., ... & Xiong, Z. (2014). Uncertainties of isoprene emissions in the MEGAN model estimated for a coniferous and broad-leaved mixed forest in Southern China. *Atmospheric Environment*, *98*, 105-110.

Sivakumar, M. V. K., Stone, R., Sentelhas, P. C., Svoboda, M., Omondi, P., Sarkar, J., & Wardlow, B. (2010). Agricultural drought indices: summary and recommendations. *Agricultural Drought Indices Proceedings of an Expert Meeting* (pp. 172–197). Murcia, Spain.

Skamarock, W. C., Klemp, J. B., Dudhia, J., Gill, D. O., Barker, D. M., Wang, W., & Powers, J. G. (2005). *A description of the advanced research WRF version 2* (No.

NCAR/TN-468+ STR). National Center For Atmospheric Research Boulder Co Mesoscale and Microscale Meteorology Div.

Slinn, S. A., & Slinn, W. G. N. (1980). Predictions for particle deposition on natural waters. *Atmospheric Environment (1967)*, *14*(9), 1013-1016.

Smiatek, G., & Bogacki, M. (2005). Uncertainty assessment of potential biogenic volatile organic compound emissions from forests with the Monte Carlo method: Case study for an episode from 1 to 10 July 2000 in Poland. *Journal of Geophysical Research: Atmospheres (1984–2012)*, *110*(D23).

Solberg, S., Hov, Ø., Søvde, A., Isaksen, I. S. A., Coddeville, P., De Backer, H., ... & Uhse, K. (2008). European surface ozone in the extreme summer 2003. *Journal of Geophysical Research: Atmospheres (1984–2012)*, *113*(D7).

Song, J., Vizuete, W., Chang, S., Allen, D., Kimura, Y., Kemball-Cook, S., …McDonald-Buller, E. (2008). Comparisons of modeled and observed isoprene concentrations in southeast Texas. *Atmospheric Environment, 42*(8), 1922-1940.

Staudt, M., Ennajah, A., Mouillot, F., & Joffre, R. (2008). Do volatile organic compound emissions of Tunisian cork oak populations originating from contrasting climatic conditions differ in their responses to summer drought? *Canadian Journal of Forest Research*, 38(12), 2965-2975.Svoboda, M., LeComte, D., Hayes, M., Heim, R., Gleason, K., Angel, J., & Stephens, S. (2002). The drought monitor. *Bulletin of the American Meteorological Society*, *83*, 1181–1190.

Stavrakou, T., Guenther, A., Razavi, A., Clarisse, L., Clerbaux, C., Coheur, P. F., ... & Müller, J. F. (2011). First space-based derivation of the global atmospheric methanol emission fluxes. *Atmospheric chemistry and physics*,*11*(10), 4873-4898.

Stavrakou, T., Müller, J. F., Bauwens, M., De Smedt, I., Van Roozendael, M., Guenther, A., ... & Xia, X. (2014). Isoprene emissions over Asia 1979–2012: impact of climate and land-use changes. *Atmospheric Chemistry and Physics*,*14*(9), 4587-4605.

Steinbrecher, R., Smiatek, G., Köble, R., Seufert, G., Theloke, J., Hauff, K., … Curci, G. (2009). Intra- and inter-annual variability of VOC emissions from natural and semi-natural vegetation in Europe and neighbouring countries. *Atmospheric Environment, 43*(7), 1380–1391. doi:10.1016/j.atmosenv.2008.09.072.

Tani, A., Tozaki, D., Okumura, M., Nozoe, S., & Hirano, T. (2011). Effect of drought stress on isoprene emission from two major *Quercus* species native to East Asia. *Atmospheric Environment*, 45(34), 6261-6266.

Tawfik, A. B., Stöckli, R., Goldstein, A., Pressley, S., & Steiner, A. L. (2012). Quantifying the contribution of environmental factors to isoprene flux interannual variability. *Atmospheric Environment*, 54, 216-224.

Texas A&M Forest Service (2012). Texas A&M Forest Service Survey Shows 301 Million Trees Killed by Drought, Retrieved February 19, 2014 from http://texasforestservice.tamu.edu/main/popup.aspx?id=16509

Texas A&M Forest Service (2013). 2011 Texas Wildfires Common Denominators of Home Destruction, Retrieved July 5, 2015, from http://texasforestservice.tamu.edu/uploadedFiles/TFSMain/Preparing_for_Wildfires/Prepare_Your_Home_for_Wildfires/Contact_Us/2011%20Texas%20Wildfires.pdf

Texas A&M Forest Service. (2014). Texas ecoregions. Retrieved July 5, 2015, from http://texastreeid.tamu.edu/content/texasecoregions/

Texas Water Development Board. (2012). 2012 State Water Plan. Retrieved September 17, 2013 from http://www.twdb.state.tx.us/publications/state_water_plan/2012/04.pdf

Thunis, P., & Cuvelier, C. (2000). Impact of biogenic emissions on ozone formation in the Mediterranean area–a BEMA modelling study. *Atmospheric Environment*, *34*(3), 467-481.

Tian, Y. (2004). Comparison of seasonal and spatial variations of leaf area index and fraction of absorbed photosynthetically active radiation from Moderate Resolution Imaging Spectroradiometer (MODIS) and Common Land Model. *Journal of Geophysical Research*, *109*(D1), D01103. doi:10.1029/2003JD003777

Tingey, D. T., Evans, R., & Gumpertz, M. (1981). Effects of environmental conditions on isoprene emission from live oak. *Planta*, 152(6), 565-570.

Tingey, D. T., Manning, M., Grothaus, L. C., & Burns, W. F. (1980). Influence of light and temperature on monoterpene emission rates from slash pine. *Plant Physiology*, *65*(5), 797-801.

Tsakiris, G., Loukas, A., Pangalou, D., Vangelis, H., Tigkas, D., Rossi, G., & Cancelliere, A. (2002). Drought characterization. *Options Méditerranéennes*, *Ser. B*(58), 85–102.

Tsigaridis, K., & Kanakidou, M. (2003). Global modelling of secondary organic aerosol in the troposphere: a sensitivity analysis. *Atmospheric Chemistry and Physics*, *3*(5), 1849-1869.

Turpin, B. J., & Huntzicker, J. J. (1995). Identification of secondary organic aerosol episodes and quantitation of primary and secondary organic aerosol concentrations during SCAQS. *Atmospheric Environment*, *29*(23), 3527-3544.

Tuzet, A., Perrier, A., Loubet, B., Cellier, P. (2011). Modelling ozone deposition fluxes: the relative roles of deposition and detoxification processes. *Agricultural and Forest Meteorology*, *151*(4), 480-492.

UNECE. (2004). Revised Manual on Methodologies and Criteria for Mapping Critical Levels/loads and Geographical Areas where they are Exceeded. www.icpmapping.org.

US Global Change Research Program. (2009). Global Climate Change Impacts in the United States. Cambridge University Press. Retrieved Feb 19, 2014, from http://downloads.globalchange.gov/usimpacts/pdfs/climate-impacts-report.pdf

Val Martin, M., Heald, C. L., & Arnold, S. R. (2014). Coupling dry deposition to vegetation phenology in the Community Earth System Model: Implications for the simulation of surface O_3. *Geophysical Research Letters*, *41*(8), 2988–2996. doi:10.1002/2014GL059651.Received

Van Nieuwstadt, M. G. L., & Sheil, D. (2004). Drought, fire and tree survival in a Borneo rain forest, East Kalimantan, Indonesia. *Journal of Ecology*, *93*(1), 191–201. doi:10.1111/j.1365-2745.2005.00954.x

Van Vliet, M. T. H., & Zwolsman, J. J. G. (2008). Impact of summer droughts on the water quality of the Meuse river. *Journal of Hydrology*, *353*(1), 1–17. doi:10.1016/j.jhydrol.2008.01.001

Vicente-Serrano, S. M. (2007). Evaluating the impact of drought using remote sensing in a Mediterranean, semi-arid region. *Natural Hazards*, *40*(1), 173-208.

Vieno, M., Dore, A. J., Stevenson, D. S., Doherty, R., Heal, M. R., Reis, S., ... & Sutton, M. A. (2010). Modelling surface ozone during the 2003 heat-wave in the UK. *Atmospheric Chemistry and Physics*, *10*(16), 7963-7978.

Vilagrosa, A., Bellot, J., Vallejo, V. R., & Gil-Pelegrin, E. (2003). Cavitation, stomatal conductance, and leaf dieback in seedlings of two co-occurring Mediterranean shrubs during an intense drought. *Journal of Experimental Botany*, *54*(390), 2015–24. doi:10.1093/jxb/erg221

Viña, A., Gitelson, A. A., Nguy-Robertson, A. L., & Peng, Y. (2011). Comparison of different vegetation indices for the remote assessment of green leaf area index of

crops. *Remote Sensing of Environment*, *115*(12), 3468–3478. doi:10.1016/j.rse.2011.08.010

Voelker, S. L., Muzika, R., & Guyette, R. P. (2008). Individual tree and stand level influences on the growth, vigor, and decline of Red Oaks in the Ozarks. *Forest Science*, *54*(1), 8–20.

Wang, X., Zhang, Y., Hu, Y., Zhou, W., Lu, K., Zhong, L., ... & Russell, A. G. (2010). Process analysis and sensitivity study of regional ozone formation over the Pearl River Delta, China, during the PRIDE-PRD2004 campaign using the Community Multiscale Air Quality modeling system. *Atmospheric Chemistry and Physics*, *10*(9), 4423-4437.

Webb, P., & Reardon, T. (1992). Drought impact and household response in East and West Africa. *Quarterly Journal of International Agriculture*, *31*, 230–246.

Wesely, M. L. (1989). Parameterization of surface resistances to gaseous dry deposition in regional-scale numerical models. *Atmospheric Environment*, *23*(6), 1293–1304.

Wesely, M. L., Eastman, J. A., Stedman, D. H., & Yalvac, E. D. (1982). An eddy-correlation measurement of NO_2 flux to vegetation and comparison to O_3 flux. *Atmospheric Environment*, *16*(4), 815–820.

Wesely, M. L., & Hicks, B. B. (2000). A review of the current status of knowledge on dry deposition. *Atmospheric Environment*, *34*(12), 2261–2282.

Wiedinmyer, C., Guenther, A., Estes, M., Strange, I. W., Yarwood, G., & Allen, D. T. (2001). A land use database and examples of biogenic isoprene emission estimates for the state of Texas, USA. *Atmospheric Environment*, *35*(36), 6465-6477.

Wiedinmyer, C., Tie, X., Guenther, A., Neilson, R., & Granier, C. (2006). Future changes in biogenic isoprene emissions: how might they affect regional and global atmospheric chemistry? *Earth Interactions*, *10*(3), 1-19.

Wild, O. (2007). Modelling the global tropospheric ozone budget : exploring the variability in current models. *Atmospheric Chemistry and Physics*, *7*(10), 2643–2660.

Wilhite, D.A. (2000). Drought as a Natural Harzard: Concepts and Definitions. In D.A. Wilhite (Ed.), *Drought: A Global Assessment* (pp. 3–18). London/New York: Routledge.

Wilhite, D. A., & Knutson, C. L. (2008). Drought management planning: conditions for success. *Options Mediterraneennes Series A*, *80*, 141-148.

Wilhite, D.A., Svoboda, M. D., & Hayes, M. J. (2007). Understanding the complex impacts of drought: A key to enhancing drought mitigation and preparedness. *Water Resources Management*, *21*(5), 763–774. doi:10.1007/s11269-006-9076-5

Wilhite, D.A., & Vanyarkho, O. (2000). Drought: Pervasive impacts of a creeping phenomenon. *Drought: A Global Assessment* (ed., pp. 245–255). London/New York.

Wilkinson, M. J., Monson, R. K., Trahan, N., Lee, S., Brown, E., Jackson, R. B., ... & Fall, R. A. Y. (2009). Leaf isoprene emission rate as a function of atmospheric CO2 concentration. *Global Change Biology*, *15*(5), 1189-1200.

Wittig, V. E., Ainsworth, E. A., Naidu, S. L., Karnosky, D. F., & Long, S. P. (2009). Quantifying the impact of current and future tropospheric ozone on tree biomass, growth, physiology and biochemistry: a quantitative meta-analysis.*Global Change Biology*, *15*(2), 396-424.

Wu, S., Mickley, L. J., Leibensperger, E. M., Jacob, D. J., Rind, D., & Streets, D. G. (2008). Effects of 2000–2050 global change on ozone air quality in the United States. *Journal of Geophysical Research: Atmospheres (1984–2012)*, *113*(D6).

Wu, Z., Wang, X., Chen, F., Turnipseed, A. A., Guenther, A. B., Niyogi, D., ... & Alapaty, K. (2011). Evaluating the calculated dry deposition velocities of reactive nitrogen oxides and ozone from two community models over a temperate deciduous forest. *Atmospheric Environment*, *45*(16), 2663-2674.

Wuebbles, D. J., Grant, K. E., Connell, P. S., & Penner, J. E. (1989). The role of atmospheric chemistry in climate change. *JAPCA*, *39*(1), 22-28.

Xue, H., Wang, J., & Ping, C. (2011). Validation of collection 5 MODIS LAI product by scaling-up method using field measurements. *Remote Sensing. International Society for Optics and Photonics*, 81742H–81742H.

Yang, W., Tan, B., Huang, D., Rautiainen, M., Shabanov, N. V., Wang, Y., ... & Myneni, R. B. (2006). MODIS leaf area index products: From validation to algorithm improvement. *Geoscience and Remote Sensing, IEEE Transactions on*, *44*(7), 1885-1898.

Yarwood, G., Gookyoung, H., Carter, W. P. L., & Whitten, G.Z. (2012). Environmental Chamber Experiments to Evaluate NOx Sinks and Recycling in Atmospheric Chemical Mechanisms. Final report prepared for the Texas Air Quality Research Program, University of Texas, Austin, Texas. Retrieved April 17, 2015, from http://aqrp.ceer.utexas.edu/projectinfo%5C10-042%5C10-042%20Final%20Report.pdf

Yarwood, G., Wilson, G., Shepard, S., & Guenther, A. (2002). User's guide to the global biosphere emissions and interactions system (GloBEIS) version 3. *ENVIRON International Corporation*, *773*.

Zargar, A., Sadiq, R., Naser, B., & Khan, F. I. (2011). A review of drought indices. *Environmental Reviews*, *19*, 333–349. doi:10.1139/A11-013

Zeppel, M. J. B., Anderegg, W. R. L., & Adams, H. D. (2013). Meetings Forest mortality due to drought : latest insights , evidence and unresolved questions on physiological pathways and consequences of tree death. *New Phytologist*, *197*, 372–374.

Zhang, Q. (2003). Drought and its impacts. China Climate Impact Assessment (2002), edited by H. Chen, pp. 12–18. *China Meteorol Press*. Beijing

Zhang, L., Brook, J. R., & Vet, R. (2002). On ozone dry deposition — with emphasis on non-stomatal uptake and wet canopies. *Atmospheric Environment*, *36*(30), 4787–4799.

Zhang, L., Brook, J. R., & Vet, R. (2003). A revised parameterization for gaseous dry deposition in air-quality models. *Atmospheric Chemistry and Physics*, *3*(6), 2067-2082.

Zhang, L., Gong, S., Padro, J., & Barrie, L. (2001). A size-segregated particle dry deposition scheme for an atmospheric aerosol module. *Atmospheric Environment*, *35*(3), 549-560.

Zhao, K., & Popescu, S. (2009). Lidar-based mapping of leaf area index and its use for validating GLOBCARBON satellite LAI product in a temperate forest of the southern USA. *Remote Sensing of Environment*, *113*(8), 1628–1645. doi:10.1016/j.rse.2009.03.006